



THE UNIVERSITY OF
WAIKATO
Te Whare Wānanga o Waikato

Research Commons

<http://researchcommons.waikato.ac.nz/>

Research Commons at the University of Waikato

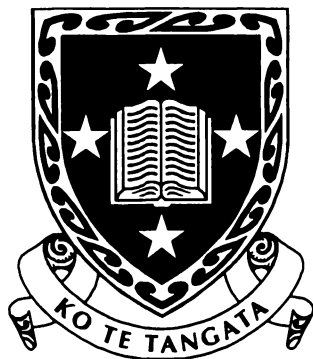
Copyright Statement:

The digital copy of this thesis is protected by the Copyright Act 1994 (New Zealand).

The thesis may be consulted by you, provided you comply with the provisions of the Act and the following conditions of use:

- Any use you make of these documents or images must be for research or private study purposes only, and you may not make them available to any other person.
- Authors control the copyright of their thesis. You will recognise the author's right to be identified as the author of the thesis, and due acknowledgement will be made to the author where appropriate.
- You will obtain the author's permission before publishing any material from the thesis.

Some Metallacyclic Complexes of the Late Transition Metals



A thesis
submitted in partial fulfilment
of the requirements for the Degree
of
Doctor of Philosophy in Chemistry
at the
University of Waikato
by
ALLEN GRAYSON OLIVER

University of Waikato

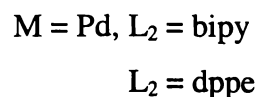
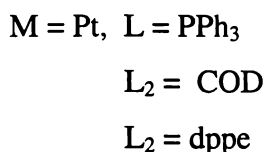
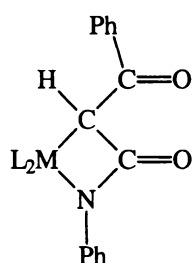
1999

Abstract

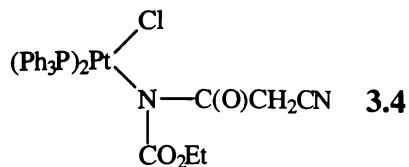
The principal aim of this thesis is the synthesis and characterisation of four-membered metallacyclic complexes. Reactions of square-planar palladium(II), platinum(II) and gold(III) dihalide complexes with a variety of amides, some in the presence of silver(I) oxide are discussed.

Chapter one reviews the literature of small-ring metallacyclic chemistry, in particular the synthesis of four-membered metallacycles, as they are, in the main, the complexes that are further reported throughout the remainder of the thesis.

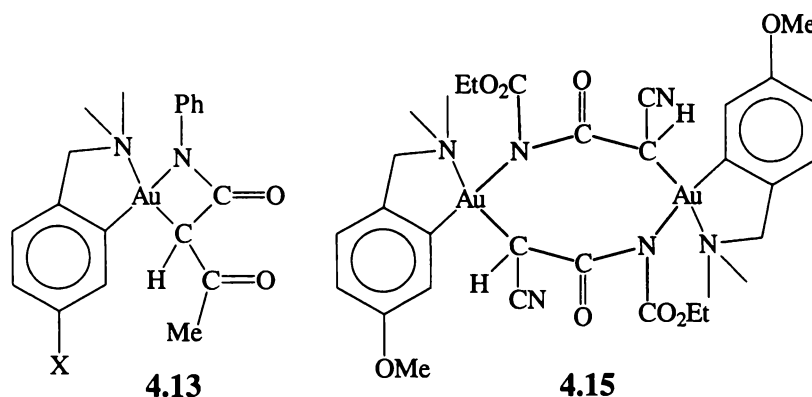
Chapter two reports the synthesis of four-membered metallalactam complexes $[M\{N(Ph)C(O)CHC(O)Ph\}L_2]$ (**2.11** – **2.15**) formed from the reactions of square-planar L_2MCl_2 complexes [$M = Pt, Pd, L = PPh_3, L_2 = 1,5$ -cyclooctadiene (COD), 1,2-bis(diphenylphosphino)ethane (dppe), 2,2'-bipyridine (bipy)] with 2-benzoylacetylphenylamide [$PhC(O)CH_2C(O)NHPh$] in the presence of silver(I) oxide. The X-ray crystal structure of $[Pd\{N(Ph)C(O)CHC(O)Ph\}(bipy)] \cdot CH_2Cl_2$ (**2.14**. CH_2Cl_2) was determined to confirm the geometry of the compounds. The reactions of acetoacetamide [$NH_2C(O)CH_2C(O)CH_3$] with *cis*- $[PtCl_2(PPh_3)_2]$, $[PtCl_2(dppe)]$ and $[PdCl_2(bipy)]$ (**2.16** – **2.18**) in the presence of silver(I) oxide are also discussed..



Chapter three describes the isolation and characterisation of a platinum(II)-amidate complex, believed to be the first characterised intermediate in silver(I) oxide mediated reactions. For short reaction times the complex *cis*- $[Pt\{N(C(O)CH_2CN)(CO_2Et)\}Cl(PPh_3)_2]$ (**3.4**) can be isolated from the reaction mixture of *cis*- $[PtCl_2(PPh_3)_2]$ with *N*-cyanoacetylurethane [$NCCH_2C(O)NHCO_2Et$] in the presence of silver(I) oxide. For long reaction times this synthesis is known to afford the four-membered metallalactam $[Pt\{N(CO_2Et)C(O)CHCN\}(PPh_3)_2]$.



Chapter four details the synthesis and characterisation of four-membered gold(III) lactam complexes. A series of metallalactam complexes were characterised from the reaction of $[\text{LAuCl}_2]$ [$\text{L} = \{\text{C}_6\text{H}_3(\text{CH}_2\text{NMe}_2)\text{-2-OMe-5}\}$ or $\{\text{C}_6\text{H}_4(\text{CH}_2\text{NMe}_2)\text{-2}\}$] with *N*-cyanoacetylurethane, 2-benzoylacetylurethane, acetoacetylurethane or acetoacetamide in the presence of silver(I) oxide. A representative of these gold(III) metallacycles, $[\{\text{C}_6\text{H}_4\text{-CH}_2\text{NMe}_2\text{-2}\}\text{Au}\{\text{N}(\text{Ph})\text{C}(\text{O})\text{CHC}(\text{O})\text{CH}_3\}]$ (**4.13**), was structurally characterised. A novel and unprecedented dimerisation occurred with $[\{\text{C}_6\text{H}_3\text{-CH}_2\text{NMe}_2\text{-2-OMe-5}\}\text{Au}\{\text{N}(\text{CO}_2\text{Et})\text{C}(\text{O})\text{CHCN}\}]$, that formed an eight-membered metallacycle (**4.15**) which was characterised by an X-ray diffraction study.

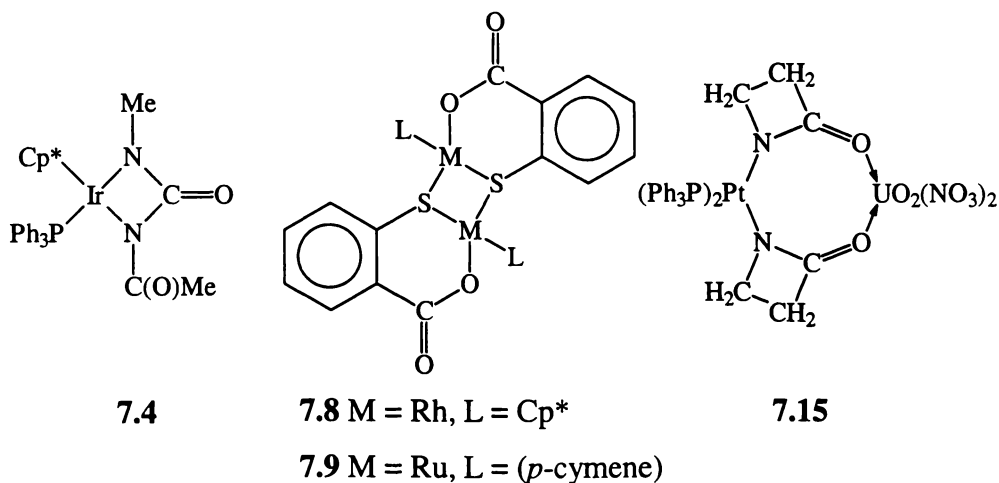


The reactions of *cis*- $[\text{PtCl}_2(\text{PPh}_3)_2]$ with either cyanoacetic acid or phenoxyacetic acid in the presence of silver(I) oxide are reported in chapter five. The reaction of phenoxyacetic acid with *cis*- $[\text{PtCl}_2(\text{PPh}_3)_2]$ was found to form the simple platinum(II) bis(carboxylate) complex, *cis*- $[\text{Pt}(\text{O}_2\text{CCH}_2\text{OPh})_2(\text{PPh}_3)_2]$ (**5.9**). Conversely, cyanoacetic acid undergoes a novel decarboxylation reaction which results in the formation of the platinum(II) bis(alkyl) complex *cis*- $[\text{Pt}(\text{CH}_2\text{CN})_2(\text{PPh}_3)_2]$ (**5.7**). The X-ray crystal structures of these two complexes are described.

Chapter six discusses the triethylamine-mediated syntheses of four-membered metallalactam complexes. The reactions of cyanoacetylurea $[\text{NH}_2\text{C}(\text{O})\text{NHC}(\text{O})\text{CH}_2\text{CN}]$ with *cis*- $[\text{PtCl}_2(\text{PPh}_3)_2]$, $[\text{PtCl}_2(\text{COD})]$, $[\text{PtCl}_2(\text{dppe})]$ and $[\text{PdCl}_2(\text{dppe})]$ in the presence of triethylamine and details of their characterisation are described. One complex, *cis*- $[\text{Pt}\{\text{N}(\text{C}(\text{O})\text{NH}_2)\text{C}(\text{O})\text{CHCN}\}(\text{PPh}_3)_2]$ (**6.5**), was

structurally characterised and was found to crystallise as an H-bonded dimer. The reactions of *N*-cyanoacetylurethane, 2-benzoylacetylurethane and acetoacetanilide with *cis*-[PtCl₂(PPh₃)₂] in the presence of silver(I) oxide are known to give well-characterised four-membered metallalactam complexes. The results of the reactions of these compounds when reacted under similar conditions, but with triethylamine as the base and halide abstractor, are also discussed.

Chapter seven describes a selection of four crystal structures. The X-ray structure of the first coordinatively saturated iridaureylene complex, $[\text{Ir}\{\text{N}(\text{Me})\text{C}(\text{O})\text{NAc}\}(\text{Cp}^*)(\text{PPh}_3)]$ (7.4), which is isoelectronic with four-membered metallalactam complexes, is described. The complex was found to adopt a "bar-stool" geometry. The structures of the complexes, $[\text{Rh}\{\text{O}_2\text{CC}_6\text{H}_4\text{-S-2}\}\text{Cp}^*]_2$ (7.8) and $[\text{Ru}\{\text{O}_2\text{CC}_6\text{H}_4\text{-S-2}\}(p\text{-cymene})]_2$ (7.9) were studied and found to be dimeric compounds. The complexes were found to adopt a pseudo-octahedral geometry, with a three-coordinate, bridging thiolate sulfur. The fourth structural analysis was that of the novel chelation product of *cis*- $[\text{Pt}\{\text{NCH}_2\text{CH}_2\text{C}(\text{O})\}_2(\text{PPh}_3)_2]$ with uranyl nitrate $[\text{UO}_2(\text{NO}_3)_2]$. The complex was found to form an eight-membered heterocycle (7.15), with the platinum bis(lactam) complex coordinating to the uranium via the lactam oxygen atoms.



Acknowledgments

First and foremost, I would like to thank my supervisor, Dr. William Henderson for his support, inspiration and at times perspiration during the course of my research. I would also like to thank my second supervisor Prof. Brian Nicholson for both the support and for instilling in me a sense of wonder about the art of X-ray crystallography.

As ever, a piece of work like this would be difficult to achieve with out financial support, and I would like to thank both the University of Waikato for a postgraduate scholarship, and the New Zealand Lottery Grants Board for their assistance in the purchase of materials and equipment. On the matter of equipment, Dr. Ralph Thomson and Mrs. Wendy Jackson have been invaluable for their insight and technical assistance. Thanks also to the rest of the technical staff at Waikato University, for without whom little or no real work would ever get done. The X-ray crystallographic units at both Auckland University and Canterbury University have both provided high quality data and I would like to thank both units, in particular the people who run them (Assoc. Prof. Clifton Rickard, Dr. L.J. Baker and Prof. Ward Robinson) for their exemplary work. I also thank the Microanalytical Unit at Otago University for elemental analysis data.

There is of course, "The C-block Lab" and all who have worked there during the years of this research (Greg, Scott, Mark, Paul, Cam, Mays, Steve, Maarten, Gwion, Meto, Lea, Brent, Clads and Corry to name a few) and the other grad's at Waikato (Karen, Stefan, Mark, Craig and Ian) who helped pass the time and make it more bearable. Also the grad's and staff at Auckland University who have been supportive during my employment there (Assoc. Prof. C. Rickard, Dr. L. J. Baker, Assoc. Prof. P. Boyd, Assoc. Prof. G. Clark, Dr. M. Glenny, Dr. M. Hodgson, Dr. S. Woodgate, Dr. S. Horner and Dr. A. Clark). My good friends (Todd Morris, Andy Hollis, Craig Haskell, Dr. Scott McIndoe, Angela McIndoe, Daryn Glasgow, Erin Gamble and Michael Wilkinson) and brothers (Ross, Tony and Ken) and sister (Lyn), who have always supported me, even if they couldn't understand half the gibberish I was spouting. My partner, Chaylah Skinner, has been a wonder during my research and deserves some credit for the final work. Lastly, and perhaps most importantly, the following people deserve some credit for this work, without them it wouldn't have started, Ron and Nancy Oliver.

*Dedicated to my parents,
Ron and Nancy Oliver*

Table of Contents

Abstract	II
Acknowledgments	V
Table of Contents	VII
List of Figures	X
List of Schemes	XII
List of Equations	XIII
List of Tables	XIII
List of Abbreviations	XVI
Chapter One. Introduction to Four-membered Metallacyclic Syntheses	1
1.1 Thesis Overview	1
1.2 Small-Ring Metallacyclic Syntheses	3
1.2.1 Insertion into C-C bonds	3
1.2.2 Dilithio / di-Grignard compounds (1,3-dianion formation)	4
1.2.2.1 Silver(I) oxide mediated syntheses (1,3-dianion synthon reactions)	5
1.2.3 Reactions of alkenes, alkynes, polyalkenes and polyalkynes with metal carbenes.....	7
1.2.4 Cyclometallation	10
1.2.4.1 Oxidative addition.....	10
1.3 Four-membered metallacyclic complexes	11
1.3.1 Metallacyclobutane and η^3 -propargyl / allenyl complexes	12
1.3.2 Metallacyclobutan-3-ones, trimethylenemethane and azadimethylenemethane complexes	14
1.3.2.1 Metallacyclobutan-3-one (oxodimethylenemethane) complexes	14
1.3.2.2 Trimethylenemethane metal complexes	16
1.3.2.3 Azadimethylenemethane complexes	18
1.3.3 Metal-nitrogen and metal-oxygen metallacycles	20
1.3.3.1 Ureylene complexes	20
1.3.3.2 Metallacyclocarbamate complexes.....	21
1.3.3.3 Metallalactone complexes	22
1.3.3.4 Metallalactam complexes	24
1.4 Summary	25
Chapter Two. Metallalactam complexes of palladium(II) and platinum(II) .	27
2.1 Introduction	27
2.2 Experimental	29
2.2.1 Synthesis of [Pt{N(Ph)C(O)CHC(O)Ph}(COD)] (2.11).....	30
2.2.2 Synthesis of [Pt{N(Ph)C(O)CHC(O)Ph}(PPh ₃) ₂] (2.12) from (2.11) by ligand displacement	31
2.2.3 Preparation of [Pt{N(Ph)C(O)CHC(O)Ph}(PPh ₃) ₂] (2.12) from cis-[PtCl ₂ (PPh ₃) ₂]	31
2.2.4 Preparation of [Pt{N(Ph)C(O)CHC(O)Ph}(dppe)] (2.13) by ligand displacement from (2.11)	32
.....	32

2.2.5 Preparation of [Pd{N(Ph)C(O)CHC(O)Ph}(bipy)] (2.14)	32
2.2.6 Preparation of [Pd{N(Ph)C(O)CHC(O)Ph}(dppe)] (2.15) from [PdCl ₂ (dppe)]	33
2.2.7 Preparation of cis-[Pt{N(H)C(O)CHC(O)CH ₃ }(PPh ₃) ₂] (2.16) from cis-[PtCl ₂ (PPh ₃) ₂]	34
2.2.8 Preparation of [Pd{N(H)C(O)CHC(O)CH ₃ }(bipy)] (2.17) from [PdCl ₂ (bipy)]	35
2.2.9 Preparation of [Pd{N(H)C(O)CHC(O)CH ₃ }(dppe)] (2.18) from [PdCl ₂ (dppe)]	35
2.2.10 X-ray diffraction study of [Pd{N(Ph)C(O)CHC(O)Ph}(bipy)].CH ₂ Cl ₂ (2.14)	36
2.3 Results and Discussion	38
2.3.1 X-ray Crystallography of Metallalactam Complexes.....	40
2.3.2 Nuclear Magnetic Resonance Spectroscopy of metallalactam complexes.....	44
2.3.3 Electrospray Mass Spectrometry of metallalactam complexes	48
2.3.3.1 Overview of Electrospray Mass Spectrometry.....	48
2.3.3.2 ES/MS studies of 2-benzoylacetanilide metallalactam complexes	49
2.3.3.3 ES/MS of acetoacetamide complexes	53
2.4 Conclusion	53
Chapter Three. Isolation of a platinum amide intermediate in silver(I) oxide mediated syntheses of platinalactam complexes.....	55
3.1 Introduction	55
3.2 Experimental.....	57
3.2.1 Synthesis of cis-[Pt{N(C(O)CH ₂ CN)(CO ₂ Et)}Cl(PPh ₃) ₂] (3.4)	58
3.2.2 Synthesis of cis-[Pt{N(C(O)CH ₂ CN)(CO ₂ Et)}Cl(PPh ₃) ₂] (3.4) from cis-[PtCl ₂ (PPh ₃) ₂] mediated by cuprous oxide	58
3.2.3 Synthesis of cis-[Pt{N(C(O)CH ₂ CN)(CO ₂ Et)}Cl(PPh ₃) ₂] (3.4) from cis-[PtCl ₂ (PPh ₃) ₂] mediated by mercuric oxide.....	59
3.2.4 In situ displacement of chloride from cis-[Pt{N(C(O)CH ₂ CN)(CO ₂ Et)}Cl(PPh ₃) ₂] (3.4) by pyridine.....	59
3.2.5 Lactam formation by prolonged reaction of cis-[Pt{N(C(O)CH ₂ CN)(CO ₂ Et)}Cl(PPh ₃) ₂] (3.4) with silver(I) oxide.....	60
3.2.6 Lactam formation by reaction of cis-[Pt{N(C(O)CH ₂ CN)(CO ₂ Et)}Cl(PPh ₃) ₂] (3.4) with sodium hydride	60
3.2.7 Reaction of cis-[Pt{N(C(O)CH ₂ CN)(CO ₂ Et)}Cl(PPh ₃) ₂] with NaBPh ₄	60
3.2.8 Short duration reaction of 2-benzoylacetanilide with cis-[PtCl ₂ (PPh ₃) ₂].....	61
3.2.9 Crystal Structure of cis-[Pt{N(C(O)CH ₂ CN)(CO ₂ Et)}Cl(PPh ₃) ₂].0.5CH ₂ Cl ₂ (3.4).....	61
3.3 Results and Discussion	63
3.3.1 Intermediate synthesis reactions	63
3.3.2 X-ray crystallography of cis-[Pt{N(C(O)CH ₂ CN)(CO ₂ Et)}Cl(PPh ₃) ₂].0.5CH ₂ Cl ₂ (3.4).....	67
3.3.3 NMR Spectroscopy of the cis-chloro amidate complex 3.4.....	70
3.3.4 ES/MS study of cis-[Pt{N(C(O)CH ₂ CN)(CO ₂ Et)}Cl(PPh ₃) ₂] (3.4)	73
3.4 Conclusions	77
Chapter Four. Organogold metallalactam complexes and a novel dimeric metallacycle	78
4.1 Introduction	78

4.2 Experimental	81
4.2.1 Synthesis of $[\{C_6H_3(CH_2NMe_2)-2-(OMe)-5\}Au\{N(CO_2Et)C(O)CHCN\}]$ (4.8)	82
4.2.1.1 Crystallisation of the dimeric complex $[\{C_6H_3(CH_2NMe_2)-2-(OMe)-5\}Au\{N(CO_2Et)C(O)CHCN\}]_2 \cdot 2CDCl_3$ (4.15)	83
4.2.2 Preparation of $[\{C_6H_3(CH_2NMe_2)-2-(OMe)-5\}Au\{N(Ph)C(O)CHC(O)Ph\}]$ (4.9).....	83
4.2.3 Preparation of $[\{C_6H_3(CH_2NMe_2)-2-(OMe)-5\}Au\{N(Ph)C(O)CHC(O)CH_3\}]$ (4.10).....	84
4.2.4 Preparation of $[\{C_6H_4(CH_2NMe_2)-2\}Au\{N(CO_2Et)C(O)CHCN\}]$ (4.11).....	85
4.2.5 Preparation of $[\{C_6H_4(CH_2NMe_2)-2\}Au\{N(Ph)C(O)CHC(O)Ph\}]$ (4.12).....	86
4.2.6 Preparation of $[\{C_6H_4(CH_2NMe_2)-2\}Au\{N(Ph)C(O)CHC(O)CH_3\}]$ (4.13)	86
4.2.7 Synthesis of $[\{C_6H_3(CH_2NMe_2)-2-(OMe)-5\}Au\{N(CONH_2)C(O)CHCN\}]$ (4.14).....	87
4.2.8 X-ray Crystallography	88
4.3 Results and Discussion	91
4.3.1 Synthesis of Organogold Metallalactam Complexes	91
4.3.2 The crystal structure of $[\{C_6H_4(CH_2NMe_2)-2\}Au\{N(Ph)C(O)CHC(O)CH_3\}]$ (4.13).....	93
4.3.3 X-ray crystal structure of $[\{C_6H_3(CH_2NMe_2)-2-(OMe)-5\}Au\{N(CO_2Et)C(O)CHCN\}]_2 \cdot 2CDCl_3$ (4.15).....	97
4.3.4 Electrospray Mass Spectrometry of Organogold Metallalactam Complexes.....	101
4.3.5 NMR Spectroscopy of Organogold Metallalactams	102
4.4 Conclusions	105
Chapter Five. Silver(I) oxide mediated reactions with carboxylic acids..	106
5.1 Introduction	106
5.2 Experimental	107
5.2.1 Synthesis of $cis-[Pt(CH_2CN)_2(PPh_3)_2]$ (5.7).....	108
5.2.2 Synthesis of $cis-[Pt(O_2CCH_2OPh)_2(COD)]$ (5.8).....	108
5.2.3 Preparation of $cis-[Pt(O_2CCH_2OPh)_2(PPh_3)_2]$ by ligand displacement (5.9)	108
5.2.4 X-ray Crystallographic studies of $cis-[Pt(CH_2CN)_2(PPh_3)_2]$ (5.7) and $cis-[Pt(O_2CCH_2OPh)_2(PPh_3)_2]$ (5.9)	109
5.3 Results and Discussion	112
5.3.1 Reaction of cyanoacetic acid with $cis-[PtCl_2(PPh_3)_2]$	112
5.3.2 X-ray crystal structure of $cis-[Pt(CH_2CN)_2(PPh_3)_2] \cdot 0.6(CH_2Cl_2)$ (5.7).....	114
5.3.3 Reactions of phenoxyacetic acid with platinum(II) dihalide complexes.....	117
5.3.4 X-ray crystal structure of $cis-[Pt(O_2CCH_2OPh)_2(PPh_3)_2] \cdot CH_2Cl_2$ (5.9).....	118
5.3.5 NMR spectroscopy	120
5.4 Conclusion	121
Chapter Six. Triethylamine mediated syntheses of four-membered metallalactam complexes	122
6.1 Introduction	122
6.2 Experimental	123
6.2.1 Synthesis of $[Pt\{N(C(O)NH_2)C(O)CHCN\}(PPh_3)_2]$ (6.5).....	124
6.2.2 Synthesis of $[Pt\{N(C(O)NH_2)C(O)CHCN\}(COD)]$ (6.6)	125

6.2.2.1 Ligand displacement of COD from [Pt{N(C(O)NH ₂)C(O)CHCN}(COD)] (6.6) by PPh ₃	125
6.2.3 Synthesis of [Pt{N(C(O)NH ₂)C(O)CHCN}(dppe)] (6.7)	126
6.2.4 Synthesis of [Pd{N(C(O)NH ₂)C(O)CHCN}(dppe)] (6.8)	126
6.2.5 Reaction of N-cyanoacetylurethane with cis-[PtCl ₂ (PPh ₃) ₂] in the presence of triethylamine	127
6.2.6 Reaction of cis-[PtCl ₂ (PPh ₃) ₂] with 2-benzoylacetanilide in the presence of triethylamine	127
6.2.7 Reaction of cis-[PtCl ₂ (PPh ₃) ₂] with acetoacetanilide, in the presence of triethylamine	128
6.2.8 X-ray crystallography of [Pt{N(C(O)NH ₂)C(O)CHCN}(PPh ₃) ₂] (6.5)	128
6.3 Results and discussion	131
6.3.1 Synthesis of metallalactam complexes mediated by triethylamine	131
6.3.2 X-ray crystal structure analysis of [Pt{N(C(O)NH ₂)C(O)CHCN}(PPh ₃) ₂].CH ₂ Cl ₂ .½[(C ₂ H ₅) ₂ O] (6.5)	132
6.3.3 NMR spectroscopy	137
6.3.4 Electrospray mass spectrometry	138
6.4 Conclusion	140
Chapter Seven. Selected X-ray crystallographic studies	141
7.1 Overview	141
7.2 Ureylene complex	141
7.3 Synthesis and structural data for [Ir{N(Me)C(O)NAC}(Cp*)(PPh ₃)] (7.4)	143
7.4 Structural analysis of the iridaureylene complex [Ir{N(Me)C(O)NAC}(Cp*)(PPh ₃)] (7.4)	145
7.5 Introduction to metal-thiosalicylate complexes	149
7.6 Synthesis of thiosalicylato complexes	151
7.7 Discussion of rhodium and ruthenium thiosalicylato complexes	154
7.7.1 Rhodium thiosalicylato complex	154
7.7.2 Ruthenium thiosalicylato complex	156
7.8 Lactam coordination complexes	159
7.9 Synthesis of cis-[Pt{NCH ₂ CH ₂ CO} ₂ (PPh ₃) ₂].UO ₂ (NO ₃) ₂ (7.15)	161
7.10 Structural analysis of [Pt{NCH ₂ CH ₂ C(O)} ₂ (PPh ₃) ₂].UO ₂ (NO ₃) ₂ (7.15)	163
Appendix 1 List of Publications	A-1
1.1 Chapter Two	A-1
1.2 Chapter Three	A-1
1.3 Chapter Five	A-1
1.4 Chapter Seven	A-1
Appendix 2 Crystallographic data tables	A-2

List of Figures

Figure 1.1 Chatt-Dewar-Duncanson π -backbonding model for metal-alkene complexes and the Walsh model for transition metal-cyclopropane complex bonding	13
Figure 1.2 Metallacyclobutan-3-one bonding.....	15
Figure 1.3 Canonical forms of trimethylenemethane complexes.....	17
Figure 1.4 N, N', N''-triphenyl guanidine platinum(II) imido-ureylene complex	21
Figure 2.1 Thermal ellipsoid plot of $[Pd\{N(Ph)C(O)CH(O)Ph\}(bipy)]$ (2.14) showing atom labeling. ...	41
Figure 2.2 View of 2.14 showing the slight puckering of the metallalactam ring and the torsion of the bipy ligand.....	43
Figure 2.3 Representative ^{31}P NMR spectrum of $[Pt\{N(Ph)C(O)CHC(O)Ph\}(PPh_3)_2]$ (2.12).....	46
Figure 2.4 Representative ES/MS spectrum of $[Pd\{N(Ph)C(O)CHC(O)Ph\}(bipy)]$ (M) (2.14)	50
Figure 3.1 Atom labeling scheme for $cis-[Pt\{N(C(O)CH_2CN)(CO_2Et)\}Cl(PPh_3)_2]$ (3.4).....	68
Figure 3.2 View of N-cyanoacetylurethane ligand of 3.4 showing distortion of ligand.....	70
Figure 3.1 Ethyl resonance region of the 1H NMR spectrum of $cis-[Pt\{N(C(O)CH_2CN)(CO_2Et)\}Cl(PPh_3)_2]$ (3.4)	71
Figure 3.2 ^{31}P NMR spectrum of $cis-[Pt\{N(C(O)CH_2CN)(CO_2Et)\}Cl(PPh_3)_2]$ (3.4)	72
Figure 3.1 ES/MS spectrum of $[Pt\{N(C(O)CH_2CN)(CO_2Et)\}Cl(PPh_3)_2]$ (M) at cone voltage = 20 V.....	74
Figure 3.2 Proposed structures for $[Pt\{N(C(O)CH_2CN)(CO_2Et)\}(PPh_3)_2]^+$	75
Figure 3.3 ES/MS spectrum of $[Pt\{N(C(O)CH_2CN)(CO_2Et)\}Cl(PPh_3)_2]$ (M) with added pyridine at cone voltage = 20 V	76
Figure 4.1 Examples of gold(III) metallacycles	79
Figure 4.2 Metallacyclic complexes of platinum, palladium and gold.....	80
Figure 4.3 Four-membered and eight-membered gold(III) metallacycles	81
Figure 4.4 X-ray crystal structure and atom labeling scheme of $[(C_6H_4(CH_2NMe_2)-2)Au\{N(Ph)C(O)CHC(O)CH_3\}]$ (4.13).....	94
Figure 4.5 View of gold coordination sphere of 4.13 showing ring puckering.....	95
Figure 4.6 X-ray crystal structure and atom-labeling scheme of $[(C_6H_3(CH_2NMe_2)-2-(OMe)-5)Au\{N(CO_2Et)C(O)CHCN\}]_2 \cdot 2CDCl_3$ (4.15).	97
Figure 4.7 View of 4.15 showing the chair-like conformation of the eight-membered metallacycle and substituents	99
Figure 4.8 Stereoscopic view of 4.15, showing the structure of the molecule and the interactions to the chloroforms of crystallisation.....	100
Figure 4.9 ES/MS spectrum of $[(C_6H_4(CH_2NMe_2)-2)Au\{N(Ph)C(O)CHC(O)CH_3\}]$ (4.13) at cone voltage = 20 V	102
Figure 4.10 Representative 1H NMR spectrum of the auralactam 4.13	103
Figure 4.11 Representative $^{13}C\{-^1H\}$ NMR spectrum of the auralactam 4.13	104
Figure 5.1 Thermal ellipsoid plot and labelling scheme for $cis-[Pt(CH_2CN)_2(PPh_3)_2]$ (5.7).....	115
Figure 5.2 Thermal ellipsoid plot showing the 'syn' geometry of the cyanomethyl ligands of $cis-[Pt(CH_2CN)_2(PPh_3)_2]$	116
Figure 5.3 Thermal ellipsoid plot and atom labelling scheme for $cis-[Pt(O_2CCH_2OPh)_2(PPh_3)_2]$ (5.9). 118	
Figure 5.4 Plan view of 5.9 depicting the anti-arrangement of the carboxylate ligands	119
Figure 6.1 Crystal structure of $cis-[Pt\{N(C(O)NH_2)C(O)CHCN\}(PPh_3)_2]$ (6.5)	133
Figure 6.2 Diagrams depicting the H-bonding scheme in $Pt\{N(C(O)NH_2)C(O)CHCN\}(PPh_3)_2]$ (6.5). .	135

Figure 6.3 Fragmentation patterns of $[Pt\{N(C(O)NH_2)C(O)CHCN\}(dppe)]$ at 20, 50 and 70 V	139
Figure 7.1 Molecular structure of $[Ir\{N(Me)C(O)NAC\}(Cp^*)(PPh_3)]$ (7.4).....	146
Figure 7.2 Stereoscopic view of $[Ir\{N(Me)C(O)NAC\}(Cp^*)(PPh_3)]$ (7.4) showing steric interactions. ..	148
Figure 7.3 Thermal ellipsoid plot of $[Rh\{OC(O)C_6H_4-2-S\}(Cp^*)_2$ (7.8) showing molecular geometry and labelling scheme.	155
Figure 7.4 Thermal ellipsoid plot of $[Ru\{OC(O)C_6H_4-2-S\}(p-cymene)]_2$ (7.9) showing the atom labelling scheme.	157
Figure 7.5 Thermal ellipsoid plot of <i>cis</i> - $[Pt\{NCH_2CH_2CO\}_2(PPh_3)_2].UO_2(NO_3)_2$ (7.15) showing atom labelling scheme.	164
Figure 7.6 Diagram showing bonding geometry about the β -propiolactam rings of 7.15.....	168

List of Schemes

Scheme 1.1 Alkene coupling with a metal carbene (Olefin Metathesis).....	8
Scheme 1.2 Azadimethylenemethane synthetic utility.....	19
Scheme 2.1 Proposed four-membered metallalactam synthesis	40
Scheme 2.2 Canonical forms of η^3 oxadimethylenemethane complexes.....	42
Scheme 2.3 Proposed fragmentation of $[Pt\{N(Ph)C(O)CHC(O)Ph\}(COD)]$ (2.11) at 90 V.....	51
Scheme 3.1 General metallalactam synthesis.....	56
Scheme 3.2 Formation of the intermediate 3.4 in the metallacyclisation of <i>N</i> -cyanoacetylurethane.....	64
Scheme 3.3 Proposed synthesis of a metallalactam through reaction with a 1,3-dianion	65
Scheme 4.1 NMR labeling scheme.....	82
Scheme 4.2 Auralactam synthesis.....	91
Scheme 4.3 Proposed dimerisation of 4.8 to give 4.15.....	92
Scheme 5.1 Synthetic pathways for the formation of <i>cis</i> - $[Pt(CH_2CN)_2(PPh_3)_2]$	113
Scheme 5.2 Decarboxylation of cyanoacetic acid.....	113
Scheme 6.1 Metallalactam or ureylene synthetic routes	132
Scheme 6.2 Proposed fragmentation pathway for $[Pt\{N(C(O)NH_2)C(O)CHCN\}(dppe)+H]^+$ (6.7).....	138

List of Equations

Equation 1.1 Tipper's metallacyclobutane synthesis.....	4
Equation 1.2 Di-Grignard preparation of a metallacyclobutane complex.....	4
Equation 1.3 1,3-dianion and oxidative addition formations of platinacyclobutan-3-ones.....	5
Equation 1.4 General silver(I) oxide synthesis of a metallalactam.....	6
Equation 1.5 Cycloaddition of an alkyne to a metal-carbene.....	8
Equation 1.6 Butadiene reaction with $[Pt(COD)_2]$	9
Equation 1.7 Thermolysis of $cis-[Pt\{CH_2CMe_3\}_2(PEt_3)_2]$	10
Equation 1.8 Oxidative addition of 1,3-dichloroacetone to $[Pt\{trans-stilbene\}(PPh_3)_2]$	11
Equation 1.9 Bergman's synthesis of a η^4 -oxodimethylenemethane complex.....	16
Equation 1.10 η^3 -Trimethylenemethane complex synthesis.....	17
Equation 1.11 Azadimethylenemethane synthesis.....	18
Equation 1.12 Azadimethylenemethane synthesis by Wojcicki et al.....	19
Equation 1.13 Metallacyclocarbamate synthesis.....	22
Equation 1.14 Palladalactone synthesis.....	23
Equation 1.15 Synthesis of a mixed-metal metallalactone.....	23
Equation 1.16 Platinalactone synthesis mediated by silver(I) oxide.....	24
Equation 1.17 Di-rhodium metallalactam synthesis.....	25
Equation 2.1 Equations for R-factors and Goodness-of-Fit.....	38

List of Tables

Table 2.1 X-ray Crystallographic data for $[Pd\{N(Ph)C(O)CHC(O)Ph\}(bipy)].CH_2Cl_2$ (2.14).....	36
Table 2.2 Selected bond lengths (Å) and bond angles (°) for $[Pd\{N(Ph)C(O)CHC(O)Ph\}(bipy)].CH_2Cl_2$ (2.14).....	44
Table 2.3 Fragmentation pattern of $[Pt\{N(Ph)C(O)CHC(O)Ph\}(COD)]$ at cone voltage = 90 V.....	51
Table 2.4 Fragmentation of $[Pt\{N(Ph)C(O)CHC(O)Ph\}(dppe)]$ (2.13) at cone voltage = 90V.....	52
Table 2.5 Fragmentation pattern of $[Pd\{N(H)C(O)CHC(O)CH_3\}(bipy)]$ (2.17) at cone voltage = 70 V..	53
Table 3.1 Crystal data and structure refinement for $cis-[Pt\{N(C(O)CH_2CN)(CO_2Et)\}Cl(PPh_3)_2].0.5CH_2Cl_2$ (3.4).....	62
Table 3.2 Selected bond lengths (Å) and bond angles (°) for $cis-[Pt\{N(C(O)CH_2CN)(CO_2Et)\}Cl(PPh_3)_2]$ (3.4).....	68
Table 3.3 Electrospray mass spectral data for $cis-[Pt\{N(C(O)CH_2CN)(CO_2Et)\}Cl(PPh_3)_2]$ (M) (3.4)	74
Table 3.4 Electrospray mass spectral data for $cis-[Pt\{N(C(O)CH_2CN)(CO_2Et)\}Cl(PPh_3)_2]$ (3.4) (M) with added pyridine.....	76
Table 4.1 Data collection and structure refinement details for $[C_6H_4(CH_2NMe_2)-2]Au\{N(Ph)C(O)CHC(O)CH_3\}$ (4.13) and $[C_6H_3(CH_2NMe_2)-2-(OMe)-5]Au\{N(CO_2Et)C(O)CHCN\}_2.2CDCl_3$ (4.15).....	89

Table 4.2 Selected bond lengths (Å) and angles (°) for of $[(C_6H_4(CH_2NMe_2)-2)Au\{N(Ph)C(O)CHC(O)CH_3\}]$ (4.13).....	95
Table 4.3 Selected bond lengths (Å) and angles (°) for of $[(C_6H_3(CH_2NMe_2)-2-(OMe)-5)Au\{N(CO_2Et)C(O)CHCN\}]_2 \cdot 2CDCl_3$ (4.15).	98
Table 4.4 Table of hydrogen-bond contacts.....	101
Table 5.1 Cell parameter, solution and final cycle refinement data for <i>cis</i> - $[Pt(CH_2CN)_2(PPh_3)_2]$ (5.7) and <i>cis</i> - $[Pt(O_2CCH_2OPh)_2(PPh_3)_2]$ (5.9).....	110
Table 5.2 Selected bond lengths (Å) and angles (°) for <i>cis</i> - $[Pt(CH_2CN)_2(PPh_3)_2]$ (5.7).....	116
Table 5.3 Selected bond lengths (Å) and angles (°) for <i>cis</i> - $[Pt(O_2CCH_2OPh)_2(PPh_3)_2]$ (5.9).....	120
Table 6.1 Crystal collection and refinement data for $[Pt\{N(C(O)NH_2)C(O)CHCN\}(PPh_3)_2] \cdot CH_2Cl_2 \cdot \frac{1}{2}Et_2O$ (6.5).....	129
Table 6.2 Selected bond lengths (Å) and bond angles (°) for <i>cis</i> - $[Pt\{N(C(O)NH_2)C(O)CHCN\}(PPh_3)_2]$ (6.5).....	134
Table 6.3 Hydrogen bonds and angles for $[Pt\{N(C(O)NH_2)C(O)CHCN\}(PPh_3)_2] \cdot CH_2Cl_2 \cdot 0.5Et_2O$ (6.5).....	136
Table 7.1 Crystal data and structure refinement for $[Ir\{N(Me)C(O)NAC\}(Cp^*)(PPh_3)] \cdot CHCl_3$ (7.4). ...	144
Table 7.2 Selected bond lengths (Å) and angles (°) for $[Ir\{N(Me)C(O)NAC\}(Cp^*)(PPh_3)]$ (7.4).	147
Table 7.3 Data collection and cell parameters for $[Rh\{OC(O)C_6H_4-2-S\}(Cp^*)]_2$ (7.8) and $[Ru\{OC(O)C_6H_4-2-S\}(p-cymene)]_2$ (7.9).....	152
Table 7.4 Selected bond lengths (Å) and bond angles (°) for $[Rh\{OC(O)C_6H_4-2-S\}(Cp^*)]_2$ (7.8).	156
Table 7.5 Selected bond lengths (Å) and bond angles (°) for $[Ru\{OC(O)C_6H_4-2-S\}(p-cymene)]_2$ (7.9)..	158
Table 7.6 Crystal data and structure refinement for <i>cis</i> - $[Pt\{NCH_2CH_2CO\}_2(PPh_3)_2] \cdot UO_2(NO_3)_2$ (7.15)	162
Table 7.7 Selected bond lengths (Å) and bond angles (°) for $[Pt\{NCH_2CH_2CO\}_2(PPh_3)_2] \cdot UO_2(NO_3)_2$ (7.15).....	165
Table A-1 Atomic coordinates and equivalent isotropic displacement parameters (Å ²) for $[Pd\{N(Ph)C(O)CHC(O)Ph\}(bipy)] \cdot CH_2Cl_2$ (2.14).....	A-2
Table A-2 Bond lengths (Å) for $[Pd\{N(Ph)C(O)CHC(O)Ph\}(bipy)] \cdot CH_2Cl_2$ (2.14).....	A-2
Table A-3 Bond angles (°) for $[Pd\{N(Ph)C(O)CHC(O)Ph\}(bipy)] \cdot CH_2Cl_2$ (2.14).....	A-3
Table A-4 Anisotropic displacement parameters (Å ²) for $[Pd\{N(Ph)C(O)CHC(O)Ph\}(bipy)] \cdot CH_2Cl_2$ (2.14).....	A-4
Table A-5 Hydrogen coordinates and isotropic displacement parameters (Å ²) for $[Pd\{N(Ph)C(O)CHC(O)Ph\}(bipy)] \cdot CH_2Cl_2$ (2.14).....	A-4
Table A-6 Atomic coordinates and equivalent isotropic displacement parameters for <i>cis</i> - $[Pt\{N(C(O)CH_2CN)(CO_2Et)\}Cl(PPh_3)_2] \cdot 0.5CH_2Cl_2$ (3.4).....	A-6
Table A-7 Bond lengths (Å) for <i>cis</i> - $[Pt\{N(C(O)CH_2CN)(CO_2Et)\}Cl(PPh_3)_2] \cdot 0.5CH_2Cl_2$ (3.4).....	A-7
Table A-8 Bond angles (°) for for <i>cis</i> - $[Pt\{N(C(O)CH_2CN)(CO_2Et)\}Cl(PPh_3)_2] \cdot 0.5CH_2Cl_2$ (3.4).....	A-7
Table A-9 Anisotropic displacement parameters (Å ²) for for <i>cis</i> - $[Pt\{N(C(O)CH_2CN)(CO_2Et)\}Cl(PPh_3)_2] \cdot 0.5CH_2Cl_2$ (3.4).....	A-8
Table A-10 Hydrogen coordinates and isotropic displacement parameters (Å ²) for <i>cis</i> - $[Pt\{N(C(O)CH_2CN)(CO_2Et)\}Cl(PPh_3)_2] \cdot 0.5CH_2Cl_2$ (3.4).....	A-10

Table A-11 Atomic coordinates and equivalent isotropic displacement parameters for $[C_6H_4(CH_2NMe_2)-2]Au\{N(Ph)C(O)CHC(O)CH_3\}$ (4.13).....	A-11
Table A-12 Bond lengths (Å) for $[C_6H_4(CH_2NMe_2)-2]Au\{N(Ph)C(O)CHC(O)CH_3\}$ (4.13)	A-11
Table A-13 Bond Angles (°) for $[C_6H_4(CH_2NMe_2)-2]Au\{N(Ph)C(O)CHC(O)CH_3\}$ (4.13).....	A-12
Table A-14 Anisotropic displacement parameters (Å ²) for $[C_6H_4(CH_2NMe_2)-2]Au\{N(Ph)C(O)CHC(O)CH_3\}$ (4.13).....	A-12
Table A-15 Hydrogen coordinates and isotropic displacement parameters (Å ²) for $[C_6H_4(CH_2NMe_2)-2]Au\{N(Ph)C(O)CHC(O)CH_3\}$ (4.13).....	A-13
Table A-16 Atomic coordinates and equivalent isotropic displacement parameters (Å ²) for $\{[C_6H_3(CH_2NMe_2)-2-(OMe)-5]Au\{N(CO_2Et)C(O)CHCN\}\}_2 \cdot 2CDCl_3$ (4.15)	A-14
Table A-17 Bond lengths [Å] for $\{[C_6H_3(CH_2NMe_2)-2-(OMe)-5]Au\{N(CO_2Et)C(O)CHCN\}\}_2 \cdot 2CDCl_3$ (4.15).....	A-14
Table A-18 Bond angles (°) for $\{[C_6H_3(CH_2NMe_2)-2-(OMe)-5]Au\{N(CO_2Et)C(O)CHCN\}\}_2 \cdot 2CDCl_3$ (4.15).....	A-15
Table A-19 Anisotropic displacement parameters (Å ²) for $\{[C_6H_3(CH_2NMe_2)-2-(OMe)-5]Au\{N(CO_2Et)C(O)CHCN\}\}_2 \cdot 2CDCl_3$ (4.15)	A-15
Table A-20 Hydrogen coordinates and isotropic displacement parameters (Å ²) for $\{[C_6H_3(CH_2NMe_2)-2-(OMe)-5]Au\{N(CO_2Et)C(O)CHCN\}\}_2 \cdot 2CDCl_3$ (4.15).....	A-16
Table A-21 Atomic coordinates and equivalent isotropic displacement parameters (Å ²) for <i>cis</i> - $[Pt(CH_2CN)_2(PPh_3)_2] \cdot 0.6CH_2Cl_2$ (5.7).....	A-17
Table A-22 Bond lengths (Å) for <i>cis</i> - $[Pt(CH_2CN)_2(PPh_3)_2] \cdot 0.6CH_2Cl_2$ (5.7).....	A-18
Table A-23 Bond angles (°) for <i>cis</i> - $[Pt(CH_2CN)_2(PPh_3)_2] \cdot 0.6CH_2Cl_2$ (5.7).....	A-18
Table A-24 Anisotropic displacement parameters (Å ²) for <i>cis</i> - $[Pt(CH_2CN)_2(PPh_3)_2] \cdot 0.6CH_2Cl_2$ (5.7). A-19	A-19
Table A-25 Hydrogen coordinates and isotropic displacement parameters (Å ²) for <i>cis</i> - $[Pt(CH_2CN)_2(PPh_3)_2] \cdot 0.6CH_2Cl_2$ (5.7).....	A-20
Table A-26 Atomic coordinates and equivalent isotropic displacement parameters (Å ²) for <i>cis</i> - $[Pt(O_2CCH_2OPh)_2(PPh_3)_2] \cdot CH_2Cl_2$ (5.9)	A-22
Table A-27 Bond lengths (Å) for <i>cis</i> - $[Pt(O_2CCH_2OPh)_2(PPh_3)_2] \cdot CH_2Cl_2$ (5.9).....	A-23
Table A-28 Bond angles (°) for <i>cis</i> - $[Pt(O_2CCH_2OPh)_2(PPh_3)_2] \cdot CH_2Cl_2$ (5.9).....	A-24
Table A-29 Anisotropic displacement parameters (Å ²) for <i>cis</i> - $[Pt(O_2CCH_2OPh)_2(PPh_3)_2] \cdot CH_2Cl_2$ (5.9).....	A-25
Table A-30 Hydrogen coordinates and isotropic displacement parameters (Å ²) for <i>cis</i> - $[Pt(O_2CCH_2OPh)_2(PPh_3)_2] \cdot CH_2Cl_2$ (5.9)	A-26
Table A-31 Atomic coordinates and equivalent isotropic displacement parameters (Å ²) for $[Pt\{N(C(O)NH_2)C(O)CHCN\}(PPh_3)_2] \cdot CH_2Cl_2 \cdot 0.5Et_2O$ (6.5).....	A-28
Table A-32 Bond lengths (Å) for $[Pt\{N(C(O)NH_2)C(O)CHCN\}(PPh_3)_2] \cdot CH_2Cl_2 \cdot 0.5Et_2O$ (6.5).....	A-29
Table A-33 Bond angles (°) for $[Pt\{N(C(O)NH_2)C(O)CHCN\}(PPh_3)_2] \cdot CH_2Cl_2 \cdot 0.5Et_2O$ (6.5).....	A-30
Table A-34 Anisotropic displacement parameters (Å ²) for $[Pt\{N(C(O)NH_2)C(O)CHCN\}(PPh_3)_2] \cdot CH_2Cl_2 \cdot 0.5Et_2O$ (6.5).....	A-31
Table A-35 Hydrogen coordinates and isotropic displacement parameters (Å ²) for $[Pt\{N(C(O)NH_2)C(O)CHCN\}(PPh_3)_2] \cdot CH_2Cl_2 \cdot 0.5Et_2O$ (6.5).....	A-32

Table A-36 Atomic coordinates and equivalent isotropic displacement parameters (\AA^2) for $[\text{Ir}\{\text{N}(\text{Me})\text{C}(\text{O})\text{NAc}\}(\text{Cp}^*)(\text{PPh}_3)].\text{CHCl}_3$ (7.4)	A-34
Table A-37 Bond lengths (\AA) for $[\text{Ir}\{\text{N}(\text{Me})\text{C}(\text{O})\text{NAc}\}(\text{Cp}^*)(\text{PPh}_3)].\text{CHCl}_3$ (7.4)	A-35
Table A-38 Bond angles ($^\circ$) for $[\text{Ir}\{\text{N}(\text{Me})\text{C}(\text{O})\text{NAc}\}(\text{Cp}^*)(\text{PPh}_3)].\text{CHCl}_3$ (7.4)	A-35
Table A-39 Anisotropic displacement parameters (\AA^2) for $[\text{Ir}\{\text{N}(\text{Me})\text{C}(\text{O})\text{NAc}\}(\text{Cp}^*)(\text{PPh}_3)].\text{CHCl}_3$ (7.4)	A-36
Table A-40 Hydrogen coordinates and isotropic displacement parameters (\AA^2) for $[\text{Ir}\{\text{N}(\text{Me})\text{C}(\text{O})\text{NAc}\}(\text{Cp}^*)(\text{PPh}_3)].\text{CHCl}_3$ (7.4)	A-37
Table A-41 Atomic coordinates and equivalent isotropic displacement parameters (\AA^2) for $[\text{Rh}\{\text{OC}(\text{O})\text{C}_6\text{H}_4\text{-2-S}\}(\text{Cp}^*)]_2$ (7.8)	A-39
Table A-42 Bond lengths (\AA) for $[\text{Rh}\{\text{OC}(\text{O})\text{C}_6\text{H}_4\text{-2-S}\}(\text{Cp}^*)]_2$ (7.8)	A-39
Table A-43 Bond angles ($^\circ$) for $[\text{Rh}\{\text{OC}(\text{O})\text{C}_6\text{H}_4\text{-2-S}\}(\text{Cp}^*)]_2$ (7.8)	A-40
Table A-44 Anisotropic displacement parameters (\AA^2) for $[\text{Rh}\{\text{OC}(\text{O})\text{C}_6\text{H}_4\text{-2-S}\}(\text{Cp}^*)]_2$ (7.8)	A-41
Table A-45 Hydrogen coordinates and isotropic displacement parameters (\AA^2) for $[\text{Rh}\{\text{OC}(\text{O})\text{C}_6\text{H}_4\text{-2-S}\}(\text{Cp}^*)]_2$ (7.8)	A-41
Table A-46 Atomic coordinates and equivalent isotropic displacement parameters (\AA^2) for $[\text{Ru}\{\text{OC}(\text{O})\text{C}_6\text{H}_4\text{-2-S}\}(\text{p-cymene})]_2$ (7.9)	A-42
Table A-47 Bond lengths (\AA) for $[\text{Ru}\{\text{OC}(\text{O})\text{C}_6\text{H}_4\text{-2-S}\}(\text{p-cymene})]_2$ (7.9)	A-42
Table A-48 Bond angles ($^\circ$) for $[\text{Ru}\{\text{OC}(\text{O})\text{C}_6\text{H}_4\text{-2-S}\}(\text{p-cymene})]_2$ (7.9)	A-43
Table A-49 Anisotropic displacement parameters (\AA^2) for $[\text{Ru}\{\text{OC}(\text{O})\text{C}_6\text{H}_4\text{-2-S}\}(\text{p-cymene})]_2$ (7.9) ...	A-44
Table A-50 Hydrogen coordinates and isotropic displacement parameters (\AA^2) for $[\text{Ru}\{\text{OC}(\text{O})\text{C}_6\text{H}_4\text{-2-S}\}(\text{p-cymene})]_2$ (7.9)	A-44
Table A-51 Atomic coordinates and equivalent isotropic displacement parameters (\AA^2) for $[\text{Pt}\{\text{NCH}_2\text{CH}_2\text{CO}\}_2(\text{PPh}_3)_2].\text{UO}_2(\text{NO}_3)_2$ (7.15)	A-45
Table A-52 Bond lengths (\AA) for $[\text{Pt}\{\text{NCH}_2\text{CH}_2\text{CO}\}_2(\text{PPh}_3)_2].\text{UO}_2(\text{NO}_3)_2$ (7.15)	A-46
Table A-53 Bond angles ($^\circ$) for $[\text{Pt}\{\text{NCH}_2\text{CH}_2\text{CO}\}_2(\text{PPh}_3)_2].\text{UO}_2(\text{NO}_3)_2$ (7.15)	A-47
Table A-54 Anisotropic displacement parameters (\AA^2) for $[\text{Pt}\{\text{NCH}_2\text{CH}_2\text{CO}\}_2(\text{PPh}_3)_2].\text{UO}_2(\text{NO}_3)_2$ (7.15)	A-48
Table A-55 Hydrogen coordinates and isotropic displacement parameters (\AA^2) for $[\text{Pt}\{\text{NCH}_2\text{CH}_2\text{CO}\}_2(\text{PPh}_3)_2].\text{UO}_2(\text{NO}_3)_2$ (7.15)	A-50

List of Abbreviations

Ac	Acetyl
Ar	Aromatic
Bu	Butyl
Et	Ethyl
Me	Methyl
Ph	Phenyl

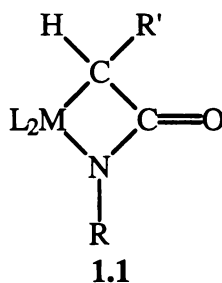
py	pyridine
bipy	2,2'-bipyridine
COD	1,5-cyclooctadiene
dppe	1,2-bis(diphenylphosphino)ethane
g	gram
mg	milligram
mmol	millimole
cm ³	cubic centimetre
h.	hour
mL	millilitre
IR	infrared
cm ⁻¹	wavenumber
v	stretching frequency
br.	broad
m.p.	melting point
°C	degrees Celcius
decomp.	decomposition
NMR	Nuclear Magnetic Resonance
MHz	megaHertz
Hz	Hertz
TMS	tetramethylsilane
ppm	parts per million
δ	chemical shift (in ppm)
-{ ¹ H}	proton decoupled
d	doublet
dd	doublet of doublets
dq	doublet of quartets
m	multiplet
q	quartet
s	singlet (NMR), strong (IR)
t	triplet
<i>J</i>	coupling constant (in Hz)
ES/MS	Electrospray Mass Spectrometry
V	voltage
Da	Dalton

m/z	mass to charge ratio (Da)
Å	Angstrom unit
°	degree
Å ³	cubic Ångstrom
K	Kelvin
g cm^{-3}	density (grams per cubic centimetre)
mm	millimetre
mm^{-1}	linear absorption coefficient (per millimetre)
e.Å^{-3}	electrons per cubic Ångstrom
THF	tetrahydrofuran
L	ligand

Chapter One. Introduction to Four-membered Metallacyclic Syntheses

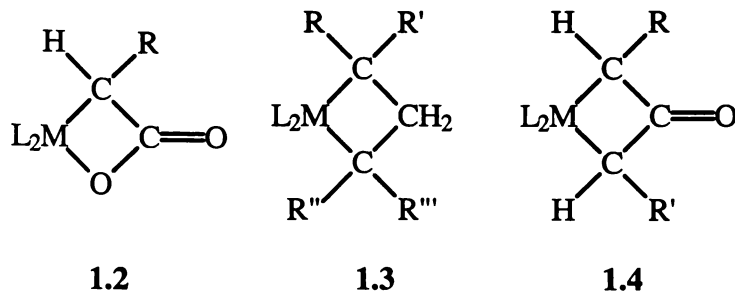
1.1 Thesis Overview

This thesis is primarily concerned with the synthesis and characterisation of a variety of metallacyclic, and metal-amide complexes. The complexes were those formed by the late transition metals, specifically the platinum group metals. Four-membered ring systems, in particular metallalactam complexes (**1.1**), were the primary focus of the research. They are predominantly the complexes that are formed when square-planar platinum group L_2MCl_2 complexes are reacted with amides in the presence of silver(I) oxide.¹



The term “metallalactam” is derived from the structure of the ring system. The base structure is a cyclic amide (lactam), and incorporates a metal heteroatom in the ring. This terminology is used throughout this thesis to describe such classes of compounds. Other derivations using this terminology are: metallalactone (**1.2**), metallacyclobutane (**1.3**) and metallacyclobutan-3-one (**1.4**). Usually the term is applied to a complex formed by an anionic ligand and a cationic metal centre rather than that of a chelating ligand and neutral metal centre, although this too is formally a metallacycle.

1 a) W. Henderson, B. K. Nicholson and A. G. Oliver, *J. Chem. Soc., Dalton Trans.*, (1994), 1831; b) W. Henderson, B. K. Nicholson and A. G. Oliver, *Polyhedron*, (1994), **13**, 3099; c) R. D. W. Kemmitt, S. Mason, M. R. Moore, J. Fawcett and D. R. Russell, *J. Chem. Soc., Chem. Comm.*, (1990), 1535; d) W. Henderson, R. D. W. Kemmitt, S. Mason, M. R. Moore, J. Fawcett and D. R. Russell, *J. Chem. Soc., Dalton Trans.*, (1992), 59; e) R. D. W. Kemmitt, S. Mason, M. R. Moore, J. Fawcett and D. R. Russell, *J. Chem. Soc., Dalton Trans.*, (1992), 851



Platinum group metals were primarily used for their stability. The platinum group metals also have some useful characteristics which aided the analysis of these complexes. For example, platinum-195 is a spin $\frac{1}{2}$ nucleus and is 33.8% abundant. When coupled with phosphorus-31 in $^{31}\text{P}\{-^1\text{H}\}$ NMR, $^1J(\text{Pt}, \text{P})$ satellites are observed. The coupling constant is dependent on the relative *trans*-influence strength of the atom *trans* to the phosphorus atom of the ligand.² This provides a useful technique to determine the outcome of a reaction. Both metals have characteristic isotope patterns, aiding in analysis by ES/MS. The stability of platinum group complexes is well known; platinum and palladium tend to form more stable complexes, though platinum tends to be slightly less reactive than palladium. Coupled with previously acquired data¹ and the characteristics mentioned above, were thus ideal candidates for the metallacyclic syntheses undertaken.

The primary reaction methodology used was heating at reflux a solution of a metal dihalide (L_2MCl_2) with an organic reagent in the presence of silver(I) oxide in dichloromethane. The use of this synthetic route has been established for a wide range of organic substrates.¹ The metal dihalides selected, were those with the halides in a *cis*- conformation, which is required for the metallacyclisation process to occur (except for $[\text{PdCl}_2(\text{PPh}_3)_2]$ which is a mixture of *cis* and *trans* isomers in solution). The organic reagent (generally an amide) had to meet one main requirement; the protons on both the amide nitrogen and the carbon *alpha* to the amide carbonyl had to be sufficiently acidic to allow deprotonation by the mildly basic silver(I) oxide. The formation of insoluble silver chloride is generally believed to be one of the principal driving forces behind these reactions.

2 T. G. Appleton and M. A. Bennett, *Inorg. Chem.*, (1978), 17, 738

1.2 Small-Ring Metallacyclic Syntheses

The following review is primarily an overview of the field of metallacyclic chemistry and will only deal briefly with an outline of the various techniques involved in the formation of metallacycles. It is not intended to be an in depth study of each of the techniques since they are outside of the scope of this thesis. Likewise, the discussion of the various structures that metallacycles can assume is also just an overview. The primary focus of this thesis is on the synthesis of four-membered metallacycles. However, larger metallacycles will be touched upon during this review. Five- and six-membered ring systems are perhaps the more common reaction product because of the reduced strain on the ring system. However, many four-membered metallacycles do appear in the literature.

There are four main synthetic routes towards the synthesis of a metallacyclic complex which have been extensively reviewed.^{3,4,5} The general synthetic techniques are:

- insertion of the metal centre into a C-C bond of an existing organic ring system
- formation of a dianionic organic moiety (usually by the formation of the dilithio or di-Grignard salt) and subsequent reaction with a metal dihalide
- the coupling product of a metal carbene with an alkene (olefin metathesis), alkyne, polyalkene or polyalkyne
- cyclometallation of a bound organic fragment *via* another substituent back to the metal centre

Several examples also exist where a metallacycle can be formed by oxidative addition of a ligand to a neutral metal centre with concurrent dehalogenation.

1.2.1 Insertion into C-C bonds

Insertion of a metal into a C-C bond is one of the earliest reported methods of synthesising a four-membered metallacycle. The product of the insertion reaction is formally a metallacyclobutane. Tipper⁶ found that platinum from hexachloroplatinic

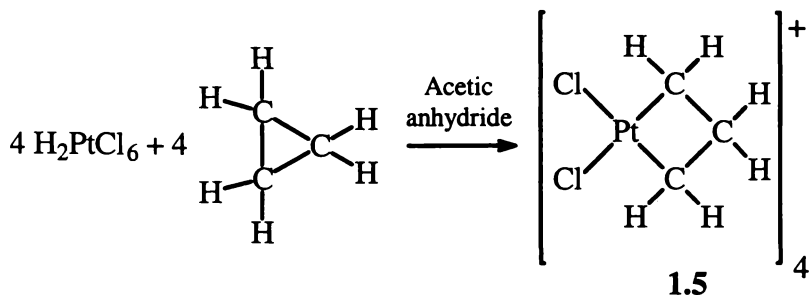
3 S. D. Chappell and D. J. Cole-Hamilton, *Polyhedron*, (1982), **11-12**, 739

4 *Principles and Applications of the Metal Carbon Bond*, Ed. A. Kelly, University Science, Mill Valley CA, (1987), Chapters 9 and 16

5 J. Cámpora, P. Palma and E. Carmoba, *Coord. Chem. Rev.*, (1999), **193**, 207

6 C. F. H. Tipper, *J. Chem. Soc.*, (1955), 2045

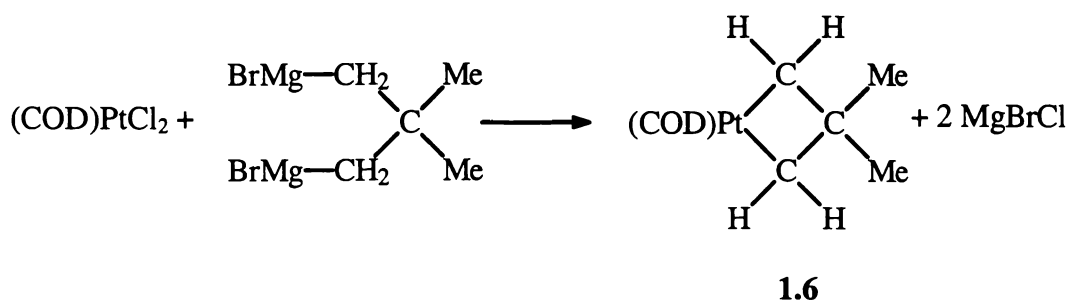
acid would insert into the C-C bond of cyclopropane (Equation 1.1) forming dichloroplatinacyclobutane tetramer (**1.5**). However, only cyclopropane would undergo this particular insertion. Substituted metallacyclobutanes required alternative synthetic methodologies, for example the platinum alkene complex $[\text{Pt}(\eta^2\text{-H}_2\text{C}=\text{CH}_2)\text{Cl}_2]_2$ will undergo oxidative addition with functionalised cyclopropanes to give functionalised metallacyclobutane complexes.¹⁶



Equation 1.1 Tipper's metallacyclobutane synthesis

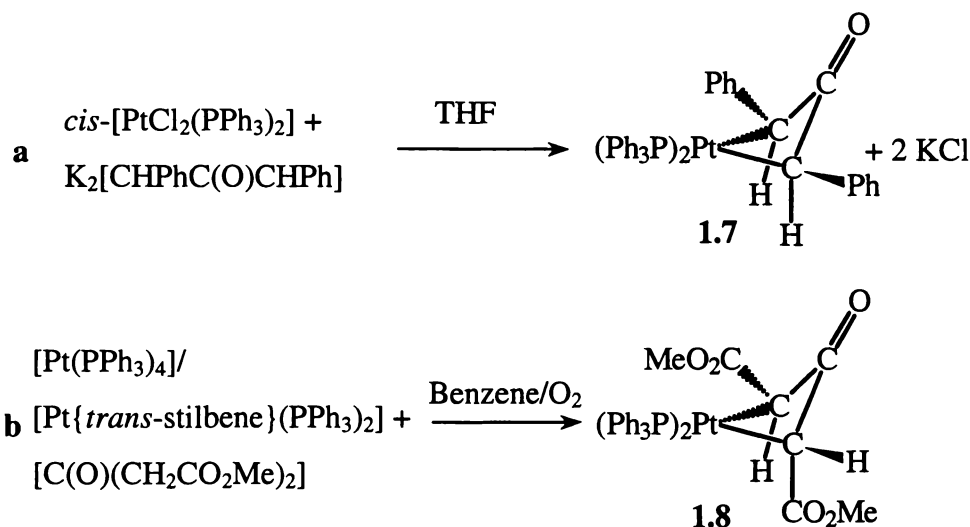
1.2.2 Dilithio / di-Grignard compounds (1,3-dianion formation)

An alternative to that of metal insertion is the utilisation of a salt of the organic moiety (for example the di-Grignard salt). The organic substrate carries a formal 2^- charge and this will readily react with a platinum dichloride complex for example, giving an inorganic salt and the platinacyclobutane **1.6**⁷ (Equation 1.2). One of the principal driving forces behind this synthetic technique is the formation of an insoluble salt. However, one of the limitations with dianion syntheses results from the fact that dry aprotic solvents are necessary since protic solvents regenerate the organic substrate. The initial synthesis of the dianionic compound is often also difficult to achieve. However, most aprotic solvents are organic and this aids in the reaction driving force of salt formation by precipitation of the salt.



Equation 1.2 Di-Grignard preparation of a metallacyclobutane complex

The reaction of $K_2[PhCHC(O)CHPh]$ with a square-planar metal dihalide {for example *cis*- $[PtCl_2(PPh_3)_2]$ } in tetrahydrofuran was found to give the four-membered platinacyclobutan-3-one $[Pt\{CHPhC(O)CHPh\}(PPh_3)_2]$ (**1.7**)⁸ (Equation 1.3a). The phenyl rings of this metallacycle were found to occupy equatorial positions. By contrast, the reaction of dimethyl 3-oxoglutarate $[C(O)(CH_2CO_2Me)_2]$ with zero-valent $[Pt(PPh_3)_4]$ or $[Pt\{trans\text{-stilbene}\}(PPh_3)_2]$ yields the platinacyclobutan-3-one $[Pt\{CH(CO_2Me)C(O)CH(CO_2Me)\}(PPh_3)_2]$ (**1.8**) (Equation 1.3b),⁹ which has the alkyl substituents in both the equatorial and axial positions. The reaction of dimethyl 3-oxoglutarate with the two platinum(0) complexes described above is an example of an oxidative addition reaction, which will be detailed later.



Equation 1.3 1,3-dianion and oxidative addition formations of platinacyclobutan-3-ones

1.2.2.1 Silver(I) oxide mediated syntheses (1,3-dianion synthon reactions)

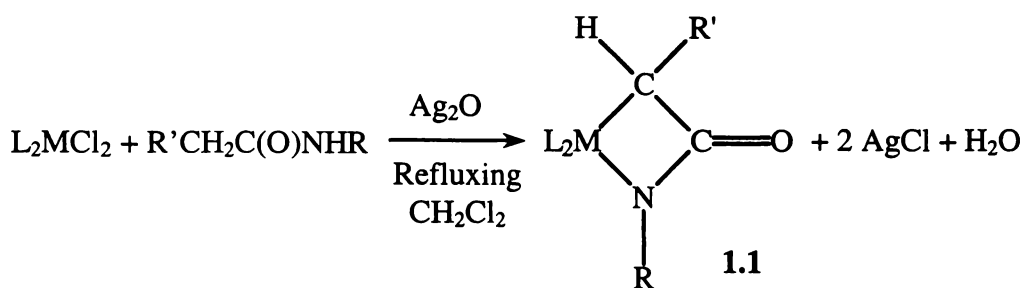
This synthetic technique has been expanded with the utilisation of silver(I) oxide as a reaction mediator.¹ The reaction proceeds in a similar (though somewhat slower) manner to that of a true 1,3-dianionic synthesis. The organic moiety in a silver(I) oxide mediated reaction could be viewed as a 1,3-dianion synthon. However, the exclusion of

⁷ R. DiCosimo and G. M. Whitesides, *J. Am. Chem. Soc.*, (1980), **102**, 3601

⁸ K. W. Chiu, W. Henderson, R. D. W. Kemmitt, L. J. S. Prouse and D. R. Russell, *J. Chem. Soc., Dalton Trans.*, (1988), 427

protic solvents in silver(I) oxide syntheses is not so crucial. 1,3-Dianion synthon reactions are not limited to just silver(I) oxide. Other strong bases, for example triethylamine, have been used with success.¹⁰ Further details for the formation of metallacycles by both silver(I) oxide and triethylamine mediated syntheses will be given throughout this thesis.

The usefulness of silver(I) oxide is now proven for a wide selection of organic reagents and late transition metal complexes. The reaction is not moisture-sensitive, indeed water is a by-product of the reaction (Equation 1.4). As mentioned earlier, for silver(I) oxide reactions to be viable and allow the formation of a four-membered metallacycle, the metal centre has to have *cis*-halides and the organic reagent have acidic protons in the 1,3-positions. The silver organic salt is formed *in situ* and is not observed in the reaction mixture.



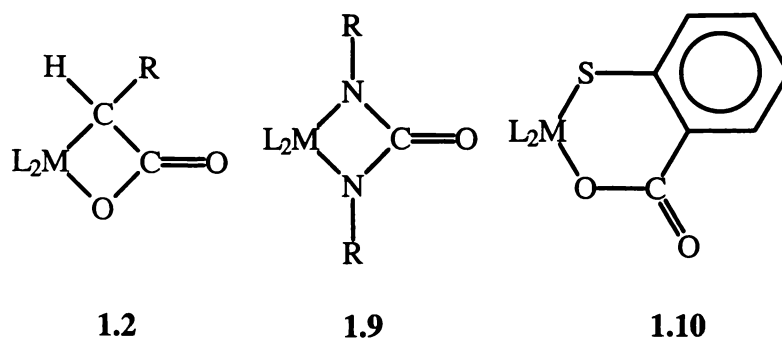
Equation 1.4 General silver(I) oxide synthesis of a metallalactam

In particular, for metallalactam complexes to be formed, which contain both M–C and M–N bonds, the CH and NH protons must be activated. Activation of the CH proton occurs by the presence of local electron-withdrawing groups on the carbon and hence, the proton can be regarded as being acidic. The amide nitrogen proton is generally sufficiently labile that additional functionalities only serve the purpose of halting any bridging between two metal centres by the nitrogen. Indeed, the carbonyl adjacent to the nitrogen increases the acidity of the nitrogen, making it more susceptible to initial deprotonation.

9 a) M. K. Deh, R. D. W. Kemmitt, P. McKenna, D. R. Russell and L. J. S. Prouse, *J. Chem. Soc., Chem. Commun.*, (1982), 505; b) D. A. Clarke, R. D. W. Kemmitt, M. A. Mazid, M. D. Schilling and D. R. Russell, *J. Chem. Soc., Chem. Commun.*, (1978), 744

10 L. J. McCaffrey, W. Henderson, B. K. Nicholson, J. E. Mackay and M. B. Dinger, *J. Chem. Soc., Dalton Trans.*, (1997), 2577

This synthetic technique has expanded to include a wide range of metallacyclic complexes. Metallalactone (1.2),¹¹ ureylene (1.9)¹² and thiosalicylato complexes (1.10)¹⁰ of the platinum group metals synthesised by silver(I) oxide mediated reactions have been reported.



To date only late transition metal species have been investigated by this methodology, mainly because of their stability with respect to water. Early transition metal complexes display inherent reactivity towards water, a by-product of silver(I) oxide mediated syntheses. Hence, the methodologies for the synthesis of early transition metal metallacyclic complexes by silver(I) oxide facilitated reactions has not been developed.

1.2.3 Reactions of alkenes, alkynes, polyalkenes and polyalkynes with metal carbenes

Perhaps the most widely utilised synthetic technique of metallacycle formation is that of the coupling of an alkene or alkyne to a coordinatively unsaturated metal carbene. In practice this method is catalytic, with a metal carbene being regenerated at the end of the catalytic cycle. Industrially this process is utilised in olefin metathesis.^{13,14} In the case of metathesis, the metallacycle is a transient intermediate in the reaction. If the alkene moiety does not cleave from the metal centre, chain extension occurs, resulting in a polymeric compound.¹⁵

The alkene or alkyne undergoes cycloaddition with the metal carbene. This methodology allows substituted metallacyclobutanes to be synthesised as can be seen in

11 W. Henderson, R. D. W. Kemmitt and A. L. Davis, *J. Chem. Soc., Dalton Trans.*, (1993), 2247

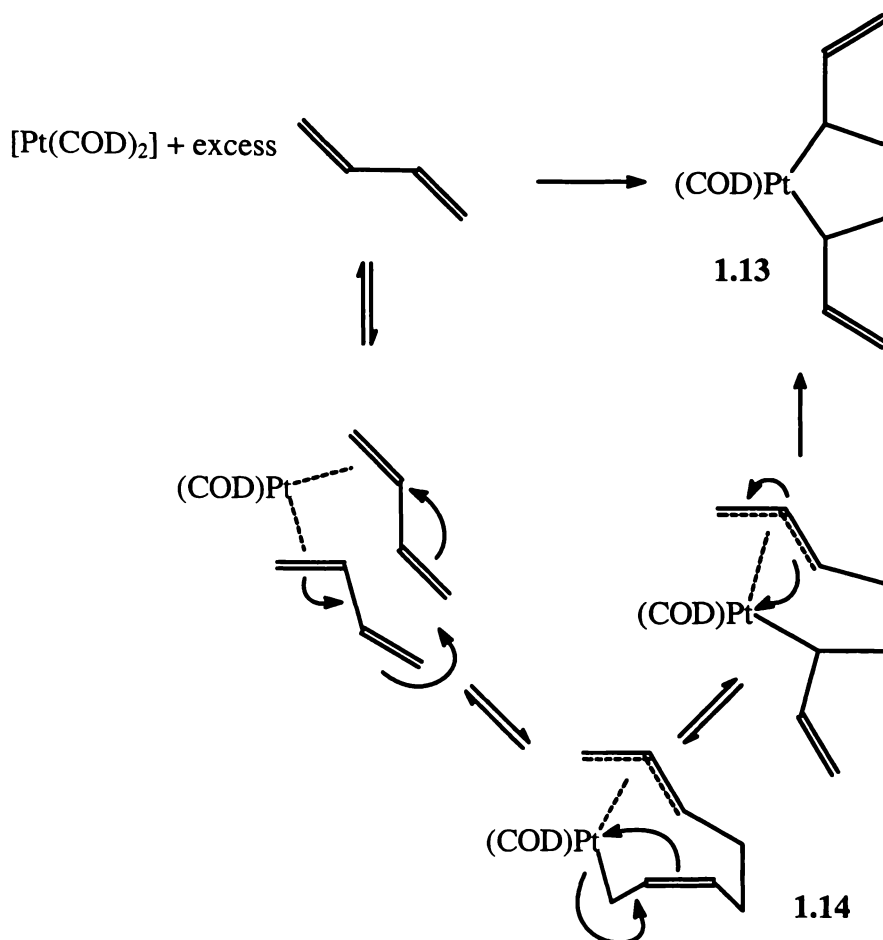
12 M. B. Dinger, W. Henderson, B. K. Nicholson and A. L. Wilkins, *J. Organomet. Chem.*, (1996), **526**, 303

13 F. N. Tebbe, G. W. Parshall and G. S. Reddy, *J. Am. Chem. Soc.*, (1978), **100**, 3611

14 T. J. Katz, *Adv. Organomet. Chem.*, (1977), **16**, 283

15 R. H. Grubbs and W. Tumas, *Science*, (1989), **243**, 907

five- or six-membered ring, due to a reduction in ring strain. Polyalkenes and polyalkynes also undergo oxidative addition reactions with low-oxidation state metal centres. For example, the reaction of an excess of butadiene with $[\text{Pt}(\text{COD})_2]$, results in the formation of a 2,5-divinylplatinacyclopentane¹⁸ (**1.13**) (Equation 1.6).



Equation 1.6 Butadiene reaction with $[\text{Pt}(\text{COD})_2]$

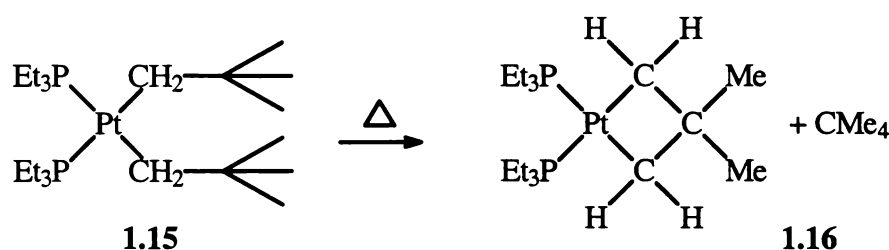
The reaction is proposed to proceed as described in equation 1.6 above, since the PMe_3 adduct of **1.14** has been isolated and structurally characterised. Unlike metathesis reactions, the complexes formed by the reactions of polyalkenes and polyalkynes are stable and several have been structurally characterised.

By contrast, 2,3-dimethylbuta-1,3-diene reacts with $[\text{Pt}(\text{COD})_2]$ to yield 2,3-dimethylplatinacyclopentadiene. Both of these reactions are also examples of oxidative addition reactions, described later. Frequently the reaction product of polyalkene or polyalkyne reactions is a five-membered metallacycle.

¹⁸ G. K. Barker, M. Green, J. A. K. Howard, J. L. Spencer and F. G. A. Stone, *J. Am. Chem. Soc.*, (1976), **98**, 3373

1.2.4 Cyclometallation

The formation of a metallacycle *via* cyclometallation is viewed as an alternative decomposition pathway to that of β -elimination. Cyclometallation arises when the β -elimination process is blocked by complete substitution at the β -carbon. For example, a *neo*-pentyl functionality ($-\text{CH}_2\text{CMe}_3$) is blocked from undergoing β -elimination by the methyl groups on the β -carbon. Cyclometallation often involves the loss of a neutral fragment, usually from an originally coordinated ligand, which becomes displaced during the process. For example, the thermolysis of *cis*-[Pt{CH₂CMe₃}₂(PEt₃)₂] (**1.15**) affords the substituted platinacyclobutane [Pt{CH₂CMe₂CH₂}(PEt₃)₂] (**1.16**) and *neo*-pentane (Equation 1.7).¹⁹



Equation 1.7 Thermolysis of *cis*-[Pt{CH₂CMe₃}₂(PEt₃)₂]

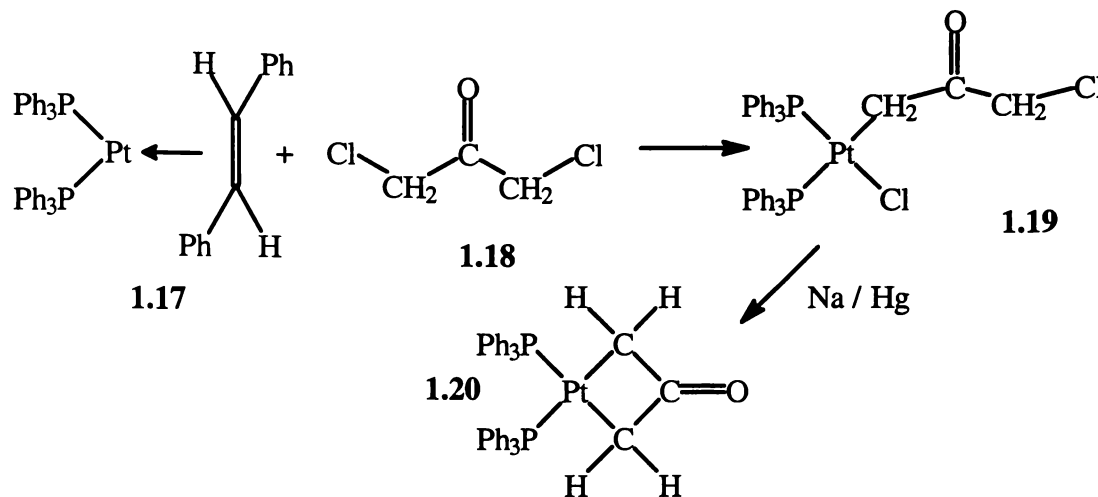
1.2.4.1 Oxidative addition

An example of oxidative addition reactions is the formation of a platinacyclobutan-3-one by the reaction of [Pt{*trans*-stilbene}(PPh₃)₂] (**1.17**) with 1,3-dichloroacetone (**1.18**) (Equation 1.8). The intermediate, *cis*-[Pt{CH₂C(O)CH₂Cl}Cl(PPh₃)₂] (**1.19**),²⁰ is then further reacted in the presence of a reducing agent, for example sodium amalgam, to produce the platinacyclobutan-3-one, [Pt{CH₂C(O)CH₂}(PPh₃)₂] (**1.20**).²¹

19 P. Foley, R. DiCosimo and G. M. Whitesides, *J. Am. Chem. Soc.*, (1980), **102**, 6713

20 W. Henderson, J. Fawcett, R. D. W. Kemmitt, P. McKenna and D. R. Russell, *Polyhedron*, (1997), **16**, 2455

21 J. Fawcett, W. Henderson, M. D. Jones, R. D. W. Kemmitt, B. Lam, S. K. Kang and T. A. Albright, *Organometallics*, (1989), **8**, 1991



Equation 1.8 Oxidative addition of 1,3-dichloroacetone to [Pt{*trans*-stilbene}(PPh₃)₂]

As described earlier, dimethyl 3-oxoglutarate undergoes a similar oxidative addition with Pt(0) complexes, to give the substituted platinacyclobutan-3-one, [Pt{CHCO₂MeC(O)CHCO₂Me}(PPh₃)₂] (1.8).⁹ This reaction differs from the one discussed above since the metallacyclic product, 1.8, is formed during the reaction, whereas the synthesis using 1,3-dichloroacetone requires further reaction with a reducing agent to afford the metallacycle.

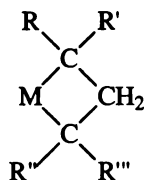
1.3 Four-membered metallacyclic complexes

The four-membered metallacyclic complexes discussed here are isoelectronic with each other. Due to their historical significance, metallacyclobutane complexes (1.3) are initially discussed and used as a bench-mark for further metallacyclic complexes. Substitution about the ring leads to complexes that more closely resemble metallalactam complexes. For example, substitution of the hydrogen atoms at the 3-position (with respect to the metal) with oxygen gives rise to a metallacyclobutan-3-one (1.4) or oxodimethylenemethane complex.

Palladium and platinum are often utilised in the study of metallacyclic complexes for the stability, and hence ease of characterisation, of the complexes that these two metals form, whereas nickel is often subordinated for reactivity studies.⁵ Often these reactivity studies are simple insertion reactions of small molecules (for example SO₂, CO and acetylene) into the metal-carbon bond. The new, chain-extended organic compound can

often be simply regenerated by the addition of hydrochloric acid to the complex. Recently, both the synthesis and reactivity of the metallacycles of the group 10 elements was extensively reviewed.⁵

1.3.1 Metallacyclobutane and η^3 -propargyl / allenyl complexes



Of the small metallacyclic complex family, metallacyclobutanes are, perhaps, one of the most widely studied groups since being first synthesised by Tipper in 1955.⁶ They are believed to play a vital role in the important industrial process of olefin metathesis. This field has been extensively reviewed.¹⁶

Metallacyclobutanes are generally slightly puckered but with dihedral angles through the ring often less than 30°. Main distortions away from planarity arise from varying substituents on the cyclobutane ring.²² The metal-carbon bonds are thought of as σ -bonds, with bond distances as expected based on the covalent radii of the metal and carbon.^{22,23} Facile reductive elimination of cyclopropane from some metallacyclobutanes lead to the Walsh bonding model. This bonding model involves orbital overlap similar to the Chatt-Dewar-Duncanson model for π -backbonding of a transition metal bonding to an alkene (Figure 1.1a). The Walsh model is based on the theoretical bonding of platinum to cyclopropane (Figure 1.1b).

22 a) D. J. Yarrow, J. A. Ibers, M. Lenarda and M. Graziani, *J. Organomet. Chem.*, (1974), **74**, 133; b) J. A. Ibers, R. DiCosimo and G. M. Whitesides, *Organometallics*, (1982), **1**, 13
23 R. J. Klingler, J. C. Huffman and J. K. Kochi, *J. Am. Chem. Soc.*, (1982), **104**, 2147

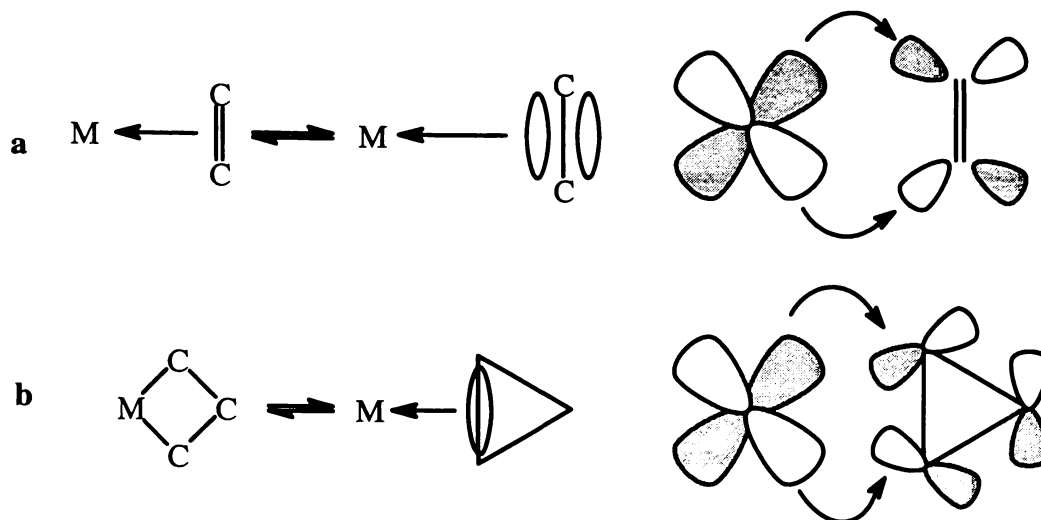
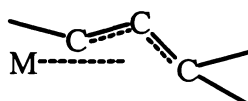


Figure 1.1 Chatt-Dewar-Duncanson π -backbonding model for metal-alkene complexes and the Walsh model for transition metal-cyclopropane complex bonding

Metal- η^3 -propargyl / allenyl complexes (1.21) are similar to metallacyclobutane complexes in that both complexes contain a four-membered metallacycle consisting of three carbon atoms and a transition metal. However, unlike metallacyclobutanes, the central carbon atom of the η^3 -propargyl / allenyl moiety has only one hydrogen atom.²⁴ Charge delocalisation over the π -bond of the propargyl / allenyl ligand and coordination to (in the case of four-membered ring systems) two vacant coordination sites on the metal centre give rise to the four-membered ring structures observed for these complexes.²⁵ The structures often have a highly folded ring, which is also characteristic of many four-membered metallacyclic complexes.



1.21

These complexes have been found to be synthetically useful for the formation of other metallacyclic complexes. For example, azadimethylenemethane²⁶ and

²⁴ A. Wojcicki, *New J. Chem.*, (1997), **21**, 733

²⁵ see, for example, a) W. E. Oberhansli and L. F. Dahl, *J. Organomet. Chem.*, (1965), **3**, 43; b) S. Doherty, J. F. Corrigan, A. J. Carty and E. Sappa, *Adv. Organomet. Chem.*, (1995), **37**, 39; c) S. A. King, D. Van Engen, H. E. Fischer and J. Schwartz, *Organometallics*, (1991), **10**, 1195

²⁶ M. W. Baize, J. L. Furilla and A. Wojcicki, *Inorg. Chim. Acta*, (1994), **223**, 1

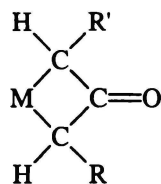
oxodimethylenemethane complexes,²⁷ can be readily synthesised by the direct reaction of the metal η^3 -propargyl complex with an appropriate nucleophile.

1.3.2 Metallacyclobutan-3-ones, trimethylenemethane and azadimethylenemethane complexes

These classes of four-membered metallacycle can be regarded as substituted metallacyclobutanes, with the substitution is at the 3-, or transannular position (with respect to the metal centre). The substitution at the 3-position results in a double-bond. However, due to the conformations that these molecules can adopt, an appreciable amount of charge delocalisation must also occur. Formally, the molecules can have discrete metal-carbon σ -bonds. Again, this does not exclude some degree of the η^3 -bonding described for metallacyclobutane and η^3 -propargyl compounds, as evidenced by the amount of folding that occurs in these complexes.

Fewer complexes of these types are reported compared with metallacyclobutanes. However, with recent advances in the chemistry of η^3 -propargyl / allenyl complexes, new synthetic methodologies have been developed giving access to these novel metallacycles.²⁴ Synthetic techniques involving silver(I) oxide mediated reactions have also given rise to some metallacyclobutan-3-ones.²⁸

1.3.2.1 Metallacyclobutan-3-one (oxodimethylenemethane) complexes



Metallacyclobutan-3-ones are four-membered metallacycles incorporating a carbonyl functionality at the 3-position. A variety of synthetic techniques has been developed which yield these complexes,^{29,30} though the predominant methodology has been the oxidative addition of 3-oxopentandioic acid esters or 2,4,6-heptantrione to various

27 A. Ohsura, T. W. Wardhana, H. Kurosawa and I. Ikeda, *Organometallics*, (1997), **16**, 3038

28 D. A. Clarke, R. D. W. Kemmitt; M. A. Mazid, P. McKenna, D. R. Russell; M. D. Schilling and L. J. S. Sherry, *J. Chem. Soc., Dalton Trans.* (1984), 1993

29 A. Ohsuka, T. Hirao, H. Kurosawa and I. Ikeda, *Organometallics*, (1995), **14**, 2538

30 R. D. W. Kemmitt, P. McKenna, D. R. Russell and L. J. S. Sherry, *J. Chem. Soc., Dalton Trans.*, (1985), 259

palladium(0) and platinum(0) complexes. This oxidative addition methodology has already been the subject of a review.³¹ Nucleophilic attack at the β -carbon of a η^3 -allylic complex by a base (for example, potassium hydroxide) has also been found to yield metallacyclobutan-3-one complexes. However, this technique, as mentioned earlier, is a relatively new methodology, and is not yet as well developed as the oxidative addition syntheses described above.

Structurally, metallacyclobutan-3-ones display a large amount of ring folding compared with their metallacyclobutane analogues, where fold angles up to 50° are not uncommon.^{28,30} The bonding in these molecules deviates considerably from the σ -bond description applied to metallacyclobutanes above. Often the C-C bonds are shorter than an "accepted" carbon-carbon single bond and the carbon-oxygen bond somewhat longer than a true double bond. The bonding in these complexes can then be best viewed as a mix between a four-membered metallacycle with pure σ -bonding, and a "bent" η^3 -form (Figure 1.2). The η^3 -form arises from charge delocalisation about the ring-system and subsequently the carbon atoms of the ring all have bonding contacts with the metal centre. The bond from the metal to the transannular ring carbon is longer than those directly adjacent to the metal, but not as great as a non-bonding contact. This alternate bonding mode gives rise to the alternative name of oxodimethylenemethane or oxyallyl complex.^{32,33} The η^3 -allylic bonding mode is the predominant form that metallacyclobutan-3-one complexes adopt.

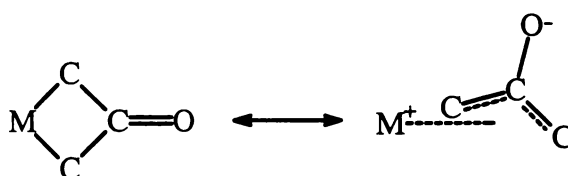
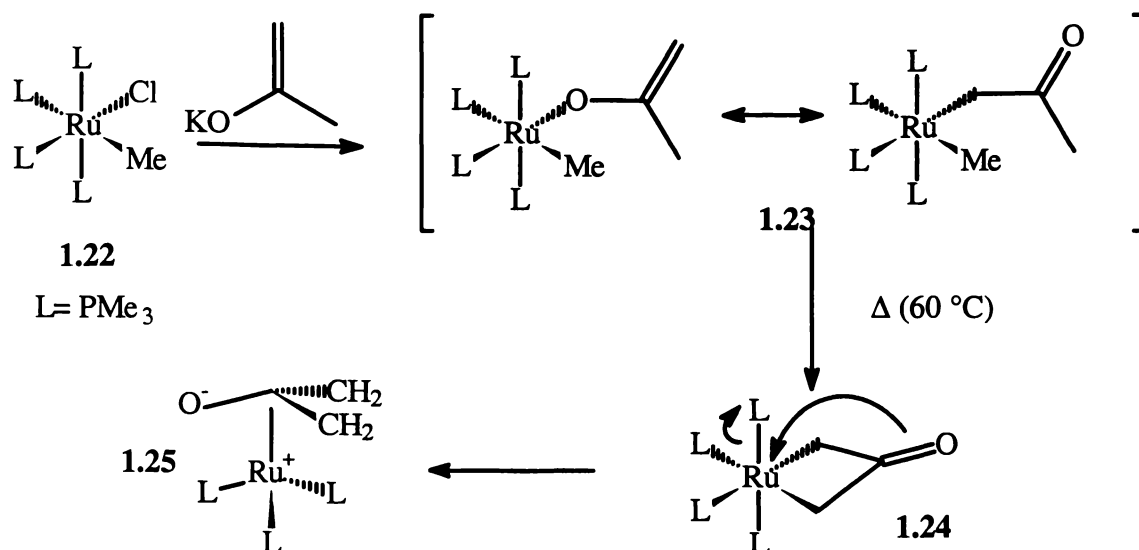


Figure 1.2 Metallacyclobutan-3-one bonding

Earlier a two-step oxidative addition process was described (refer 0). The addition of 1,3-dichloroacetone (**1.18**) to *cis*-[Pt{*trans*-stilbene}(PPh₃)₂] (**1.17**) and subsequent reaction with sodium amalgam results in the formation of an unsubstituted metallacyclobutan-3-one (**1.20**).²¹

31 R. D. W. Kemmitt and M. R. Moore, *Transition Met. Chem.*, (1993), **18**, 348

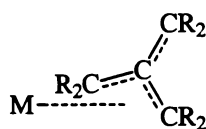
32 B. M. Trost and S. J. Schneider, *J. Am. Chem. Soc.* (1989), **111**, 4430



Equation 1.9 Bergman's synthesis of a η^4 -oxodimethylenemethane complex

Bergman reported the novel synthesis of a η^4 -oxodimethylenemethane complex in 1990.³⁴ The reaction of $[\text{RuCl}(\text{Me})(\text{PMe}_3)_4]$ (**1.22**) with potassium acetone enolate (Equation 1.9) affords the equilibrating complex **1.23**. If this complex is heated to 60 °C, loss of methane results and the ruthenacyclobutan-3-one **1.24** forms. This complex then decomposes, *via* loss of PMe_3 , forming the ruthenium η^4 -oxodimethylenemethane complex **1.25**, which was structurally characterised.

1.3.2.2 Trimethylenemethane metal complexes



Trimethylenemethane (TMM) complexes are the “alkene” variant of metallacyclobutan-3-one complexes. That is, the carbonyl oxygen is replaced with a CR_2 fragment. These complexes show considerable charge delocalisation, and can be described by one of three canonical forms. The first is a η^3 -allylic bonding mode (Figure 1.3a), similar to that for the η^3 -propargyl / allenyl complexes described above. The second canonical structure is a metallacyclobutan-3-ene (Figure 1.3b), and the final form is a η^4 -trimethylenemethane complex (Figure 1.3c).

33 M. Frey, T. A. Jenny and H. Stoeckli-Evans, *Organometallics* (1990), **9**, 1806

34 J. F. Hartwig; R. G. Bergman and R. A. Andersen, *J. Am. Chem. Soc.* (1990), **112**, 5670

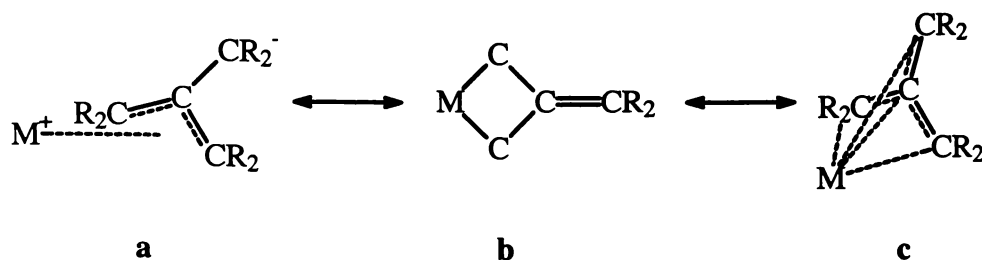
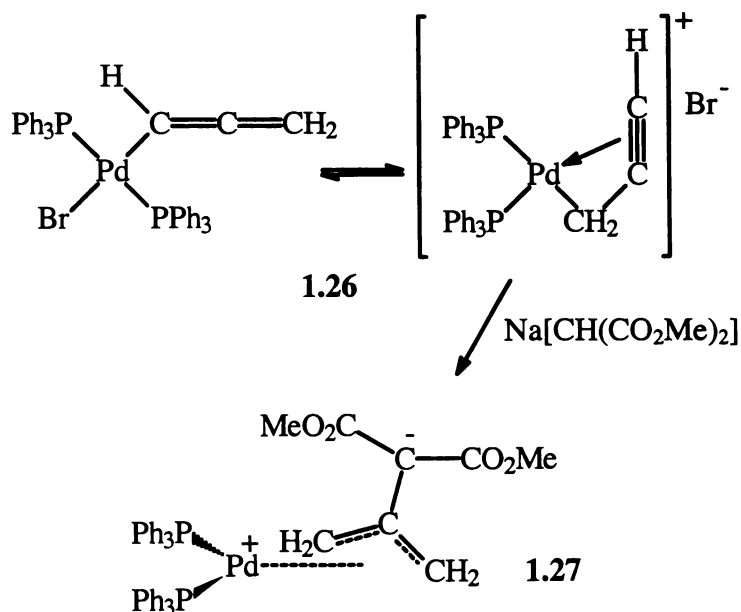


Figure 1.3 Canonical forms of trimethylenemethane complexes

Complexes containing the η^3 -bonding^{35,36} (Figure 1.3a) and η^4 -bonding^{37,38} modes (Figure 1.3c) have been structurally characterised. As outlined earlier, nucleophilic attack at the central carbon of an η^3 -allylic complex will result in the formation of these complexes. For example, the reaction of *trans*-[Pd{CH=C=CH₂}Br(PPh₃)₂] (**1.26**) with one equivalent of Na[CH(CO₂Me)₂] results in the formation of [Pd{ η^3 -CH₂C(C(CO₂Me)₂)CH₂}(PPh₃)₂] (**1.27**) (Equation 1.10).³⁶



Equation 1.10 η^3 -Trimethylenemethane complex synthesis

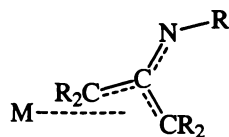
35 V. Plantevin, P. W. Blosser, J. C. Gallucci and A. Wojcicki, *Organometallics*, (1994), **13**, 365

36 C.-C. Su, J.-T. Chen, G.-H. Lee and Y. Wang, *J. Am. Chem. Soc.*, (1994), **110**, 4999

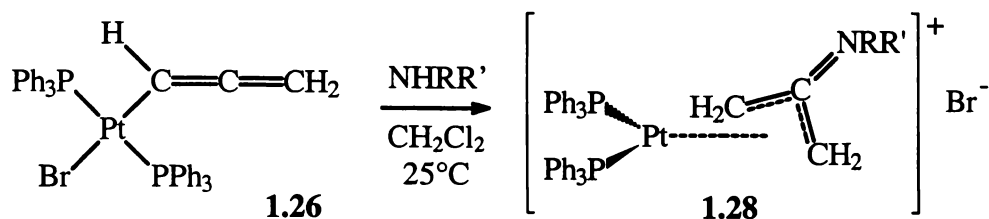
37 B. M. Trost and S. A. King, *J. Am. Chem. Soc.*, (1990), **112**, 408

38 M. D. Jones and R. D. W. Kemmitt, *Adv. Organomet. Chem.* (1987), **27**, 279

1.3.2.3 Azadimethylenemethane complexes

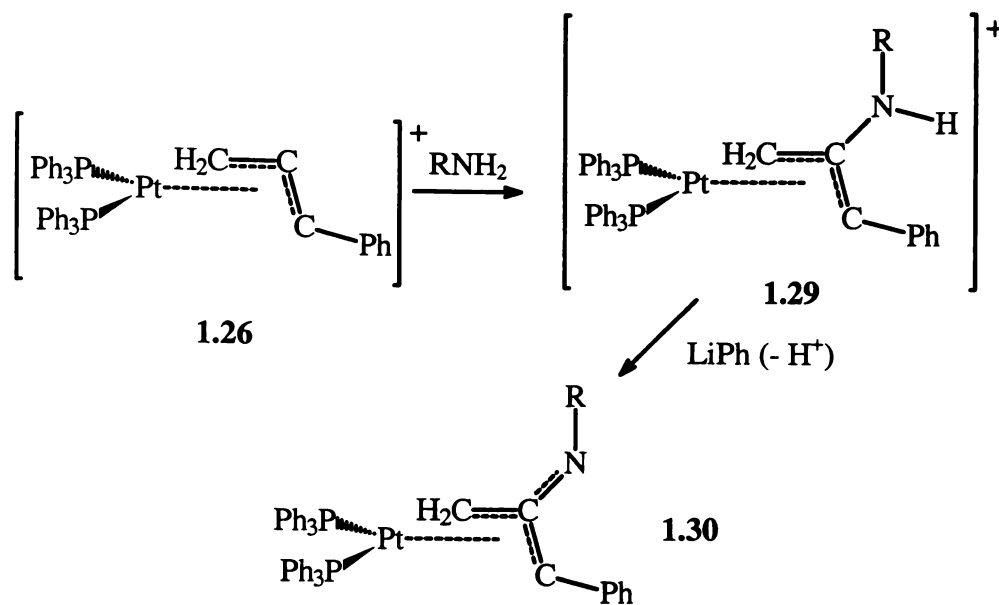
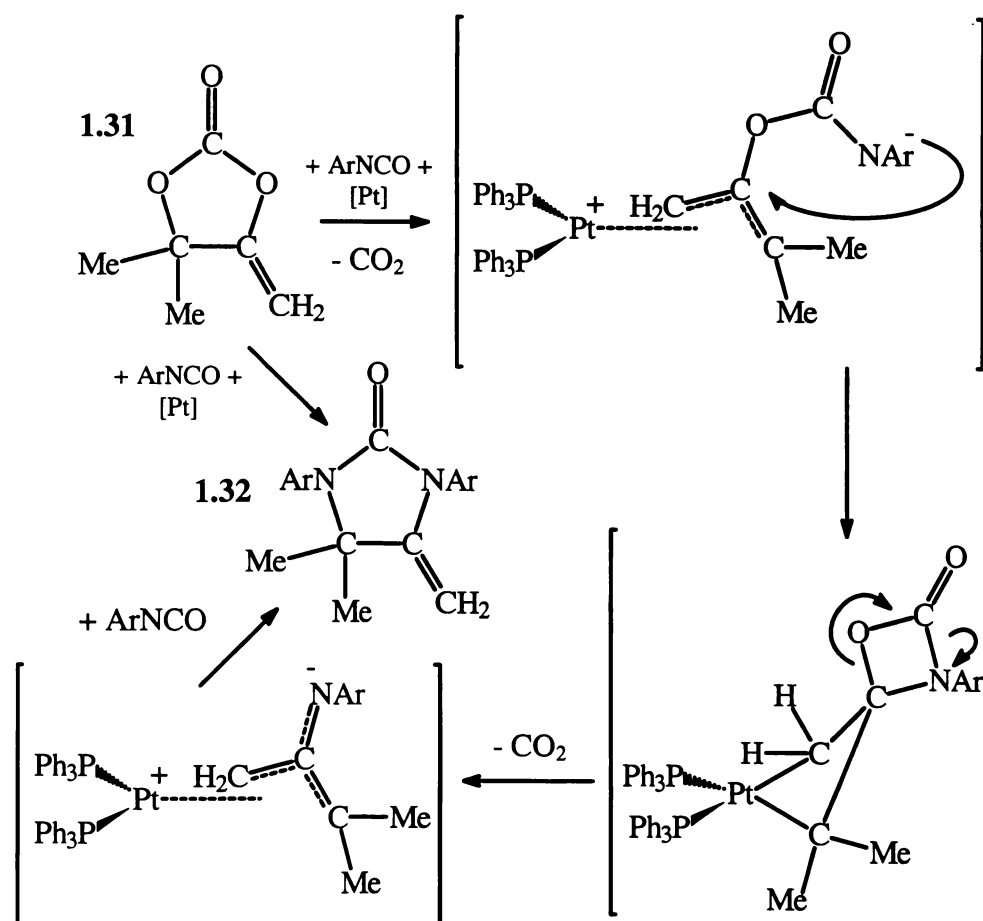


Azadimethylenemethane complexes are again a species related to metallacyclobutan-3-ones. However, the carbonyl oxygen is replaced with an imine functionality. An early reported example of this class of compound proved to have a facile synthesis. The reaction of a secondary amine with the β -carbon of *trans*-[Pt(HC=C=CH₂)Br(PPh₃)₂] (**1.26**) under standard conditions gives the azadimethylenemethane complex **1.28** (Equation 1.11).³⁹

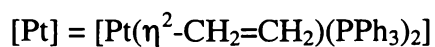


Equation 1.11 Azadimethylenemethane synthesis

However, this complex (**1.28**), is a charged species. Azadimethylenemethane complexes with an NR functionality have been synthesised, again by reaction of a metal- η^3 -propargyl complex [Pt(η^3 -CH₂=C=CPh)(PPh₃)₂]⁺ (**1.26**) with a primary amine (*p*-Me-C₆H₄NH₂ or *p*-O₂N-C₆H₄NH₂). The intermediate complex **1.29** was then deprotonated by a strong base yielding the neutral azadimethylenemethane complex **1.30** (Equation 1.12).²⁶

Equation 1.12 Azadimethylenemethane synthesis by Wojcicki *et al.*

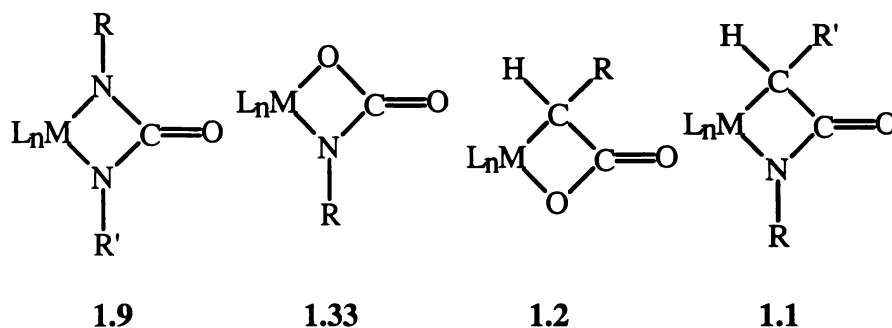
Scheme 1.2 Azadimethylenemethane synthetic utility



The usefulness of these azadimethylenemethane complexes has been demonstrated by the reaction of 5,5-dimethyl-4-methylene-1,3-dioxolan-2-one (**1.31**) with a range of aromatic isocyanates, in the presence of $[\text{Pt}(\eta^2\text{-CH}_2=\text{CH}_2)(\text{PPh}_3)_2]$.⁴⁰ The reaction product **1.32**, was found to have the 1,3-oxygen atoms in the ring replaced with an N(Ar) functionality (Scheme 1.2). The scale of the reaction {0.05 mole equivalent of $[\text{Pt}(\eta^2\text{-CH}_2=\text{CH}_2)(\text{PPh}_3)_2]$ to 1 mole equivalent of 5,5-dimethyl-4-methylene-1,3-dioxolan-2-one (**1.31**)} indicates that the process is catalytic.

1.3.3 Metal-nitrogen and metal-oxygen metallacycles

Four-membered metallacycles with a metal-nitrogen or metal-oxygen bond in the ring cover a wide range of complexes, for example ureylenes (**1.9**), metallacyclocarbamates (**1.33**), metallalactones (**1.2**) and metallalactams (**1.1**). Again these complexes are all isoelectronic with metallacyclobutan-3-one (**1.4**) and metallacyclobutane complexes (**1.3**).



1.3.3.1 Ureylene complexes

Ureylene complexes cover a wide selection of transition metals; from the first row^{41,42} to the third,^{12,43} as well as several novel gold(III) ureylene complexes.⁴⁴ The methods for their synthesis are also varied as the metals from which they are formed. The diverse range of syntheses available for these compounds has prompted a review of

40 K. Ohe, H. Matsuda, T. Morimoto, S. Ogoshi, N. Chatani and S. Murai, *J. Am. Chem. Soc.*, (1994), **116**, 4125

41 Y. Matura, N. Yauoka, T. Ueki, N. Kasai and M. Kakudo, *Bull. Chem. Soc. Jpn.*, (1969), **42**, 881

42 G. D. Forster and G. Hogarth, *J. Chem. Soc., Dalton Trans.*, (1993), 2539

43 A. A. Danopoulos, G. Wilkinson, T. K. N. Sweet and M. B. Hursthouse, *J. Chem. Soc., Chem. Comm.*, (1996), 1835

44 M. B. Dinger and W. Henderson, *J. Organomet. Chem.*, (1998), **557**, 231

these complexes.⁴⁵ In contrast with the highly folded metallacyclobutan-3-one complexes, ureylenes often have a planar ring system. In this respect they closely resemble metallacyclobutanes.

A novel and related metallacycle (**1.34**) (Figure 1.4) produced by the reaction of *cis*-[PtCl₂COD] with triphenylguanidine in the presence of silver(I) oxide has been reported.⁴⁶ Again, the complex **1.34** is isoelectronic with the azadimethylenemethane and trimethylenemethane complexes. The complex is an imido-ureylene and occupies the mid-ground between azadimethylenemethane and ureylene complexes by being a mix of both. The ring of the metallacycle is planar, more like a metal-nitrogen bonded ureylene than the metal-carbon bonded azadimethylenemethane complexes described earlier (section 1.3.2.3).

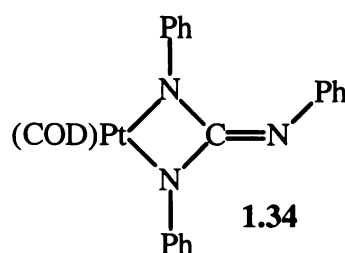


Figure 1.4 N, N', N''-triphenyl guanidine platinum(II) imido-ureylene complex

1.3.3.2 Metallacyclo carbamate complexes

This class of heterocyclic compound is of interest as a model for metathesis reactions, as with many of these metallacyclic complexes, and for their use in the preparation of catalytically important metal-imido complexes. Metallacyclo carbamate complexes are readily accessed by a formal [2+2] electrocyclic reaction of an isocyanate with a metal-oxo complex (Equation 1.13).^{47,48,49a} Metal-imido complexes are of value in catalytic processes since the imido group stabilises the often high oxidation states of the metals,

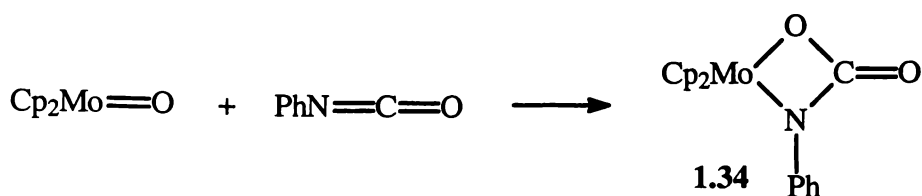
45 S. Cenini and G. La Monica, *Inorg. Chim. Acta.* (1976), **18**, 279

46 M. B. Dinger and W. Henderson, *J. Chem. Soc., Chem. Comm.*, (1996), 211

47 P. Jernkoff, G. L. Geoffroy, A. L. Rheingold and S. J. Geib, *J. Chem. Soc., Chem. Commun.*, (1987), 1610

48 S. Schmid and J. Sträle, *Z. Naturforsch.*, (1991), **46b**, 235

while at the same time being sterically small and occupying only one coordination site on the metal.⁴⁹



Equation 1.13 Metallacyclocarbamate synthesis

1.3.3.3 Metallalactone complexes

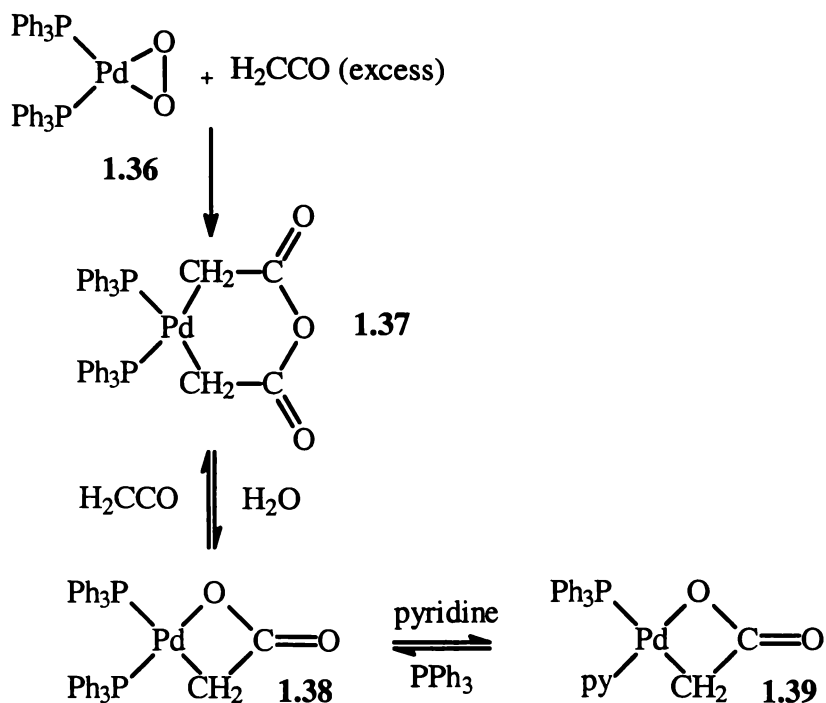
Of the characterised four-membered metallacycles that contain a metal-nitrogen or metal-oxygen bond, a significant number are metallalactone complexes. Several examples with platinum group metals incorporated in the ring have been structurally characterised.^{50,51,52} Early work on metallalactones centred on the reactions of ketene (CH_2CO) with *cis*-[Pd ($\eta^2\text{-O}_2$)(PPh₃)₂] (**1.36**) and the resulting compound **1.37** was described as being a palladium C,O-chelate of acetic acid (refer Equation 1.14). Subsequent ligand substitution gave the reported structures (**1.38** and **1.39**).⁵⁰

49a) R. S. Pilato, C. E. Housmekerides, P. Jernakoff, D. Rubin, G. L. Geoffroy and A. L. Rheingold, *Organometallics*, (1990), **9**, 2333; b) D. E. Wigley, *Progress in Inorganic Chemistry*, (1994), **42**, pp 239 - 483, ed. K. D. Kartin, John Wiley & Sons. Inc.

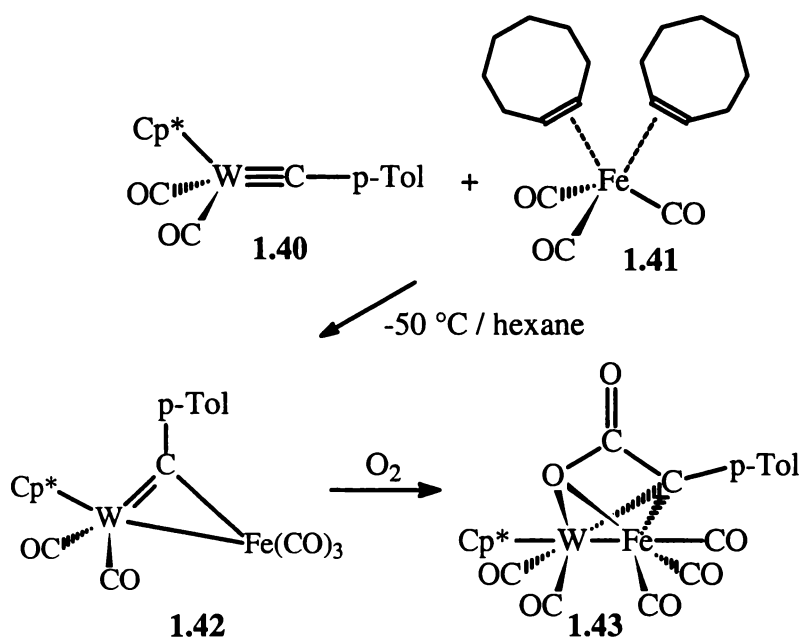
50 a) S. Baba, T. Ogura, S. Kawaguchi, H. Tokunan, Y. Kai and N. Kasai, *J. Chem. Soc., Chem. Comm.*, (1972), 910; b) Y. Kai, N. Yauoka and N. Kasai, *Bull. Chem. Soc. Jpn.*, (1979, **52**, 737

51 L. Pandolfo, G. Paiaro, G. Valle and P. Ganis, *Gazz. Chim. Ital.*, (1985), **115**, 65

52 a) W. A. Herrmann, U. Kusthardt, A. Schafer and E. Herdtweck, *Angew. Chem., Int. Ed. Engl.*, (2986), **25**, 817; b) J. R. Bleeke, R. Behm, Y.-F. Xie, T. W. Clayton Jr. and K. D. Robinson, *J. Am. Chem. Soc.*, (1994), **116**, 4093



Equation 1.14 Palladalactone synthesis

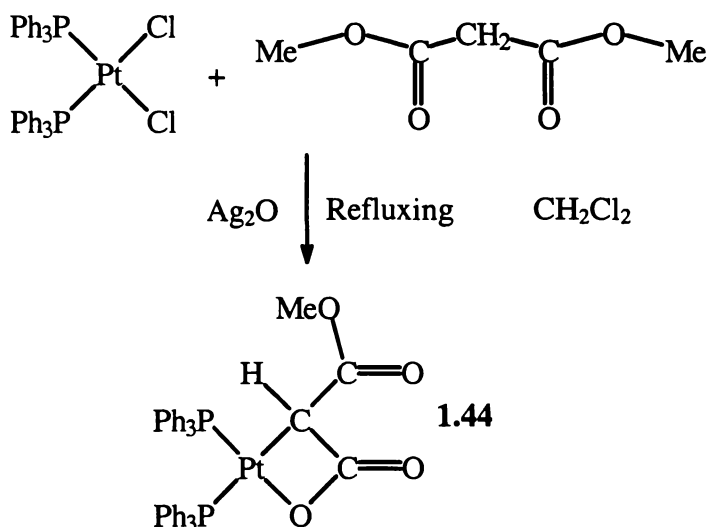


Equation 1.15 Synthesis of a mixed-metal metallalactone

A mixed-metal bridged di-metallic metallalactone has also been reported, consisting of a first row transition metal (iron) and a third row transition metal (tungsten).⁵³ This compound was synthesised as part of a study into the bonding of tungsten to other

transition metals. The tungsten precursor, $[\text{W}(\equiv\text{CC}_6\text{H}_4\text{Me-4})(\text{CO})_2(\text{Cp}^*)]$ (**1.40**) was reacted with $[\text{Fe}(\text{CO})_3(\eta^2\text{-cyclooctene})_2]$ (**1.41**) giving $[\text{FeW}(\mu\text{-CC}_6\text{H}_4\text{Me-4})(\text{CO})_5(\text{Cp}^*)]$ (**1.42**) (Equation 1.15). This then reacted with oxygen present in the reaction vessel and also scavenged carbon monoxide affording the di-metal metallalactone **1.43**. $[\text{FeW}(\mu\text{-CC}_6\text{H}_4\text{Me-4})(\text{CO})_5(\text{Cp}^*)]$ (**1.42**) and similar compounds were found to be an excellent scavengers of carbon monoxide.

The reaction of dimethylmalonate with *cis*- $[\text{PtCl}_2(\text{PPh}_3)_2]$ in the presence of silver(I) oxide (Equation 1.16) has been found to yield at intermediate (24 h.) reaction times a complex mixture of compounds.⁵⁴ Prolonged reaction affords the single complex $[\text{Pt}\{\text{OC}(\text{O})\text{CHCO}_2\text{CH}_3\}(\text{PPh}_3)_2]$ (**1.44**), characterised by multinuclear NMR spectroscopy. However, the complex could not be successfully crystallised and characterised by an X-ray diffraction study.



Equation 1.16 Platinalactone synthesis mediated by silver(I) oxide

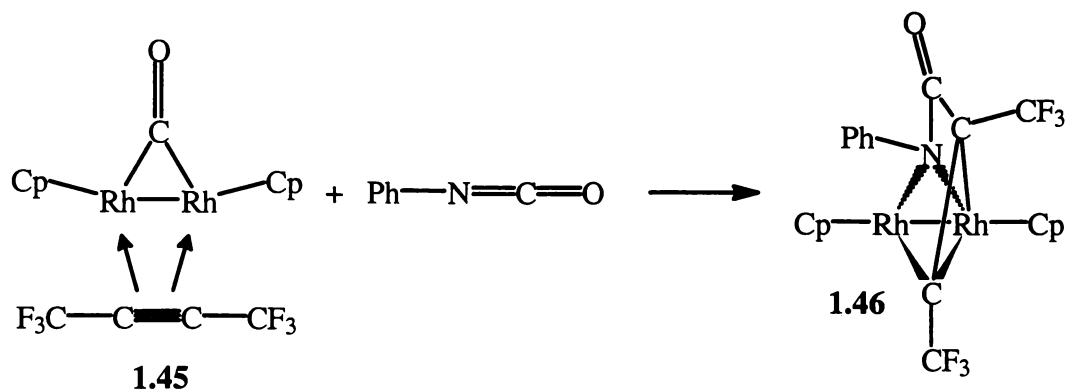
1.3.3.4 Metallalactam complexes

Several structurally characterised examples of metallalactam complexes have been reported. One, is again, a bridged di-metallic species.⁵⁵ Unlike the metallalactone above, this complex has rhodium for both metal centres and was synthesised in a

⁵⁴ W. Henderson, R. D. W. Kemmitt and A. L. Davis, *J. Chem. Soc., Dalton Trans.*, (1993), 2247

⁵⁵ R. S. Dickson, R. J. Nesbit, H. Pateras, J. M. Patrick and A. H. White, *J. Organomet. Chem.*, (1984), 265, C25

manner similar to that of the metallacyclocarbamates described above (1.3.3.2). Phenyl isocyanate is reacted with either the monocarbonyl complex $[\text{Cp}_2\text{Rh}_2(\text{CO})\{\text{CF}_3\text{C}_2\text{CF}_3\}]$ (1.45) or the dicarbonyl analogue, $[\text{Cp}_2\text{Rh}_2(\text{CO})_2\{\text{CF}_3\text{C}_2\text{CF}_3\}]$, yielding the complex $[\text{Cp}_2\text{Rh}_2\{\mu\text{-C}(\text{CF}_3)\text{C}(\text{CF}_3)\text{C}(\text{O})\text{N}(\text{Ph})\}]$ (1.46) (Equation 1.17).



Equation 1.17 Di-rhodium metallalactam synthesis

Several metallalactam complexes have also been characterised as the products of silver(I) oxide mediated reactions.^{1a,56} The reaction of amides with a metal dihalide in the presence of silver(I) oxide was found to be generally more rapid (18 h.) than that of dimethylmalonate with similar metal dihalides (48 h.) (section 1.3.3.3). Presumably the reaction proceeds more rapidly due to the higher acidity, and hence more rapid abstraction of the amide hydrogen, compared with the displacement of methanol from dimethylmalonate.

1.4 Summary

Four-membered metallacycles are a synthetically and industrially important class of compounds. The variety of techniques available for the synthesis and the number of groups of compounds that can be formed, have made them widely studied since their first synthesis in 1955.⁶ The synthetic methodology using silver(I) oxide as a reaction mediator has been successfully extended to include most of the classes of four-membered metallacycles. However, little is known about the mechanism of these reactions. Also with the recent synthesis of the square-planar gold dihalide complexes

56 W. Henderson, J. Fawcett, R. D. W. Kemmitt, C. Proctor and D. R. Russell, *J. Chem. Soc., Dalton Trans.*, 1994, 3085

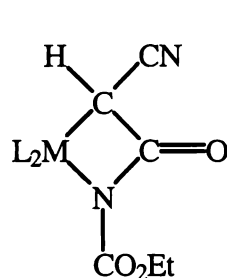
[{C₆H₃(CH₂NMe₂)-2-(R)-5}AuCl₂] (R = OMe or H)⁵⁷ a new field of metallacyclic chemistry, auracyclic complexes, has opened up. While silver(I) oxide has proven to be an efficient mediator of these metallacycle formation reactions, other alternatives, for example triethylamine,¹⁰ exist. In the following chapters further examples of four-membered metallalactam complexes synthesised both by silver(I) oxide and triethylamine routes will be described as well as two novel gold(III) metallacycles. Some mechanistic information is also gleaned from the characterisation of a complex which is an intermediate in metallalactam synthesis

57 a) P. A. Bonnardel and R. V. Parish, *J. Chem. Soc., Dalton Trans.*, (1996), 318; b) M.-D. Bermúdez, F.-J. Carrión and P. G. Jones, *J. Organomet. Chem.*, (1984), **268**, 191

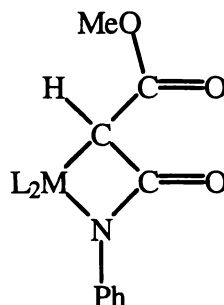
Chapter Two. Metallalactam complexes of palladium(II) and platinum(II)

2.1 Introduction

Silver(I) oxide has been found to mediate the synthesis of several novel metallalactam complexes from reactions of the appropriate metal dihalide with either *N*-cyanoacetylurethane (**2.1**)¹ or acetoacetanilide (**2.2**).² This methodology has been developed to allow the synthesis of a wide variety of complexes containing various functionalities ranging from metal-amides (**2.3**)^{3a} to metallalactone (**2.4**)^{3b} and ureylene (**2.5**)^{3c} ring systems. The range of metals utilised in these silver(I) oxide mediated reactions has been limited to the platinum group due to the presence of water as a by-product of the reaction. Early transition metal complexes tend to be more air- and moisture-sensitive and require alternative methodologies to prepare similar complexes.



2.1



2.2

2.1a) M = Pt, L = PPh₃

b) L₂ = COD

c) L₂ = dppe

d) M = Pd, L₂ = dppe

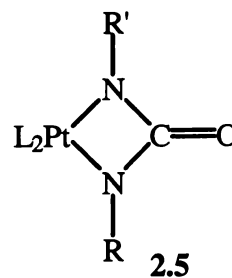
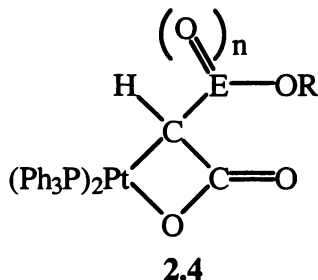
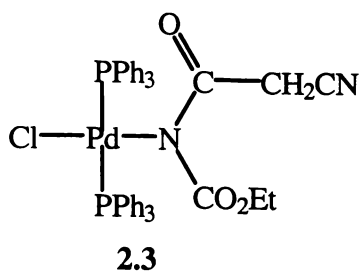
2.2a) M = Pt, L = PPh₃

b) L₂ = dppe

c) M = Pd, L₂ = bipy

1 W. Henderson, B. K. Nicholson and A. G. Oliver, J. Chem. Soc., Dalton Trans., (1994), 1831

2 W. Henderson, J. Fawcett, R. D. W. Kemmitt, C. Proctor and D. R. Russell, J. Chem. Soc., Dalton Trans., (1994), 3085



2.4 E = C, n = 1, R = Me, Et **2.5** L = PPh₃, R = Ar, C(O)Me, R' = Alkyl, Ar, C(O)Me
 E = S, n = 2, R = Ph L₂ = COD, R = Ar, C(O)Me, R' = Alkyl, Ar, C(O)Me

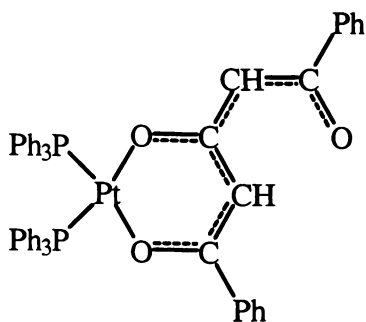
In an effort to determine whether or not alternative bonding modes similar to those found for acetylacetonate complexes of platinum(II) and palladium(II) (**2.6**, **2.7**, **2.8**) could be synthesised *via* a silver(I) oxide mediated pathway, 2-benzoylacetylurethane was selected as a candidate. The hydrogen atoms on the α -carbon are more acidic than those of the well studied *N*-cyanoacetylurethane, perhaps approaching the acidity of the amide hydrogen. Studies of platinum group complexes of 1,3-diketones indicate that several modes of bonding to the metal centre are possible.^{4,5,6} The main bonding mode of acetonate ligands to the metal centre is through the ketonic oxygen atoms (**2.6**), which is exemplified by the reaction of [PhC(O)CH₂C(O)CH₂C(O)Ph] with *cis*-[PtCl₂(PPh₃)₂].⁵ In contrast however, the methyl derivative, [MeC(O)CH₂C(O)CH₂C(O)Me] bonds *via* the acetyl carbon atoms, giving rise to a metallabutanone (**2.7**) structure as shown below.⁶ Others are complexed only through the α -carbon (**2.8**), allowing two organic substrates to bond to the metal centre.

3 a) W. Henderson, B. K. Nicholson, A. G. Oliver, *Polyhedron*, (1994), 3094; b) W. Henderson, R. D. W. Kemmitt and A. L. Davis, *J. Chem. Soc., Dalton Trans.*, (1993), 2247; c) M. B. Dinger, W. Henderson, B. K. Nicholson and A. L. Wilkins, *J. Organomet. Chem.*, (1996), **526**, 303

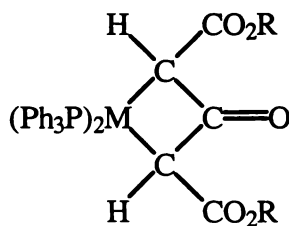
4 S. Kawaguchi, *Coord. Chem. Rev.*, (1986), **70**, 51

5 A. Imran, R. D. W. Kemmitt, A. J. W. Markwick, P. McKenna, D. R. Russell and L. J. S. Sherry, *J. Chem. Soc., Dalton Trans.*, (1985), 549

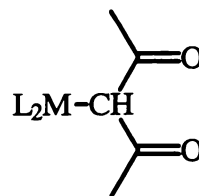
6 R. D. W. Kemmitt, M. A. Mazid, P. McKenna, D. R. Russell and L. J. S. Sherry, *J. Chem. Soc., Dalton Trans.*, (1984), 1993



2.6



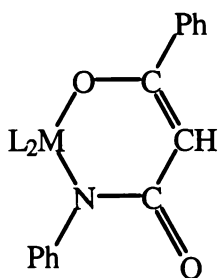
2.7 M = Pd, Pt



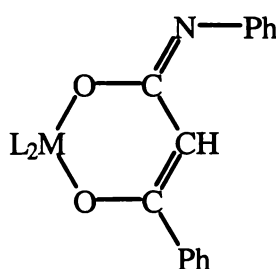
2.8

R = Me, Et

2-Benzoylacetylurethane was chosen as a likely candidate to determine whether amides could form an alternative bonding configuration to that of *N*-cyanoacetylurethane and acetoacetanilide. It is similar to $[\text{PhC(O)CH}_2\text{C(O)CH}_2\text{C(O)Ph}]$ and may bond in a manner like one of the two six-membered metallacycles depicted below (2.9, 2.10). Enolisation of the ligand would presumably be the most likely rearrangement if this did occur (2.9). In addition acetoacetamide $[\text{NH}_2\text{C(O)CH}_2\text{C(O)CH}_3]$ was used to extend the utility of these silver(I) oxide syntheses towards metallacycles with an unsubstituted nitrogen in the ring, perhaps providing a pathway for future synthesis of organic lactams with less substitution on the ring.



2.9



2.10

2.2 Experimental

General experimental procedures are as described previously.¹ $[\text{PtCl}_2(\text{COD})]$,⁷ $[\text{PdCl}_2(\text{COD})]$,⁸ $[\text{PdCl}_2(\text{bipy})]$,⁹ 1,2-bis(diphenylphosphino)ethane¹⁰ (dppe) and silver(I)

7 J. X. McDermott, J. F. White and G. M. Whitesides, *J. Am. Chem. Soc.*, (1976), 6521

8 D. Drew and J. R. Doyle, *Inorg. Synth.*, (1972), 13, 52

9 B. J. McCormick, E. N. Jaynes, jun. R. I. Kaplan, *Inorg. Synth.*, (1972), 13, 216

10 P. Veya, *Organometallics*, (1993), 12, 4365

oxide¹¹ were prepared by literature methods. Acetoacetamide, 2-benzoylacetyl (Aldrich) and triphenylphosphine (Pressure Chemical Co.) were used as received. Mass spectra were recorded on a VG Platform II electrospray mass spectrometer using CH₃CN/H₂O as the carrier solvent. ¹H and ¹³C-{¹H} NMR data were recorded on a Brüker AC300P NMR spectrometer at 300.13 MHz and 75.47 MHz respectively. CDCl₃ was used as lock, with chemical shifts referenced to internal TMS (δ 0.0). ³¹P-{¹H} NMR data were recorded on a JEOL FX90Q NMR spectrometer at 36.23 MHz. Samples were referenced to external 85% H₃PO₄ and were recorded in CH₂Cl₂ with a D₂O insert for lock. IR spectra were recorded as KBr discs on a BIO-RAD FTS-40 Infrared Spectrometer. All melting points were recorded on a Reichert Thermopan Apparatus in air, and are uncorrected. Elemental microanalyses were carried out at the University of Otago Microanalytical Unit. Differential scanning calorimetry (DSC) was performed on a Perkin-Elmer DSC6. Accurate X-ray intensity data were collected at the University of Auckland by a Nonius CAD4 diffractometer.

2.2.1 Synthesis of $[\text{Pt}\{\text{N}(\text{Ph})\text{C}(\text{O})\text{CHC}(\text{O})\text{Ph}\}(\text{COD})]$ (2.11)

A solution of [PtCl₂(COD)] (0.140 g, 0.375 mmol), 2-benzoylacetyl (0.092 g, 0.385 mmol) and Ag₂O (0.266 g, excess) was heated at reflux in dichloromethane (20 cm³) for 18 h. The silver salts were removed by filtration affording a tan solution, which was reduced in volume under vacuum. The tan product was precipitated by the addition of light petroleum, then obtained by filtration and dried (0.139 g, 69%).

Elemental analysis: C, 51.2; H, 4.2; N, 2.6. C₂₃H₂₄NO₂Pt requires C, 51.1; H, 4.5; N, 2.6%.

IR: ν(CO) 1663 cm⁻¹ (vs).

m.p.: 163-165 °C (decomp.).

ES/MS (20 V): [M+H]⁺ *m/z* 541, (100%); [2M+H]⁺ *m/z* 1081, (40%).

¹H NMR: δ 8.1 - 6.9 [m, 12H, Ph], 5.15- 5.35 [m, 2H, COD CH], 4.90 - 4.84 [m, 1H, COD CH, ²J(Pt, H) 62.5], 4.16 - 4.09 [m, 1H, COD CH, ²J(Pt, H) 59.5], 3.87 [s, 1H, ring CH, ²J(Pt, H) 100], 2.70 - 1.90 [m, 8H, COD CH₂].

¹³C-{¹H} NMR: δ 197.3 [s, C(O)Ph, ²J(Pt, C) 51], 173.9 [s, ring CO, ²J(Pt, C) 162], 144.5 - 124.1 [m, Ph], 106.6 [s, COD CH, ¹J(Pt, C) 62], 105.8 [s, COD CH, ¹J(Pt, C)

62], 87.9 [s, COD CH, $^1J(\text{Pt}, \text{C})$ 167], 86.1 [s, COD CH, $^1J(\text{Pt}, \text{C})$ 157], 40.5 [s, ring CH, $^1J(\text{Pt}, \text{C})$ 435], 32.3 [s, COD CH₂], 30.5 [s, COD CH₂], 29.3 [s, COD CH₂], 28.1 [s, COD CH₂].

2.2.2 Synthesis of $[\text{Pt}\{\text{N}(\text{Ph})\text{C}(\text{O})\text{CHC}(\text{O})\text{Ph}\}(\text{PPh}_3)_2]$ (2.12) from (2.11) by ligand displacement

$[\text{Pt}\{\text{N}(\text{Ph})\text{C}(\text{O})\text{CHC}(\text{O})\text{Ph}\}(\text{COD})]$ (2.11) (0.038 g, 0.071 mmol) and triphenylphosphine (0.039 g, 0.15 mmol) were dissolved in dichloromethane (0.5 cm³) and allowed to stand for 10 min. The product was precipitated by the addition of light petroleum (5 cm³) and the solvents removed by filtration, yielding a tan residue after drying (0.066 g, 97%).

Elemental analysis: C, 64.0; H, 4.2; N, 1.5. C₅₁H₄₁NO₂P₂Pt requires C, 64.1; 4.3; N, 1.5%.

IR: $\nu(\text{CO})$ 1636 cm⁻¹ (br, s).

m.p.: 173-174 °C (decomp.).

ES/MS (20V): $[\text{M}+\text{H}]^+$ m/z 957, (100%); $[\text{Pt}(\mu^2\text{-C}_6\text{H}_4\text{-PPh}_2)(\text{PPh}_3)+\text{NH}_3]^+$ m/z 736, (15%).

^1H NMR: δ 7.80 - 6.50 (m, 45H, Ph), 3.53 - 3.36 [dd, ring CH, $^2J(\text{Pt}, \text{H})$ 41.2, $^3J(\text{P}, \text{H})$ 4.9, $^3J(\text{P}, \text{H})$ 4.0].

$^{13}\text{C}\{-^1\text{H}\}$ NMR: δ 201.2 [s, C(O)Ph, $^2J(\text{Pt}, \text{C})$ 32, $^3J(\text{P}, \text{C})$ 4], 174.1 [s, ring CO, $^2J(\text{Pt}, \text{C})$ 75, $^3J(\text{P}, \text{C})$ 7], 144.0 - 123.1 (m, Ph), 45.9 [d, ring CH, $^2J(\text{P}, \text{C})$ 64 $^1J(\text{Pt}, \text{C})$ 390].

$^{31}\text{P}\{-^1\text{H}\}$ NMR: AB spin system δ 16.33 [P *trans* C, $^1J(\text{Pt}, \text{P})$ 2351, $^2J(\text{P}, \text{P})$ 17], 10.00 [P *trans* N, $^1J(\text{Pt}, \text{P})$ 3733, $^2J(\text{P}, \text{P})$ 17].

2.2.3 Preparation of $[\text{Pt}\{\text{N}(\text{Ph})\text{C}(\text{O})\text{CHC}(\text{O})\text{Ph}\}(\text{PPh}_3)_2]$ (2.12) from *cis*-[PtCl₂(PPh₃)₂]

cis-[PtCl₂(PPh₃)₂] was prepared *in situ* by the addition of triphenylphosphine (0.097 g, 0.37 mmol) to [PtCl₂(COD)] (0.065 g, 0.17 mmol) in dichloromethane (10 cm³). 2-Benzoylacetylacetanilide (0.044 g, 0.19 mmol) and silver(I) oxide (0.289 g, excess) were added to this stirred solution with additional dichloromethane (10 cm³) and heated at reflux for 24 h. Silver salts were removed by filtration and solvent removed under reduced pressure affording a tan powder. This was subsequently recrystallised from a dichloromethane solution by the addition of light petroleum and the solid collected by

filtration (0.118 g, 72%). The ES/MS and ^{31}P - $\{^1\text{H}\}$ NMR data obtained were consistent with the data collected above in experiment 2.2.2.

ES/MS (20 V): $[\text{M}+\text{H}]^+$ m/z 957, (100%).

^{31}P - $\{^1\text{H}\}$ NMR: AB spin system δ 16.36 [d, P *trans* C, $^1J(\text{Pt}, \text{P})$ 2351, $^2J(\text{P}, \text{P})$ 17], 10.00 [d, P *trans* N, $^1J(\text{Pt}, \text{P})$ 3763, $^2J(\text{P}, \text{P})$ 17].

2.2.4 Preparation of $[\text{Pt}\{\overline{\text{N}(\text{Ph})\text{C}(\text{O})\text{CHC}(\text{O})\text{Ph}}\}(\text{dppe})]$ (2.13) by ligand displacement from (2.11)

1,2-Bis(diphenylphosphino)ethane (dppe) (0.026 g, 0.066 mmol) was added to a solution of $[\text{Pt}\{\overline{\text{N}(\text{Ph})\text{C}(\text{O})\text{CHC}(\text{O})\text{Ph}}\}(\text{COD})]$ (2.11) (0.034 g, 0.064 mmol) in dichloromethane (0.5 cm³), which was allowed to stand for 10 min. A tan compound was precipitated by the addition of light petroleum (5 cm³) to this solution. The tan product was filtered and dried (yield 0.042 g, 89%).

Elemental analysis: C, 59.4; H, 4.4; N, 1.7%. C₄₁H₄₀NO₂P₂Pt requires C, 59.4; H, 4.3; N, 1.7%.

IR: $\nu(\text{CO})$ 1632 cm⁻¹ (br, s).

m.p.: 131-133 °C (decomp.).

ES/MS (20 V): $[\text{M}+\text{H}]^+$ m/z 831, (100%).

^1H NMR: δ 8.34 (m, 32H, Ph), 3.81-3.77 [dd, 1H, ring CH, $^2J(\text{Pt}, \text{H})$ 72.0, $^3J(\text{P}, \text{H})$ 9.1, $^3J(\text{P}, \text{H})$ 1.9].

^{13}C - $\{^1\text{H}\}$ NMR: δ 199.3 [d, C(O)Ph, $^3J(\text{P}, \text{C})$ 3], 174.5 [d, ring CO, $^2J(\text{Pt}, \text{C})$ 142, $^3J(\text{P}, \text{C})$ 8], 146.4 - 123.0 (m, Ph), 44.3 [d, ring CH, $^1J(\text{Pt}, \text{C})$ 323, $^2J(\text{P}, \text{C})$ 61], 31.7 - 28.2 (m, dppe CH₂).

^{31}P - $\{^1\text{H}\}$ NMR: AB spin system δ 44.33 [P *trans* C, $^1J(\text{Pt}, \text{P})$ 2607], 35.88 [P *trans* N, $^1J(\text{Pt}, \text{P})$ 3234].

2.2.5 Preparation of $[\text{Pd}\{\overline{\text{N}(\text{Ph})\text{C}(\text{O})\text{CHC}(\text{O})\text{Ph}}\}(\text{bipy})]$ (2.14)

A stirred suspension of $[\text{PdCl}_2(\text{bipy})]$ (0.177 g, 0.837 mmol), 2-benzoylacetyl anilide (0.128 g, 0.536 mmol) and silver(I) oxide (0.412 g, excess) in dichloromethane (20 cm³) was heated at reflux for 24 h. Filtration of the silver salts afforded a bright orange solution, which yielded a pale orange microcrystalline powder upon removal of the

solvent. The product was recrystallised by liquid-liquid diffusion from a dichloromethane / methanol solvent (0.5 : 0.1 cm³) layered with light petroleum (5 cm³) and a final yield obtained (0.210 g, 78%). Orange crystals of X-ray crystallographic quality were obtained from this diffusion crystallisation and a crystallographic study performed. Elemental analysis and NMR spectroscopy indicate that a variable amount of solvent of crystallisation (dichloromethane) is present in the crystal, even after drying under vacuum.

Found C, 55.2; H, 3.5; N, 7.5. C₂₅H₁₉N₃O₂Pd.CH₂Cl₂ requires C, 53.5; H, 3.6; N, 7.2%.

IR: $\nu(\text{CO})$ 1603 cm⁻¹ (br, s).

m.p.: 167-168 °C (decomp.).

ES/MS (20 V): [M+H]⁺ m/z 499, (100%); [2M+H]⁺ m/z 1000, (40%).

¹H NMR: δ 9.1 - 7.0 (m, 18H, Ar), 5.29 (s, 0.5H, CH₂Cl₂ of crystallisation), 3.58 (s, 1H, ring CH).

¹³C-¹H NMR: δ 201.2 [s, C(O)Ph], 171.7 (s, ring CO), 154.8 - 121.9 (m, Ar), 35.9 (s, ring CH).

2.2.6 Preparation of [Pd{N(Ph)C(O)CHC(O)Ph}(dppe)] (2.15) from [PdCl₂(dppe)]

[PdCl₂(dppe)] was prepared *in situ* by the addition of dppe (0.096 g, 0.24 mmol) to a stirred solution of [PdCl₂(COD)] (0.069 g, 0.24 mmol) in dichloromethane (10 cm³). To this mixture 2-benzoylacetyl (0.058 g, 0.24 mmol), silver (I) oxide (0.259 g, excess) and additional dichloromethane (10 cm³) were added and the mixture heated at reflux for 18 h. The silver salts were removed by filtration and the solvent removed under reduced pressure. The product, a yellow powder, was recrystallised from dichloromethane / light petroleum and dried under vacuum giving the final yield (0.151 g, 88%). As with 2.14 above, the final product was found to contain a variable amount of solvent of crystallisation even after drying, as shown by NMR spectroscopy and the elemental analyses of the complex.

Elemental analysis: C, 64.8; H, 5.2; N, 1.9. C₄₁H₃₆O₂NP₂Pd.CH₂Cl₂ requires C, 64.2; H, 4.9; N, 1.8%.

IR: $\nu(\text{CO})$ 1618, 1587 cm⁻¹ (s).

m.p. : 152-153 °C (decomp.).

ES/MS: [M+H]⁺ m/z 743 (100%).

^1H NMR: δ 8.15 - 6.25 (m, 30H, Ph), 5.29(s, 1H, CH_2Cl_2), 3.42 - 3.30 [dd, 1H, ring CH, $^3J(\text{P}, \text{H})$ 29, $^3J(\text{P}, \text{H})$ 5], 2.63-1.95 [m, 4H, dppe CH_2].

^{13}C - $\{^1\text{H}\}$ NMR: δ 197.9 [s, $\text{C}(\text{O})\text{Ph}$], 176.7 (s, ring CO), 141.7 - 119.2 (m, Ar), 53.6 (s, CH_2Cl_2), 39.1 [dd, ring CH, $^2J(\text{P}, \text{C})$ 65, $^2J(\text{P}, \text{C})$ 4], 28.9 - 28.2 (m, dppe CH_2).

^{31}P - $\{^1\text{H}\}$ NMR: AB spin system δ 51.6 [d, $^2J(\text{P}, \text{P})$ 31], 47.3 [d, $^2J(\text{P}, \text{P})$ 31].

2.2.7 Preparation of $\text{cis-}[\text{Pt}\{\overline{\text{N}(\text{H})\text{C}(\text{O})\text{CHC}(\text{O})\text{CH}_3}\}(\text{PPh}_3)_2]$ (2.16) from $\text{cis-}[\text{PtCl}_2(\text{PPh}_3)_2]$

$\text{cis-}[\text{PtCl}_2(\text{PPh}_3)_2]$ was prepared *in situ* by the addition of triphenylphosphine (0.183 g, 0.699 mmol) to $\text{cis-}[\text{PtCl}_2(\text{COD})]$ (0.126 g, 0.375 mmol) in dichloromethane (10 cm^3). To this stirred solution, acetoacetamide (0.043 g, 0.42 mmol) and silver(I) oxide (0.313 g, excess) were added with additional dichloromethane (10 cm^3) and the mixture heated at reflux for 72 h. The silver salts were filtered off, yielding a deep brown solution. The solvent was removed under reduced pressure and the product recrystallised by the addition of light petroleum to a dichloromethane solution of the compound, affording a tan powder. This tan powder was isolated by filtration and dried under vacuum (0.144 g, 47%).

Elemental analysis: C, 55.1; H, 3.4; N, 1.7. $\text{C}_{39}\text{H}_{35}\text{NO}_2\text{P}_2\text{Pt}\cdot 0.5\text{CH}_2\text{Cl}_2$ requires C, 55.8; H, 4.2; N, 1.6%.

IR: $\nu(\text{CO})$ 1599 cm^{-1} (br).

m.p.: 159 - 162 $^\circ\text{C}$ (decomp.).

ES/MS (20 V): $[\text{M}+\text{H}]^+$ m/z 807, (100%).

^1H NMR: δ 7.55 - 6.95 (m, Ph), 4.85 - 4.75 [d, CH, $^2J(\text{Pt}, \text{H})$ 58], 1.24 (s, CH_3).

^{13}C - $\{^1\text{H}\}$ NMR: δ 172.9 (s, ring CO), 167.2 [s, $\text{C}(\text{O})\text{CH}_3$], 135.3 - 127.2 (m, Ph), 29.5 (s, CH_3), 24.7 [d, ring CH, $^2J(\text{P}, \text{C})$ 8].

^{31}P - $\{^1\text{H}\}$ NMR: AB spin system δ 17.10 [d, $^1J(\text{Pt}, \text{P})$ 3071, $^2J(\text{P}, \text{P})$ 24], 11.98 [d, $^1J(\text{Pt}, \text{P})$ 3643, $^2J(\text{P}, \text{P})$ 24].

2.2.8 Preparation of $[\text{Pd}\{\overline{\text{N}(\text{H})\text{C}(\text{O})\text{CHC}(\text{O})\text{CH}_3}\}(\text{bipy})]$ (2.17) from $[\text{PdCl}_2(\text{bipy})]$

In a similar reaction to that described in section 2.2.7 above, $[\text{PdCl}_2(\text{bipy})]$ (0.111 g, 0.525 mmol), acetoacetamide (0.058 g, 0.57 mmol) and silver(I) oxide (0.261 g, excess) were heated at reflux in dichloromethane (20 cm³) for 24 h. Silver salts were removed by filtration affording an orange solution. The solvent was removed under reduced pressure and the final product, a yellow microcrystalline solid, was recrystallised from dichloromethane / diethyl ether (0.087 g, 46%). A considerably large amount of water of crystallisation was observed in the ¹H NMR spectrum of this complex, effectively saturating out any other signals. This resonance was partially removed by saturation of the signal at a frequency set to that of the water resonance. Differential scanning calorimetry revealed a broad, endothermic peak at 96 to 121 °C. Upon cooling to room temperature the solid appeared unchanged. A weight loss of 0.04 mg (2% by weight) was noted.

Elemental analysis: C, 39.8; H, 3.9; N, 9.9. C₁₄H₁₃N₃O₂Pd.3H₂O requires C, 40.4; H, 4.6; N, 10.1%.

IR: $\nu(\text{CO})$ 1582 cm⁻¹ (br).

m.p.: 144 - 146 °C (decomp.).

ES/MS (20 V): $[\text{M}+\text{H}]^+$ m/z 361, (100%); $[2\text{M}+\text{H}]^+$ m/z 725, (10%).

¹H NMR: δ 8.50 - 6.75 (m, 8H, bipy), 2.10 (s, suppressed H₂O), 1.93 (s, 1H, CH), 1.37 (s, 2H, CH₃).

¹³C-¹H NMR: δ 176.7 (s, ring CO), 172.1 [s, C(O)CH₃], 160.0 - 124.2 (m, bipy), 48.4 (s, CH), 25.9 (s, CH₃).

2.2.9 Preparation of $[\text{Pd}\{\overline{\text{N}(\text{H})\text{C}(\text{O})\text{CHC}(\text{O})\text{CH}_3}\}(\text{dppe})]$ (2.18) from $[\text{PdCl}_2(\text{dppe})]$

Acetoacetamide (0.014 g, 0.14 mmol) and silver(I) oxide (0.283 g, excess) were added to a stirred solution of $[\text{PdCl}_2(\text{dppe})]$ (0.075 g, 0.013 mmol) in dichloromethane (20 cm³). The mixture was heated at reflux for 18 h. The silver salts were removed in the usual manner. The volume of solvent was reduced to ca. 2 cm³ and light petroleum added (20 cm³) to precipitate a tan solid, which was filtered and dried (0.055 g, 70%). The solid obtained was identified by ³¹P NMR spectroscopy and found to contain a mixture of products.

IR: $\nu(\text{CO})$ 1566 cm^{-1} (br, s).

m.p.: 153 - 156 °C.

ES/MS (20 V): $[\text{M}+\text{H}]^+$ m/z 603, (100%); $[\text{M}+\text{NH}_4]^+$ m/z 619, (70%).

$^{31}\text{P}\{-^1\text{H}\}$ NMR: δ 64.7 {s, *cis*- $[\text{PdCl}_2(\text{dppe})]$ }, AB spin system (major product); 57.5 [d, $^2J(\text{P}, \text{P})$ 32], 47.0 (d, $^2J(\text{P}, \text{P})$ 32), AB spin system (minor product); 57.2 [d, $^2J(\text{P}, \text{P})$ 24], 47.9 [d, $^2J(\text{P}, \text{P})$ 24].

2.2.10 X-ray diffraction study of $[\text{Pd}\{\text{N}(\text{Ph})\text{C}(\text{O})\text{CHC}(\text{O})\text{Ph}\}(\text{bipy})].\text{CH}_2\text{Cl}_2$ (**2.14**)

X-ray crystallographic data for the complex **2.14** and the details of the solution and refinement are summarised in Table 2.1. **Error! Reference source not found.** Preliminary studies were performed by X-ray precession photography, giving approximate cell dimensions and data consistent with monoclinic $\text{P2}_1/\text{c}$ space group. Accurate X-ray data were collected at the University of Auckland and were corrected for Lorentz and polarisation effects. The solution to the structure was determined by the direct methods option of SHELXS-86.¹² Atoms not located (including the dichloromethane of crystallisation) in the original difference map were located from successive electron density maps. All non-hydrogen atoms were allowed anisotropic thermal parameters, and hydrogen atoms were included in calculated positions with thermal parameters tied to 1.2 times the U_{iso} of the atom to which they are bonded. The final difference Fourier map showed significant electron density (1.96 $\text{e}.\text{\AA}^{-3}$) located near the palladium (0.91 \AA), perhaps due to a poor absorption correction.

Table 2.1 X-ray Crystallographic data for $[\text{Pd}\{\text{N}(\text{Ph})\text{C}(\text{O})\text{CHC}(\text{O})\text{Ph}\}(\text{bipy})].\text{CH}_2\text{Cl}_2$ (**2.14**)

<i>Crystal data</i>	
Empirical formula	$\text{C}_{25}\text{H}_{19}\text{N}_3\text{O}_2\text{Pd}.\text{CH}_2\text{Cl}_2$
Formula weight	584.76
Crystal system	Monoclinic
Space group	$\text{P2}_1/\text{c}$
a (\AA)	10.688(3)
b (\AA)	12.074(7)
c (\AA)	18.480(4)
β ($^\circ$)	101.81(2)

V (Å ³)	2334.3(16)
Z	4
D(c) (g cm ⁻³)	1.664

Data Collection

Diffractometer	Nonius CAD4
Radiation	Mo-K α
Crystal size (mm)	0.33 x 0.33 x 0.25
θ range for data collection (°)	1.95 to 24.95
Data collection mode	ω -scans
Index ranges	-12 \leq h \leq 0 0 \leq k \leq 13 -21 \leq l \leq 21
Reflections collected	4291
Independent reflections	4062 [R(int) = 0.0299]
Absorption coefficient (mm ⁻¹)	1.054
F(000)	1176

Structure determination and refinement

Solution by	Direct methods
Refinement method	Full-matrix least-squares on F^2
Data / restraints / parameters	4062 / 0 / 307
Goodness-of-fit on F^2	1.039
Final R indices [$I > 2\sigma(I)$]	$R_1 = 0.0562$, $wR^2 = 0.1435$
R indices (all data)	$R_1 = 0.0851$, $wR^2 = 0.1621$
Weighting Scheme:	$w = 1/[\sigma^2(F_o^2) + (0.1079P)^2 + 1.5377P]$ where $P = (F_o^2 + 2F_c^2)/3$
Largest difference peak (e.Å ⁻³)	1.957
Largest difference hole (e.Å ⁻³)	-1.643
Programs used:	
Solution by	SHELXS-86 ¹²
Refinement by	SHELXL-93 ¹³

Equation 2.1 Equations for R-factors and Goodness-of-Fit

$$R_1 = \frac{\sum ||F_o| - |F_c||}{\sum |F_o|}$$

$$wR^2 = \sqrt{\frac{\sum [w(F_o^2 - F_c^2)^2]}{\sum [w(F_o^2)^2]}}$$

$$\text{Goodness-of-Fit (on } F^2) = S = \sqrt{\frac{\sum [w(F_o^2 - F_c^2)^2]}{(n-p)}}$$

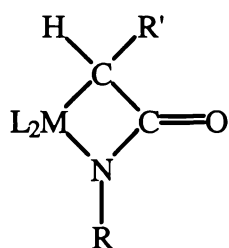
w = weighting scheme, see above

n = Number of reflections

p = number of parameters refined

2.3 Results and Discussion

Reactions of the square-planar complexes [PtCl₂(COD)], *cis*-[PtCl₂(PPh₃)₂], [PtCl₂(dppe)], [PdCl₂(dppe)] and [PdCl₂(bipy)] with 2-benzoylacetylacetone in the presence of silver(I) oxide in refluxing dichloromethane afforded in reasonably high yield, metallacyclic complexes of the type [L₂M{N(Ph)C(O)CHC(O)Ph}]. Syntheses performed using *cis*-[PtCl₂(PPh₃)₂], [PdCl₂(dppe)] and [PdCl₂(bipy)] together with acetoacetamide and silver(I) oxide also yielded metallalactam complexes of the type [L₂M{N(H)C(O)CHC(O)Me}]. The complexes *cis*-[PtCl₂(PPh₃)₂], [PtCl₂(dppe)] and [PdCl₂(dppe)] can readily be generated *in situ* or externally prior to the reaction from [PtCl₂(COD)] or [PdCl₂(COD)], giving a range of methods for the synthesis of these metallalactam complexes. These syntheses are analogous to those for the previously described platina- and palladalactam complexes (2.1, 2.2),^{1,2,3a} and again the compounds are air stable, allowing for a straightforward work-up procedure.



R = Ph, R' = C(O)Ph: **2.11** M = Pt, L₂ = COD;

2.12 M = Pt, L = PPh₃; **2.13** M = Pt, L₂ = dppe;

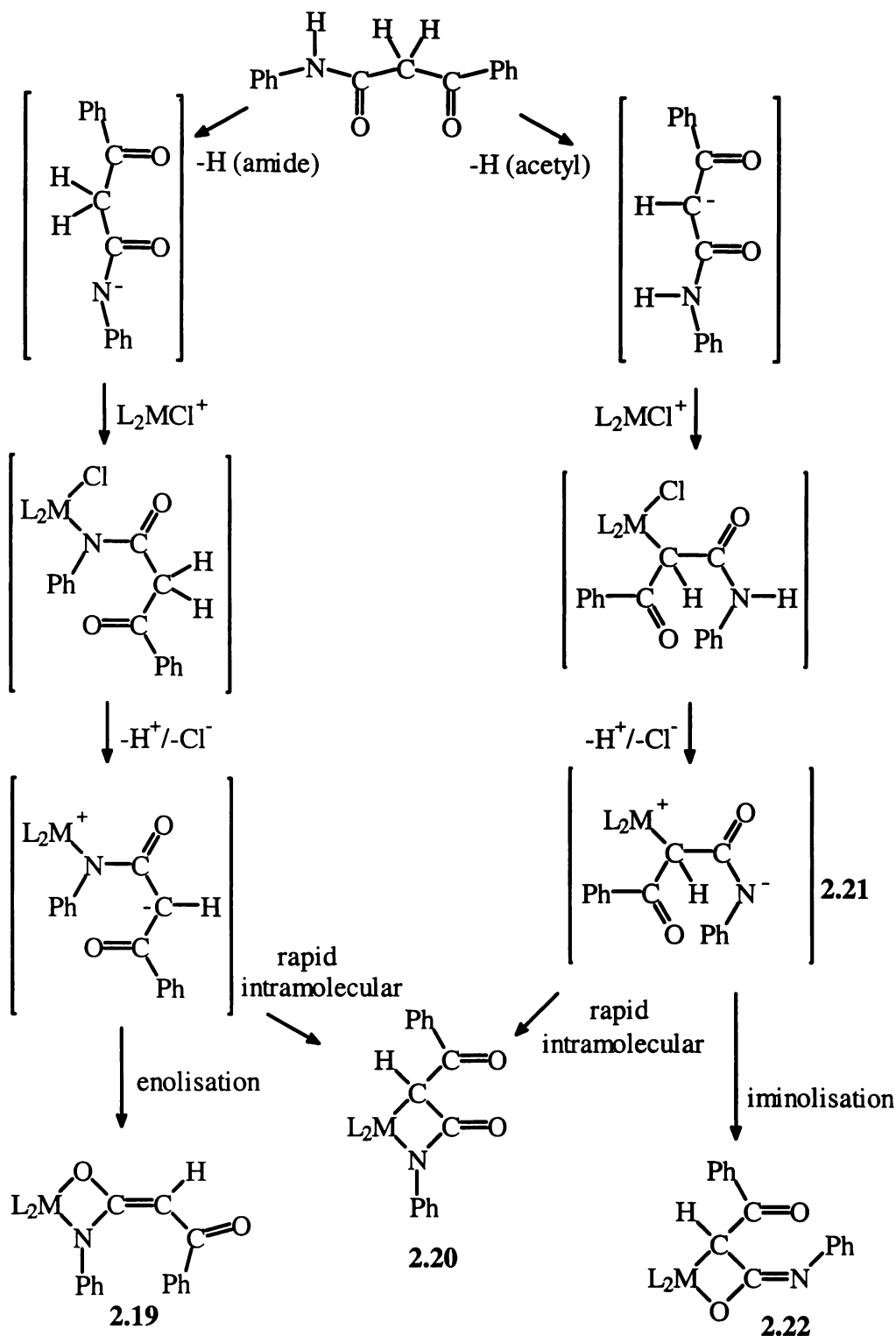
2.14 M = Pd, L₂ = bipy; **2.15** M = Pd, L₂ = dppe;

R = H, R' = C(O)Me: **2.16** M = Pt, L = PPh₃;

2.17 M = Pd, L₂ = bipy; **2.18** M = Pd, L₂ = dppe

The crystallographic study carried out indicates that 2-benzoylacetylacetone does not undergo a rearrangement to form either of the six-membered metallacyclic models (**2.9**, **2.10**) proposed earlier. Presumably the metal-nitrogen bond forms early in the reaction mechanism, which would rule out the *O, O* species (**2.10**). A concerted deprotonation of the acetyl carbon and dehalogenation of the metal would predictably be the next step in the reaction mechanism (Scheme 2.1 below). The organic fragment would either have to undergo an enolisation, producing the *N, O* bonded species (**2.9**) or alternatively a four-membered metallacyclocarbamate **2.19** or, more simply a bond between the carbon and the metal could form creating a four-membered metallalactam **2.20**. Alternatively if the acetyl carbon was deprotonated initially which then coordinated to the metal centre, a metal alkyl (**2.21**) species could be envisaged as an intermediate. This complex would then undergo further dehalogenation at the metal centre, and deprotonation at the amide nitrogen. Again a rapid intramolecular reaction would result in the formation of a metallalactam **2.20**, or enolisation could occur resulting in an iminol-type complex **2.22**.

Complex **2.16** appears to contain a proportion of water of crystallisation. NMR spectroscopy and differential scanning calorimetry suggest that solvent of crystallisation is present. ¹H NMR shows a broad peak (δ 2.10), which was suppressed to obtain data on the other environments. Differential scanning calorimetry (DSC) shows that the complex has an endothermic peak between 95 - 120 °C indicative of solvent loss from the matrix. The $[\text{Pd}\{\overline{\text{N}(\text{H})\text{C}(\text{O})\text{CHC}(\text{O})\text{CH}_3}\}(\text{bipy})]$ complex (**2.17**) otherwise appeared unaffected after treatment with heat. Elemental analysis supports the proposal that water of crystallisation is present. Water is a by-product of the reaction and while not expected to be incorporated with the metallalactam complex, is not entirely surprising. In many of the organic precursors to these metallalactam complexes an acetyl or benzoyl functionality is present. The polar carbonyl associated with these functionalities may allow hydrogen-bonding to water or another similar polar molecule to the metallalactam in the solid state. In these cases the presumed lactam hydrogen also provides an alternative site for hydrogen-bonding to a polar molecule to occur.



Scheme 2.1 Proposed four-membered metallalactam synthesis

2.3.1 X-ray Crystallography of Metallalactam Complexes

The X-ray crystal structure of $[\text{Pd}\{\overline{\text{N(Ph)C(O)CHC(O)Ph}}\}(\text{bipy})]$ (**2.14**) shows that 2-benzoylacetyl anilide, when reacted with a square-planar metal dihalide complex in the presence of silver(I) oxide forms a four-membered metallalactam (Figure 2.1), and is

similar to those described previously (2.1, 2.2).^{1,2} Neither of the two six-membered ring metallacycles (2.9, 2.10) described earlier appear to be possible reaction products. One dichloromethane of crystallisation is located in a void in the crystal lattice, and lies 3.114 Å from O(2). A least-squares mean-plane analysis of the planar four-membered ring reveals that no atom of the lactam ring and palladium co-ordination sphere [Pd, N(1), C(1), C(2), N(2) and N(3)] lies more than 0.052(7) Å [for C(2)] from that plane. O(2) is also co-planar with the lactam ring and lies 0.120(8) Å out of the plane, indicating that little in the way of η^3 -allyl bonding occurs.

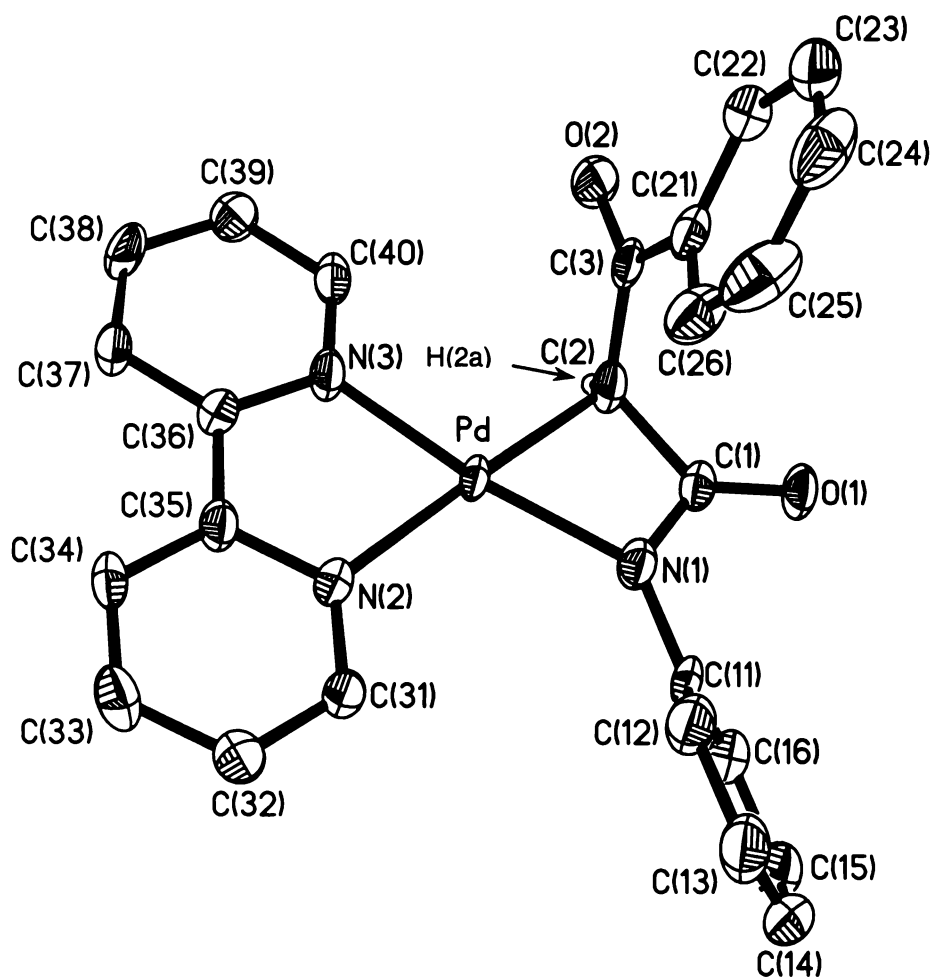
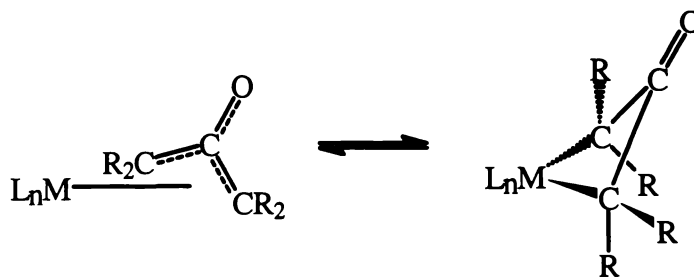


Figure 2.1 Thermal ellipsoid plot of $[\text{Pd}\{\text{N}(\text{Ph})\text{C}(\text{O})\text{CH}(\text{O})\text{Ph}\}(\text{bipy})]$ (2.14) showing atom labeling.

Thermal ellipsoids are viewed at 50% probability. Hydrogen atoms, except H2a and the dichloromethane of crystallisation have been removed for clarity.

The features of this metallacyclic ring are similar to those of the complex $[\text{Pd}\{\text{N}(\text{Ph})\text{C}(\text{O})\text{CHC}(\text{O})\text{CH}_3\}(\text{bipy})]$ (**2.2c**), reported previously.² An interesting difference between the two structures is the difference in planarity of the ring systems. The acetoacetanilide analogue (**2.2c**) has a fold angle of 17.5° through the planes defined by $\text{N}(1)\text{--Pd--C}(2)$ and $\text{N}(1)\text{--C}(1)\text{--C}(2)$.² This contrasts with the palladalactam **2.14** described here which has a smaller fold angle of $5.2(1)^\circ$ through the analogous planes (see Figure 2.2). Unlike acetylacetonate and other oxadimethylenemethane complexes, in which the metallacyclic ring is often puckered due to η^3 -allyl bonding (Scheme 2.2), these metallalactam compounds have little puckering in the ring.^{1,2,3a,14} The lack of puckering in this molecule indicates that there may be less η^3 -bonding associated with this complex, as η^3 -allyl complexes generally display considerable folding through the plane of the ring.¹⁴ It has been suggested that in the case of the acetoacetanilide palladalactam (**2.2c**) some η^3 -allyl character may have caused this folding.² Presumably the change of the functionality bonded to ring the carbon C(2) may have also aided in this slight conformational change. However, the benzoyl moiety and the N-phenyl ring both lie at an angle to the plane of the metallalactam ring [$75.4(2)$ and $60.2(2)^\circ$, respectively] giving little in the way of aid in electron delocalisation. Another plausible reason for this flattening of the metallacycle may be crystal packing forces. The transannular bond distance in complex **2.14**, from the palladium to C(1), of $2.564(6)$ Å is comparable to that of the previously reported example (**2.2c**) of this type, which has a transannular Pd·····C bond distance of $2.535(13)$ Å.²



Scheme 2.2 Canonical forms of η^3 oxadimethylenemethane complexes

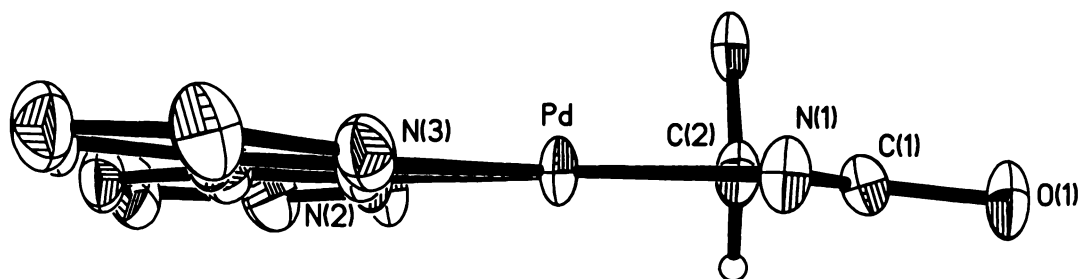


Figure 2.2 View of 2.14 showing the slight puckering of the metallalactam ring and the torsion of the bipy ligand.

As with other four-membered metallacycles^{1,2}, an acute chelate “bite” angle of 67.0(2)° is observed at the metal for the lactam functionality [N(1)–Pd–C(2)]. The rigid constraint of the geometry at the sp^2 -hybridised carbonyl carbon, C(1), is presumably a controlling factor. The bonds from the palladium to the bipyridyl nitrogen atoms, N(2) and N(3) are noticeably different. The palladium to N(2) bond, *trans* to the high *trans*-influence carbon atom C(2), is significantly longer [2.104(5) Å] than that of palladium to N(3) [2.043(5) Å] [*trans* to the low *trans*-influence nitrogen N(1)]. This effect is well known,¹⁵ and in the case of platinum phosphine complexes provides a basis for characterisation by phosphorus NMR spectroscopy (see section 2.3.2). Considerable distortion is also present about the sp^2 hybridised lactam nitrogen N(1). These deviations are most noticeable in the bond angles about this atom, with only C(1)–N(1)–C(11) [122.9(5)°] approaching the ideal of 120°. The other two bond angles are 98.0(4) and 138.3(4)° for Pd–N(1)–C(1) and Pd–N(1)–C(11), respectively. No other unusual features about the geometries of the carbon atoms and carbonyl functionalities about the lactam ring are observed.

The bond lengths and angles for the phenyl rings are unsurprising, with an average C–C bond length of 1.387 Å, and an average C–C–C bond angle of 120.0°. The 2,2'-bipyridyl ligand displays no extraordinary characteristics, with C–C bond lengths typical for an aromatic ring system (average C–C bond length 1.392 Å). The plane of the bipy ligand is twisted slightly with respect to the plane of the metallacyclic ring [4.6(1)°]. To reduce the steric strain introduced by an interaction of hydrogen atoms on

C(34) and C(37), the pyridine moieties are rotated slightly, with a $4.1(1)^\circ$ twist between the planes of the two pyridines.

Table 2.2 Selected bond lengths (Å) and bond angles ($^\circ$) for [Pd{N(Ph)C(O)CHC(O)Ph}(bipy)].CH₂Cl₂ (**2.14**)

Pd–N(1)	2.021(5)	Pd–N(3)	2.042(5)
Pd–C(2)	2.053(6)	Pd–N(2)	2.104(5)
Pd·····C(1)	2.564(6)	N(1)–C(1)	1.324(8)
N(1)–C(11)	1.420(8)	O(1)–C(1)	1.239(7)
O(2)–C(3)	1.249(7)	C(1)–C(2)	1.521(8)
C(2)–C(3)	1.483(9)	C(3)–C(21)	1.485(9)
N(1)–Pd–N(3)	169.7(2)	N(1)–Pd–C(2)	67.0(2)
N(3)–Pd–C(2)	103.0(2)	N(1)–Pd–N(2)	110.7(2)
N(3)–Pd–N(2)	79.25(19)	C(2)–Pd–N(2)	177.7(2)
N(1)–Pd·····C(1)	30.7(2)	N(3)–Pd·····C(1)	139.1(2)
C(2)–Pd–C(1)	36.4(2)	N(2)–Pd·····C(1)	141.41(19)
C(1)–N(1)–C(11)	122.9(5)	C(1)–N(1)–Pd	98.0(4)
C(11)–N(1)–Pd	138.3(4)	O(1)–C(1)–N(1)	129.6(6)
O(1)–C(1)–C(2)	126.0(6)	N(1)–C(1)–C(2)	104.3(5)
O(1)–C(1)·····Pd	176.2(5)	N(1)–C(1)·····Pd	51.3(3)
C(2)–C(1)·····Pd	53.2(3)	C(3)–C(2)–C(1)	121.2(5)
C(3)–C(2)–Pd	112.7(4)	C(1)–C(2)–Pd	90.4(4)
O(2)–C(3)–C(2)	118.1(6)	O(2)–C(3)–C(21)	119.0(6)
C(2)–C(3)–C(21)	122.9(5)		

2.3.2 Nuclear Magnetic Resonance Spectroscopy of metallalactam complexes

Where applicable, the success of a reaction was determined by ^{31}P NMR. Phosphorus NMR, when coupled with spin $\frac{1}{2}$ ^{195}Pt nuclei, is a powerful tool for analysing the outcome of a reaction due to the *trans*-influence that various atoms have on the $^1J(\text{Pt}, \text{P})$ coupling constants. Miyamoto *et al.* have studied the differing *trans*-influences that a variety of atoms have on the $^1J(\text{Pt}, \text{P})$ coupling constants of trialkylphosphine

platinum(II) complexes.¹⁶ However, the coupling constants for trialkylphosphine platinum(II) complexes tend to be smaller than those observed for triarylphosphine platinum(II) complexes.^{1,2,3} In conjunction with the previously reported NMR characteristics of these metallalactam complexes, any new compound can be quickly and easily identified.

The ³¹P NMR spectra of **2.12**, **2.13**, **2.15**, **2.16** and **2.18** show the characteristic AB doublet of doublets spin system associated with two inequivalent phosphorus atoms. The ¹J(Pt, P) coupling constants for a phosphorus nucleus *trans* to a carbon atom is of the order of 2500 Hz for a triphenylphosphine or 1,2-bis(diphenylphosphino)ethane ligand. For a phosphorus atom *trans* to a nitrogen atom the coupling constant rises to 3400 - 3700 Hz. The organic substituents bonded to the phosphorus atom have some effect on these constants, so for comparison triphenylphosphine was used as the primary ligand. Miyamoto *et al.* used triethylphosphine¹⁶ in their study of the *trans*-influence of carbon, nitrogen and oxygen, giving marginally lower ¹J(Pt, P) coupling constants than are found here. For complex **2.12** the ¹J(Pt, P) coupling constants (2351 and 3733 Hz) are as expected for triphenylphosphine phosphorus atoms *trans* to carbon and nitrogen, respectively (Figure 2.3).¹ The ²J(P, P) couplings for bis(triphenylphosphine) metallalactam complexes are typically 17-25 Hz,^{1,2} which were observed here also. 1,2-Bis(diphenylphosphino)ethane platinalactam complexes often display small ²J(P, P) coupling constants,¹ and in complex (**2.13**) these are smaller than the resolution of the NMR spectrometer and are only identifiable as satellites by a broadening of the main resonance. The ¹J(Pt, P) couplings are as would normally be expected (P *trans* to C 2607 and P *trans* to N 3234 Hz).

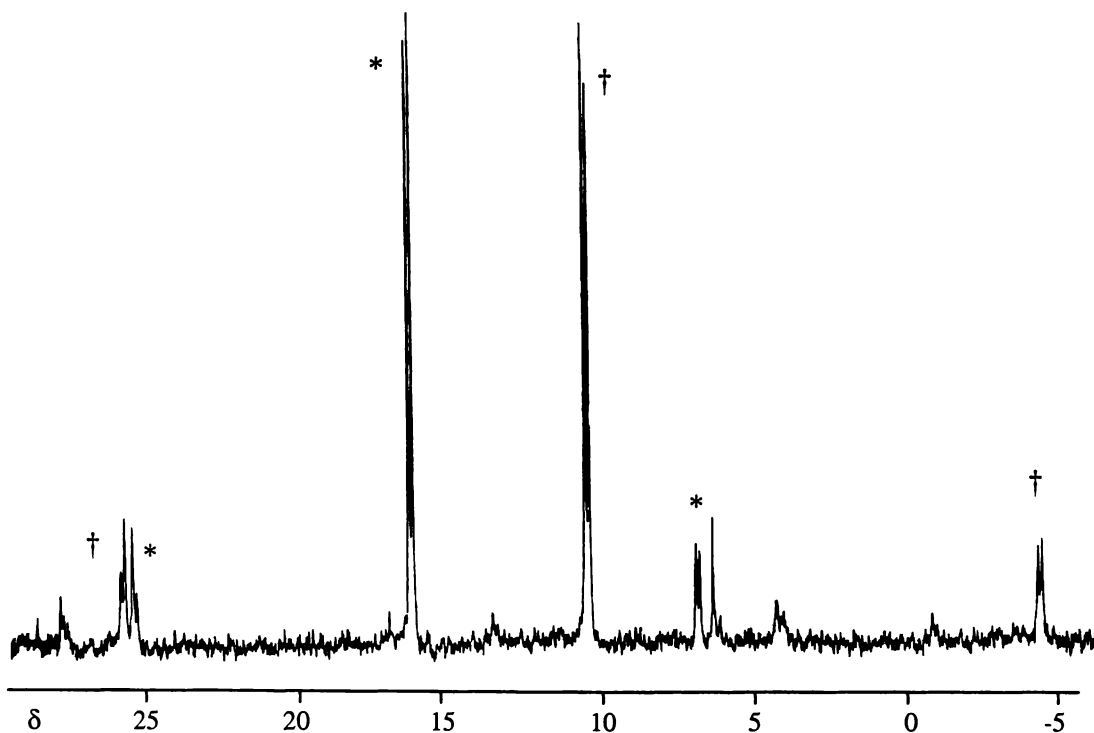


Figure 2.3 Representative ^{31}P NMR spectrum of $[\text{Pt}\{\text{N}(\text{Ph})\text{C}(\text{O})\text{CHC}(\text{O})\text{Ph}\}(\text{PPh}_3)_2]$ (2.12)

The ^{31}P NMR spectrum of complex (2.15) has an AB spin system as its only feature. Palladium has no spin $\frac{1}{2}$ nuclei, therefore no satellites are observed. As with other palladalactam complexes the resonances are observed further downfield (δ 51.6 and 47.3), than those of the (dppe)-platinalactam complexes (typically around δ 45 and 35).^{3a}

The $[\text{Pt}\{\text{N}(\text{Ph})\text{C}(\text{O})\text{CHC}(\text{O})\text{Ph}\}(\text{COD})]$ complex (2.11) shows features in the ^{13}C NMR that have been previously described in metallalactam complexes of this type.¹ The asymmetry of the lactam ring is sufficient to cause all of the COD carbon atoms to be in different environments. Further assignment of these carbons is also possible through the varying *trans*-influences that carbon and nitrogen effect on the $^1J(\text{Pt}, \text{C})$ and $^2J(\text{Pt}, \text{C})$ coupling constants. The resonances at δ 106.6 and 105.8 are due to the ethylene carbons *trans* to the ring carbon C(1) and the coupling constants for these resonances [$^1J(\text{Pt}, \text{C})$ 62] also reflect an effect from a high *trans*-influence atom. The other ethylene carbon signals (δ 87.9 and 86.1) are due to the carbon atoms *trans* to the lactam ring nitrogen. Additionally the lactam ring carbon is tetrahedral, causing the COD carbons to be in inequivalent environments through the plane of the molecule.

This effect is observed with the COD methylene carbons which gives rise to four individual peaks. Two of the peaks (δ 32.3 and 30.5) have a slight broadening at the base of the peak which is unresolved $^2J(\text{Pt}, \text{C})$ coupling, indicating that they are likely to be *trans* to the low *trans*-influence ring nitrogen.

The carbon NMR spectra of the bis(triphenylphosphine)- and (dppe)-platinalactam complexes (**2.12** and **2.13**) also display similar features to those of the COD-platinalactam (**2.11**). Only one $^3J(\text{P}, \text{C})$ coupling is observed for the carbonyl resonances [$^3J(\text{P}, \text{C})$ 7 and 8 Hz for **2.12** and **2.13** respectively]. Presumably the $^3J(\text{P}, \text{C})$ coupling constants for both phosphorus atoms are similar, resulting in a slight broadening of the doublets observed. The carbonyl signals have 2J and 3J coupling to platinum and phosphorus respectively, however the phosphorus coupling to the ring carbonyl is somewhat stronger than that of the side-chain carbonyl, presumably due to the connectivity of these two atoms. For example $[\text{Pt}\{\text{N}(\text{Ph})\text{C}(\text{O})\text{CHC}(\text{O})\text{Ph}\}(\text{PPh}_3)_2]$ (**2.12**) has a $^2J(\text{Pt}, \text{C})$ coupling of 75 Hz to the ring carbonyl resonance, while the benzoyl carbonyl resonance only has a $^2J(\text{Pt}, \text{C})$ of 32 Hz.

The ring CH signal also provides information on the strengths of *trans* coupling as opposed to *cis* coupling. The 2J coupling to the *trans* phosphorus is 64 Hz, while the *cis* coupling is not resolved. The 1J coupling to platinum is about 400 Hz as seen in other similar complexes.^{1-3a}

Perhaps the most interesting feature of the proton NMR is the ring CH proton. In the platinum complexes a 2J coupling to platinum is observed; typically these satellites have a coupling constant of 50 - 100 Hz.¹ In the bis(triphenylphosphine)- and (dppe)-platinalactam complexes (**2.12** and **2.13**) the ring proton displays an AXX' type spin system, arising from coupling to the two inequivalent phosphorus atoms in a similar manner to that seen by the phosphorus atoms in the phosphorus NMR spectra. The larger $^3J(\text{P}, \text{H})$ coupling constant for complexes **2.12** and **2.13** (4.9 and 9.1 Hz, respectively) is presumably due to coupling to the *trans* phosphorus. Due to the lack of phosphorus in the COD platinalactam (**2.11**) only platinum satellites are observed on the ring proton resonance.

The proton NMR spectra of the acetoacetamide derived metallalactam complexes (**2.16** – **2.18**) show no unusual feature. However, due to the fact that there are only three

environments in the acetoacetamide moiety this is not surprising. The amide proton resonance is noteworthy by its absence from these spectra. In the spectrum of the parent acetoacetamide compound, the amide resonance is small and broad, evidence of solvent exchange. This too may occur in these metallalactam complexes reducing the signal's intensity.

The NMR spectra of complex **2.16** are somewhat surprising in that only a few couplings are observed in both the proton and carbon spectra. The ring CH resonance (δ 4.85 - 4.75) only shows a $^2J(\text{Pt}, \text{H})$ coupling. Any phosphorus coupling was noted as a slight broadening of the resonances of this doublet, while in the carbon NMR spectrum of this complex no phosphorus or platinum couplings are observed to the ring carbonyl or acetyl carbon. The ring carbonyl carbon is broad in the carbon spectrum of complex **2.16**, which may be unresolved 3J phosphorus-carbon coupling. The platinum satellites were not resolved from the background.

The ^{31}P NMR spectrum of the products of complex **2.18** shows that at least three complexes are evident; one at δ 64.7, is unreacted *cis*-[PdCl₂(dppe)]. ES/MS of the product mix indicates that the species present have the same mass and are indistinguishable from one another by this method. Fractional crystallisation of the products was also unsuccessful in separating the two remaining compounds.

2.3.3 *Electrospray Mass Spectrometry of metallalactam complexes*

2.3.3.1 *Overview of Electrospray Mass Spectrometry*

Electrospray mass spectrometry is a relatively new technique for the analysis of a variety of compounds, ranging from proteins to organometallic and inorganic complexes.¹⁷ This technique allows the analysis of involatile compounds to be undertaken. Unlike other mass spectrometry methods, the ionisation that occurs in electrospray mass spectrometry is of a "soft" nature. Two methods of analysis are available, positive and negative ion modes. Compounds observed under positive ion mode conditions generally accept a proton from the carrier solvent forming an $[\text{M}+\text{H}]^+$ species. In negative ion mode a proton is lost to the solvent. In this study positive ion

mode was used exclusively. The complexes in this study readily accept a proton from the carrier solvent ($\text{CH}_3\text{CN} / \text{H}_2\text{O}$); the electronegative carbonyl oxygen atoms are ideal for acquiring a proton. Some of the complexes also accept an ammonium cation, forming an $[\text{M}+\text{NH}_4]^+$ species. Ammonia is present in the acetonitrile as a stabiliser. Aggregation of two or more complexes, giving $[2\text{M}+\text{H}]^+$, $[3\text{M}+\text{H}]^+$ or higher species, is sometimes observed with organometallic compounds. Often, upon fragmentation, a coordination site becomes available on the metal centre. Two proposals for the filling of this vacant site are by the formation of an intramolecular bond with an existing moiety e.g. the formation of a dative bond with a carbonyl oxygen, or by coordination of a solvent molecule to the vacant site. Conditions within the spectrometer can be altered to induce fragmentation (increased cone voltage), which provides information about the connectivity of the molecule or to improve the sensitivity (increased mass resolution) which gives an isotopic distribution pattern for the observed species. ES/MS is an ideal analytical tool to identify compounds of a low to medium molecular weight (*ca.* 1000 Da), this mass allows identification of the parent ion, and is within the mass range of the quadrupole analyser to observe whether or not any aggregate species have also formed.

2.3.3.2 ES/MS studies of 2-benzoylacetanilide metallalactam complexes

Under mild electrospray conditions (cone voltage = 20V) these compounds readily form an $[\text{M}+\text{H}]^+$ species in solution (Figure 2.4). At low cone voltages (e.g. 20 V) little fragmentation of the molecules is evidenced, instead these molecules form aggregates of $[2\text{M}+\text{H}]^+$ and to a lesser extent $[3\text{M}+\text{H}]^+$ along with a very small amount of $[4\text{M}+\text{H}]^+$ species.

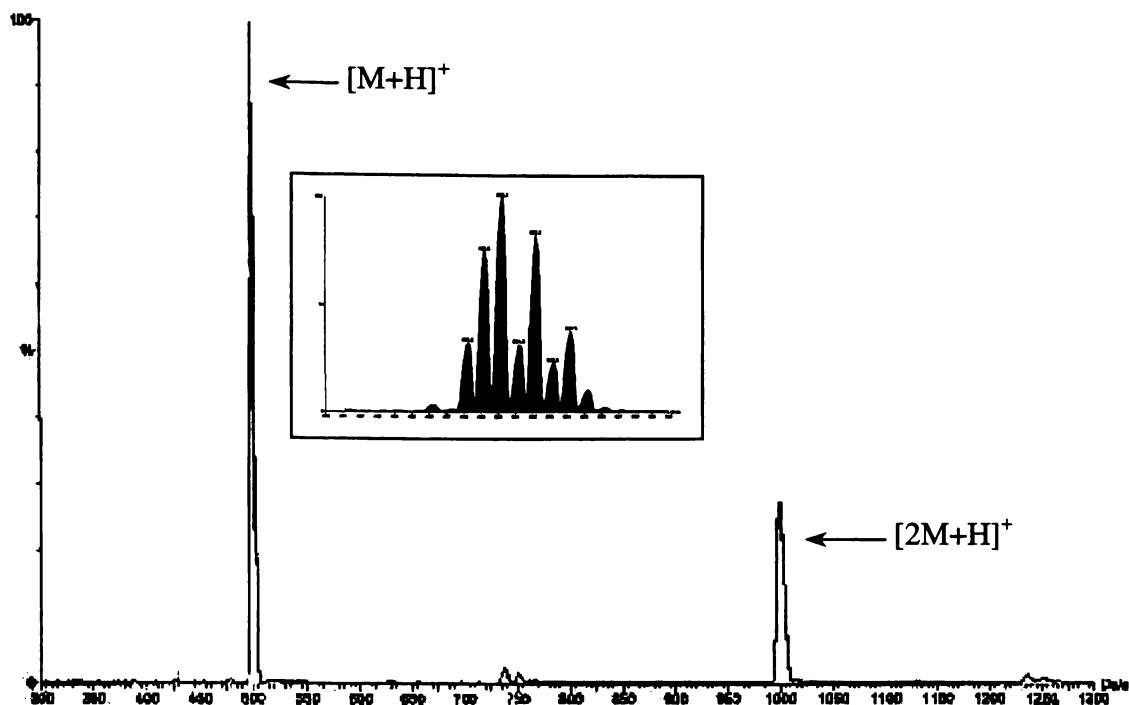


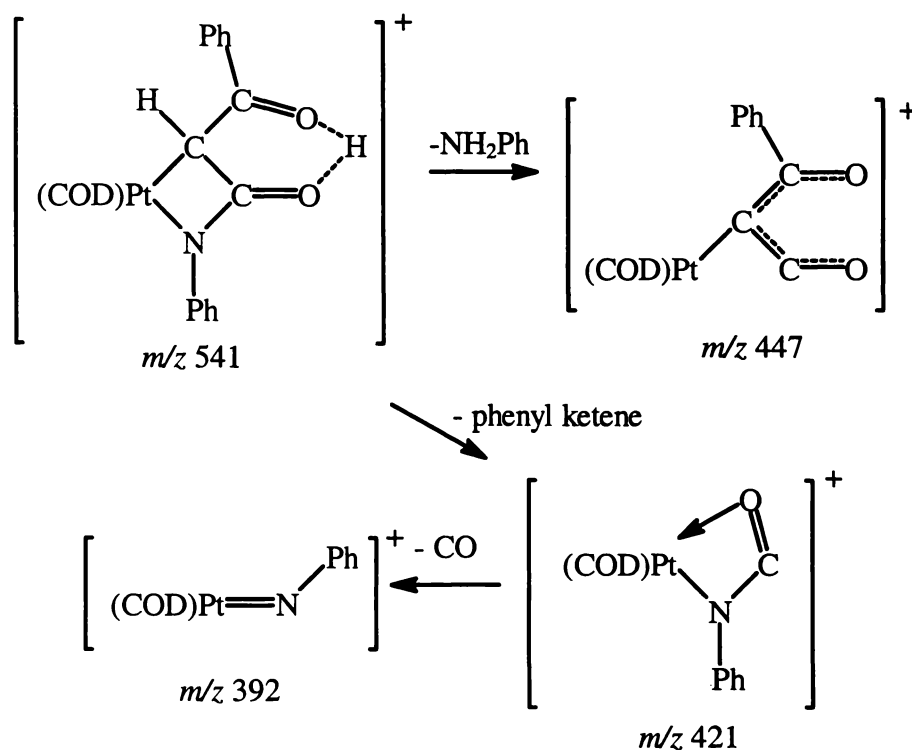
Figure 2.4 Representative ES/MS spectrum of $[\text{Pd}\{\text{N}(\text{Ph})\text{C}(\text{O})\text{CHC}(\text{O})\text{Ph}\}(\text{bipy})]$ (**M**) (2.14)

Inset shows isotope pattern for $[\text{M}+\text{H}]^+$ peak at m/z 499.

The $[\text{Pt}\{\text{N}(\text{Ph})\text{C}(\text{O})\text{CHC}(\text{O})\text{Ph}\}(\text{COD})]$ complex (**2.11**) shows two major peaks at low cone voltage (20 V), the base peak, $[\text{M}+\text{H}]^+$, at m/z 541 (100%) and an aggregation $[\text{2M}+\text{H}]^+$ peak at m/z 1081 (40%). No other peaks are observed for this complex at this voltage. When the cone voltage is increased to 90V fragmentation of the species is induced (summarised in table 2.3). The parent $[\text{M}+\text{H}]^+$ ion at m/z 541 is slightly reduced in intensity to 40% and the most intense peak at m/z 447 corresponds to the loss of $[\text{NHPH}]^-$ from the complex forming a $[\text{Pt}\{\text{C}(\text{C}(\text{O}))\text{C}(\text{O})\text{Ph}\}(\text{COD})]^+$ species. Loss of phenyl ketene from the parent molecule results in the peak observed at m/z 421 $[\text{Pt}\{\text{N}(\text{Ph})\text{C}(\text{O})\}(\text{COD})]^+$. This species can lose carbon monoxide giving the m/z 392 peak (40% intensity). Eventually loss of the amide occurs, leaving only the $[\text{PtH}(\text{COD})]^+$ moiety [m/z 302 (30%)] (see scheme 2.3).

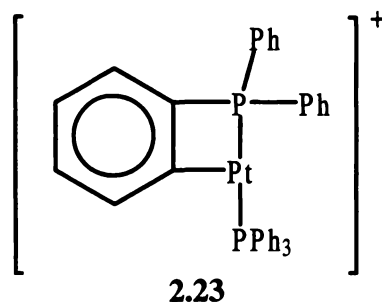
Table 2.3 Fragmentation pattern of $[\text{Pt}\{\text{N}(\text{Ph})\text{C}(\text{O})\text{CHC}(\text{O})\text{Ph}\}(\text{COD})]$ at cone voltage = 90 V

Species	Mass (m/z)	Relative Intensity (%)
$[\text{Pt}\{\text{N}(\text{Ph})\text{C}(\text{O})\text{CHC}(\text{O})\text{Ph}\}(\text{COD})+\text{H}]^+$	541	40
$[\text{Pt}\{\text{C}(\text{C}(\text{O}))\text{C}(\text{O})\text{Ph}\}(\text{COD})]^+$	447	100
$[\text{Pt}\{\text{N}(\text{Ph})\text{C}(\text{O})\}(\text{COD})]^+$	421	20
$[\text{Pt}\{\text{N}(\text{Ph})\}(\text{COD})]^+$	392	40
$[\text{Pt}(\text{COD})\text{H}]^+$	302	30

**Scheme 2.3** Proposed fragmentation of $[\text{Pt}\{\text{N}(\text{Ph})\text{C}(\text{O})\text{CHC}(\text{O})\text{Ph}\}(\text{COD})]$ (**2.11**) at 90 V

In the case of $[\text{Pt}\{\text{N}(\text{Ph})\text{C}(\text{O})\text{CHC}(\text{O})\text{Ph}\}(\text{PPh}_3)_2]$ (**2.12**), loss of the lactam moiety appears to induce a PPh_3 cyclometallation reaction. Presumably one of the phenyl rings on triphenylphosphine can cyclometallate to the platinum atom, forming a stable four-membered metallacycle (**2.23**). This gives rise to an $[\text{M}]^+$ species of m/z 718 often observed in electrospray mass spectra of bis(triphenylphosphine) platinum(II)

compounds.¹⁸ This is a tentative assignment of the m/z 718 peak as it is only observed under electrospray mass spectrometry conditions.



Fragmentation of the complexes is not always similar. For example complex **2.13** has a more straightforward fragmentation pathway at a cone voltage of 90V as outlined in table 2.4. The predominant peak is due to the parent ion $[M+H]^+$, $M = [Pt\{N(Ph)C(O)CHC(O)Ph\}(dppe)]$, at m/z 831 and at m/z 738 (20%) is a peak corresponding to loss of $[NHPh]^+$, as observed previously. The second most intense peak (50%) appears at m/z 685, presumably due to $[Pt\{N(Ph)\}(dppe)]^+$. No evidence of a $[Pt\{N(Ph)C(O)\}(dppe)]$ species is observed. Two small peaks at m/z 594 and 610 (5 and 10 % respectively) are attributed to cyclometallated $[Pt(dppe)]^+$ and cyclometallated $[Pt(dppe)+NH_3]^+$. Presumably, the bis(diphenylphosphino)ethane ligand can cyclometallate in a manner similar to, but less easily than, that observed for triphenylphosphine ligands.

Table 2.4 Fragmentation of $[Pt\{N(Ph)C(O)CHC(O)Ph\}(dppe)]$ (**2.13**) at cone voltage = 90V

<i>Species</i>	<i>Mass (m/z)</i>	<i>Relative Intensity (%)</i>
$[Pt\{N(Ph)C(O)CHC(O)Ph\}(dppe)+H]^+$	831	100
$[Pt\{C(C(O))C(O)Ph\}(dppe)]^+$	738	20
$[Pt\{N(Ph)\}(dppe)]^+$	685	50
cyclometallated $[Pt(dppe)+NH_3]^+$	610	10
cyclometallated $[Pt(dppe)]^+$	594	5

18 a) J. Fawcett, W. Henderson, R. D. W. Kemmitt, D. R. Russell and A. Upreti, *J. Chem. Soc., Dalton Trans.*, (1996), 1897; b) J. M. Law, W. Henderson and B. K. Nicholson, *J. Chem. Soc., Dalton Trans.*, (1997), 4587

2.3.3.3 ES/MS of acetoacetamide complexes

The acetoacetamide complexes (**2.16** – **2.18**) show similar electrospray behaviour to the benzoylacetanilide complexes described above. At low cone voltages the parent $[M+H]^+$ ion is observed as the major peak. Associated with this is a $[2M+H]^+$ ion. At higher voltages (*ca.* 70V) the acetoacetamide moiety becomes fragmented as outlined in Table 2.5. The fragmentation of the acetoacetamide complex **2.17** is not as straightforward as that of the benzoylacetanilide derivatives. Several fragmentation pathways are possible which result in ionic species that have the same m/z ratio. However, even under these forcing conditions an appreciable amount of the parent $[M+H]^+$ species survives.

Table 2.5 Fragmentation pattern of $[\text{Pd}\{\text{N}(\text{H})\text{C}(\text{O})\text{CHC}(\text{O})\text{CH}_3\}(\text{bipy})]$ (**2.17**) at cone voltage = 70 V

<i>Species</i>	<i>Mass (m/z)</i>	<i>Relative intensity (%)</i>
$[\text{Pd}\{\text{N}(\text{H})\text{C}(\text{O})\text{CHC}(\text{O})\text{CH}_3\}(\text{bipy})+\text{H}]^+$	362	80
$[\text{Pd}\{\text{C}(\text{C}(\text{O}))\text{C}(\text{O})\text{CH}_3\}(\text{bipy})]^+$	or 345	10
$[\text{Pd}\{\text{N}(\text{H})\text{C}(\text{O})\text{CHC}(\text{O})\}(\text{bipy})]^+$		
$[\text{Pd}\{\text{C}(\text{C}(\text{O})\text{C}(\text{O}))\}(\text{bipy})]^+$	331	30
$[\text{Pd}\{\text{CC}(\text{O})\text{CH}_3\}(\text{bipy})]^+$	or 319	10
$[\text{Pd}\{\text{N}(\text{H})\text{C}(\text{O})\text{CH}\}(\text{bipy})]^+$		
$[\text{Pd}\{\text{CC}(\text{O})\}(\text{bipy})]^+$	300	100
$[\text{Pd}\{\text{N}(\text{H})\}(\text{bipy})]^+$	277	20

2.4 Conclusion

Silver(I) oxide has proven to be a consistently effective reagent for the synthesis of a wide variety of small four-membered metallacycles, with consistently predictable products. 2-Benzoylacetanilide does not appear to undergo any intramolecular rearrangement during the course of the reaction, which would have given one of two proposed six-membered heterocycles (**2.9**, **2.10**). Instead the four-membered metallalactam is formed as characterised by a single crystal X-ray diffraction study. Easy analysis of the reaction products is facilitated by both multinuclear NMR spectroscopy and by the relatively new technique of electrospray mass spectrometry.

With further pursuit, the limited success of the reaction of acetoacetamide with a selection of metal dihalide complexes may be transformed into a novel way for the synthesis of *N*-unsubstituted four-membered metallalactams. This in turn could lead to further functionalisation resulting in synthetically useful compounds.

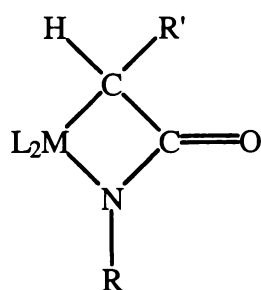
However, the mechanism of silver(I) oxide mediated reactions is still not well understood. Though silver(I) oxide is relatively cheap to prepare, an alternative base may also mediate the synthesis of four-membered metallalactams. The following chapters will discuss these investigations.

Chapter Three. Isolation of a platinum amide intermediate in silver(I) oxide mediated syntheses of platinalactam complexes

3.1 Introduction

Silver(I) oxide mediated syntheses are an established method for the preparation of a wide variety of late transition metal metallacycles.^{1,2} However, little is known about the mechanism of these reactions. Silver(I) oxide mediated reactions proceed under mild conditions and as yet no species has been isolated which could be proposed as an intermediate in the metallacyclisation process.

The synthesis and characterisation of a four-membered platinalactam complex (**3.1a**) has been reported.¹ The organic reagent employed in that synthesis was *N*-cyanoacetylurethane. The characterised complex (**3.1a**) had 1,5-cyclooctadiene as the ancillary ligand, which gave access to a range of complexes with various alternative ancillary ligands, including the triphenylphosphine derivative (**3.1b**).¹ The compound [PdCl₂(PPh₃)₂], a mixture of *cis* and *trans* isomers in solution, when reacted with *N*-cyanoacetylurethane in the presence of silver(I) oxide was found to form the complex *trans*-[Pd{N(C(O)CH₂CN)(CO₂Et)}Cl(PPh₃)₂] (**3.2**).³



3.1a M = Pt; L₂ = COD, R = CN, C(O)Ph, C(O)CH₃, R' = CO₂Et, Ph, H

b) L = PPh₃, R = CN, C(O)Ph, C(O)CH₃, R' = CO₂Et, Ph, H

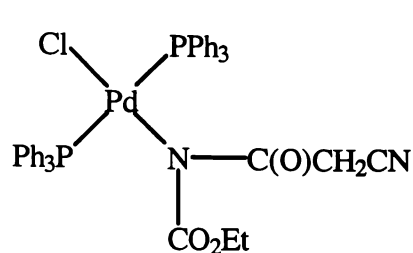
c) L₂ = dppe, R = CN, C(O)Ph, C(O)CH₃, R' = CO₂Et, Ph, H

d) M = Pd; L₂ = dppe, R = CN, C(O)Ph, C(O)CH₃, R' = CO₂Et, Ph, H

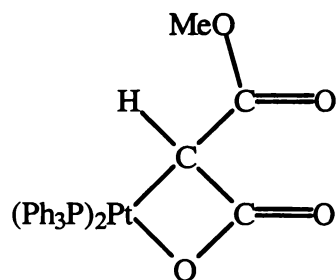
1 W. Henderson, A. G. Oliver and B. K. Nicholson, *J. Chem. Soc., Dalton Trans.*, (1994), 1831

2 See for example: a) W. Henderson, R. D. W. Kemmitt, L. J. S. Prouse and D. R. Russell, *J. Chem. Soc., Dalton Trans.*, (1989), 259; b) W. Henderson, R. D. W. Kemmitt and A. L. Davis, *J. Chem. Soc., Dalton Trans.*, (1993), 2247; c) M. B. Dinger and W. Henderson, *J. Organomet. Chem.*, (1997), 547; d) D. A. Clarke, R. D. W. Kemmitt, M. A. Mazid, D. R. Russell, M. D. Shilling and L. J. S. Sherry, *J. Chem. Soc., Dalton Trans.*, (1984), 243

3 W. Henderson, B. K. Nicholson and A. G. Oliver, *Polyhedron*, (1994), 13, 3099

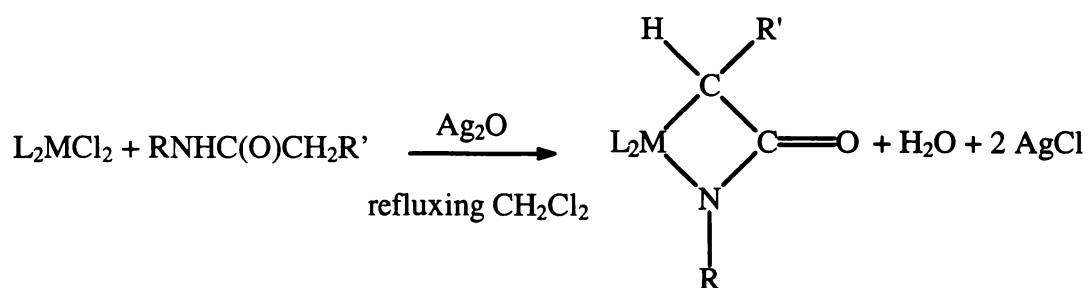


3.2



3.3

Silver(I) oxide acts as both a halide abstractor and as a strong base (Scheme 3.1). It is not known if the reaction occurs at the surface of suspended silver(I) oxide, or if a sparingly soluble silver complex is involved in the reaction. The formation of insoluble silver chloride is a driving force for the equilibrium, and would be contributing factor for product formation in either of these hypotheses.



Scheme 3.1 General metallalactam synthesis

NMR studies of reactions of dimethylmalonate with *cis*-PtCl₂(PPh₃)₂ in the presence of silver(I) oxide show that at intermediate times (24 h.) a complex mixture of compounds is present in the reaction solution. Although the reaction here is slightly different, and must involve hydrolysis or dealkylation of the dimethylmalonate, it suggests that silver(I) oxide reactions do not follow a simple pathway. At the completion of the reaction (48 h.) only one product, the platinalactone (3.3), is present.⁴ The reaction may be stepwise, with either the (lactam) oxygen or (lactam ring) carbon atom of the organic ligand bonding to the metal centre followed by deprotonation of the other heteroatom to form the metallacycle or effectively concerted, with the metallacycle forming in its entirety at the reaction site. Though dimethylmalonate appears to follow a complicated

4 W. Henderson, R. D. W. Kemmitt and A. L. Davis, *J. Chem. Soc., Dalton Trans.*, (1993), 2247

reaction pathway, this may not be true for other systems. By comparison, the reaction of *N*-cyanoacetylurethane with square-planar L_2MCl_2 complexes is known to yield well characterised metallalactam complexes (3.1) for long (18 h.) reaction times. However, there have been no studies undertaken to determine what products are present for short reaction times for reactions involving amides.

3.2 Experimental

Syntheses were performed as described previously. $[PtCl_2(COD)]^5$ and silver(I) oxide⁶ were prepared by standard literature procedures. Triphenylphosphine (Pressure Chemical Co.), mercuric oxide (May and Baker Ltd.), 1,5-cyclooctadiene, cuprous oxide, sodium hydride, sodium tetraphenylborate (BDH), pyridine (Sigma), 2-benzoylacetylurethane and *N*-cyanoacetylurethane (Aldrich) were used as supplied. Dichloromethane and light petroleum (40 – 60 °C) were distilled from CaH_2 , and tetrahydrofuran and diethyl ether from sodium benzophenone ketyl before use. Methanol (AR grade) was used as supplied and acetone (LR grade) was distilled over magnesium sulfate prior to use. NMR spectra were recorded on a Brüker AC300P (1H , ^{13}C - $\{^1H\}$ and ^{31}P - $\{^1H\}$) and JEOL FX90Q (^{31}P - $\{^1H\}$). Spectra were recorded at 300.133 MHz for 1H and 75.47 MHz for ^{13}C - $\{^1H\}$ referenced to internal TMS (δ 0.00) with a $CDCl_3$ lock. ^{31}P - $\{^1H\}$ spectra were recorded at 121.74 and 36.23 MHz respectively, in CH_2Cl_2 , with a D_2O lock, referenced to external 85% H_3PO_4 (δ 0.00). Infrared spectra were recorded on a Bio-Rad FTS-40 infrared spectrometer as solid KBr discs. Melting points were obtained from a Reichert Thermopan apparatus and are uncorrected. X-ray intensity data were collected on a Nicolet R3 Automatic Diffractometer at the University of Canterbury. Elemental analysis data were collected at the University of Otago Microanalytical Unit. Electrospray mass spectra were collected on a VG Platform II Mass Spectrometer with an acetonitrile (HPLC grade)/water (doubly distilled, deionised) (50:50) carrier solvent.

5 J. X. McDermott, J. F. White and G. M. Whitesides, *J. Am. Chem. Soc.*, (1976), **98**, 6521

6 H. L. Riley and H. B. Baker, *J. Chem. Soc.*, (1960), 1378

3.2.1 Synthesis of *cis*-[Pt{N(C(O)CH₂CN)(CO₂Et)}Cl(PPh₃)₂] (3.4)

To a stirred solution of [PtCl₂(COD)] (0.201 g, 0.537 mmol) in dichloromethane (20 cm³), was added triphenylphosphine (0.284 g, 1.08 mmol), *N*-cyanoacetylurethane (0.085 g, 0.54 mmol) and silver(I) oxide (0.273 g, excess). The mixture was stirred for 15 minutes and filtered to remove silver salts. The filtrate volume was reduced under reduced pressure and the product precipitated by the addition of light petroleum. The precipitate was collected by filtration and dried under reduced pressure (yield 0.425 g, 87%). Crystals of single crystal X-ray diffraction quality were obtained from dichloromethane / diethyl ether by liquid / liquid diffusion.

Elemental analysis: C, 55.3; H, 4.0; N, 2.9. Calculated C₄₂H₃₇N₂ClO₃P₂Pt: C, 55.4; H, 4.1; N, 3.1%.

IR: $\nu(\text{CN})$ 2255 cm⁻¹; $\nu(\text{CO})$ 1689, 1638 cm⁻¹.

m.p: 200 - 203°C (decomp.).

ES/MS (20 V): [M-Cl+CH₃CN]⁺ m/z 915, (92%); [M-Cl]⁺ m/z 874, (100%).

¹H NMR: δ 7.8 - 7.6 (m, 30H, Ph), AB spin system 4.26 [dq, 2H, diastereotopic ethyl CH₂ (H5a), ² $J(\text{H}, \text{H})$ 11, ³ $J(\text{H}, \text{H})$ 7], 4.05 [dq, 2H, diastereotopic ethyl CH₂ (H5b) ² $J(\text{H}, \text{H})$ 11, ³ $J(\text{H}, \text{H})$ 7], AB spin system 3.69 [d, 1H, diastereotopic CH₂CN (H2a), ² $J(\text{H}, \text{H})$ 20], 2.86 [d, 1H, diastereotopic CH₂CN (H2b), ² $J(\text{H}, \text{H})$ 20], 1.50 [t, 3H, ethyl CH₃, ³ $J(\text{H}, \text{H})$ 7].

¹³C-¹H NMR: δ 168.8 (s, ester CO); 158.2 (s, acetyl CO); 136 - 127 (m, Ph); 116.3 (s, CN), 61.4 (s, ethyl CH₂); 53.5 (s, CH₂CN); 14.9 (s, ethyl CH₃).

³¹P-¹H: AB spin system δ 14.20 [d, P *trans* Cl, ¹ $J(\text{Pt}, \text{P})$ 3957, ² $J(\text{P}, \text{P})$ 20]; 7.07 [d, P *trans* N, ¹ $J(\text{Pt}, \text{P})$ 3330, ² $J(\text{P}, \text{P})$ 20].

3.2.2 Synthesis of *cis*-[Pt{N(C(O)CH₂CN)(CO₂Et)}Cl(PPh₃)₂] (3.4) from *cis*-[PtCl₂(PPh₃)₂] mediated by cuprous oxide

cis-[PtCl₂(PPh₃)₂] was prepared *in situ* by the addition of triphenylphosphine (0.130 g, 0.496 mmol) to a stirred solution of [PtCl₂(COD)] (0.077 g, 0.21 mmol) in dichloromethane (10 cm³). To this were added *N*-cyanoacetylurethane (0.038 g 0.25 mmol), cuprous oxide (0.248 g, excess) and additional dichloromethane (10 cm³). The mixture was heated under reflux for 6 days. Insoluble copper salts were removed by

filtration and the solvent removed under reduced pressure from the tan coloured filtrate. The product was identified by $^{31}\text{P}\{-^1\text{H}\}$ NMR for comparison with 3.2.1 above. No attempts were made at recrystallisation of the product.

$^{31}\text{P}\{-^1\text{H}\}$ NMR: AB spin system δ 14.14 [d, P *trans* Cl, $^1J(\text{Pt}, \text{P})$ 3957, $^2J(\text{P}, \text{P})$ 20], 7.00 [d, P *trans* N, $^1J(\text{Pt}, \text{P})$ 3330, $^2J(\text{P}, \text{P})$ 20].

3.2.3 Synthesis of *cis*-[Pt{N(C(O)CH₂CN)(CO₂Et)}Cl(PPh₃)₂] (3.4) from *cis*-[PtCl₂(PPh₃)₂] mediated by mercuric oxide

In a manner similar to that described above, [PtCl₂(COD)] (0.080 g, 0.21 mmol) and triphenylphosphine (0.118 g, 0.449 mmol) were mixed in dichloromethane (10 cm³). To this stirred solution, *N*-cyanoacetylurethane (0.037 g, 0.24 mmol), yellow mercuric oxide (0.442 g, excess), and dichloromethane (10 cm³) were added. The mixture was heated at reflux for 2 days after which mercury salts were removed by filtration. The volume of solvent was reduced under reduced pressure and $^{31}\text{P}\{-^1\text{H}\}$ NMR data collected on the crude products. Two AB spin systems were observed in the phosphorus NMR spectrum, the major product (93%) was attributed to the *cis*-chloro amidate complex (3.4), while the minor component (7%) was associated with the metallalactam complex 3.1b.¹

$^{31}\text{P}\{-^1\text{H}\}$ NMR: AB spin system (major product) δ 13.33 [d, P *trans* Cl, $^1J(\text{Pt}, \text{P})$ 3969, $^2J(\text{P}, \text{P})$ 19], 6.91 [d, P *trans* N, $^1J(\text{Pt}, \text{P})$ 3373, $^2J(\text{P}, \text{P})$ 19]; AB spin system (minor product) δ 19.98 [d, P *trans* C, $^1J(\text{Pt}, \text{P})$ 2535, $^2J(\text{P}, \text{P})$ 18], 10.03 [d, P *trans* N, $^1J(\text{Pt}, \text{P})$ 3828, $^2J(\text{P}, \text{P})$ 18].

3.2.4 *In situ* displacement of chloride from *cis*-[Pt{N(C(O)CH₂CN)(CO₂Et)}Cl(PPh₃)₂] (3.4) by pyridine

A small amount of *cis*-[Pt{N(C(O)CH₂CN)(CO₂Et)}Cl(PPh₃)₂] (3.4) (*ca.* 1 mg) was dissolved in an acetonitrile/water solution in a 2 mL cuvette. To this 2 drops of pyridine were added. The solution was mixed and directly injected into the ES/MS for analysis.

ES/MS (20 V): [M-Cl+py]⁺ *m/z* 953, (100%); [M-Cl]⁺ *m/z* 875, (15%)

3.2.5 Lactam formation by prolonged reaction of *cis*-[Pt{N(C(O)CH₂CN)(CO₂Et)}Cl(PPh₃)₂] (**3.4**) with silver(I) oxide

The *cis*-chloro amidate complex **3.4** (0.041 g, 0.045 mmol) was heated under reflux in a mixture of dichloromethane (20 cm³) and silver(I) oxide (0.229 g, excess) for 18 h. The insoluble silver salts were removed by filtration. Subsequently the solvent was removed under reduced pressure and a ³¹P-¹H} NMR spectrum recorded of the crude product for comparison with previous experiments. The phosphorus NMR spectrum indicated that only one compound was present, and the obtained coupling constant data were consistent for the metallalactam **3.1b**.¹

³¹P-¹H} NMR: AB spin system δ 20.14 [d, P *trans* Cl, ¹J(Pt, P) 2518, ²J(P, P) 17], 11.41 [d, P *trans* N, ¹J(Pt, P) 3808, ²J(P, P) 17].

3.2.6 Lactam formation by reaction of *cis*-[Pt{N(C(O)CH₂CN)(CO₂Et)}Cl(PPh₃)₂] (**3.4**) with sodium hydride

To a stirred suspension of *cis*-[Pt{N(C(O)CH₂CN)(CO₂Et)}Cl(PPh₃)₂] (**3.4**) (0.034 g, 0.038 mmol) in tetrahydrofuran (10 cm³), sodium hydride (0.201 g, excess) was added under nitrogen. After gas evolution had stopped the solution was separated from the solid residue by decantation. The solvent was removed under reduced pressure and the products identified by ³¹P-¹H} NMR. Only one AB spin system was observed, with data consistent with that of the complex **3.1b**, indicating that the product was pure by phosphorus NMR.

³¹P-¹H} NMR: AB spin system δ 19.51 [d, P *trans* Cl, ¹J(Pt, P) 2548, ²J(P, P) 20], 10.41 [d, P *trans* N, ¹J(Pt, P) 3845, ²J(P, P) 20].

3.2.7 Reaction of *cis*-[Pt{N(C(O)CH₂CN)(CO₂Et)}Cl(PPh₃)₂] with NaBPh₄.

Sodium tetraphenylborate (0.014g, 0.042 mmol) was added to a suspension of *cis*-[Pt{N(C(O)CH₂CN)(CO₂Et)}Cl(PPh₃)₂] (**3.1**) (0.016g, 0.018 mmol) in methanol (10 cm³). The mixture was stirred for 18 h. The solvent was removed under reduced pressure and the product identified by ³¹P-¹H} NMR spectroscopy.

$^{31}\text{P}\{-^1\text{H}\}$ NMR: AB spin system δ 19.37 [d, P *trans* C, $^1J(\text{Pt}, \text{P})$ 2554, $^2J(\text{P}, \text{P})$ 24], 10.21 [d, P *trans* N, $^1J(\text{Pt}, \text{P})$ 3866, $^2J(\text{P}, \text{P})$ 20]

3.2.8 Short duration reaction of 2-benzoylacetanilide with *cis*-[PtCl₂(PPh₃)₂]

A mixture of *cis*-[PtCl₂(PPh₃)₂] (0.013 g, 0.016 mmol), 2-benzoylacetanilide (0.004 g, 0.02 mmol) and silver(I) oxide (0.133 g, excess) in dichloromethane (20 cm³) was stirred for 15 min at room temperature. The solution was separated from the silver slats by filtration and excess solvent removed under reduced pressure. $^{31}\text{P}\{-^1\text{H}\}$ NMR spectroscopy of the crude products reveal that two complexes, in an approximately 60% : 40% ratio were present. The NMR data obtained was consistent with the formation of both a *cis*-chloro-amidate and *cis*-chloro-alkyl complexes. The two complexes could not be separated by either fractional crystallisation or by chromatography.

$^{31}\text{P}\{-^1\text{H}\}$ NMR: AB spin system (major product) δ 15.43 [d, P *trans* Cl, $^1J(\text{Pt}, \text{P})$ 3863, $^2J(\text{P}, \text{P})$ 24], 7.73 [d, P *trans* N, $^1J(\text{Pt}, \text{P})$ 3330, $^2J(\text{P}, \text{P})$ 20]; AB spin system (minor product) 20.46 [d, P *trans* C, $^1J(\text{Pt}, \text{P})$ 2554, $^2J(\text{P}, \text{P})$ 24], 11.76 [d, P *trans* Cl, $^1J(\text{Pt}, \text{P})$ 3866, $^2J(\text{P}, \text{P})$ 20],

3.2.9 Crystal Structure of *cis*-[Pt{N(C(O)CH₂CN)(CO₂Et)}Cl(PPh₃)₂].0.5CH₂Cl₂ (3.4)

Pale tan crystals of *cis*-[Pt{N(C(O)CH₂CN)(CO₂Et)}Cl(PPh₃)₂].0.5CH₂Cl₂ were obtained by vapour diffusion of diethyl ether into a dichloromethane solution of 3.4. A suitable crystal for preliminary X-ray precession studies was selected and was mounted on a glass fibre with apiezon grease. Preliminary precession photography, using Cu-K α X-radiation with a Ni filter for zero and first upper levels, showed information consistent with the triclinic, $\bar{P}1$ space group. Preliminary cell dimensions were obtained from these photographs. Accurate intensity data were collected on a Nicolet R3 diffractometer at the University of Canterbury. Details for the data collection, structural analysis and refinement are recorded in Table 3.1. Significant electron density (1.90 e. \AA^{-3}) was observed in the final difference Fourier map. It is located 0.69 \AA from the platinum. The terminal carbon of the ethyl ester was found to be disordered over two sites, and has been modelled as two 50% occupancy carbons.

Table 3.1 Crystal data and structure refinement for *cis*-
[Pt{N(C(O)CH₂CN)(CO₂Et)}Cl(PPh₃)₂].0.5CH₂Cl₂ (**3.4**).

<i>Crystal Data</i>	
Empirical formula	C ₄₂ H ₃₇ N ₂ ClO ₃ P ₂ Pt. 0.5CH ₂ Cl ₂
Formula weight	951.67
Crystal system	Triclinic
Space group	P $\bar{1}$
<i>a</i> (Å)	11.165(4)
<i>b</i> (Å)	12.054 (2)
<i>c</i> (Å)	17.399(5)
α (°)	71.73(2)
β (°)	76.04(2)
γ (°)	71.25(3)
<i>V</i> (Å ³)	2079.7(10)
<i>Z</i>	2
<i>D</i> (c) (g cm ⁻³)	1.520
<i>Data Collection</i>	
Diffractometer	Nicolet R3
Radiation	Mo-K α
Wavelength (Å)	0.71073
Temperature (K)	130(2)
Crystal size (mm)	0.50 x 0.36 x 0.22
Data collection mode	ω -scans
θ range for data collection(°)	1.85 to 22.50
Index ranges	0 ≤ <i>h</i> ≤ 12 -11 ≤ <i>k</i> ≤ 12 -18 ≤ <i>l</i> ≤ 18
Reflections collected	5736
Independent reflections	5391 [R(int) = 0.0289]
Absorption coefficient (mm ⁻¹)	3.618
F(000)	944

Structural analysis and refinement

Solution by	Patterson methods
Refinement method	Full-matrix least-squares on F^2
Data / restraints / parameters	5391 / 234 / 464
Goodness-of-fit on F^2	1.038
Final R indices [$I > 2\sigma(I)$]	$R_1 = 0.0430$, $wR^2 = 0.1025$
R indices (all data)	$R_1 = 0.0594$, $wR^2 = 0.1093$ $w = 1/[\sigma^2(F_o^2) + (0.0583P)^2 + 6.7916P]$, where $P = (F_o^2 + 2F_c^2)/3$
where $P = (F_o^2 + 2F_c^2)/3$	
Largest difference peak	$1.902 \text{ e.}\text{\AA}^{-3}$
Largest difference hole	$-0.681 \text{ e.}\text{\AA}^{-3}$
Programs used	
Solution by	SHELXS-86 ⁷
Refinement by	SHELXL-96 ⁸

3.3 Results and Discussion

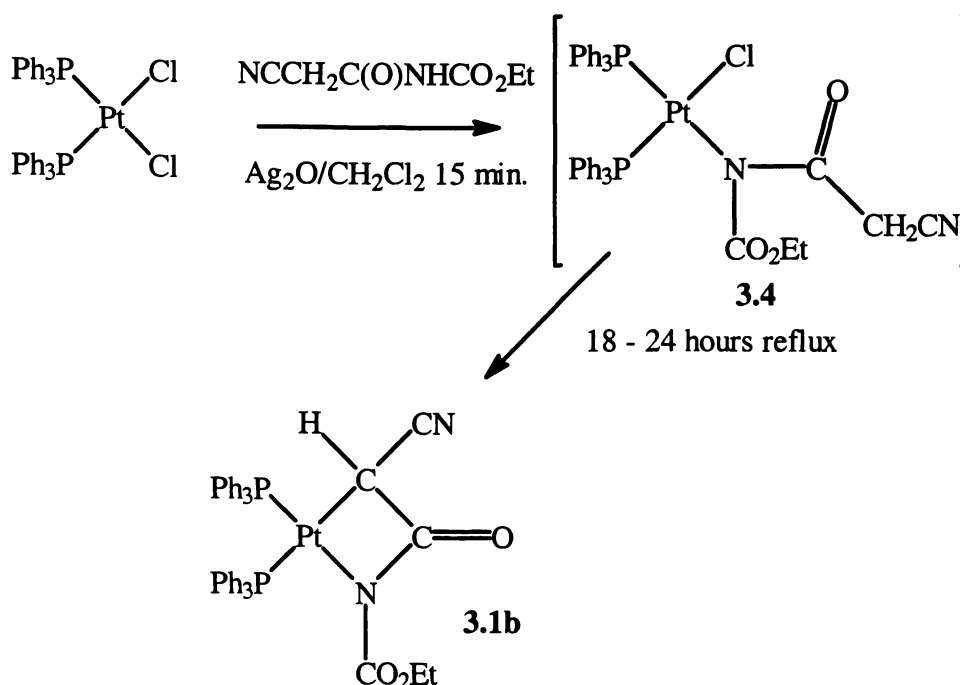
3.3.1 Intermediate synthesis reactions

The complex **3.4** was first observed during a routine silver(I) oxide mediated synthesis of the platinalactam (**3.1b**, $R = \text{CO}_2\text{Et}$, $R' = \text{CN}$).¹ This intermediate complex was found to form rapidly in the mild conditions of a stirred, room temperature mixture. This indicates that the proton on the urethane nitrogen is easily abstracted, even under these mild conditions. This is not unexpected, as the two carbonyl groups adjacent to this nitrogen should greatly increase its acidity. The acidity of the acetyl proton [$\text{NCCH}_2\text{C}(\text{O})\text{NH}(\text{CO}_2\text{Et})$] is also considerably enhanced, by being flanked by a cyanide and a carbonyl functionality. Even after the relatively short reaction time of 15 minutes, the formation of some metallalactam complex (**3.1b**) was confirmed by the presence of characteristic doublet phosphorus resonances at δ 19.10 and 10.93. Prolonged reaction

⁷ G. M. Sheldrick, SHELXS-86, *Program for the solution of X-ray structures*, Universität Göttingen, 1986

⁸ G. M. Sheldrick, SHELXL-96, *Program for the refinement of X-ray structures*, Universität Göttingen, 1996

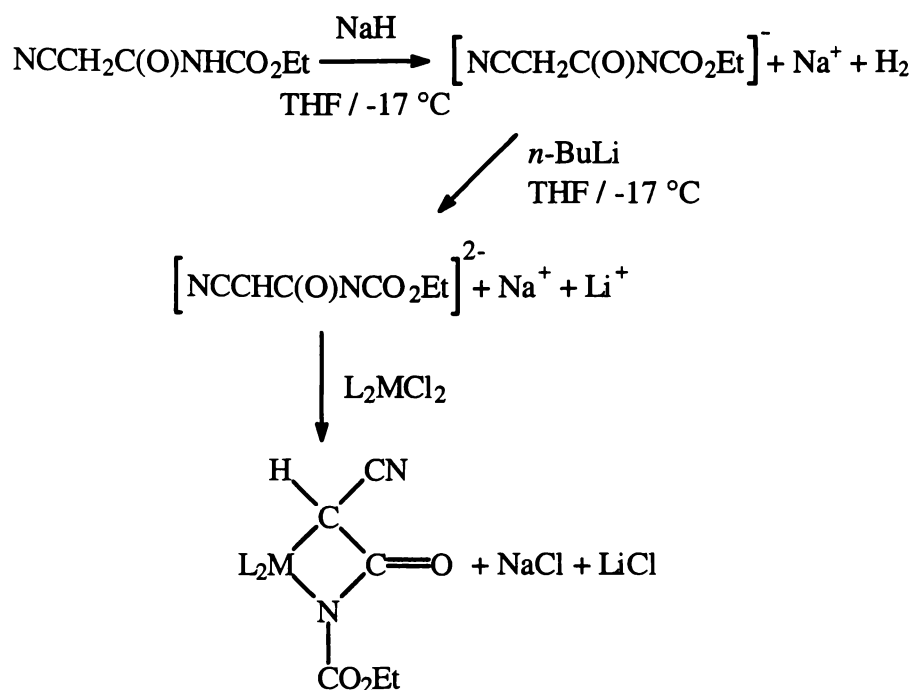
of the intermediate complex **3.4** with additional silver(I) oxide resulted in the formation of the platinalactam **3.1b** in good yield (scheme 3.2).



Scheme 3.2 Formation of the intermediate **3.4** in the metallacyclisation of *N*-cyanoacetylurethane

A variety of metal oxides were investigated for their reactivity in comparison with silver(I) oxide. Their reactivities towards mediating metallacyclisation processes were less than that of silver(I) oxide. They did however, provide an alternative route to synthesising *cis*-[Pt{N(C(O)CH₂CN)(CO₂Et)}Cl(PPh₃)₂] (**3.4**). Of the four metal oxides tried, cuprous oxide, mercuric oxide, ferric oxide and aluminium oxide, only the first two showed any reactivity. Cuprous oxide mediated the synthesis of the intermediate **3.4**, after 6 days of heating under reflux in dichloromethane, while the reaction with mercuric oxide required 24 h. of heating under reflux to yield an appreciable amount of the intermediate. Both required significantly longer times than the 15 minutes required with silver(I) oxide. Yields in both cases were also lower than with silver(I) oxide. Prolonged heating at reflux of the mercuric oxide mixture eventually afforded a small quantity of the platinalactam complex **3.1b**. As mercuric oxide was the only relatively successful candidate, and due to its toxicity, further syntheses involving mercuric oxide were discontinued.

An alternative synthetic route involving a 1,3-dianionic species, was also investigated. Sodium hydride and *n*-butyl lithium were employed to generate the organic salt $[\text{NCCHC}(\text{O})\text{NCO}_2\text{Et}]^{2-} \cdot \text{Na} \cdot \text{Li}$ (scheme 3.3). However, this method resulted in the degradation of the organic precursor by the base, giving little recoverable metallalactam product.



Scheme 3.3 Proposed synthesis of a metallalactam through reaction with a 1,3-dianion

The effect of sodium hydride on *cis*-[Pt{N(C(O)CH₂CN)(CO₂Et)}Cl(PPh₃)₂] (**3.4**) was also investigated and reaction with this produced the desired platinalactam $[\text{Pt}\{\text{N}(\text{CO}_2\text{Et})\text{C}(\text{O})\text{CHCN}\}(\text{PPh}_3)_2]$ (**3.1b**). Unlike the use of an organic salt generated from sodium hydride / *n*-butyl lithium, mentioned earlier, the treatment of the intermediate with sodium hydride did not degrade the organic ligand. One of the driving forces of silver(I) oxide mediated syntheses is the formation of insoluble silver chloride. It also appears that the formation of sodium chloride in THF is also sufficient to drive the reaction. This hypothesis is supported by the fact that sodium tetraphenylborate can induce metallacyclisation. Sodium hydride is very basic, so the formation of platinalactam was expected. However, sodium tetraphenylborate is essentially non-basic. Sodium tetraphenylborate was employed to provide a counterion $[\text{BPh}_4]^-$ during the attempted displacement of the chloride from **3.4** by triphenylphosphine. ES/MS studies indicated that the chloride could be readily

displaced by a neutral ligand and it was hoped that a cationic complex could be formed by this procedure.

Initial investigations into the reaction of 2-benzoylacetyl anilide with *cis*-[PtCl₂(PPh₃)₂] in the presence of silver(I) oxide for short reaction times yielded a mixture of two compounds. Based on ³¹P NMR spectra of the reaction products the two components of the reaction were a *cis*-chloro amidate complex, presumably similar to the intermediate 3.4. The ¹J(Pt, P) satellites (2554, 3866 Hz) of the second, minor component indicated that a *cis*-chloro alkyl was present. Presumably the amine NH and the acetyl CH₂ protons of 2-benzoylacetyl anilide have a similar acidity, allowing both an N/Cl and a C/Cl intermediate species to form. Unfortunately separation of the two complexes by both chromatography and by fractional crystallisation could not be achieved.

A ³¹P NMR resonance, with ¹J couplings characteristic of phosphorus *trans* to oxygen, has been observed in a number of spectra. Also, a species which has a mass peak and isotope pattern which correspond well with the predicted isotopomer values for [Pt(OH)₂(PPh₃)₂] has been recorded by ES/MS. Often this species is only a small percentage of the products. However, if this compound is observed at an early stage in the reaction, prolonged reaction times eventually yield only this complex. It is proposed that this reaction product arises from a competing reaction, and may be due to the use of lower quality silver(I) oxide. Use of a source of silver(I) oxide purified by Soxhlet extraction with water did not produce any of this unwanted product.

Several of the results presented here are the result of *in situ* reactions of *cis*-[Pt{N(C(O)CH₂CN)(CO₂Et)}Cl(PPh₃)₂] (3.4) with various compounds during ES/MS studies. The fact that a relatively mild base, such as sodium tetraphenylborate, can complete the metallacyclisation process is quite surprising. In some cases organic bases have been found to effect the metallacyclisation reaction, in particular triethylamine has been found to be quite efficient.⁹ However, reactions using organic bases generally have more impurities in the products compared to silver(I) oxide mediated reactions.

Pyridine will displace the chloride ion and act as a neutral ligand in an electrospray environment, not an entirely unexpected result considering that a coordinated

acetonitrile complex of $[\text{Pt}\{\text{N}(\text{C}(\text{O})\text{CH}_2\text{CN})(\text{CO}_2\text{Et})\}(\text{PPh}_3)_2+\text{NCCH}_3]^+$ ($[\text{M}-\text{Cl}+\text{NCCH}_3]^+$) is observed as the predominant species at low cone voltages in ES/MS spectra for the intermediate **3.4**. It was thought that pyridine would be sufficiently basic to be able to abstract a proton from the *N*-cyanoacetyl functionality and complete the metallacyclisation process, with pyridinium chloride produced as a reaction by-product. Unfortunately this did not prove to be the case and no metallacyclisation was observed.

3.3.2 X-ray crystallography of *cis*- $[\text{Pt}\{\text{N}(\text{C}(\text{O})\text{CH}_2\text{CN})(\text{CO}_2\text{Et})\}\text{Cl}(\text{PPh}_3)_2]\cdot 0.5\text{CH}_2\text{Cl}_2$ (**3.4**)

The single crystal X-ray structure of *cis*- $[\text{Pt}\{\text{N}(\text{C}(\text{O})\text{CH}_2\text{CN})(\text{CO}_2\text{Et})\}\text{Cl}(\text{PPh}_3)_2]$ (**3.4**) shows that the *N*-cyanoacetylurethane moiety is *cis* to the chloride (Figure 3.1). The compound is similar to a previously reported palladium complex **3.2**, that had adopted a *trans* geometry.³ The coordination around the platinum centre is the expected square-planar configuration for d^8 platinum(II). No atom lies more than 0.052(3) Å [N(1)] from the mean plane of the coordination sphere.

The bond lengths from platinum to each of the coordinating atoms are not unusual. The bond length from Pt—P(2) is marginally shorter [2.237(3) Å] than that of its partner P(1) [2.251(2) Å], as a result of the differing *trans* influences of chlorine [*trans* to P(2)] and nitrogen. The bond angles around the platinum centre all approach 90°, the ideal for a square planar complex (see Table 3.2). The N—Pt—Cl bond is slightly more acute at an angle of 85.7(2)°, presumably due to steric pressure applied from the triphenylphosphine and amide ligands. The steric bulk of the triphenylphosphine ligands also appear to cause the P—Pt—P bond angle to become more obtuse [98.3(1)°]. In the platinalactam **3.1a**, the “bite” angle of the organic moiety deviates considerably from 90° with an N—Pt—C angle of 67.0(3)°¹; presumably the more rigid constraint of a carbonyl in the ring system causes this distortion.

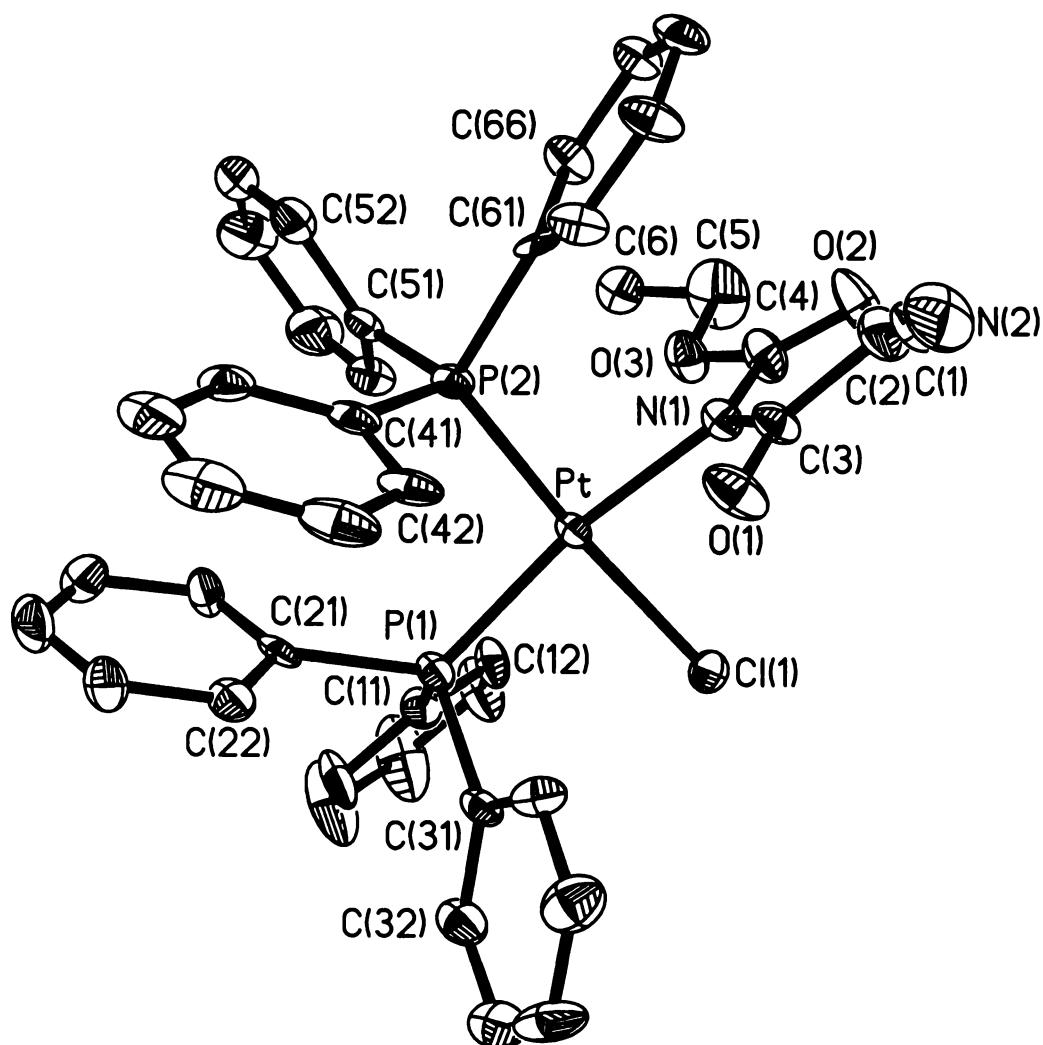


Figure 3.1 Atom labeling scheme for *cis*-[Pt{N(C(O)CH₂CN)(CO₂Et)}Cl(PPh₃)₂] (**3.4**)
Thermal displacement ellipsoids are depicted at 50% probability. Hydrogen atoms and dichloromethane of crystallisation omitted for clarity.

Table 3.2 Selected bond lengths (Å) and bond angles (°) for *cis*-
[Pt{N(C(O)CH₂CN)(CO₂Et)}Cl(PPh₃)₂] (**3.4**)

Pt-N(1)	2.080(7)	Pt-P(2)	2.237(2)
Pt-P(1)	2.250(2)	Pt-Cl(1)	2.356(2)
N(1)-C(3)	1.351(11)	N(1)-C(4)	1.363(12)
N(2)-C(1)	1.147(13)	O(1)-C(3)	1.217(11)
O(2)-C(4)	1.214(11)	O(3)-C(4)	1.346(11)
O(3)-C(5)	1.459(12)	O(3)-C(5')	1.458(12)
C(1)-C(2)	1.448(16)	C(2)-C(3)	1.514(12)

C(5)-C(6)	1.45(2)	C(5')-C(6')	1.42(2)
P(1)-C(11)	1.800(9)	P(1)-C(21)	1.819(9)
P(1)-C(31)	1.835(10)	P(2)-C(51)	1.808(9)
P(2)-C(41)	1.812(9)	P(2)-C(61)	1.837(9)
N(1)-Pt-P(2)	89.7(2)	N(1)-Pt-P(1)	171.1(2)
P(1)-Pt-P(2)	98.30(9)	N(1)-Pt-Cl(1)	85.7(2)
P(2)-Pt-Cl(1)	175.32(9)	P(1)-Pt-Cl(1)	86.36(9)
C(3)-N(1)-C(4)	123.7(8)	C(3)-N(1)-Pt	113.4(6)
C(4)-N(1)-Pt	122.8(6)	C(4)-O(3)-C(5)	116.1(7)
N(2)-C(1)-C(2)	178.3(11)	C(1)-C(2)-C(3)	111.7(8)
O(1)-C(3)-N(1)	120.7(8)	O(1)-C(3)-C(2)	118.2(8)
N(1)-C(3)-C(2)	120.9(8)	O(2)-C(4)-O(3)	123.0(9)
O(2)-C(4)-N(1)	126.9(9)	O(3)-C(4)-N(1)	110.0(8)
C(6)-C(5)-O(3)	106.2(11)	C(6')-C(5')-O(3)	119(2)

The plane of the organic ligand [defined by C(2), C(3), O(1), N(1), C(4), O(2), O(3)] lies almost perpendicular to the plane of the platinum co-ordination plane [87.8(1)°]. Presumably steric constraints imposed by the triphenylphosphine ligands force this arrangement. The *N*-cyanoacetylurethane ligand itself is twisted, with the major deformation being a twist about the acetyl C—C bond [C(1)—C(2)—C(3)—O(1) torsion angle = 10.1(1)°]. The ethyl ester also lies out of the least-squares plane of the ligand [C(5) 0.258(16), C(6) 0.769(22) and C(6') 1.478(35) Å] (see Figure 3.2) and is disordered with C(6) occupying two positions.

The triphenylphosphine ligands are typical, with an average C—C bond length of 1.383 Å and an average C—C—C bond angle of 120.0°. The dichloromethane of crystallisation only has a partial occupancy and as such it has been modelled as a one-half dichloromethane.

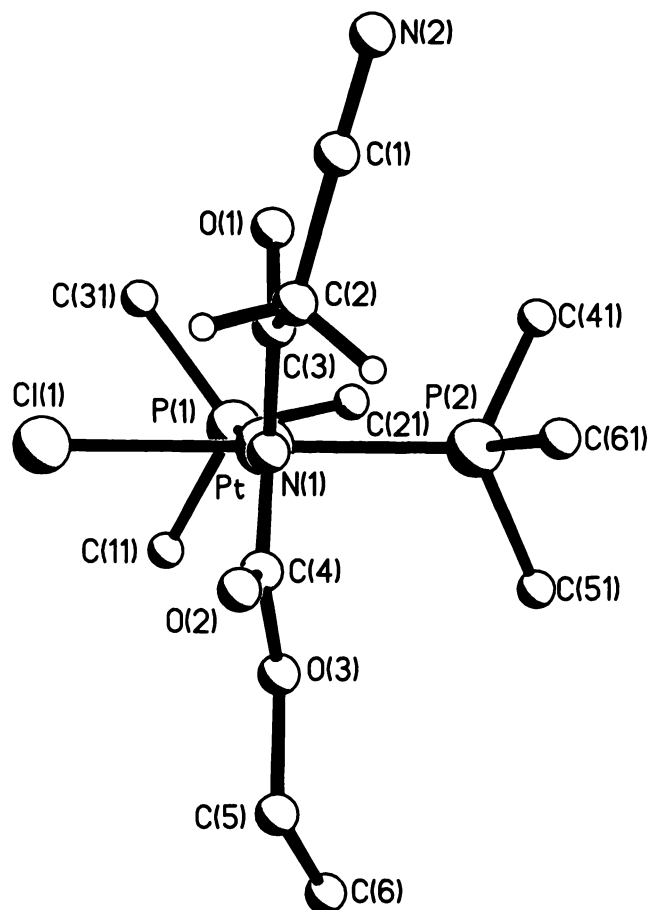


Figure 3.2 View of *N*-cyanoacetylurethane ligand of **3.4** showing distortion of ligand. Only *ipso* carbons of phenyl rings shown for clarity.

3.3.3 NMR Spectroscopy of the *cis*-chloro amidate complex **3.4**

$^{31}\text{P}\{-^1\text{H}\}$ NMR was the primary tool in this investigation, providing a rapid analysis of the compounds formed during the reactions. Considerable data exist on the *trans*-influence of various atoms with respect to 1J platinum-phosphorus couplings.¹⁰ Subsequent metallacyclisation studies have also increased this body of knowledge.¹⁻⁴

The proton NMR spectrum of the intermediate **3.4** is similar to that of the previously described *trans*- $[\text{Pd}\{\text{N}(\text{C}(\text{O})\text{CH}_2\text{CN})(\text{CO}_2\text{Et})\}\text{Cl}(\text{PPh}_3)_2]$ (**3.2**)³, and indicates that the conformation of C(2) and C(5) is locked. Because the molecule is asymmetric, the protons bonded to these carbons become inequivalent, giving rise to diastereotopism. This diastereotopism is observed as an AB spin system for the C(2)-cyanoacetyl

hydrogens H(2a) and H(2b), with both the protons coupling to each other due to the inherent asymmetry of the molecule (figure 3.3). The C(5)-methylene protons of the ethyl ester, H(5a) and H(5b), also appear as an AB spin system. Each of the H5 resonances appears as a doublet of quartets arising from a 2J coupling to their inequivalent partner and a 3J coupling to the methyl protons on C(6) (figure 3.3).

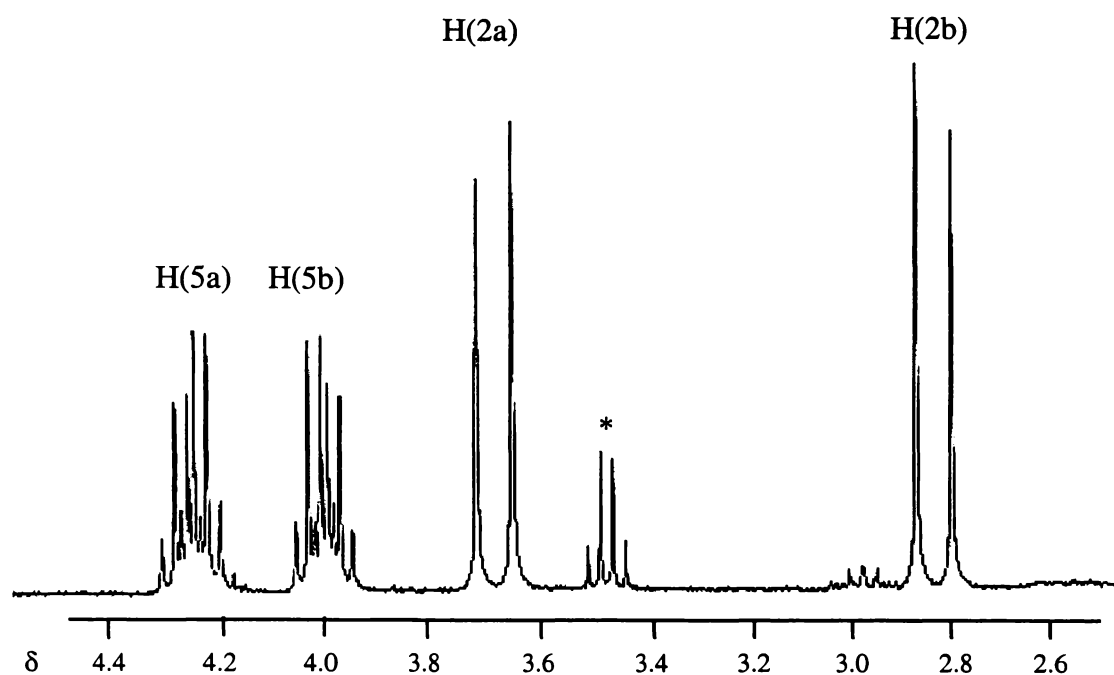


Figure 3.3 Ethyl resonance region of the ^1H NMR spectrum of *cis*- $[\text{Pt}\{\text{N}(\text{C}(\text{O})\text{CH}_2\text{CN})(\text{CO}_2\text{Et})\text{Cl}(\text{PPh}_3)_2\}]$ (**3.4**)

* Peak due to presence of unreacted *N*-cyanoacetylurethane

The carbon NMR spectrum also displays similar features to that of the metallacycle¹, however some of the resonances are found shifted downfield as a consequence of being in a less strained environment. For example the ester carbonyl resonance appears at δ 168.84, as opposed to δ 155.4 for the platinalactam. The cyanide resonance is also shifted upfield, by a similar magnitude. Correlation between these shifts and the change in the infrared stretching frequency for these bonds can also be made. Only one carbonyl stretch was observed for the platinalactam that appeared at 1738 cm^{-1} , whereas for the intermediate, two carbonyl stretching frequencies are observed (1689 and 1638 cm^{-1}). The cyanide stretching frequency has also moved by 54 cm^{-1} , (to 2255 cm^{-1}) and is closer to the stretching frequency of 2260 cm^{-1} observed for *N*-cyanoacetylurethane.

A similar effect was noted for *trans*-[Pd{N(C(O)CH₂CN)(CO₂Et)}Cl(PPh₃)₂] (**3.2**) which showed a diminished intensity of the cyanide resonance, as well as a shift of position.

The observation of an AB spin system by phosphorus NMR indicated that two phosphorus environments were present in the molecule (see figure 3.4). ¹J coupling constants of 3957 and 3330 Hz indicated that the phosphorus atoms were *trans* to a fairly low *trans*-influence (oxygen or chlorine) atom and a moderately strong *trans*-influence (nitrogen) atom, respectively. The coupling constant of 3957 Hz lies in the middle ground found for ¹J(Pt, P) values of oxygen and chlorine. Oxygen tends to be somewhat higher than chlorine (~4100 Hz), while chlorine is somewhat lower than the value observed here (~3700 Hz). However, these two coupling constants (3957 and 3330 Hz) are similar to those observed for other *cis* chloro-amidate platinum(II) bis(triphenylphosphine) complexes.^{11,12}

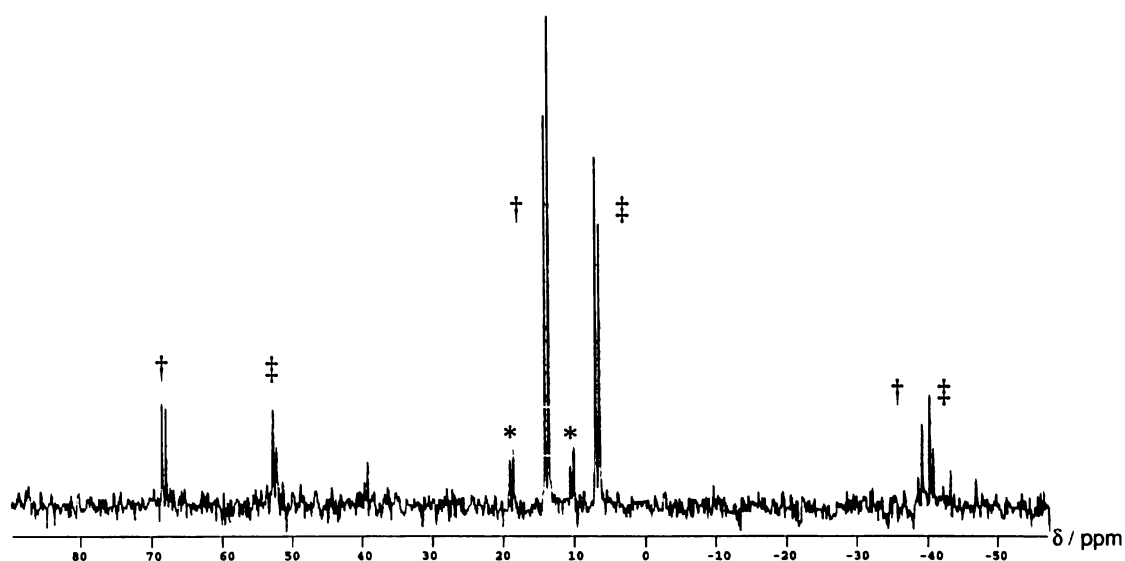


Figure 3.4 ³¹P NMR spectrum of *cis*-[Pt{N(C(O)CH₂CN)(CO₂Et)}Cl(PPh₃)₂] (**3.4**)

* Peaks due to the platinalactam **3.1b**

11 J. Fawcett, W. Henderson, R. D. W. Kemmitt, D. R. Russell and A. Upreti, *J. Chem. Soc., Dalton Trans.*, (1996), 1897

12 W. Henderson, B. K. Nicholson and L. J. McCaffrey, *Inorg. Chim. Acta*, (1998), **285**, 145

3.3.4 ES/MS study of *cis*-[Pt{N(C(O)CH₂CN)(CO₂Et)}Cl(PPh₃)₂] (3.4)

The complex *cis*-[Pt{N(C(O)CH₂CN)(CO₂Et)}Cl(PPh₃)₂] (3.4) is an ideal candidate for study by electrospray mass spectrometry. The labile chloride allows easy generation of a charged species and also leaves a vacant coordination site on the platinum which can be easily accessed by other species present in the electrospray environment.

Under conditions used in ES/MS the complex 3.4 readily loses chloride, even at low cone voltages (20 V, figure 3.5). This has been observed in several similar cases.^{13,14} At low cone voltages, the predominant species observed is the one due to chloride loss from *cis*-[Pt{N(C(O)CH₂CN)(CO₂Et)}Cl(PPh₃)₂] (*m/z* 875). It is likely that the species adopts one of two forms and is stabilised by a dative bond from one of the carbonyl oxygen atoms to the platinum (figure 3.6). This would form a four-membered metallacycle with a fairly unstrained ring structure. This enhanced stability imparted by this dative bond may also be the reason that this species is observed at high cone voltages (see table 3.3). Unfortunately the mass of this species matches that of the metallalactam [3.1b+H]⁺. The *cis*-[Pt{N(C(O)CH₂CN)(CO₂Et)}(PPh₃)₂]⁺ species also readily accepts acetonitrile from the solvent, giving rise to the ion at *m/z* 916, while the coordinatively saturated platinalactam does not as easily accept a donor molecule like acetonitrile. A small amount of the parent [M+H]⁺ complex does survive to be analysed by the spectrometer, but is considerably less than that of the cyclometallated species in Figure 3.6. The various species observed and cone voltages used are summarised in Table 3.3.

13 J. M. Law, W. Henderson and B. K. Nicholson, *J. Chem. Soc., Dalton Trans.*, (1997), 4587

14 C. Evans and W. Henderson, *Inorg. Chim. Acta*, (1999), **294**, 183

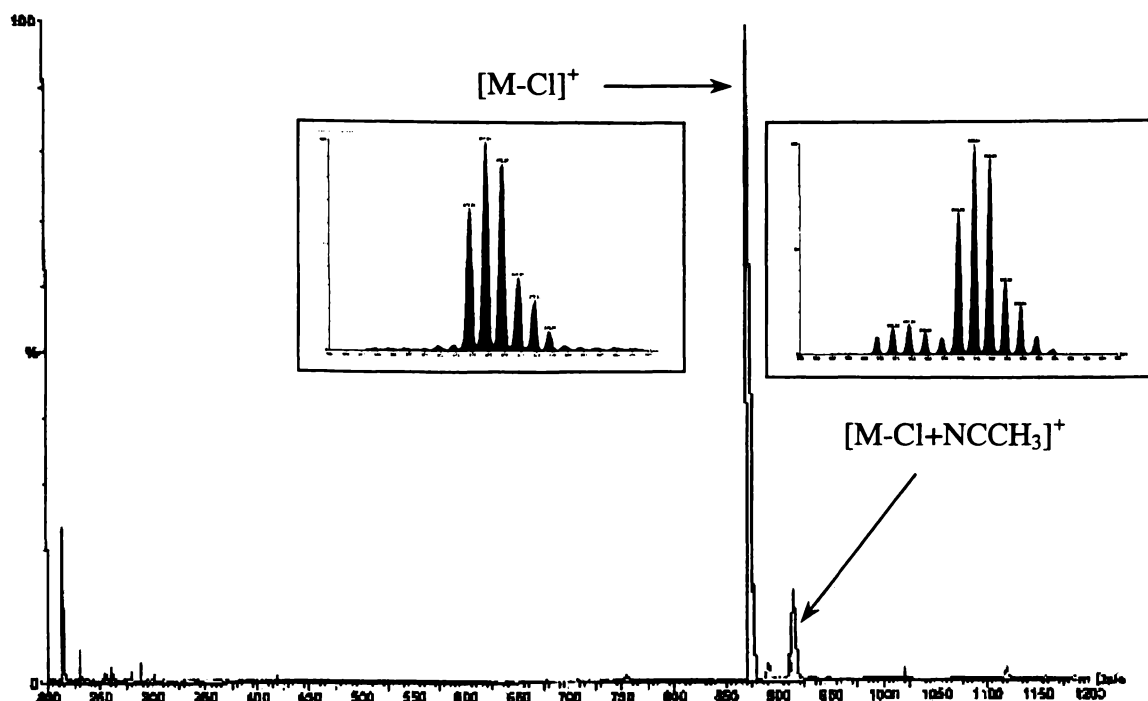


Figure 3.5 ES/MS spectrum of $[\text{Pt}\{\text{N}(\text{C}(\text{O})\text{CH}_2\text{CN})(\text{CO}_2\text{Et})\}\text{Cl}(\text{PPh}_3)_2]$ (**M**) at cone voltage = 20 V

Insets depict isotopic patterns for peaks at m/z 874 and 914 Da.

Table 3.3 Electrospray mass spectral data for *cis*- $[\text{Pt}\{\text{N}(\text{C}(\text{O})\text{CH}_2\text{CN})(\text{CO}_2\text{Et})\}\text{Cl}(\text{PPh}_3)_2]$ (**M**) (**3.4**)

Cone Voltage	Species	m/z (Da)	Relative Intensity (%)
10	$[\text{M}-\text{Cl}+\text{NCCH}_3]^+$	916	60
	$[\text{M}-\text{Cl}]^+$	875	100
20	$[\text{M}-\text{Cl}+\text{NCCH}_3]^+$	916	100
	$[\text{M}-\text{Cl}]^+$	875	75
40	$[\text{M}-\text{Cl}]^+$	875	100
60	$[\text{M}-\text{Cl}]^+$	875	100
	$[\text{Pt}(\eta^2\text{-C}_6\text{H}_4\text{PPh}_2)(\text{PPh}_3)]^+$	719	65
90	$[\text{M}-\text{Cl}]^+$	875	10
	$[\text{Pt}(\eta^2\text{-C}_6\text{H}_4\text{PPh}_2)(\text{PPh}_3)+\text{NCCH}_3]^+$	760	100
	$[\text{Pt}(\eta^2\text{-C}_6\text{H}_4\text{PPh}_2)(\text{PPh}_3)]^+$	719	73

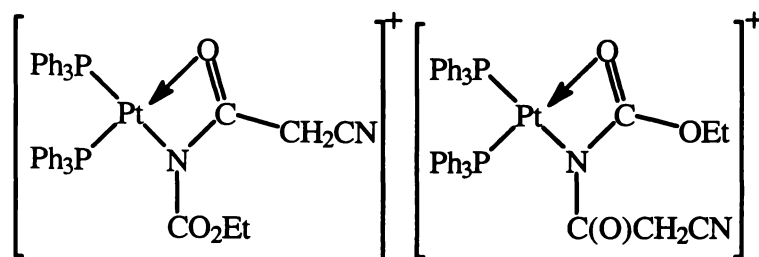
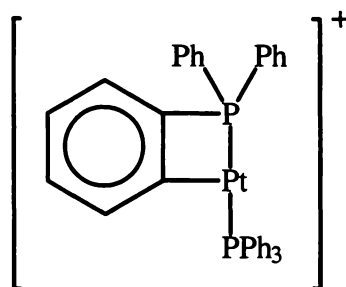


Figure 3.6 Proposed structures for $[\text{Pt}\{\text{N}(\text{C}(\text{O})\text{CH}_2\text{CN})(\text{CO}_2\text{Et})\}(\text{PPh}_3)_2]^+$

At higher cone voltages, degradation of the complex can be induced. Initially the complex loses the lightly coordinated acetonitrile and at 40 V the predominant species is $[\text{M}-\text{Cl}]^+$ (m/z 875). Increasing the voltage further results in the loss of the amide moiety, producing a species with a m/z ratio of 719. This species is believed to be a cyclometallated triphenylphosphine platinum(II) complex (**3.5**) and has been observed in the ES/MS spectra of other bis(triphenylphosphine) platinum(II) complexes.^{11,13,14}



3.5

Organic bases, for example triethylamine, have been used as mediators in these type of small ring metallacyclisation reactions with considerable success. Pyridine was employed in a similar fashion to determine whether it would promote the formation of the platinalactam **3.1b**. Unfortunately pyridine does not appear to be an adequate metallacyclisation mediator, however it was found that it provides an excellent source of neutral ligand for bonding to vacant coordination sites on metal centres. In this case at low cone voltage the predominant species is $[\text{M}-\text{Cl}+\text{py}]^+$ (figure 3.7). Pyridine is readily lost with increasing cone voltages, leaving just the $[\text{M}-\text{Cl}]^+$ species already discussed. Pyridine may be a useful tool in identifying complexes containing a functionality that is lost in the initial stages of the electrospray procedure (in this case chloride), to leave an accessible coordination site.

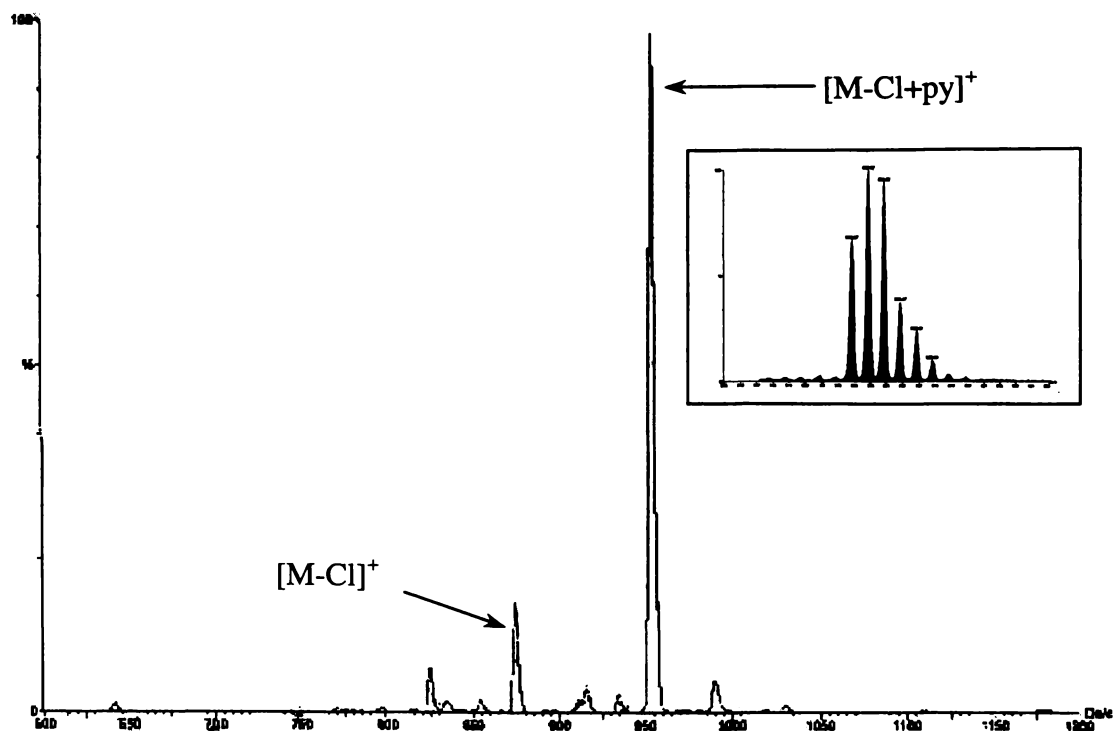


Figure 3.7 ES/MS spectrum of $[\text{Pt}\{\text{N}(\text{C}(\text{O})\text{CH}_2\text{CN})(\text{CO}_2\text{Et})\}\text{Cl}(\text{PPh}_3)_2]$ (**M**) with added pyridine at cone voltage = 20 V

Inset shows isotopic distribution pattern for $[\text{M}-\text{Cl}+\text{py}]^+$.

Table 3.4 Electrospray mass spectral data for *cis*- $[\text{Pt}\{\text{N}(\text{C}(\text{O})\text{CH}_2\text{CN})(\text{CO}_2\text{Et})\}\text{Cl}(\text{PPh}_3)_2]$ (**3.4**) (**M**) with added pyridine

Cone Voltage	Species	<i>m/z</i> (Da)	Relative Intensity (%)
20	$[\text{M}-\text{Cl}+\text{py}]^+$	953	100
	$[\text{M}-\text{Cl}]^+$	875	17
40	$[\text{M}-\text{Cl}+\text{py}]^+$	953	28
	$[\text{M}-\text{Cl}]^+$	875	100
60	$[\text{M}-\text{Cl}]^+$	875	100
	$[\text{Pt}(\eta^2\text{-C}_6\text{H}_4\text{PPh}_2)(\text{PPh}_3)+\text{NCCH}_3]^+$	760	22
	$[\text{Pt}(\eta^2\text{-C}_6\text{H}_4\text{PPh}_2)(\text{PPh}_3)]^+$	719	16
90	$[\text{M}-\text{Cl}]^+$	875	7
	$[\text{Pt}(\eta^2\text{-C}_6\text{H}_4\text{PPh}_2)(\text{PPh}_3)+\text{NCCH}_3]^+$	760	100
	$[\text{Pt}(\eta^2\text{-C}_6\text{H}_4\text{PPh}_2)(\text{PPh}_3)]^+$	719	88

3.4 Conclusions

The complex, *cis*-[Pt{N(CO₂Et)(C(O)CH₂CN)}Cl(PPh₃)₂] (3.4) is the isolable intermediate in the process of silver(I) oxide mediated metallacyclisation reactions. The fact that the complex can be readily synthesised and isolated from the reaction mixture supports the hypothesis that silver(I) oxide mediated reactions follow a stepwise mechanism. That is, the initial bond from the organic reagent to the metal centre is *via* the atom with the highest acidity (in this case the urethane nitrogen), followed by completion of the metallacycle through further halide loss and hydrogen abstraction.

Alternative metallacyclic mediators were also identified in cuprous and mercuric oxides, and in the unlikely sodium tetraphenylborate. These results support the theory that the reaction equilibrium is driven by salt formation. Following this, investigations were extended to include a new metal centre, gold(III) into the suite of metals already available as metallacyclic precursors. The somewhat limited success with other metal oxides as reaction mediators also prompted an investigation into the formation of metallalactam complexes utilising different bases, which are the topics of discussion in the following chapters.

Chapter Four. Organogold metallalactam complexes and a novel dimeric metallacycle

4.1 Introduction

Metallacyclic complexes of the platinum group metals are useful models for some catalytic processes.¹ Silver(I) oxide mediates the synthesis of metallacyclic complexes with generally favourable results for a wide range of L_2MCl_2 precursors and organic substrates.^{2,3,4,5} Predominantly the metals used have been from the platinum group, both for their stability, and for the range of techniques available for the characterisation of the compounds produced.

Until recently, little was known about the metallacyclic chemistry of gold. Gold(III) complexes are square planar and isoelectronic (d^8) with platinum(II), about which there is a considerable body of knowledge. The recent availability of the square-planar gold(III) dichloride complexes $[LAuCl_2]$, $[L = \{C_6H_3(CH_2NMe_2)_2-(OMe)_5\}$ (4.1a)⁶ or $L = \{C_6H_4(CH_2NMe_2)_2\}$ (4.1b)]⁷ has expanded this area of research. Recently, the novel auracyclobutan-3-one $[LAu\{\overbrace{CH(CO_2Me)C(O)CH(CO_2Me)}\}]$ (4.2)⁸ auracyclobutane $([LAu\{\overbrace{C(CN)_2CH_2C(CN)_2}\})$ (4.3)⁹, and auraureylene $[LAu\{\overbrace{N(R)C(O)N(R')}\})$ (4.4)¹⁰ complexes have been synthesised and characterised (Figure 4.1).

1 M. Lautens, W. Klute and W. Tam, *Chem. Rev.*, (1996), **96**, 49

2 W. Henderson; B.K. Nicholson and A. G. Oliver, *J. Chem. Soc., Dalton Trans.*, (1994), 1831

3 W. Henderson, J. Fawcett, R. D. W. Kemmitt, C. Proctor and D. R. Russell, *J. Chem. Soc., Dalton Trans.*, (1994), 3085

4 W. Henderson, A. G. Oliver, C. E. F. Rickard and L.-J. Baker, *Inorg. Chim. Acta.*, (1999) 292, 260

5 D. A. Clarke, R. D. W. Kemmitt, M. A. Mazid, D. R. Russell, M. D. Shilling and L. J. S. Sherry, *J. Chem. Soc., Dalton Trans.*, (1984), 1993; W. Henderson, R. D. W. Kemmitt, L. J. S. Prouse and D. R. Russell, *J. Chem. Soc., Dalton Trans.*, (1990), 1853; W. Henderson, R. D. W. Kemmitt and A. L. Davis, *J. Chem. Soc., Dalton Trans.*, (1993), 2247

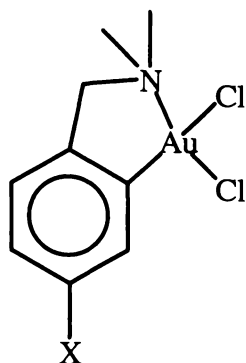
6 P. A. Bonnardel and R. V. Parish, *J. Chem. Soc., Dalton Trans.*, (1996), 3185

7 M.-D. Bermúdez, F.-J. Carrión and P. G. Jones, *J. Organomet. Chem.*, (1984), **268**, 191

8 M. B. Dinger and W. Henderson, *J. Organomet. Chem.*, (1997), **547**, 243

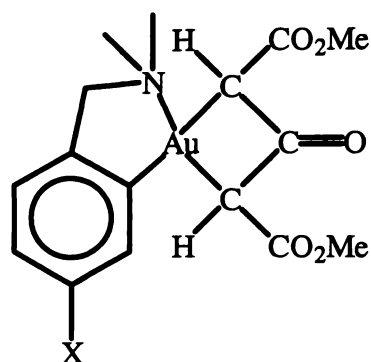
9 M. B. Dinger and W. Henderson, *J. Organomet. Chem.*, (1999), **577**, 219

10 M. B. Dinger and W. Henderson, *J. Organomet. Chem.*, (1998), **557**, 231

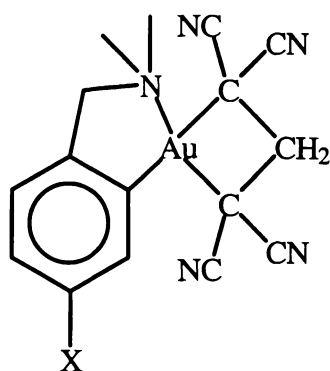


4.1a X = OMe

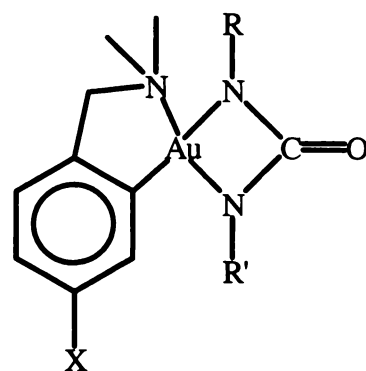
b X = H



4.2 X = OMe, H



4.3 X = OMe, H

4.4 X = OMe, H; R = Ph, C(O)Me,
R' = Ph, C(O)Me**Figure 4.1** Examples of gold(III) metallacycles

The reactivity of these gold(III) dihalides appears to mimic square-planar platinum(II) and palladium(II) L_2MCl_2 complexes in most cases. There are, however, differences in the reactivity of these metals, notably the different products when thioureas are reacted with $[L_2PtCl_2]$ and $[LAuCl_2]$. The product of the reaction with platinum(II) is a mixed-donor four-membered metallacycle $cis-[Pt\{\overbrace{N(Ph)C=N(Ph)S}^{\text{}}\}L_2]$ (4.5),¹¹ while with the gold(III) complexes (4.1) the dimethylthiourea undergoes an unusual desulfurisation resulting in mixed-metal aggregate cations (4.6) (Figure 4.2).¹² The reactivity of gold(III) dihalides with organic reagents in the presence of silver(I) oxide appears to be greater than platinum(II) or palladium(II) dihalide compounds.

11 a) W. Henderson, R. D. W. Kemmitt, S. Mason, M. R. Moore, J. Fawcett and D. R. Russell, *J. Chem. Soc., Dalton Trans.*, (1992), 59; b) S. Okeya, Y. Fujiwara, S. Kawashima, Y. Hayashi, K. Isobe, Y. Makamura, H. Shimomura and Y. Kushi, *Chem. Lett.*, (1993), 32, 1823; c) W. Henderson and B. K. Nicholson, *Polyhedron*, (1996), 15, 4015

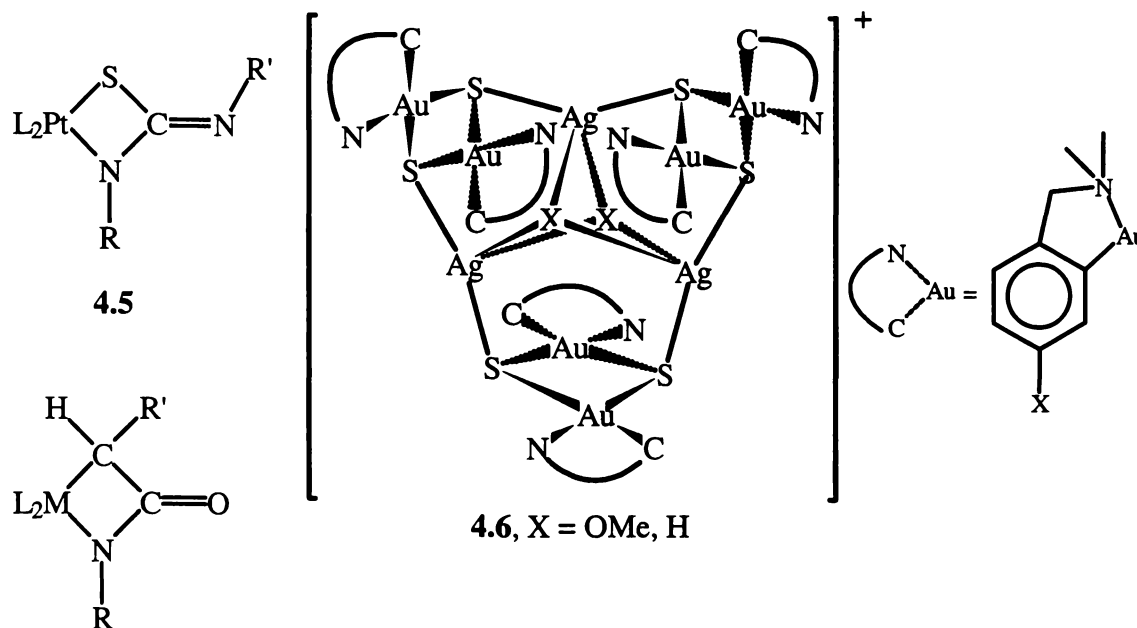


Figure 4.2 Metallacyclic complexes of platinum, palladium and gold

Gold(I) complexes have found a niche in medicine as effective anti-arthritis drugs.^{13,14} However, gold(III), unlike its isoelectronic counterpart platinum(II), has proved to be less effective in any drug role. This may be due to the high lability and oxidising power of the gold(III) centre,¹³ though fewer gold(III) complexes have been synthesised and tested compared to platinum(II) complexes. Complexes of gold(III) with amide ligands are of interest as models for the binding of gold(III) to peptides.¹⁵

In this chapter is reported the synthesis of the first metallalactam complexes of gold(III), similar to those described previously for platinum(II) and palladium(II) (4.7a-f).^{2,3,4} Both a monomeric four-membered auralactam of the type $[LAu\{N(R)C(O)CH(R')\}]$; [L

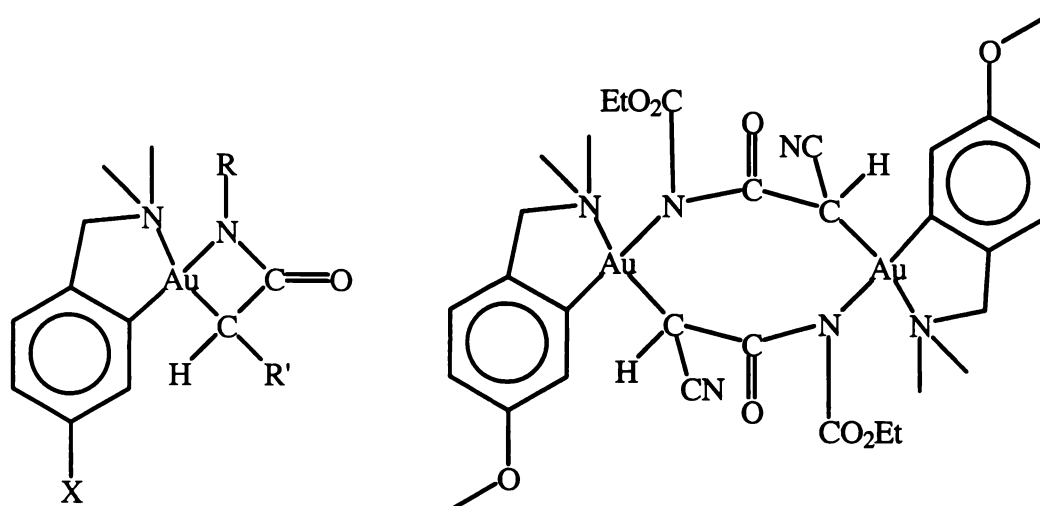
12 M. B. Dinger, W. Henderson, B. K. Nicholson and W. T. Robinson, *J. Organomet. Chem.*, (1998), **560**, 169

13 P. J. Sadler, *Adv. Inorg. Chem.*, (1991), **36**, 1

14 S. J. Berners-Price and P. J. Sadler, *Coord. Chem. Rev.*, (1996), **151**, 1

15 S. L. Best, T. K. Chattopadhyay, M. I. Djuran, R. A. Palmer, P. J. Sadler, I. Sóvágó and K. Varnagy, *J. Chem. Soc., Dalton Trans.*, (1997), 2587

= {C₆H₃(CH₂NMe₂)-2-(OMe)-5}, {C₆H₄(CH₂NMe₂)-2}, R = Ph, C(O)Et, R' = C(O)Me, C(O)Ph, CN] (4.8 – 4.13) and a novel dimerisation product (4.15) were completely characterised. The reaction of cyanoacetylurea [NH₂C(O)NHC(O)CH₂CN] with 4.1a in the presence of silver(I) oxide giving 4.14, is also reported. Reactions of cyanoacetylurea with palladium(II) and platinum(II) dihalide complexes are described in detail in chapter six.



4.8) X = OMe, R = CO₂Et, R' = CN

4.15

4.9) X = OMe, R = Ph, R' = C(O)Ph

4.10) X = OMe, R = Ph, R' = C(O)Me

4.11) X = H, R = CO₂Et, R' = CN

4.12) X = H, R = Ph, R' = C(O)Ph

4.13) X = H, R = Ph, R' = C(O)Me

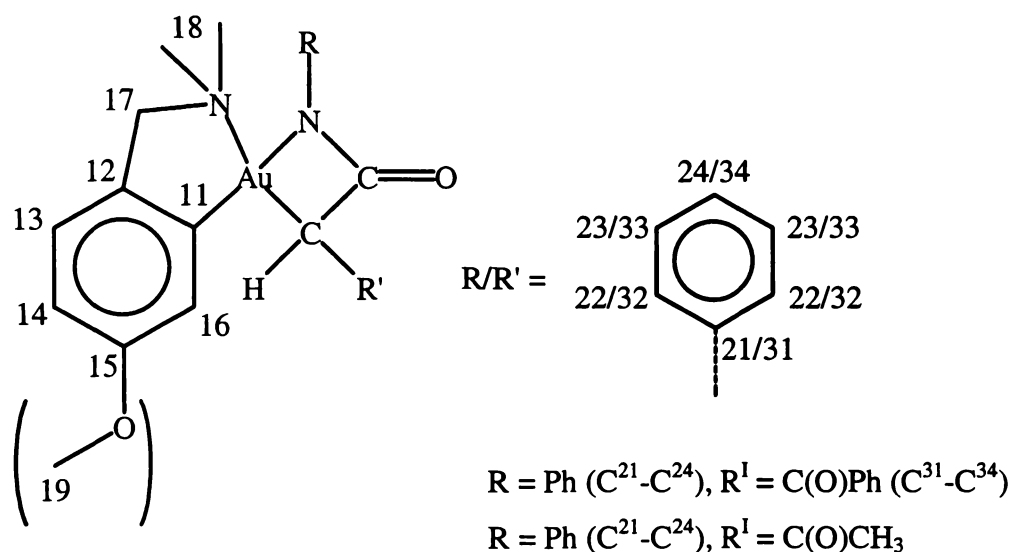
4.14) X = OMe, R = C(O)NH₂, R' = CN

Figure 4.3 Four-membered and eight-membered gold(III) metallacycles

4.2 Experimental

The complexes [$\{C_6H_3(CH_2NMe_2)-2-(OMe)-5\}AuCl_2$] (4.1a)⁶ and [$\{C_6H_4(CH_2NMe_2)-2\}AuCl_2$] (4.1b)⁷ were prepared following literature methods. Silver(I) oxide was prepared by a literature method.¹⁶ *N*-cyanoacetylurethane, 2-benzoylacetylurethane and acetoacetylurethane (Aldrich) were used as supplied. Solvents were distilled before use, dichloromethane and light petroleum from CaH₂ and diethyl ether from sodium benzophenone ketyl. All reactions were carried out under a dry nitrogen atmosphere

and were shielded from light. NMR spectra were recorded on a Brüker AC300P or a Brüker DRX400 in deuteriochloroform. ^1H NMR were recorded at 300.133 or 400.131 MHz respectively and referenced to tetramethylsilane (TMS) (δ 0) as an internal standard. ^{13}C NMR spectra were obtained at 75.47 or 100.61 MHz and referenced to internal TMS (δ 0). Experimental NMR data were assigned per Scheme 4.1 ES/MS spectra were recorded on a VG Platform II electrospray mass spectrometer in positive ion mode. The ESMS carrier solvent was a 1:1 acetonitrile/water mixture. Infrared spectra were collected on a Bio-Rad FTS-40 infrared spectrophotometer. Melting points were determined on a Reichert Thermopan apparatus in air. Accurate X-ray intensity data were collected on a Siemens SMART CCD diffractometer.



Scheme 4.1 NMR labeling scheme

4.2.1 Synthesis of $\{[\text{C}_6\text{H}_3(\text{CH}_2\text{NMe}_2)\text{-2-(OMe)-5}]\text{Au}\{\text{N}(\text{CO}_2\text{Et})\text{C}(\text{O})\text{CHCN}\}\}$ (4.8)

A mixture of $\{[\text{C}_6\text{H}_3(\text{CH}_2\text{NMe}_2)\text{-2-(OMe)-5}]\text{AuCl}_2\}$ (0.046 g, 0.11 mmol), *N*-cyanoacetylurethane (0.017 g, 0.11 mmol) and silver(I) oxide (0.045 g, excess) in degassed dichloromethane (20 cm³) were heated at reflux for 3 h. The silver salts were removed by filtration with no precautions to exclude air, and the solvent removed from the filtrate under reduced pressure giving a pale tan solid. The product was redissolved in dichloromethane (ca. 1 cm³) and precipitated by addition to light petroleum (ca. 40 cm³), yielding a pale tan microcrystalline solid (0.046 g, 83%). The product was identified by NMR spectroscopy and electrospray mass spectrometry.

Elemental analysis: C, 36.5; H, 3.8; N, 8.0. $C_{16}H_{20}N_3AuO_4$ requires C, 37.3; H, 3.9; N, 8.2%.

IR: $\nu(CN)$ 2224, $\nu(CO)$ 1746, 1700 cm^{-1} .

m.p.: 210 - 213 °C (decomp.).

ES/MS (20V): $[M+H]^+$ m/z 516, (100%); $[M+NH_4]^+$ m/z 533, (30%); $[2M+NH_4]^+$ m/z 1048, (90%).

1H NMR: δ 7.10 [d, 1H, H^{13} , $^3J(H^{13}, H^{14})$ 8], 7.05 [d 1H, H^{16} , $^4J(H^{16}, H^{14})$ 2], 6.81 [dd, 1H, H^{14} , $^3J(H^{14}, H^{13})$ 8, $^4J(H^{14}, H^{16})$ 2], 4.26 [q, 2H, ethyl CH_2 , $^3J(H, H)$ 7], AB spin system, 4.17 [d, 1H, H^{17a} , $^2J(H, H)$ 16], 4.13 [d, 1H, H^{17b} , $^2J(H, H)$ 16], 3.81 (s, 3H, H^{19}), 3.26 (s, 6H, H^{18}), 1.67 (s, 1H, ring CH), 1.35 [t, 3H, ethyl CH_3 , $^3J(H, H)$ 7].

^{13}C - $\{^1H\}$ NMR: δ 166.0 [s, ring C(O)], 158.6 (s, C^{12}), 139.5 [s, ester C(O)], 138.2 (s, C^{11}), 124.1 (s, C^{15}), 117.4 (s, C^{13}), 117.2 (s, C^{16}), 116.1 (s, CN), 114.5 (s, C^{14}), 72.4 (s, C^{17}), 62.5 (s, ethyl CH_2), 55.6 (s, C^{19}), 51.8 (s, C^{18a}), 51.7 (s, C^{18b}), 18.4 (s, ring CH), 14.5 (s, ethyl CH_3).

4.2.1.1 Crystallisation of the dimeric complex $[\{C_6H_3(CH_2NMe_2)-2-(OMe)-5\}Au\{N(CO_2Et)C(O)CHCN\}]_2 \cdot 2CDCl_3$ (4.15)

Colourless crystals of the dimeric complex (4.15) precipitated from an NMR solution of 4.8 in deuteriochloroform during an 18 hour data collection. Gold colloid was also observed, indicating that over an extended period of time the complex is thermally and/or photosensitive. EDAX analysis of a crushed crystal indicated that gold and chlorine were present and IR spectroscopy confirmed the presence of cyanide and carbonyl stretching frequencies in a selection of the crystals. Preliminary X-ray precession photography gave data consistent with the monoclinic, $P2_1/c$ space group.

4.2.2 Preparation of $[\{C_6H_3(CH_2NMe_2)-2-(OMe)-5\}Au\{N(Ph)C(O)CHC(O)Ph\}]$ (4.9)

$[\{C_6H_3(CH_2NMe_2)-2-(OMe)-5\}AuCl_2]$ (0.052 g, 0.12 mmol), 2-benzoylacetyl anilide (0.029 g, 0.12 mmol) and silver(I) oxide (0.062 g, excess) were heated at reflux in degassed dichloromethane (20 cm^3) for 2.5 h. Removal of the silver salts by filtration afforded a deep yellow solution and subsequent removal of the solvent under reduced pressure afforded a dark tan solid. The tan product was recrystallised by precipitation

from a dichloromethane solution (*ca.* 2 cm³) of **4.2** by the addition of light petroleum (*ca.* 30 cm³). This solid was filtered in air and dried *in vacuo* (0.048g, 66%)

Elemental Analysis: C, 50.4; H, 4.2; N, 4.8. C₂₅H₂₅N₂AuO₃ requires: C, 50.2; H, 4.2; N, 4.7%.

IR: $\nu(\text{CO})$ 1643 cm⁻¹.

m.p.: 197 - 201 °C (decomp.).

ES/MS (20V): [M+H]⁺ *m/z* 599, (100%).

¹H NMR: δ 8.17 [dd, 2H, H³², ³J(H³², H³³) 8, ⁴J(H³³, H³⁴) 2], 7.50 [t, 1H, H³⁴, ³J(H³⁴, H³³) 7, ⁴J(H³⁴, H³²) 2], 7.43 [dist. t, 2H, H²³, ³J(H²³, H^{22/24}) 8], 7.35 [dist. t, 2H, H³³, ³J(H³³, H^{32/34}) 8], 7.24 [d, 2H, H²², ³J(H²², H²³) 8, ⁴J(H²², H²⁴) 1], 7.11 [t, 1H, H²⁴, ³J(H²⁴, H²³) 8, ⁴J(H²⁴, H²²) 1], 6.98 [d, 1H, H¹³, ³J(H¹³, H¹⁴) 8], 6.72 [d, 1H, H¹⁶, ⁴J(H¹⁶, H¹⁴) 3], 6.64 [dd, 1H, H¹⁴, ³J(H¹⁴, H¹³) 8, ⁴J(H¹⁴, H¹⁶) 3], 4.19 (s, ring CH), AB spin system, 3.97 [d, 1H, H^{17a}, ²J(H, H) 14], 3.88 [d, 1H, H^{17b}, ²J(H, H) 14], 2.75 (s, 3H, H¹⁸), 2.74 (s, 3H, H¹⁸).

¹³C-¹H NMR: 196.9 [s, C(O)Ph], 170.3 [s, ring C(O)], 158.2 (s, C¹²), 141.9 (s, C¹¹), 141.5 (s, C²¹), 138.8 (s, C³¹), 137.6 (s, C¹⁵), 132.6 (s, C³⁴), 129.2 (s, C³³), 129.0 (s, C³²), 128.5 (s, C²³), 126.4 (s, C²²), 125.1 (s, C²⁴), 124.1 (s, C¹³), 117.6 (s, C¹⁶), 114.1 (s, C¹⁴), 71.5 (s, C¹⁷), 55.2 (s, C¹⁹), 50.8 (s, C^{18a}), 50.7 (s, C^{18b}), 44.4 (s, ring CH).

4.2.3 Preparation of $[\{\text{C}_6\text{H}_3(\text{CH}_2\text{NMe}_2)\text{-2-(OMe)-5}\}\text{Au}\{\text{N(Ph)C(O)CHC(O)CH}_3\}]$ (**4.10**)

In degassed dichloromethane (20 cm³), $[\{\text{C}_6\text{H}_3(\text{CH}_2\text{NMe}_2)\text{-2-(OMe)-5}\}\text{AuCl}_2]$ (0.052 g, 0.12 mmol), acetoacetanilide (0.023 g, 0.13 mmol) and silver(I) oxide (0.229 g, excess) were heated at reflux for 4 h. The silver salts were removed by filtration in air affording a pale tan solution. The solvent was removed under reduced pressure giving the crude product as a tan powder. The product was redissolved in dichloromethane (*ca.* 3cm³) and precipitated by the addition of diethyl ether (*ca.* 50 cm³). The tan precipitate was filtered and dried (0.040 g, 63%).

Elemental Analysis: C, 44.9; H, 4.1; N, 5.6. C₂₀H₂₃N₂AuO₃ requires: C, 44.8; H, 4.3; N, 5.2%.

IR: $\nu(\text{CO})$ 1641 cm⁻¹.

m.p.: 186 - 191 °C (decomp.).

ES/MS (20V): $[M+H]^+$ m/z 537, (100%).

1H NMR: 7.38 [t, 2H, H^{23} , $^3J(H^{23}, H^{22/24})$ 8], 7.22 [dd, 2H, H^{22} , $^3J(H^{22}, H^{23})$ 8, $^4J(H^{22}, H^{21})$ 1], 7.14 [t, 1H, H^{24} , $^3J(H^{24}, H^{23})$ 8], 7.09 [d, 1H, H^{16} , $^4J(H^{16}, H^{14})$ 2], 7.06 [d, 1H, H^{13} , $^3J(H^{13}, H^{14})$ 8], 6.74 [dd, 1H, H^{14} , $^3J(H^{14}, H^{13})$ 8, $^4J(H^{14}, H^{16})$ 2], AB spin system, 4.03 [d, 1H, H^{17a} , $^2J(H, H)$ 22], 3.98 [d, 1H, H^{17b} , $^2J(H, H)$ 22], 3.86 (s, 3H, H^{19}), 3.41 (s, 1H, ring CH), 2.82 (s, 3H, H^{18a}), 2.79 (s, 3H, H^{18b}), 2.41 [s, 3H, $C(O)CH_3$].

^{13}C - $\{^1H\}$ NMR: 203.1 [s, $C(O)CH_3$], 170.4 [s, ring $C(O)$], 158.5 (s, C^{12}), 141.7 (s, C^{11}), 141.3 (s, C^{21}), 137.4 (s, C^{15}), 129.2 (s, C^{23}), 126.4 (s, C^{22}), 125.2 (s, C^{24}), 123.9 (s, C^{13}), 116.9 (s, C^{16}), 114.3 (s, C^{14}), 71.5 (s, C^{17}), 55.6 (s, OCH_3), 50.9 (s, C^{18a}), 50.8 (s, C^{18b}), 48.2 (s, ring CH), 27.7 [s, $C(O)CH_3$].

4.2.4 Preparation of $[\{C_6H_4(CH_2NMe_2)_2\}Au\{N(CO_2Et)C(O)CHCN\}]$ (4.11)

A stirred mixture of $[\{C_6H_3(CH_2NMe_2)_2\}AuCl_2]$ (0.050 g, 0.12 mmol), *N*-cyanoacetylurethane (0.020 g, 0.13 mmol) and silver(I) oxide (0.287 g, excess) were heated at reflux in degassed dichloromethane (20 cm³) for 4 h. Light was excluded during the reaction. Silver salts were removed by filtration, and solvent removed under reduced pressure from the solution giving a pale yellow solid. The complex was recrystallised by vapour diffusion of diethyl ether into dichloromethane. The light yellow crystalline solid was collected and dried under vacuum (0.030 g, 50%).

Elemental Analysis: C, 33.9; H, 4.0; N, 8.9. $C_{15}H_{18}N_3AuO_3$ requires: C, 37.1; H, 3.7; N, 8.7%.

IR: $\nu(CN)$ 2225 cm⁻¹, $\nu(CO)$ 1745, 1691 cm⁻¹.

m.p.: 220 - 223 °C (decomp).

ES/MS (20V): $[M+H]^+$ m/z 487, (100%).

1H NMR: δ 7.47 [d, 1H, H^{14} , $^3J(H^{14}, H^{13/15})$ 8], 7.10 [d, 1H, H^{16} , $^3J(H^{16}, H^{15})$ 8], 7.05 [d, 1H, H^{13} , $^4J(H^{13}, H^{15})$ 2], 6.81 [dd, 1H, H^{15} , $^3J(H^{15}, H^{16})$ 8, $^4J(H^{15}, H^{13})$ 2], 4.26 [q, 2H, ethyl CH_2 , $^3J(H, H)$ 7], AB spin system, 4.07 [d, 1H, H^{17a} , $^2J(H, H)$ 15], 4.02 [d, 1H, H^{17b} , $^2J(H, H)$ 15], 3.40 (s, 6H, H^{18}), 1.68 (s, 1H, ring CH), 1.38 [t, H, ethyl CH_3 , $^3J(H, H)$ 7].

^{13}C - $\{^1H\}$ NMR: δ 174.8 [s, ring $C(O)$], 166.1 [s, ester $C(O)$], 156.6 (s, C^{12}), 146.5 (s, C^{11}), 132.5 (s, C^{15}), 128.5 (s, C^{13}), 127.7 (s, C^{16}), 123.6 (s, C^{14}), 117.5 (s, CN), 72.8 (s, C^{17}), 62.4 (s, ester CH_2), 52.0 (s, C^{18a}), 51.8 (s, C^{18b}), 18.3 (s, ring CH), 14.5 (s, ester CH_3).

4.2.5 Preparation of $[\{C_6H_4(CH_2NMe_2)_2\}Au\{N(Ph)C(O)CHC(O)Ph\}]$ (4.12)

A stirred mixture of $[\{C_6H_4(CH_2NMe_2)_2\}AuCl_2]$ (0.118 g, 0.355 mmol), 2-benzoylacetyl anilide (0.087 g, 0.36 mmol) and silver (I) oxide (0.487 g, excess) was heated at reflux in dichloromethane (20 cm³) for 2 h under nitrogen. Silver salts were removed by filtration affording a deep yellow solution. Solvent was removed under reduced pressure giving a yellow solid. An off-white microcrystalline solid was recrystallised from dichloromethane / diethyl ether and dried *in vacuo* (0.147 g, 73%).

Elemental Analysis: C, 53.5; H, 4.8; N, 5.5. C₂₄H₂₃N₂AuO₂ requires: C, 50.7; H, 4.1; N, 4.9%.

IR: $\nu(CO)$ 1642 cm⁻¹.

m.p.: 184 - 187 °C (decomp.).

ES/MS (20 V): $[M+H]^+$ m/z 569, (100%).

¹H NMR: 8.17 [dd, 2H, H³², ³J(H³², H³³) 8, ⁴J(H³², H³⁴) 2], 7.74 [dd, 1H, H¹⁴, ³J(H¹⁴, H^{13/15}) 8], 7.59 [t, 1H, H³⁴, ³J(H³⁴, H³³) 7, ⁴J(H³⁴, H³²) 2], 7.48 [dist. t, 2H, H³³, ³J(H³³, H^{32/34}) 8], 7.43 [dist. T, 2H, H²³, ³J(H²³, H^{22/24}) 8], 7.36 [d, 2H, H²², ³J(H²², H²³) 8, ⁴J(H²², H²⁴) 1], 7.24 [t, 1H, H²⁴, ³J(H²⁴, H²³) 8, ⁴J(H²⁴, H²²) 1], 7.17 [d, 1H, H¹³, ³J(H¹³, H¹⁴) 8], 6.73 [d, 1H, H¹⁶, ⁴J(H¹⁶, H¹⁴) 3], 6.95 [dd, 1H, H¹⁴, ³J(H¹⁴, H¹³) 8, ⁴J(H¹⁴, H¹⁶) 3], 4.22 (s, ring CH), AB spin system, 4.09 [d, 1H, H^{17a}, ²J(H, H) 14], 4.03 [d, 1H, H^{17b}, ²J(H, H) 14], 3.01 (br. s, 6H, H¹⁸).

¹³C-¹H NMR: 196.9 [s, C(O)Ph], 170.2 [s, ring C(O)], 158.2 (s, C¹²), 145.5 (s, C¹¹), 141.5 (s, C²¹), 138.8 (s, C³¹), 137.5 (s, C¹⁵), 132.6 (s, C³⁴), 129.2 (s, C²³), 128.9 (s, C³²), 128.5 (s, C³³), 126.4 (s, C²²), 125.1 (s, C²⁴), 123.4 (s, C¹³), 122.8 (s, C¹⁶), 120.1 (s, C¹⁴), 72.0 (s, C¹⁷), 51.0 (s, C^{18a}), 50.7 (s, C^{18b}), 45.4 (s, ring CH).

4.2.6 Preparation of $[\{C_6H_4(CH_2NMe_2)_2\}Au\{N(Ph)C(O)CHC(O)CH_3\}]$ (4.13)

A degassed dichloromethane solution (20 cm³) of $[\{C_6H_3(CH_2NMe_2)_2\}AuCl_2]$ (0.034 g, 0.084 mmol), acetoacetanilide (0.016 g, 0.089 mmol) and silver(I) oxide was heated at reflux for 2.5 h. Silver salts were removed by filtration affording a pale yellow solution. The solvent was removed under reduced pressure and the tan product recrystallised from dichloromethane / diethyl ether (0.060 g, 36%). Crystals of single

crystal X-ray diffraction quality were grown by vapour diffusion of diethyl ether into a dichloromethane solution of **4.13**.

Elemental Analysis: C, 45.0; H, 4.1; N, 5.7. $C_{19}H_{21}N_2AuO_2$ requires: C, 45.1; H, 4.2; N, 5.5%.

IR: $\nu(\text{CO})$ 1641 cm^{-1} .

m.p.: 184 - 187 °C (decomp.).

ES/MS (20 V): $[\text{M}+\text{H}]^+$ m/z 507, (100%).

^1H NMR: δ 7.45 [d, H^{15} , $^3J(\text{H}, \text{H})$ 7], 7.37 [dist. t, H^{23} , $^3J(\text{H}, \text{H})$ 7], 7.21 [dd, H^{22} , $^3J(\text{H}, \text{H})$ 7], 7.20 [t, H^{24} , $^3J(\text{H}, \text{H})$ 8], 7.15 [t, H^{16} , $^3J(\text{H}, \text{H})$ 7], 7.15 [t, H^{13} , $^3J(\text{H}, \text{H})$ 8], 7.13 [t, H^{14} , $^3J(\text{H}, \text{H})$ 8], AB spin system, 4.10 [d, 1H, H^{17a} , $^2J(\text{H}, \text{H})$ 14], 3.99 [d, 1H, H^{17b} , $^2J(\text{H}, \text{H})$ 14], 3.40 (s, 1H, ring CH), 2.83 (s, 3H, H^{18}), 2.79 (s, 3H, H^{18}), 2.40 [s, 3H, $\text{C}(\text{O})\text{CH}_3$].

$^{13}\text{C}\{-^1\text{H}\}$ NMR: δ 201.3 [s, $\text{C}(\text{O})\text{CH}_3$], 169.5 [s, ring $\text{C}(\text{O})$], 158.4 (s, C^{12}), 146.4 (s, C^{21}), 145.4 (s, C^{11}), 132.6 (s, C^{15}), 128.5 (s, C^{23}), 128.1 (s, C^{13}), 127.4 (s, C^{24}), 123.9 (s, C^{22}), 123.5 (s, C^{14}), 122.6 (s, C^{16}), 72.8 (s, C^{17}), 52.0 (s, C^{18a}), 51.8 (s, C^{18b}), 48.4 (s, ring CH), 14.5 [s, $\text{C}(\text{O})\text{CH}_3$].

4.2.7 Synthesis of $[\{\text{C}_6\text{H}_3(\text{CH}_2\text{NMe}_2)\text{-2-(OMe)-5}\}\text{Au}\{\text{N}(\text{CONH}_2)\text{C}(\text{O})\text{CHCN}\}]$ (**4.14**)

A mixture of *cis*- $[\{\text{C}_6\text{H}_3(\text{CH}_2\text{NMe}_2)\text{-2-(OMe)-5}\}\text{AuCl}_2]$ (0.052 g, 0.12 mmol), cyanoacetylurea (0.016 g, 0.13 mmol) and silver(I) oxide (0.111 g, excess) were heated at reflux under nitrogen in degassed dichloromethane (20 cm^3) for 3 h. Light was excluded from the reaction. Silver salts were separated from a tan solution by filtration in air. The solvent was removed *in vacuo* giving a pale tan solid. This product was recrystallised by the addition of diethyl ether (30 cm^3) to a dichloromethane solution of the product (2 cm^3), and the resulting precipitate was filtered in air and dried (0.034 g, 57%).

Elemental Analysis: C, 31.50; H, 3.0; N, 9.9. $C_{14}H_{17}N_4AuO_3 \cdot \text{CH}_2\text{Cl}_2$ requires: C, 31.5; H, 3.4; N, 9.8%.

IR: $\nu(\text{CO})$ 1642 cm^{-1} .

m.p.: 191 - 194 °C (decomp.).

ES/MS (20 V): $[\text{M}+\text{H}]^+$ m/z 487, (100%).

^1H NMR: δ 7.64 (br. s, NH_2), 7.08 [d, 1H, H^{13} , $^3J(\text{H}^{13}, \text{H}^{14})$ 8], 7.01 [d, 1H, H^{16} , $^4J(\text{H}^{16}, \text{H}^{14})$ 3], 6.77 [dd, 1H, H^{14} , $^3J(\text{H}^{14}, \text{H}^{13})$ 8, $^4J(\text{H}^{14}, \text{H}^{16})$ 3], AB spin system, 4.26 [d, 1H, H^{17a} , $^2J(\text{H}, \text{H})$ 14], 4.23 [d, 1H, H^{17b} , $^2J(\text{H}, \text{H})$ 14], 4.14 (s, 1H, ring CH), 3.81 (s, 3H, H^{19}), 3.36 (s, 6H, H^{18}).

^{13}C - $\{^1\text{H}\}$ NMR: δ 202.0 [s, $\text{C}(\text{O})\text{CH}_3$], 169.4 [s, ring $\text{C}(\text{O})$], 158.3 (s, C^{15}), 138.9 (s, C^{11}), 137.8 (s, C^{12}), 124.1 (s, C^{13}), 117.2 (s, C^{16}), 114.4 (s, C^{14}), 72.4 (s, C^{17}), 55.6 (s, ring CH), 52.6 (s, C^{18a}), 52.5 (s, C^{18b}), 16.2 [s, $\text{C}(\text{O})\text{CH}_3$].

4.2.8 X-ray Crystallography

Both data sets were collected on a Siemens SMART CCD diffractometer. Data for **4.13** was collected covering a full sphere of reciprocal space, while the data for **4.15** covered an arbitrary hemisphere of reciprocal space. Data were corrected for Lorentz and polarisation effects. An empirical absorption correction based on comparisons of the intensities of redundant and equivalent reflections was made.

The location of the gold atom of the complex $[\text{C}_6\text{H}_4(\text{CH}_2\text{NMe}_2)\text{-}2\text{Au}\{\text{N}(\text{Ph})\text{C}(\text{O})\text{CHC}(\text{O})\text{CH}_3\}]$ (**4.13**) was determined by Patterson methods (SHELXS-97)¹⁷. Remaining atoms were located from residual electron density maps, and refined routinely [full-matrix least-squares based on F^2 (SHELXL-97)]¹⁸. All non-hydrogen atoms were refined anisotropically. Hydrogen atoms were included in calculated positions, with U_{iso} 1.5 times that of the atom to which they are bonded for methyl hydrogens and 1.2 times for all other hydrogen atoms. Table 4.1 details the cell and final cycle refinement parameters. The final difference Fourier map showed significant electron density ($1.84 \text{ e}\cdot\text{\AA}^{-3}$) located at the origin (0, 0, 0). This may be due to an improper application of the absorption correction.

The structure of the complex $[\{\text{C}_6\text{H}_3(\text{CH}_2\text{NMe}_2)\text{-}2\text{-(OMe)-}5\text{Au}\{\text{N}(\text{CO}_2\text{Et})\text{C}(\text{O})\text{CHCN}\}]_2\cdot 2\text{CDCl}_3$ (**4.15**) was determined by direct methods (SHELXS-96)¹⁹. Cell parameters and refinement details for the final cycle of least-

17 G. M. Sheldrick, SHELXS-97, Program for the solution of single crystal X-ray structures, (1997), Universität Göttingen, Germany

18 G. M. Sheldrick, SHELXL-97, Program for the refinement of single crystal X-ray structures, (1997), Universität Göttingen, Germany

19 G. M. Sheldrick, SHELXS-96, Program for the solution of single crystal X-ray structures, (1996), Universität Göttingen, Germany

squares refinement are given in Table 4.1 below. Atoms not located in the initial map were located from subsequent electron density maps. Refinement was a full-matrix least-squares method, based on F^2 . All heavy atoms were refined with anisotropic thermal parameters. Hydrogen atoms were included in calculated positions with methyl hydrogens assigned thermal parameters 1.5 times the U_{iso} of the atom to which they were bonded and all others with thermal parameters 20% greater than the U_{iso} of the atom to which they were bonded. The final difference Fourier map showed some residual electron density ($1.26 \text{ e.}\text{\AA}^{-3}$) located 1.04 \AA from the gold atom.).

Table 4.1 Data collection and structure refinement details for $[\text{C}_6\text{H}_4(\text{CH}_2\text{NMe}_2)\text{-}2]\text{Au}\{\text{N}(\text{Ph})\text{C}(\text{O})\text{CHC}(\text{O})\text{CH}_3\}$ (4.13) and $[\{\text{C}_6\text{H}_3(\text{CH}_2\text{NMe}_2)\text{-}2\text{-}(\text{OMe})\text{-}5\}\text{Au}\{\text{N}(\text{CO}_2\text{Et})\text{C}(\text{O})\text{CHCN}\}]_2 \cdot 2\text{CDCl}_3$ (4.15)

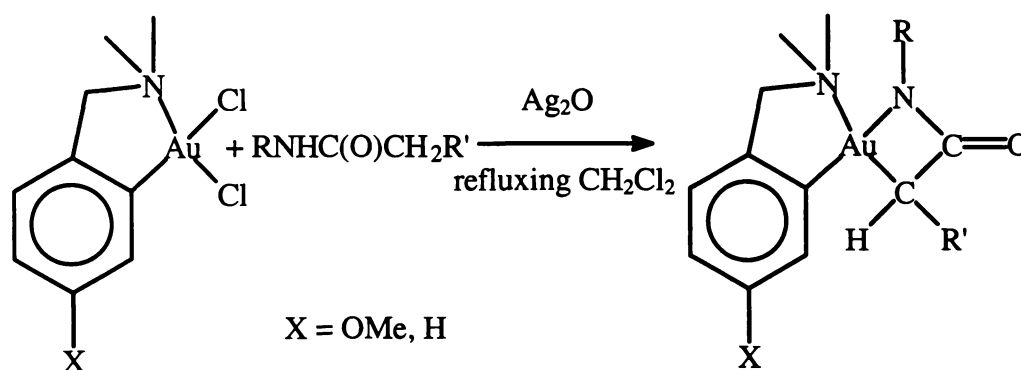
<i>Crystal data</i>	4.13	4.15
Empirical formula	$\text{C}_{19}\text{H}_{21}\text{AuN}_2\text{O}_2$	$\text{C}_{16}\text{H}_{20}\text{AuN}_3\text{O}_4 \cdot \text{CDCl}_3$
Formula weight	506.34	636.70
Crystal system	Triclinic	Monoclinic
Space group	$\bar{P}1$	$\text{P}2_1/\text{c}$
Unit cell dimensions		
a (Å)	8.721(1)	12.359(1)
b (Å)	10.7841(1)	15.1831(1)
c (Å)	11.0297(1)	12.5665(1)
α (°)	61.6520(1)	90
β (°)	84.37(1)	113.740(1)
γ (°)	79.537(1)	90
Volume (Å ³)	897.662(12)	2158.52(2)
Z	2	4
$D(c)$ (g cm ⁻³)	1.873	1.959
<i>Data Collection</i>		
Diffractometer	Siemens SMART CCD	Siemens SMART CCD
Radiation	Mo-K α	Mo-K α
Wavelength (Å)	0.71073	0.71073
Temperature (K)	203(2)	203(2)
Crystal size (mm)	0.40 x 0.30 x 0.22	0.34 x 0.30 x 0.22

θ range for data collection ($^{\circ}$)	2.10 to 28.13	1.80 to 28.17
Index ranges	$-11 \leq h \leq 11$ $-14 \leq k \leq 13,$ $-14 \leq l \leq 13$	$-16 \leq h \leq 14$ $0 \leq k \leq 20,$ $0 \leq l \leq 16$
Reflections collected	8901	4955
Independent reflections	3935 [R(int) = 0.0193]	4955 [R(int) = 0.0000]
Absorption coefficient (mm^{-1})	8.207	7.211
Maximum transmission	0.2654	0.2998
Minimum transmission	0.1378	0.1929
F(000)	488	1228
<i>Structure analysis and refinement</i>		
Solution by	Patterson	Direct methods
Refinement method	Full-matrix least-squares on F^2	Full-matrix least-squares on F^2
Data / restraints / parameters	3935 / 0 / 220	4955 / 0 / 251
Goodness-of-fit on F^2	1.104	1.065
Final R indices [$I > 2\sigma(I)$]	$R_1 = 0.0188,$ $wR^2 = 0.0475$	$R_1 = 0.0213,$ $wR^2 = 0.0524$
R indices (all data)	$R_1 = 0.0197,$ $wR^2 = 0.0480$	$R_1 = 0.0236,$ $wR^2 = 0.0536$
Weighting Scheme:	$w = 1/[\sigma^2(F_o^2) + (0.0135P)^2 + 1.1058P]$ where $P = (F_o^2 + 2F_c^2)/3$	$w = 1/[\sigma^2(F_o^2) + (0.0237P)^2 + 3.6911P]$ where $P = (F_o^2 + 2F_c^2)/3$
Largest difference peak ($e.\text{\AA}^{-3}$)	1.845	1.257
Largest difference hole ($e.\text{\AA}^{-3}$)	-1.087	-1.663
Programs used		
Solution by	SHELXS-97 ¹⁷	SHELXS-96 ¹⁹
Refinement by	SHELXL-97 ¹⁸	SHELXL-97 ¹⁸

4.3 Results and Discussion

4.3.1 Synthesis of Organogold Metallalactam Complexes

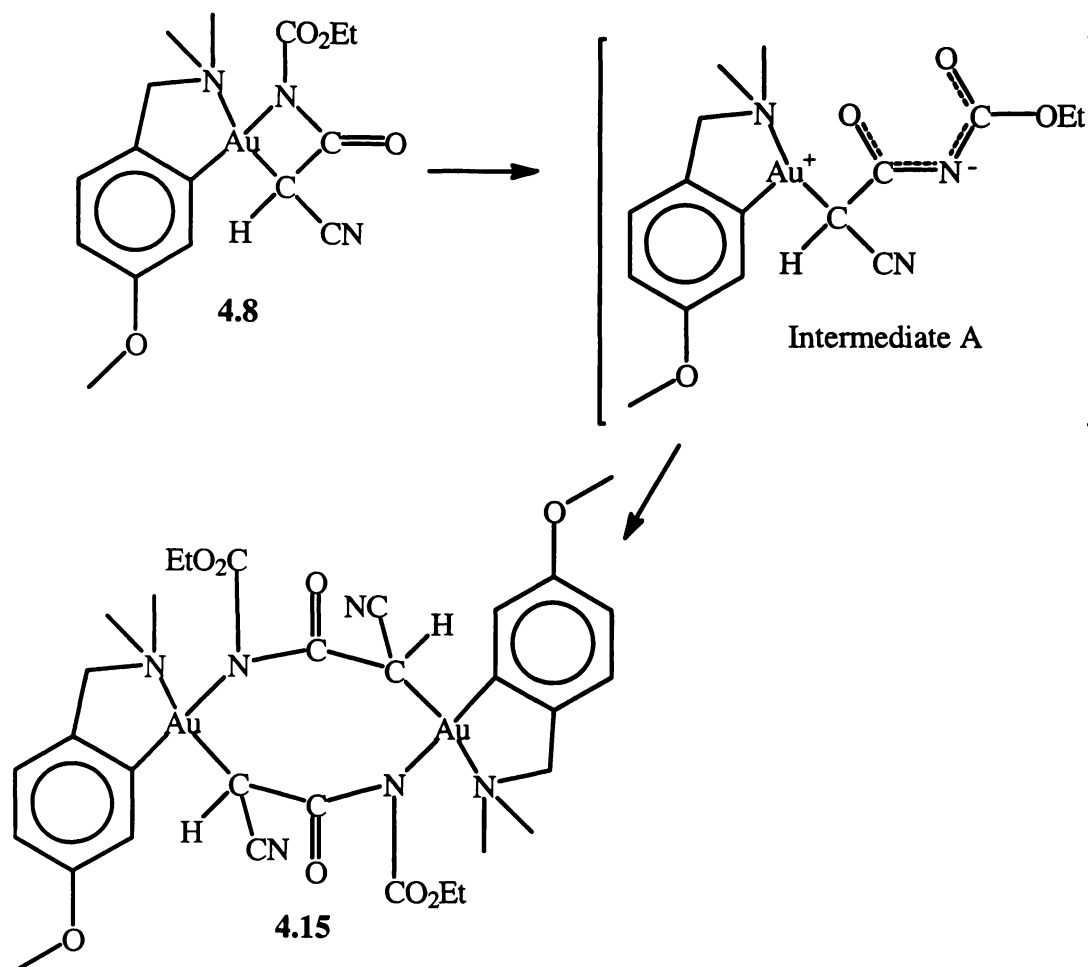
The reaction of [$\{C_6H_3(CH_2NMe_2)-2-(OMe)-5\}AuCl_2$] (**4.1a**) and [$\{C_6H_4(CH_2NMe_2)-2\}AuCl_2$] (**4.1b**) with *N*-cyanoacetylurethane, 2-benzoylacetylurethane and acetoacetanilide, in the presence of silver(I) oxide afford good yields of the metallacyclic complexes **4.8** – **4.13** (Figure 4.3, Scheme 4.2). Initial characterisation of these complexes indicated that the desired four-membered auralactam complexes had been synthesised. On the basis of NMR spectroscopy and ES/MS, for example, the complex (**4.10**) formed by the reaction of [$\{C_6H_3(CH_2NMe_2)-2-(OMe)-5\}AuCl_2$] (**4.1a**) with acetoacetanilide is the expected four-membered metallacycle. These complexes, once formed, are relatively inert with respect to air, however it does appear that some decomposition does occur. A slight purple colouration, indicative of gold colloid, was observed on the surface of several of the compounds after several days, although the products were shielded from light.



Scheme 4.2 Auralactam synthesis

One unusual result obtained here was the novel dimerisation of one of these auralactams (**4.8**) to produce an eight-membered metallacycle (**4.15**) upon standing in a deuteriochloroform solution. The complex **4.15** is insoluble in a wide range of solvents, e.g. chloroform (from which it was originally crystallised), methanol, dilute ammonia solution and diethyl ether. This dimerisation is unexpected and unprecedented in organogold and platinum group metallacyclic chemistry. Since the gold–nitrogen bond of the metallacycle is more labile than the gold–carbon bond, it can be proposed that it would preferentially cleave forming a three-coordinate intermediate complex (intermediate A below). The highly strained nature of the four-membered metallalactam

may also contribute towards this bond cleavage and molecular rearrangement. Dimerisation of two of these intermediates would result in the formation of the observed eight-membered metallacyclic complex **4.15** (Scheme 4.3).



Scheme 4.3 Proposed dimerisation of **4.8** to give **4.15**

Dimerisation of the related platinum(II) four-membered metallalactam **4.7a** has not been observed. The ligand exchange rates of gold(III), nickel(II), palladium(II) and platinum(II), with respect to the exchange of cyanide have been studied.²⁰ The results of these studies indicate that the lability at gold(III), with respect to ligand dissociation, is about two orders of magnitude greater than that of platinum(II). This high lability and the increased stability imparted by resonance delocalisation of the formal negative charge over the carbonyl groups adjacent to the urethane nitrogen (Scheme 4.3, intermediate A above), may account for the ring opening of the four-membered

auralactam, and the subsequent dimerisation for the *N*-cyanoacetylurethane derived auralactam.

The 2-benzoylacetanilide and acetoacetanilide auracycles did not appear to form any dimeric complexes. This would support the previous hypothesis that the urethane leaving group provides some additional stability, which an $[\text{N}(\text{Ph})]^-$ leaving group would not have. Alternatively the complex may form completely in one concerted step, however this is unlikely based on results of other characterisation techniques. Although ESMS indicates that an $[2\text{M}+\text{H}]^+$ species of **4.8** exists in solution, predominantly an $[\text{M}+\text{H}]^+$ species was observed. All of the monomeric complexes (**4.8** – **4.13**) were characterised in the solution state, while this dimeric complex (**4.15**) appears to be highly insoluble in a wide range of solvents.

4.3.2 The crystal structure of $[\{\text{C}_6\text{H}_4(\text{CH}_2\text{NMe}_2)\text{-}2\}\text{Au}\{\text{N}(\text{Ph})\text{C}(\text{O})\text{CHC}(\text{O})\text{CH}_3\}]$ (**4.13**)

The single crystal X-ray structure of $[\{\text{C}_6\text{H}_4(\text{CH}_2\text{NMe}_2)\text{-}2\}\text{Au}\{\text{N}(\text{Ph})\text{C}(\text{O})\text{CHC}(\text{O})\text{CH}_3\}]$ (**4.13**) (Figure 4.4) shows a distorted square-planar gold(III) centre with a coordinating cyclo-aurated *N,N*-dimethylbenzylamine ligand forming a five-membered metallacycle bonded to the gold(III) via the *ortho* aryl carbon and a dative bond from the amine nitrogen. A deprotonated acetoacetanilide moiety bonded to the gold(III) atom forms the four-membered metallalactam functionality.

The largest deviation from the Au, N(1), N(2), C(2), C(11) least-squares plane is 0.041(1) Å for Au (see Figure 4.5). The bond angles about the gold centre deviate considerably from an ideal square planar geometry. The largest distortion is the necessarily constricted N(2)-Au-C(2) “bite” angle of 66.65(12)°. Similar acute angles have been observed for platina- $[67.0(3)^\circ]^2$ and palladalactam $[67.1(2)^\circ]^{3,4}$ complexes. The gold-carbon bond lengths reflect the different hybridisation of the carbon atoms, with the gold- sp^2 carbon bond [Au-C(11)] being shorter [2.027(3) Å] than the gold- sp^3 carbon [Au-C(2) 2.076(3) Å]. These gold-carbon bond lengths are comparable with those found in previous examples [Au-C(benzyl) 2.001(3) to 2.065(5) Å,^{8-10,12} Au-C(*trans* dimethyl N) 2.05(2) and 2.109(5) Å^{8,9}]. The gold-nitrogen bonds also differ with the dative bond of Au-N(1) being longer [2.157(3) Å] than the covalent bond of Au-N(2) [2.097(3) Å]. The dimethyl nitrogen-gold bond is slightly longer than those

found in previous auracyclic complexes [2.057(3) to 2.14(1) Å].^{8-10,12} However, N(2) (*trans* to the benzyl carbon) has a gold–nitrogen bond length almost identical to that found in the isostructural auroreylene complex (4.4, R, R' = CO₂Me) [Au–N(ureylene) 2.092(7) Å].¹⁰ The geometry of the four-membered metallacycle brings C(1) into a close approach to the gold atom, with a transannular contact of 2.616(3) Å. The auralactam ring, perhaps in conjunction with this close transannular contact, has a fold angle of 10.5(4)° through the Au, N(2), C(2) and N(2), C(1), C(2) planes (Figure 4.5). The fold angle is not excessive for metallalactam complexes that have fold angles ranging from 5 to 17°.^{2,3,4}

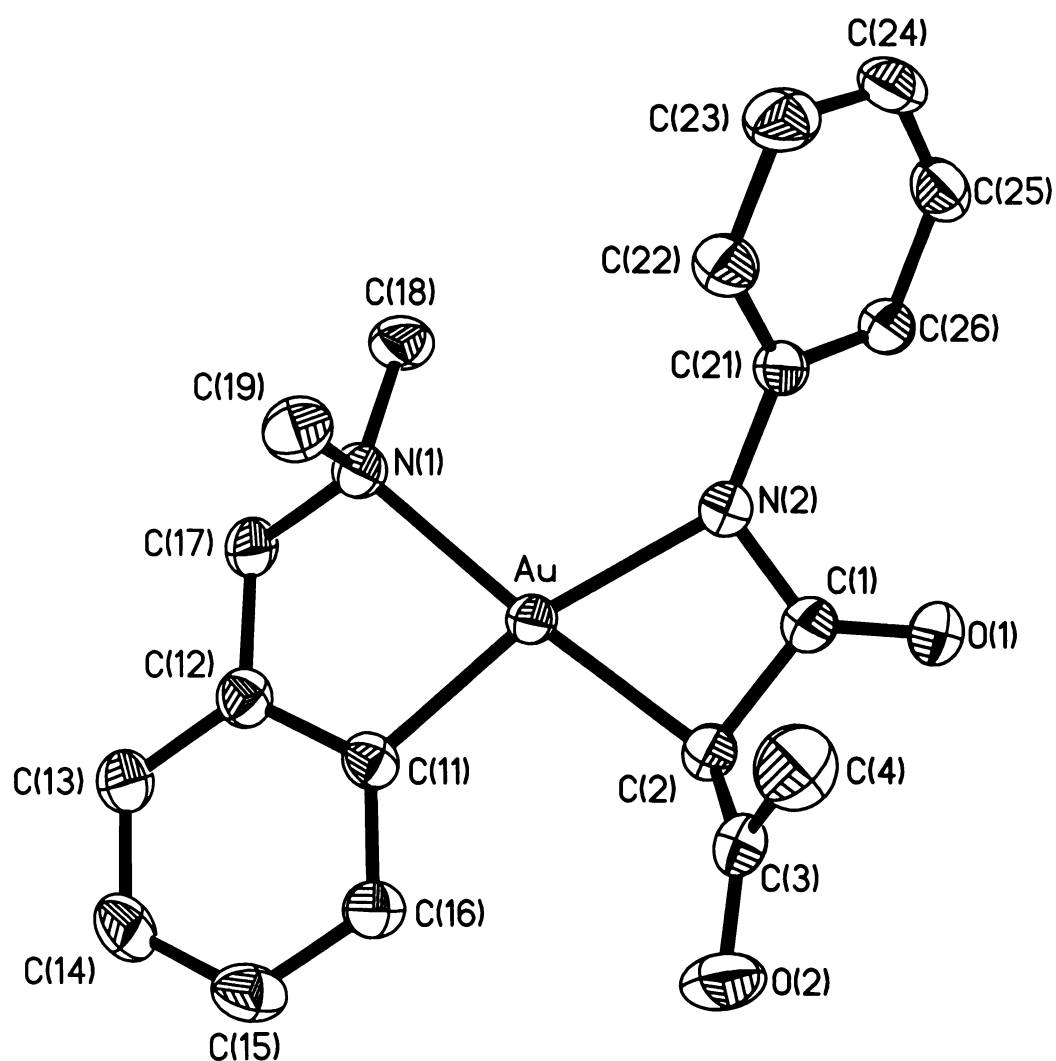


Figure 4.4 X-ray crystal structure and atom labeling scheme of $[\{C_6H_4(CH_2NMe_2)-2\}Au\{N(Ph)C(O)CHC(O)CH_3\}]$ (4.13)

Thermal displacement ellipsoids at 50% probability. Hydrogen atoms are removed for clarity.

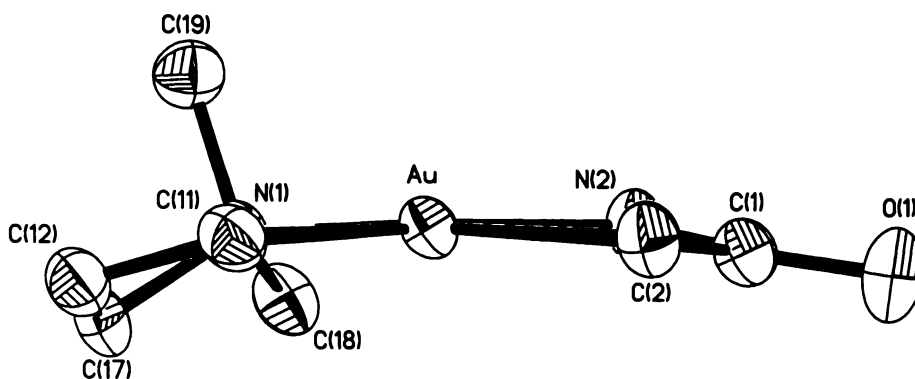


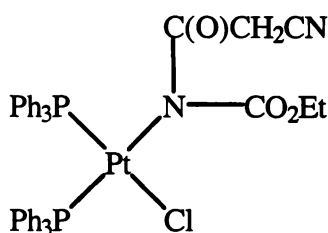
Figure 4.5 View of gold coordination sphere of **4.13** showing ring puckering

Table 4.2 Selected bond lengths (Å) and angles (°) for of $[\{\text{C}_6\text{H}_4(\text{CH}_2\text{NMe}_2)\text{-}2\}\text{Au}\{\text{N}(\text{Ph})\text{C}(\text{O})\text{CHC}(\text{O})\text{CH}_3\}]$ (**4.13**)

Au–C(11)	2.027(3)	Au–C(2)	2.076(3)
Au–N(2)	2.097(3)	Au–N(1)	2.157(3)
Au·····C(1)	2.616(3)	O(1)–C(1)	1.226(4)
N(2)–C(1)	1.356(4)	N(2)–C(21)	1.425(4)
C(1)–C(2)	1.536(5)	C(2)–C(3)	1.495(5)
O(2)–C(3)	1.220(5)	C(3)–C(4)	1.504(6)
C(11)–Au–C(2)	102.06(13)	C(11)–Au–N(2)	168.64(12)
C(2)–Au–N(2)	66.65(12)	C(11)–Au–N(1)	81.74(12)
C(2)–Au–N(1)	174.54(12)	N(2)–Au–N(1)	109.42(11)
C(11)–Au·····C(1)	137.61(12)	N(1)–Au·····C(1)	139.67(10)
C(1)–N(2)–C(21)	123.4(3)	C(1)–N(2)–Au	96.1(2)
C(21)–N(2)–Au	140.5(2)	O(1)–C(1)–N(2)	130.3(3)
O(1)–C(1)–C(2)	124.9(3)	N(2)–C(1)–C(2)	104.7(3)
O(1)–C(1)·····Au	174.9(3)	C(3)–C(2)–C(1)	113.7(3)
C(2)–C(3)–C(4)	118.5(3)	C(1)–C(2)–Au	91.5(2)
C(3)–C(2)–Au	113.8(2)	O(2)–C(3)–C(4)	120.0(4)
O(2)–C(3)–C(2)	121.5(4)		

The acetoacetanilide moiety bonds to the gold(III) centre with the nitrogen *cis* to the NMe₂ group. This presumably arises from the initial step in the metallacyclic synthesis. The chlorine atom on the gold precursor, $[\{\text{C}_6\text{H}_4(\text{CH}_2\text{NMe}_2)\text{-}2\}\text{AuCl}_2]$, *trans* to the aryl

carbon [C(11)] will be markedly more labile than the chlorine *trans* to the nitrogen [N(1)] and so will be substituted first during the reaction. The amide proton on acetoacetanilide is more acidic than either of the C–H protons and will be the first to be removed from the organic substrate. The reaction of *cis*-[PtCl₂(PPh₃)₂] with *N*-cyanoacetylurethane in the presence of silver(I) oxide for short reaction times yielded *cis*-[Pt{N(C(O)CH₂CN)(CO₂Et)}Cl(PPh₃)₂] (**4.16**), which has been proposed as an intermediate in silver(I) oxide mediated metallacyclisation reactions (see chapter three).²¹ That is, initially the nitrogen of the organic reagent bonds to the metal centre, followed by cyclisation through the acetyl carbon. Alternatively, the bonding of the soft σ -donor carbon may induce anti-symbiosis in the gold atom,²² resulting in the acetyl carbon bonding *cis* to the aryl carbon C(11), as observed in other square-planar gold(III) complexes.⁸⁻¹⁰ A combination of these two factors is the mostly likely hypothesis for the observed orientation, with the nitrogen atoms *cis* to one another.



4.16

The geometry of the *N,N*-dimethylbenzylamine ligand is similar to those of previously reported organogold metallacyclic structures.^{6-10,12} The benzylamine “bite” angle of 81.74(12)° [N(1)-Au-C(11)] approaches the ideal 90°. Compensating for this acute angle and that of [N(2)-Au-C(2)] [66.65(12)°], the angles between the two ligands [N(1)-Au-N(2) and C(11)-Au-C(2)] have become more obtuse [109.42(11) and 102.06(13)° respectively]. Other examples of gold(III) metallacycles also show similar distortions with C-Au-N angles of 80.6 to 92.5°.^{6-10,12} The five-membered ring formed by Au-C(11)-C(12)-C(17)-N(1) has a significant fold-angle of 34.9(2)° between the planes defined by Au-C(11)-C(12)-N(1) and N(1)-C(12)-C(17) (Figure 4.5).

21 W. Henderson, B. K. Nicholson and A. G. Oliver, *Inorg. Chim. Acta*, (1999), **292**, 260

22 R. G. Pearson, *Inorg. Chem.*, (1973), **12**, 712

4.3.3 X-ray crystal structure of $\{[\text{C}_6\text{H}_3(\text{CH}_2\text{NMe}_2)\text{-2-(OMe)-5}]\text{Au}\{\text{N}(\text{CO}_2\text{Et})\text{C}(\text{O})\text{CHCN}\}\}_2 \cdot 2\text{CDCl}_3$ (4.15)

The X-ray structure of $\{[\text{C}_6\text{H}_3(\text{CH}_2\text{NMe}_2)\text{-2-(OMe)-5}]\text{Au}\{\text{N}(\text{CO}_2\text{Et})\text{C}(\text{O})\text{CHCN}\}\}_2 \cdot 2\text{CDCl}_3$ (4.15) (Figure 4.6) shows that 4.8 has dimerised to form a novel eight-membered metallacycle. The molecule crystallises about a crystallographic inversion centre at 0, 0, 0.5. This complex is formed as the product of an unprecedented dimerisation reaction between two four-membered metallalactam complexes. The complex crystallises with one molecule of deuteriochloroform in the asymmetric unit.

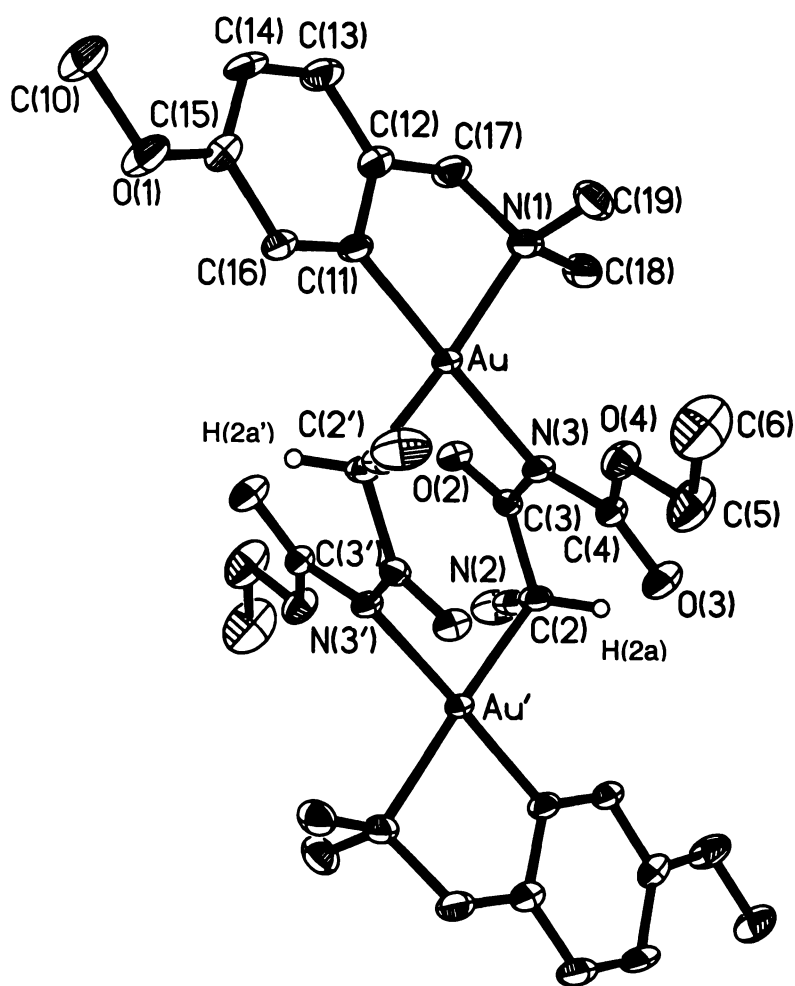


Figure 4.6 X-ray crystal structure and atom-labeling scheme of $\{[\text{C}_6\text{H}_3(\text{CH}_2\text{NMe}_2)\text{-2-(OMe)-5}]\text{Au}\{\text{N}(\text{CO}_2\text{Et})\text{C}(\text{O})\text{CHCN}\}\}_2 \cdot 2\text{CDCl}_3$ (4.15).

Thermal displacement ellipsoids are at 50% probability. Hydrogen atoms [except H(2a) and H(2a)'] and chloroforms of crystallisation are removed for clarity.

The coordination sphere around the gold(III) [Au, N(1), N(3), C(2'), C(11)] centre is a slightly distorted square-plane with no atom displaced more than 0.071(1) Å (Au) from the plane. The gold-nitrogen bonds are slightly longer [2.116(3) Å {Au-N(3)} and 2.137(3) Å {Au-N(1)}] than the gold-carbon bonds [2.031(3) Å {Au-C(11)} and 2.098(3) Å {Au-C(2')}] . As with the four-membered auralactam **4.13**, the longer gold-nitrogen bond [Au-N(1) 2.137(3) Å] reflects the dative, rather than covalent, coordination of the benzylamine nitrogen. This distortion of the square plane is also slightly enhanced by a disparity in gold-carbon bond lengths. The longer gold-carbon bond [Au-C(2') 2.098(3) Å] lies *trans* to the longer gold-nitrogen [Au-N(1) 2.137(3) Å] bond. This gold-carbon bond is slightly longer than that of the four-membered auralactam **4.13** [2.076(3) Å], presumably due to the differing substituents on the carbon (cyanide vs. acetyl). This unconstrained geometry around the eight-membered ring is also reflected in the large bond angles about the gold(III) centre compared to the four-membered auralactam **4.13**. The most acute angle is 81.78(11)° for C(11)-Au-N(1), which is part of the five-membered ring formed by the benzylamine ligand. As seen with $[\{C_6H_4(CH_2NMe_2)-2\}Au\{N(Ph)C(O)CHC(O)CH_3\}]$ (**4.13**) the *para*-methoxy *N,N*-dimethylbenzylamine ligand displays some torsion through its structure, with the five-membered ring defined by Au-C(11)-C(12)-C(17)-N(1) showing a considerable puckering with a fold angle of 39.1(2)° through the Au, N(1), C(11), C(12) and the C(12), C(17), N(1) planes.

Table 4.3 Selected bond lengths (Å) and angles (°) for of $[\{C_6H_3(CH_2NMe_2)-2-(OMe)-5\}Au\{N(CO_2Et)C(O)CHCN\}]_2 \cdot 2CDCl_3$ (**4.15**).

Au-C(11)	2.031(3)	Au-C(2')	2.098(3)
Au-N(3)	2.116(3)	Au-N(1)	2.137(3)
C(2)-Au'	2.098(3)	N(3)-C(4)	1.384(4)
N(2)-C(1)	1.152(5)	O(3)-C(4)	1.211(4)
N(3)-C(3)	1.374(4)	O(4)-C(5)	1.450(4)
O(2)-C(3)	1.237(4)	C(2)-C(3)	1.523(4)
O(4)-C(4)	1.353(4)	C(5)-C(6)	1.499(5)
C(1)-C(2)	1.464(4)		
C(11)-Au-C(2')	92.89(12)	C(11)-Au-N(3)	175.52(10)
C(2')-Au-N(3)	90.53(10)	C(11)-Au-N(1)	81.78(11)
C(2')-Au-N(1)	173.03(10)	N(3)-Au-N(1)	95.04(9)

C(3)–N(3)–C(4)	124.3(2)	C(3)–N(3)–Au	114.3(2)
C(4)–N(3)–Au	119.8(2)	N(2)–C(1)–C(2)	178.7(3)
C(4)–O(4)–C(5)	115.7(2)	C(1)–C(2)–Au'	106.2(2)
C(1)–C(2)–C(3)	108.9(2)	O(2)–C(3)–N(3)	118.7(3)
C(3)–C(2)–Au'	111.0(2)	N(3)–C(3)–C(2)	121.6(3)
O(2)–C(3)–C(2)	119.6(3)	O(3)–C(4)–N(3)	128.5(3)
O(3)–C(4)–O(4)	123.6(3)	O(4)–C(5)–C(6)	107.1(3)
O(4)–C(4)–N(3)	107.8(2)		

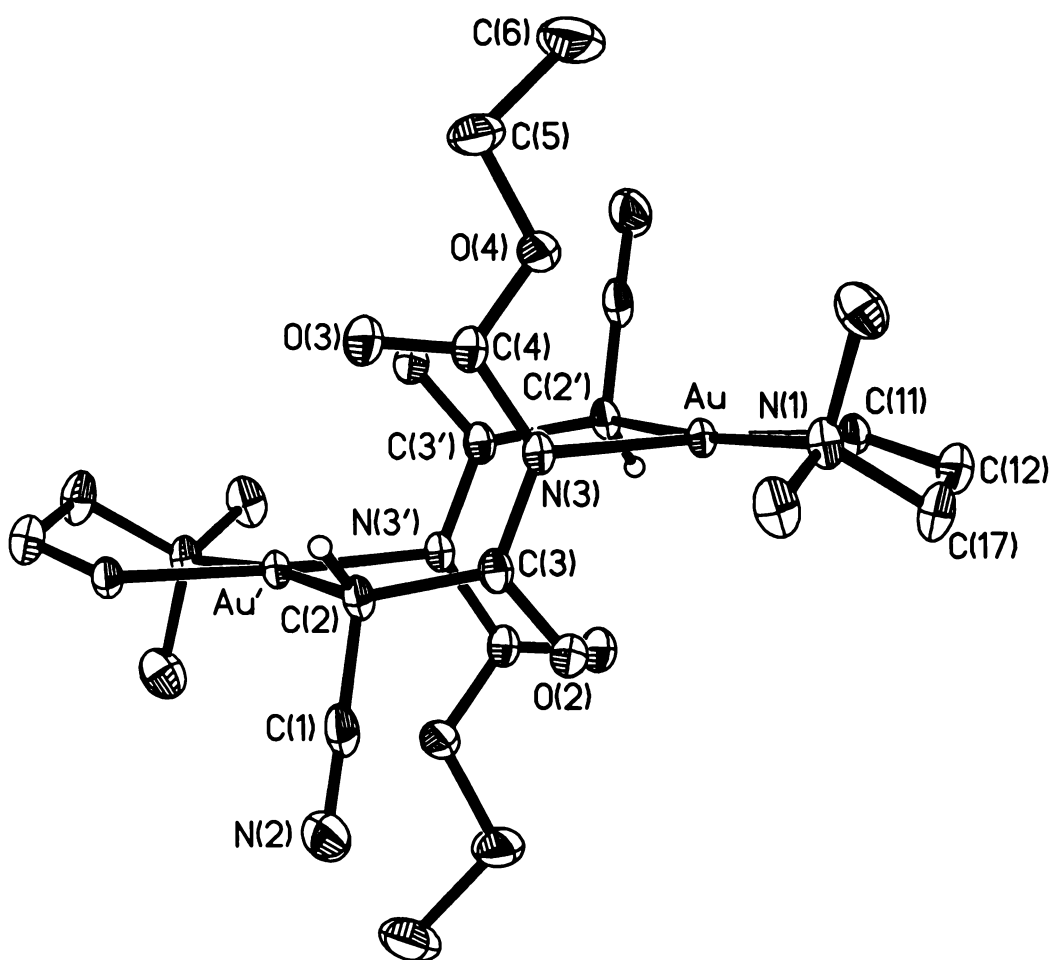
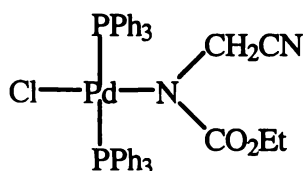


Figure 4.7 View of **4.15** showing the chair-like conformation of the eight-membered metallacycle and substituents

The plane of the bridging cyanoacetylurethane moiety lies almost perpendicular [83.82(5)°] to the gold coordination plane (Figure 4.7). In the previously described

structure of *trans*-[Pd{N(C(O)CH₂CN)(CO₂Et)}Cl(PPh₃)₂] (4.17)²³ the cyanoacetylurethane ligand has atoms that are co-planar with one another. Here the atoms of the cyanoacetylurethane group are twisted about the plane of the ligand, which may be to accommodate the eight-membered metallacycle. A stereoscopic depiction of the molecule (Figure 4.8) demonstrates this torsion about the eight-membered ring system. The atoms [N(3), O(2), O(4), C(3), C(4), C(5), C(6)] are effectively co-planar, with a maximum deviation of 0.094(3) Å [C(4)], while the cyanide functionality is skewed from the plane of the cyanoacetylurethane moiety; N(2) lies 0.232(10) Å out of this plane. The urethane carbonyl oxygen [O(3)] is twisted with respect to this plane, and lies 0.234(7) Å outside of the mean plane. The chloroform lies within a reasonable hydrogen-bonding distance of O(2) and is probably interacting with the cyanide [C(20).....O(2) 3.211(2) and C(20).....N(2) 3.451(3) Å] (Figure 4.8, Table 4.4).



4.17

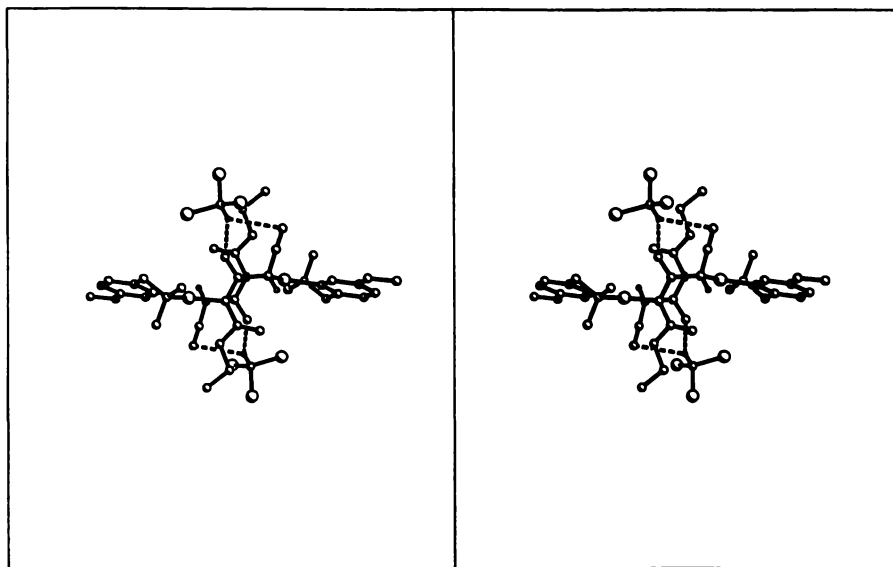


Figure 4.8 Stereoscopic view of 4.15, showing the structure of the molecule and the interactions to the chloroforms of crystallisation.

Table 4.4 Table of hydrogen-bond contacts

D-H (Å)	H·····A (Å)	D·····A (Å)	<(DHA) (°)	Atoms
0.99	2.30	3.211(2)	152.6	C(20)-H(20A)·····O(2')
0.99	2.79	3.451(3)	124.6	C(20)-H(20A)·····N(2')

D = Donor atom

A = Acceptor atom

4.3.4 Electrospray Mass Spectrometry of Organogold Metallalactam Complexes

The electrospray mass spectra of these auralactam complexes are straightforward, as gold is monoisotopic (see insets, Figure 4.9). At high mass resolution on the analyser, these complexes do not have the “fingerprint” isotopic distribution that many other transition metal complexes exhibit. The complexes also show little interaction with other species in solution. For example, the ES/MS spectrum of the complex **4.8** obtained at a cone voltage of 20V contains only three major peaks. These may be assigned as the parent $[M+H]^+$ ion at m/z 516 (100%), $[M+NH_4]^+$ at m/z 533 (30%) and an aggregate at m/z 1048 (90%) from $[2M+NH_4]^+$. While this complex (**4.8**) also appears to readily form the dimeric complex **4.15**, it is unlikely the $[2M+NH_4]^+$ peak observed here is representative of this dimer as frequently pallada- and platina-cycles have a $[2M+H]^+$ or a $[2M+NH_4]^+$ peak associated with them. Also with increased cone voltages this $[2M+NH_4]^+$ peak is not observed in the ES/MS spectra, indicating that it is an aggregate held together by electrostatic interactions. The insolubility of the dimeric complex **4.15** is another factor to consider. The dimeric species crystallised from deuteriochloroform could not be re-dissolved in that and other solvents. In contrast, the monomeric complex **4.8** was readily soluble in wide range of solvents. An electrospray mass spectrum of the dimer **4.15** was thus unable to be obtained due to this insolubility.

At increased cone voltages the complex shows little fragmentation; at 40V a peak at m/z 469 appears, presumably due to the loss of ethoxide from the ester i.e. $[M-(OEt)]^+$. At 120V, an appreciable amount of the parent auralactam survives. This phenomenon was observed for other related auracyclic complexes also.^{8-10,12} One reason for the increased stability of these auracycles is the enhanced chelation effect of having two metallacyclic ring systems. The pallada- and platinalactams, which often have only one metallacyclic ring, tend to display greater fragmentation at higher cone voltages.

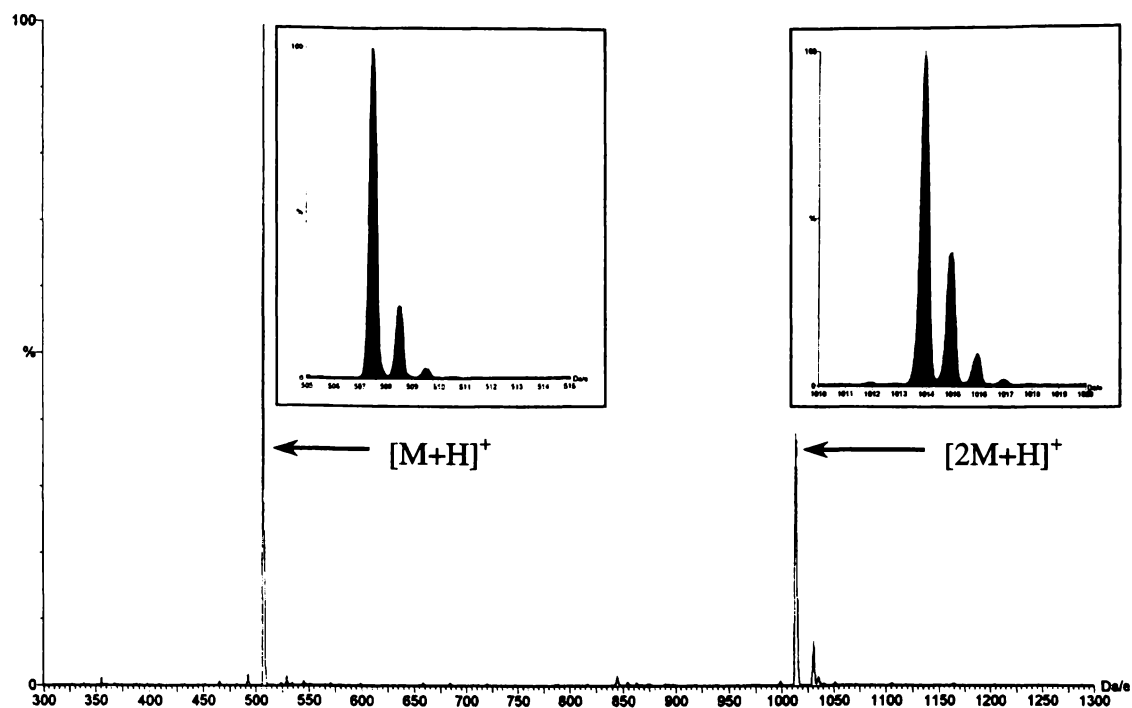


Figure 4.9 ES/MS spectrum of $[\{C_6H_4(CH_2NMe_2)_2\}Au\{N(Ph)C(O)CHC(O)CH_3\}]$ (4.13) at cone voltage = 20 V

4.3.5 NMR Spectroscopy of Organogold Metallalactams

The original research on the parent gold(III) dihalide complexes (4.1a,b)^{6,7} and further studies extensively documents the NMR spectra of these and other related complexes.^{8-10,12} Unlike the related platina-² and palladacycles^{3,4}, which often have NMR active atoms associated with the ancillary ligands, for example phosphorus in phosphine ligands, which assists in the characterisation of the reaction product, these auralactams have no NMR signatures aside from carbon and hydrogen. ¹⁵N NMR spectroscopy was not considered to be a viable technique for the purposes of this investigation. DEPT 135, XH correlation spectroscopy (XHCORR), Heteronuclear Multiple Quantum Correlation spectroscopy (HMQC) and Heteronuclear Multiple Bond Correlation spectroscopy (HMBC) were used to assign the resonances. Rotating Frame Overhauser Enhancement spectroscopy (ROESY) was used to determine the aromatic resonances of 4.9 and 4.12. The carbon and proton NMR resonances were labelled according to Scheme 4.1.

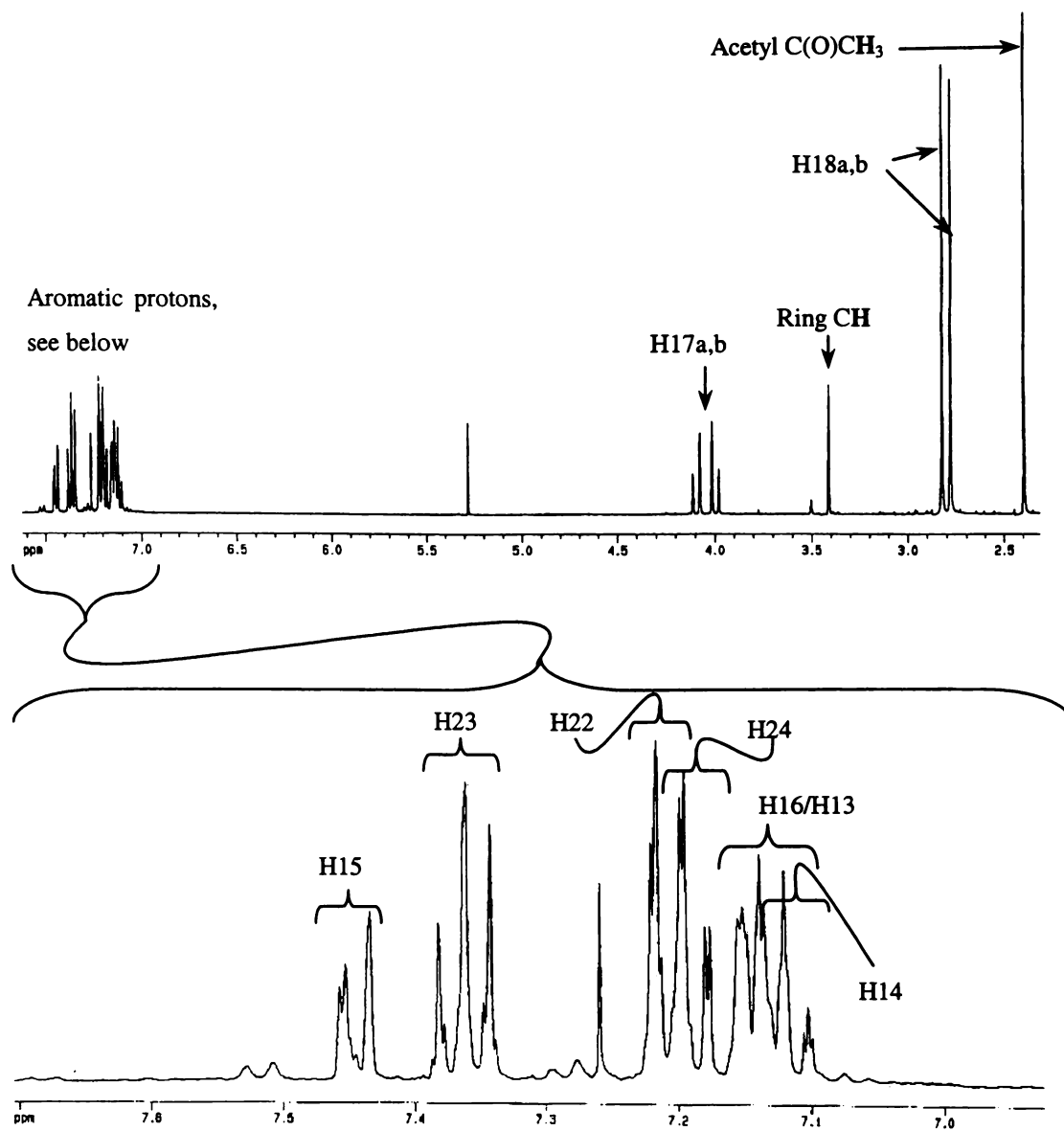
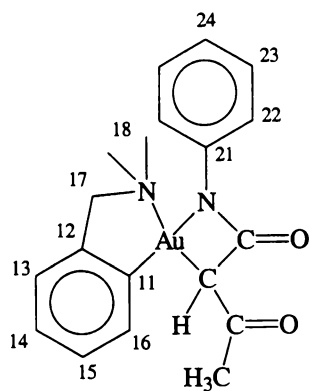


Figure 4.10 Representative ^1H NMR spectrum of the auralactam **4.13**
Expansion below shows the aromatic region of the ^1H NMR spectrum.



In complexes **4.8** – **4.10**, two of the three aromatic proton signals (H^{14} and H^{16} , Scheme 4.1) show long range 4J coupling, a feature not resolved in the original spectra measured on a lower field instrument. The coupling is typically small (2 – 3 Hz).

The benzylic protons ($H^{17a,b}$) are inequivalent and so give rise to a diastereotopic 2J coupling which is observed as an AB spin system (see Figure 4.10). This inequivalency arises from the inherent asymmetry of the lactam ring. Several of the complexes (**4.8**, **4.11**, **4.12**, **4.14**) show only a single broad resonance for the geminal dimethyl protons (H^{18}), however the remaining three compounds show two distinct methyl proton signals. The single broad resonance may be due to the two methyl signals have more similar chemical shifts than those of **4.9**, **4.10** and **4.13**. The ethyl ester CH_2 quartet resonances of the *N*-cyanoacetylurethane derivatives **4.8** and **4.11** are shifted downfield to δ 4.26 and 4.25, compared to the free ligand and those observed for the platinum² and palladium^{3,4} complexes **4.7a,b** (δ 4.15 - 3.06).

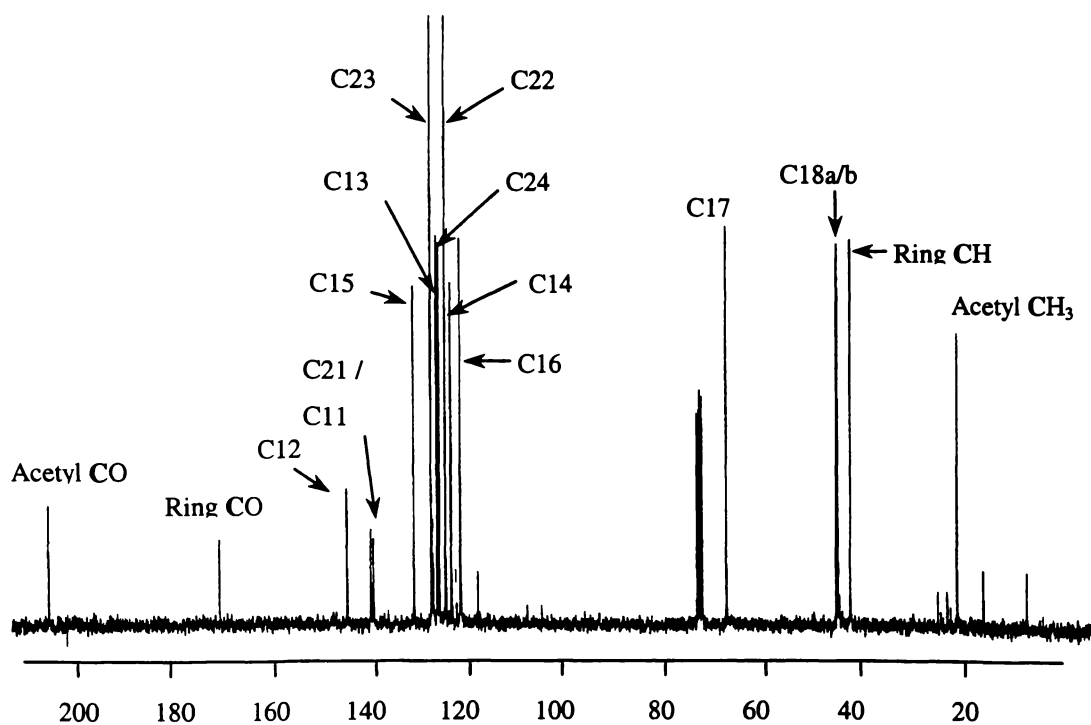


Figure 4.11 Representative ^{13}C - $\{^1H\}$ NMR spectrum of the auralactam **4.13**

The de-shielding effect that the gold atom has on the dimethylbenzylamine aromatic carbons gives each resonance a distinct chemical shift as can be seen above in Figure 4.11. This effect has been observed and noted for the previous examples of organogold metallacycles^{6,8-10,12} and aids in the assignment of cross-peaks in HMBC and HMQC experiments. In several examples (**4.8**, **4.11**, **4.12**, **4.14**), the geminal dimethyl proton

resonances (H18) were not observed. However, the carbon resonances associated with these two groups (C18a,b) were observed in all of the metallalactam complexes studied. The difference in chemical shift between the two methyl carbon signals is 0.1 – 0.2 ppm.

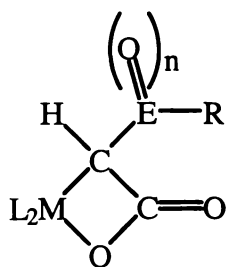
4.4 Conclusions

The structure of the four-membered auralactam **4.13** is similar to other late transition metal metallalactams. This complex may provide insight into the utility of drugs containing gold(III) and their binding to peptides. In particular the high lability of gold(III), which in one case presented here results in the formation of an unprecedented dimeric complex **4.15**. The robustness of these gold(III) metallacycles is exemplified by their behaviour during ES/MS analysis. While most platinum group metallalactams are highly fragmented at high cone voltages, these auralactams still have a significant proportion that remains intact. This maybe due to these gold(III) complexes having two heterocycles which may increase their stability. The compound **4.15** shows that the ligand dissociation/exchange ability of gold(III) is considerably higher than that of any of the platinum group metals. No other complexes of this type (metallalactam) have been observed to undergo a ring opening and subsequent coupling reaction.

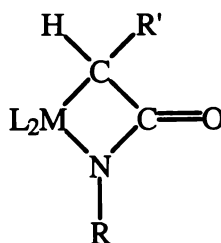
Chapter Five. Silver(I) oxide mediated reactions with carboxylic acids

5.1 Introduction

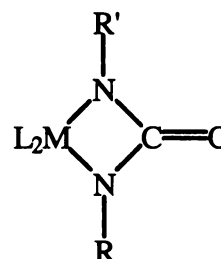
Silver(I) oxide has been shown to mediate the synthesis of the platinalactone complex **5.1a** from phenylsulfonyl acetic acid and an appropriate platinum dihalide.¹ Based on previous syntheses with amides and ureas, this result is logical, with the four-membered metallacyclic product being obtained. However, other research indicated that the platinalactone complex **5.1b** could be synthesised from dimethyl malonate $[\text{CH}_2(\text{CO}_2\text{Me})_2]$ and *cis*- $[\text{PtCl}_2(\text{PPh}_3)_2]$.² This reaction is not as straightforward as those of phenylsulfonyl acetic acid or amides³ and ureas⁴ which produce metallalactone (**1a**), metallalactam (**5.2**) and ureylene (**5.3**) complexes successively. At intermediate reaction times (24 h), a phosphorus NMR spectrum showed that a complex mixture of compounds were present. However, after 48 h the reaction had resolved itself into one product, the platinalactone complex (**5.1b**).



5.1a E = S, n = 2, R = Ph



5.2



5.3

5.1b E = C, n = 1, R = OMe

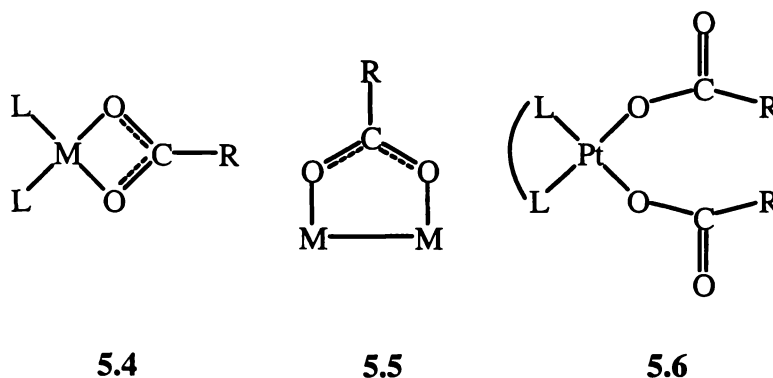
1 a) W. Henderson, R. D. W. Kemmitt, J. Fawcett and L. J. S. Prouse, *J. Chem. Soc., Dalton Trans.*, (1986), 1791; b) W. Henderson, R. D. W. Kemmitt, L. J. S. Prouse and d. R. Russell, *J. Chem. Soc., Dalton Trans.*, (1989), 259

2 W. Henderson, R. D. W. Kemmitt and A. L. Davis, *J. Chem. Soc., Dalton Trans.*, (1993), 2247

3 a) W. Henderson, B. K. Nicholson and A. G. Oliver, *J. Chem. Soc., Dalton Trans.*, (1994), 1831; b) W. Henderson, J. Fawcett, R. D. W. Kemmitt, C. Proctor and D. R. Russell, *J. Chem. Soc., Dalton Trans.*, (1994), 3085; c) W. Henderson, B. K. Nicholson and A. G. Oliver, *Inorg. Chim. Acta*, (1999), **292**, 260

4 a) M. B. Dinger and W. Henderson, *J. Organomet. Chem.*, (1998), **557**, 231; b) M. B. Dinger, W. Henderson, B. K. Nicholson, and A. L. Wilkins, *J. Organomet. Chem.*, (1996), **526**, 303

Carboxylate ligands coordinated to metal centres predominantly adopt a chelating (5.4) or a bridging mode (5.5),⁵ and when two carboxylate ligands are in a *cis*- conformation, they tend to the latter type, often bridging several metal centres. Mak *et al.* isolated and characterised several short-chain platinum(II) carboxylic acid derivatives, which adopted a unidentate bonding mode in complexes of the type (5.6).⁶



Cyanoacetic acid (NCCH₂CO₂H) and phenoxyacetic acid (PhOCH₂CO₂H) were used to extend the applicability of functionalised acetic acids towards metallalactone synthesis. The following report discusses the varied results that these two compounds gave when reacted with platinum(II) dihalide complexes in the presence of silver(I) oxide.

5.2 Experimental

Reactions were performed as described previously (see section 2.2). Solvents were distilled before use and silver(I) oxide,⁷ *cis*-[PtCl₂(PPh₃)₂]⁸ and [PtCl₂(COD)]⁹ were prepared by standard literature methods. Cyanoacetic acid, phenoxyacetic acid (BDH) and triphenylphosphine (Pressure Chemical Co.) were used as supplied. ¹H, ¹³C and ³¹P NMR were recorded on a Brüker AC300P spectrometer. ¹H NMR spectra were collected at 300.13 MHz, ¹³C NMR data were recorded at 75.47 MHz and ³¹P NMR spectra recorded at 121.47 MHz. ¹H and ¹³C NMR spectra were referenced to internal

5 C. Oldham, *Comprehensive Coordination Chemistry* (1987), Vol. 2, Ch. 15.6, 435, eds. G. Wilkinson, R. D. Gillard and J. A. McCleverty, Oxford Pergamon

6 T. C. W. Mak, A. L. Tan, P. M. N. Low, Z.-Y. Zhou, W. Zheng, B.-M. Wu and T. S. A. Hor, *J. Chem. Soc., Dalton Trans.*, (1996), 2207

7 H. L. Riley and H. B. Baker, *J. Chem. Soc.*, (1960), 1378

8 D. L. Oliver and G. K. Anderson, *Polyhedron*, (1992), 11, 2415

9 J. X. McDermott, J. F. White and G. M. Whitesides, *J. Am. Chem. Soc.*, (1976), 98, 6521

TMS (δ 0.00) and ^{31}P spectra referenced to external 85% H_3PO_4 (δ 0.00). Accurate X-ray intensity data were collected on a Siemens SMART CCD diffractometer at the University of Auckland.

5.2.1 Synthesis of *cis*-[Pt(CH₂CN)₂(PPh₃)₂] (5.7)

A stirred mixture of *cis*-[PtCl₂(PPh₃)₂] (0.058 g, 0.073 mmol), cyanoacetic acid (0.14 g, 0.39 mmol) and silver(I) oxide (0.164 g, excess) was heated at reflux in dichloromethane (20 cm³) for 3 h. under nitrogen. Silver salts were removed by filtration in air and the solvent removed under reduced pressure yielding a pale yellow microcrystalline solid. The compound was recrystallised from dichloromethane / diethyl ether and dried under vacuum (yield 0.052 g, 85%). Yellow crystals were obtained from dichloromethane / diethyl ether by vapour diffusion.

NMR: ^1H : δ 7.85 – 6.85 (m, Ph), 3.65 (s, CH₂).

^{13}C -{ ^1H }: δ 136.5 – 124.0 (m, Ph), 110.6 (s, C \equiv N), 53.52 (s, CH₂).

^{31}P -{ ^1H }: δ 23.53 [s, $^1J(\text{Pt}, \text{P})$ 2376].

5.2.2 Synthesis of *cis*-[Pt(O₂CCH₂OPh)₂(COD)] (5.8)

cis-[Pt(O₂CCH₂OPh)₂(COD)] was synthesised by heating at reflux a mixture of [PtCl₂(COD)] (0.097 g, 0.258 mmol), phenoxyacetic acid (0.081 g, 0.503 mmol) and silver(I) oxide (0.233 g, excess) in dichloromethane (20 cm³) for 3 h. Silver salts were removed by filtration affording a deep brown solution. Solvent was removed under reduced pressure and petroleum spirits added giving a tan precipitate which was filtered in air and dried (yield 0.065 g, 55%).

5.2.3 Preparation of *cis*-[Pt(O₂CCH₂OPh)₂(PPh₃)₂] by ligand displacement (5.9)

cis-[Pt(O₂CCH₂OPh)₂(PPh₃)₂] was prepared by ligand displacement of 1,5-cyclooctadiene (COD) from *cis*-[Pt(O₂CCH₂OPh)₂(COD)] (0.045 g, 0.117 mmol) in dichloromethane (10 cm³) by the addition of triphenylphosphine (0.065 g, 0.247 mmol). Recrystallisation by vapour diffusion of diethyl ether into a dichloromethane solution gave X-ray quality crystals of an acceptable size (0.25 x 0.23 x 0.08 mm).

NMR: ^1H : δ 7.7 – 6.6 (m, Ph); 1.65 (s, CH_2).

^{31}P - $\{^1\text{H}\}$: δ 15.48 [s, $^1J(\text{Pt}, \text{P})$ 4084].

5.2.4 X-ray Crystallographic studies of *cis*- $[\text{Pt}(\text{CH}_2\text{CN})_2(\text{PPh}_3)_2]$ (5.7) and *cis*- $[\text{Pt}(\text{O}_2\text{CCH}_2\text{OPh})_2(\text{PPh}_3)_2]$ (5.9)

Data collection for the two samples followed a similar procedure. A suitable crystal was coated in paratone oil, mounted on a glass fibre and frozen under a nitrogen cold stream at $-70\text{ }^\circ\text{C}$. Preliminary cell data and point group information were determined from 45 standard frames collected over three detector positions. A sphere of data were collected for the low symmetry (triclinic) *cis*- $[\text{Pt}(\text{CH}_2\text{CN})_2(\text{PPh}_3)_2]$ (5.7) complex using monochromated Mo-K α radiation, as detailed in Table 5.1 below. A hemisphere of data were collected for the higher symmetry (monoclinic point group) *cis*- $[\text{Pt}(\text{O}_2\text{CCH}_2\text{OPh})_2(\text{PPh}_3)_2]$ (5.9) compound, again using monochromated Mo-K α radiation. Both data sets were corrected for Lorentz and polarisation effects and for linear absorption using empirical methods.¹⁰

The location of the platinum atom for *cis*- $[\text{Pt}(\text{CH}_2\text{CN})_2(\text{PPh}_3)_2]$ (5.7) was determined by Patterson methods (SHELXS-97).¹¹ The remaining atoms were located in the electron density map of subsequent refinement cycles. The model was refined by full-matrix least squares methods against F^2 (SHELXL-97)¹² with all heavy atoms allowed anisotropic thermal displacement. Hydrogen atoms were placed geometrically and allowed to ride on the carrier atom with thermal parameters 20% greater than the carrier atom. Successive refinement cycles indicated that significant residual electron density located about the inversion centre was present. This could not be assigned to any particular molecule. Thus, the SQUEEZE option of the PLATON program was employed to correct this diffuse residual density.¹³

SQUEEZE attempts to determine the volume of any voids within the lattice. This calculation is made using a grid system (typically a 0.2 Å grid) applied to the unit cell.

10 R. H. Blessing, *Acta Crystallogr.*, (1995), A51, 33

11 G. M. Sheldrick, SHELXS-97. *Program for the Solution of Crystal Structures.* (1997), Universität Göttingen, Germany.

12 G. M. Sheldrick, SHELXL-97. *Program for the Refinement of Crystal Structures.* (1997), Universität Göttingen, Germany.

Grid points located more than 1.2 Å from the nearest van der Waals radius of an atom are said to be within the void. The program then begins an iterative process to determine the number of electrons that are located within any void regions in the cell. This process is similar to an electron density calculation used in a difference Fourier map. The process repeats until the electron count from successive iterations is constant. The intensity data is then corrected by removing the F associated with the solvent (F_s) from the observed intensity (F_o), essentially leaving only data associated with the molecule of interest. It should be noted that the data output from this program is modified, and is not the true experimental data.

The solution to *cis*-[Pt(O₂CCH₂OPh)₂(PPh₃)₂] (**5.9**) was determined by the direct methods option of SHELXS-97.¹¹ Atoms not located in the initial difference map were found in the subsequent refinements. The structure was refined by least-squares full-matrix based on F^2 (SHELXL-97)¹² and developed routinely. Non-hydrogen atoms were assigned anisotropic thermal parameters and hydrogen atoms were included in calculated positions with thermal parameters 1.2 times the U_{iso} of the atom to which they are bonded.

Table 5.1 Cell parameter, solution and final cycle refinement data for *cis*-[Pt(CH₂CN)₂(PPh₃)₂] (**5.7**) and *cis*-[Pt(O₂CCH₂OPh)₂(PPh₃)₂] (**5.9**)

<i>Crystal data</i>	5.7	5.9
Empirical formula	C ₄₀ H ₃₄ N ₂ P ₂ Pt. 0.6(CH ₂ Cl ₂)	C ₅₂ H ₄₄ O ₆ P ₂ Pt.(CH ₂ Cl ₂)
Formula weight	842.18	1106.83
Crystal system	Triclinic	Monoclinic
Space group	P $\bar{1}$	P2 ₁ /c
Unit cell dimensions		
a (Å)	10.2264(2)	11.4782(1)
b (Å)	10.3606(1)	17.9393(3)
c (Å)	18.0965(3)	23.3995(2)
α (°)	87.360(1)	90
β (°)	81.604(1)	101.006(1)
γ (°)	74.839(1)	90
Volume (Å ³)	1830.72(5)	4729.59(10)

Z	2	4
D(c) (g cm ⁻³)	1.528	1.554

Data Collection

Diffractometer	Siemens SMART CCD	Siemens SMART CCD
Radiation	Mo-K α	Mo-K α
Wavelength (Å)	0.71073	0.71073
Temperature (K)	203(2)	203(2)
Crystal size (mm)	0.25 x 0.21 x 0.06	0.25 x 0.23 x 0.08
θ range for data collection (°)	2.08 to 26.00	1.44 to 26.45 °
Index ranges	-12 \leq h $<$ 12 -12 \leq k \leq 12, 0 \leq l \leq 22	-14 \leq h \leq 14 0 \leq k \leq 22, 0 \leq l \leq 22
Reflections collected	13799	26767
Independent reflections	7070 [R(int) = 0.0494]	8799 [R(int) = 0.0450]
Absorption coefficient (mm ⁻¹)	4.023	3.198
Maximum transmission	0.7976	0.8149
Minimum transmission	0.4385	0.6705
F(000)	834	2216

Structure analysis and refinement

Solution by:	Patterson methods	direct methods
Refinement method	Full-matrix least-squares on F^2	Full-matrix least-squares on F^2
Data / restraints / parameters	7070 / 0 / 406	8799 / 0 / 562
Goodness-of-fit on F^2	0.968	1.065
Final R indices [$I > 2\sigma(I)$]	$R_1 = 0.0472$, $wR^2 = 0.1071$	$R_1 = 0.0475$, $wR^2 = 0.1066$
R indices (all data)	$R_1 = 0.0622$, $wR^2 = 0.1127$	$R_1 = 0.0736$, $wR^2 = 0.1191$
Weighting Scheme	$w = 1/[\sigma^2(F_o^2) + (0.0571P)^2 + 0.0000P]$ where $P = (F_o^2 + 2F_c^2)/3$	$w = 1/[\sigma^2(F_o^2) + (0.0463P)^2 + 21.2066P]$ where $P = (F_o^2 + 2F_c^2)/3$
Largest difference peak	2.930 (located 1.05 Å from	1.779

(e.Å ⁻³)	Pt)	
Largest difference hole	-1.703	-1.380
(e.Å ⁻³)		
Programs used		
Solution by	SHELXS-97 ¹¹	SHELXS-97 ¹¹
Refinement by	SHELXL-97 ¹²	SHLXL-97 ¹²

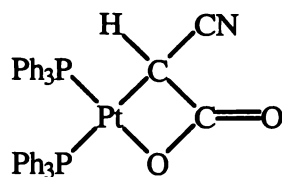
5.3 Results and Discussion

5.3.1 Reaction of cyanoacetic acid with *cis*-[PtCl₂(PPh₃)₂]

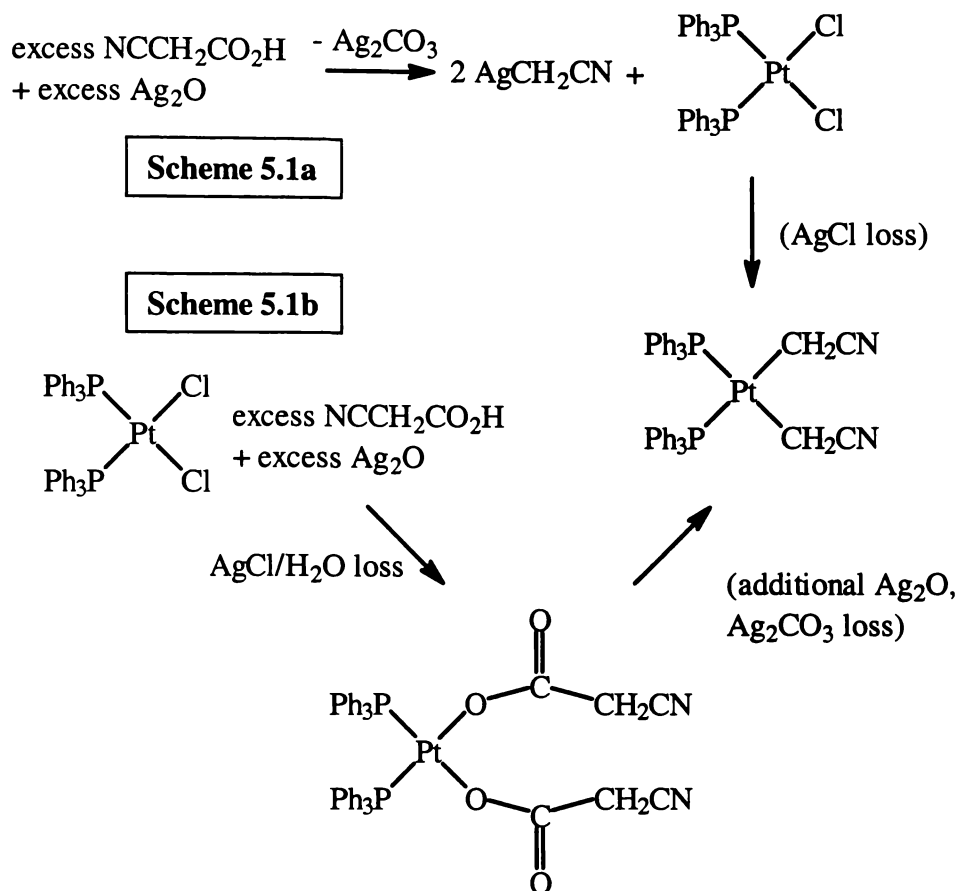
Attempts to synthesise a metallalactone complex (5.10), analogous to the previously reported *N*-cyanoacetylurethane derived platinalactam (5.2, R = CO₂Et, R' = CN), using cyanoacetic acid and *cis*-[PtCl₂(PPh₃)₂] met with failure. However, a novel decarboxylation reaction was observed giving *cis*-[Pt(CH₂CN)₂(PPh₃)₂]. The structure of only one other bis-cyanomethyl complex, [Ir(CH₂CN)₂(CO)₂]⁻ [(Ph₃P)₂N]⁺, has been reported.¹⁴ Due to the lack of steric constraints about the iridium centre, the cyanomethyl ligands lie almost at right angles to one another. One anomalous result was observed in a study into the formation of platinum dicarboxylate complexes. The reaction of [Pt(CO₃)(PPh₃)₂] with PhC≡CCO₂H was found to produce the bis(phenylalkynyl) complex *cis*-[Pt(C≡CPh)₂(PPh₃)₂] by loss of CO₂ from both the carbonate and carboxylate groups.¹⁵ Therefore, while the decarboxylation observed here was unexpected, it was not unprecedented. The decarboxylation of cyanoacetic acid may occur as an initial reaction prior to further reaction with the metal dihalide (see Scheme 5.1a), or the decarboxylation process may occur after a metal dicarboxylate complex has formed (Scheme 5.1b). Decarboxylation of cyanoacetic acid, forming insoluble silver carbonate prior to any reaction with the metal dihalide, is perhaps more plausible.

14 F. Porta, F. Ragaini, S. Cenini and F. DeMartin, *Organometallics*, (1990), 9, 929

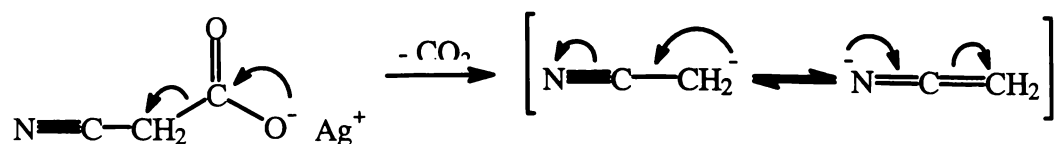
15 A. D. Burrows, D. M. P. Mingos, S. E. Lawrence, A. J. P. White and D. J. Williams, *J. Chem. Soc., Dalton Trans.*, (1997), 1295



5.10

**Scheme 5.1** Synthetic pathways for the formation of *cis*-[Pt(CH₂CN)₂(PPh₃)₂]

Some carboxylic acids are known to undergo a *Hunsdiecker* reaction, in the presence of silver halides. The *Hunsdiecker* reaction is essentially a decarboxylation of the carboxylic acid. Resonance stabilisation of the resulting fragment would prolong its existence (Scheme 5.2), enough for it to react further with a cationic species (in this case a dehalogenated platinum).

**Scheme 5.2** Decarboxylation of cyanoacetic acid

Also consistent with this, the reactions of platinum(II) hydroxo complexes, some in the presence of silver(I) oxide, with CH_3CN gave *cis*- $[\text{Pt}(\text{CH}_2\text{CN})(\text{X})\text{L}_2]$, (X = cyclohexene; OH; Cl or CH_3) complexes.^{16,17} The facile synthesis of the complex $[\text{Pd}(\text{CH}_2\text{CN})_2(\text{PPh}_3)_2]$, from $[\text{PdCl}_2(\text{PPh}_3)_2]$ and LiCH_2CN , provides access to a range of aggregation and degradation products, including a ligand free $[\text{Pd}(\text{CH}_2\text{CN})_2]$ complex.¹⁸

5.3.2 X-ray crystal structure of *cis*- $[\text{Pt}(\text{CH}_2\text{CN})_2(\text{PPh}_3)_2] \cdot 0.6(\text{CH}_2\text{Cl}_2)$ (5.7)

The geometry around the platinum centre of *cis*- $[\text{Pt}(\text{CH}_2\text{CN})_2(\text{PPh}_3)_2]$ shows the expected four coordinate, square-planar environment, with the phosphine ligands in a *cis*-arrangement as shown in Figure 5.1. Selected bond lengths and bond angles are provided in Table 5.2. The bond angle $\text{P}(1)\text{-Pt-P}(2)$ is slightly more obtuse [$98.09(9)^\circ$] than perfect square-planar coordination, while the $\text{C}(2)\text{-Pt-C}(4)$ and the $\text{C}(4)\text{-Pt-P}(2)$ bond angles have closed up [$85.3(3)$ and $85.6(4)^\circ$, respectively]. The remaining bond angle [$\text{C}(2)\text{-Pt-P}(1)$] is near ideal at $90.9(2)^\circ$. Steric considerations clearly give rise to these distortions from regular geometry. The Pt-C bond lengths [$2.104(7)$ and $2.138(7)\text{\AA}$ for Pt-C(2) and Pt-C(4), respectively] are comparable with, if fractionally longer than bond lengths in the related platinum(II) chloromethyl complexes $\{[\text{Pt}(\text{CH}_2\text{Cl})_2\text{L}_2]; \text{L}_2 = \text{bis}(\text{diphenylphosphino})\text{methane (dppm); (2S,4S)-Ph}_2\text{PCHMeCH}_2\text{CHMePPh}_2 \text{ (S,S-skewphos) [2.069(8) to 2.109(10) \AA, respectively}\}$.^{19,20}

The most interesting feature of this compound is the orientation of the cyanomethyl ligands which have adopted a *syn*-arrangement (Figure 5.2). The only other reported bis-cyanomethyl complex, $[\text{Ir}(\text{CH}_2\text{CN})_2(\text{CO})_2]^- [(\text{Ph}_3\text{P})_2\text{N}]^+$, has the ligands oriented almost perpendicular to each other.¹⁴ A lack of steric interference from the *cis*-carbonyl ligands would allow this, but intuitively an *anti*-conformation should be preferable on steric grounds. However, the cyanomethyl ligands do not completely eclipse each

16 D. P. Arnold and M. A. Bennett, *J. Organomet. Chem.*, (1980), **199**, 119 and references therein

17 M. A. Cairns, K. R. Dixon and M. A. R. Smith, *J. Organomet. Chem.*, (1977), **135**, C33

18 H. Pracejus, G. Oehemeand and K.-C. Röber, *J. Organomet. Chem.*, (1976), **105**, 127

19 N. W. Alcock, P. G. Pringle, P. Bergamini, S. Sostero and O. Traverso, *J. Chem. Soc., Dalton Trans.*, (1990), 1553

20 P. Bergamini, E. Costa, S. Sostero, C. Ganter, J. A. Hogg, A. G. Orpen and P. G. Pringle, *J. Organomet. Chem.*, (1993), **455**, C13

other; the C(1)–C(2).....C(4)–C(2) dihedral angle is $-20.6(7)^\circ$. The related $\{[\text{Pt}(\text{CH}_2\text{Cl})_2\text{L}_2]; \text{L}_2 = \text{dppm or } S,S\text{-skewphos}\}$ complexes display quite different geometries for the orientation of the chloromethyl ligands. The chloromethyl ligands of $[\text{Pt}(\text{CH}_2\text{Cl})_2(\text{dppm})]$ are oriented so that the chlorine atoms lie in the plane of the platinum coordination sphere,¹⁹ while the chloromethyl ligands of $[\text{Pt}(\text{CH}_2\text{Cl})_2(S,S\text{-skewphos})]$ are oriented approximately perpendicular to one another.²⁰

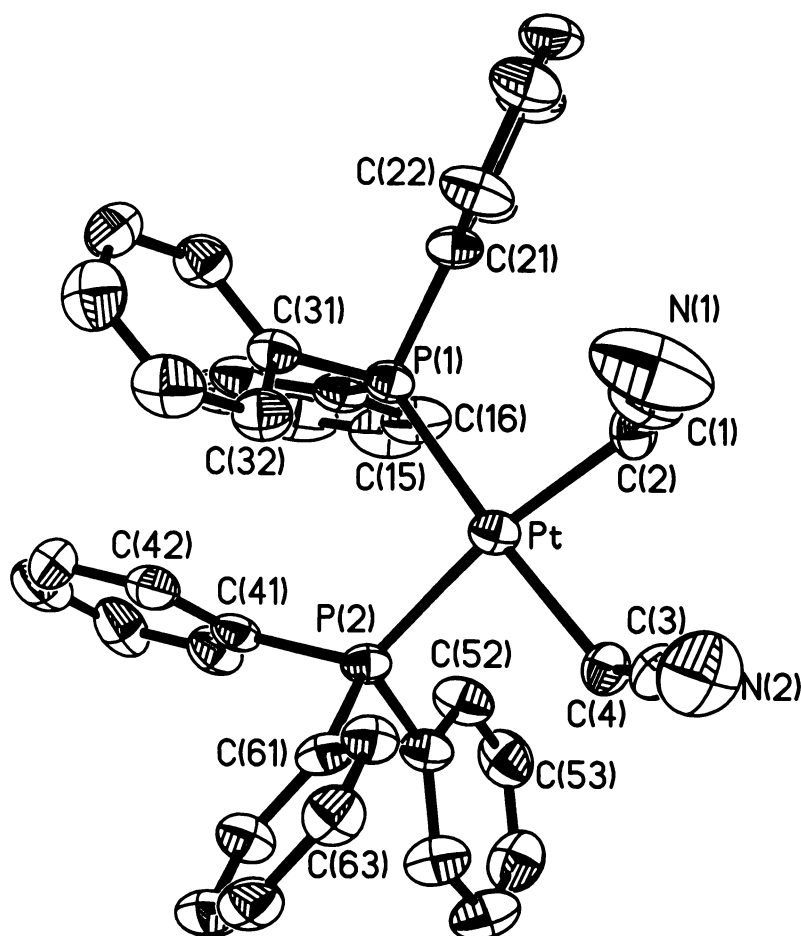


Figure 5.1 Thermal ellipsoid plot and labelling scheme for *cis*- $[\text{Pt}(\text{CH}_2\text{CN})_2(\text{PPh}_3)_2]$ (5.7)

Thermal displacement ellipsoids are viewed at 50% probability. Hydrogen atoms are omitted for clarity.

Residual electron density not associated with the *cis*- $[\text{Pt}(\text{CH}_2\text{CN})_2(\text{PPh}_3)_2]$ molecule was located during the refinement of this molecule and is located about the inversion centre of the unit cell. However, because this residual density appeared to be a diffuse,

disordered solvent molecule and could not be reliably modelled, the SQUEEZE option of the PLATON program was employed to calculate the void size, the electron count within the void, and to correct the X-ray intensity data for this additional electron density.¹³ The SQUEEZE analysis indicated that a 50 electron, 205 Å³ void existed within the lattice. The void was centred about the inversion centre, halving both the electron count and the volume of the void. Both dichloromethane and diethyl ether were used in the crystallisation of the complex and both have 42 electrons. This gives 0.6 of a solvent molecule per molecule of *cis*-[Pt(CH₂CN)₂(PPh₃)₂]. ¹H NMR of the crystals indicated that some dichloromethane was present, which was used as the solvent molecule for calculation purposes.

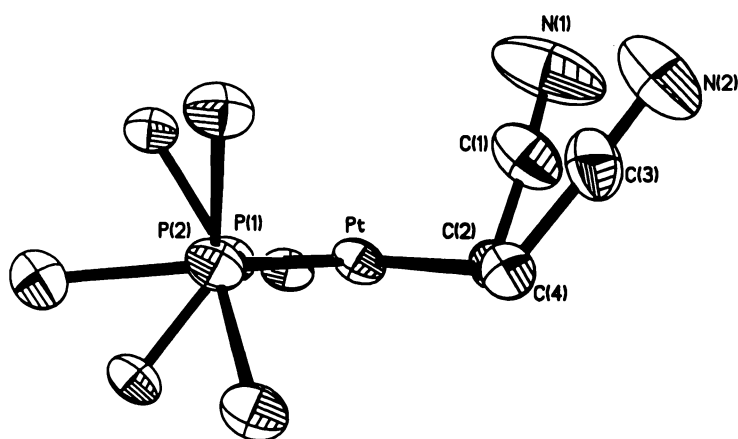


Figure 5.2 Thermal ellipsoid plot showing the 'syn' geometry of the cyanomethyl ligands of *cis*-[Pt(CH₂CN)₂(PPh₃)₂].

Only the phenyl *ipso* carbons are shown for clarity.

Table 5.2 Selected bond lengths (Å) and angles (°) for *cis*-[Pt(CH₂CN)₂(PPh₃)₂] (5.7)

Pt–C(2)	2.104(7)	Pt–C(4)	2.138(7)
Pt–P(1)	2.2953(18)	Pt–P(2)	2.3161(18)
N(1)–C(1)	1.136(10)	C(1)–C(2)	1.413(10)
N(2)–C(3)	1.150(10)	C(3)–C(4)	1.433(10)
P(1)–C(11)	1.826(7)	P(1)–C(21)	1.840(7)
P(1)–C(31)	1.822(7)	P(2)–C(41)	1.830(7)
P(2)–C(51)	1.836(7)	P(2)–C(61)	1.824(7)
C(2)–Pt–C(4)	85.3(3)	C(2)–Pt–P(1)	90.9(2)
C(4)–Pt–P(1)	175.7(2)	C(2)–Pt–P(2)	170.8(2)

C(4)–Pt–P(2)	85.6(2)	P(1)–Pt–P(2)	98.09(6)
N(1)–C(1)–C(2)	176.7(12)	C(1)–C(2)–Pt	112.1(5)
N(2)–C(3)–C(4)	178.0(9)	C(3)–C(4)–Pt	111.8(5)

5.3.3 Reactions of phenoxyacetic acid with platinum(II) dihalide complexes

The reaction of phenoxyacetic acid with *cis*-[PtCl₂(COD)] in the presence of silver(I) oxide yields the bis-carboxylato complex [Pt(O₂CCH₂OPh)₂(COD)] (**5.8**), tentatively characterised by multinuclear NMR spectroscopy. Ligand displacement of the COD by triphenylphosphine gave *cis*-[Pt(O₂CCH₂OPh)₂(PPh₃)₂] (**5.9**) which was able to be structurally characterised, and hence provides characterisation of the parent COD complex (**5.8**). The complex *cis*-[Pt(O₂CCH₂OPh)₂(PPh₃)₂] also demonstrates the unidentate bonding mode that carboxylate ligands can adopt, previously observed by Mak *et al.*⁶ One notable difference between the previously reported crystal structures of *cis*-carboxylato platinum(II) complexes and that presented here is the ancillary ligands. In the reported crystal structures of the complexes, *cis*-[Pt(O₂CR)₂L₂] [R = Me or Ph; L₂ = Fe(C₅H₄PPh₂)₂ (dppf); R = CF₃; L₂ = Ph₂PCH₂PPh₂ (dppm)], chelating phosphines were employed, enforcing a *cis*- arrangement of the acetate ligands.⁶

It appears from these crystallographic studies, that phenoxyacetic acid does not undergo decarboxylation to give a bis(phenoxyethyl) complex similar to the cyanomethyl complex (**5.7**) described above. However, if the proposal that a *Hunsdiecker* reaction was taking place during the synthesis of *cis*-[Pt(CH₂CN)₂(PPh₃)₂], in which some stabilisation was imparted to an intermediate through resonance delocalisation of the charge, this may not occur with phenoxyacetic acid. Phenoxyacetic acid would be simply unable to delocalise the charge, and hence have a species that could survive to react further with a platinum cation to give a bis(phenoxyethyl) complex.

Studies have been undertaken with amides to determine whether they too can form a bis(amide) complex and several complexes which are platinum bis(lactam) complexes have been successfully characterised.^{21,22} Presumably, the small volume of the lactams used would allow another to coordinate to the metal centre with few steric interactions.

5.3.4 X-ray crystal structure of *cis*-[Pt(O₂CCH₂OPh)₂(PPh₃)₂].CH₂Cl₂ (5.9)

The coordination around the platinum centre of *cis*-[Pt(O₂CCH₂OPh)₂(PPh₃)₂] (5.9) is a distorted square-plane (Figure 5.3) as a result of the steric bulk of the triphenylphosphine and phenoxyacetate ligands. Thus the P(1)–Pt–P(2) bond angle [98.00(6)°] is more obtuse than the O(1)–Pt–P(1) bond angle [85.54(15)°]. The remaining two bond angles [O(11)–Pt–O(1) and O(11)–Pt–P(2)] are closer to ideal [87.75(19) and 89.93(14)° respectively]. Selected bond lengths and angles are provided in Table 5.3.

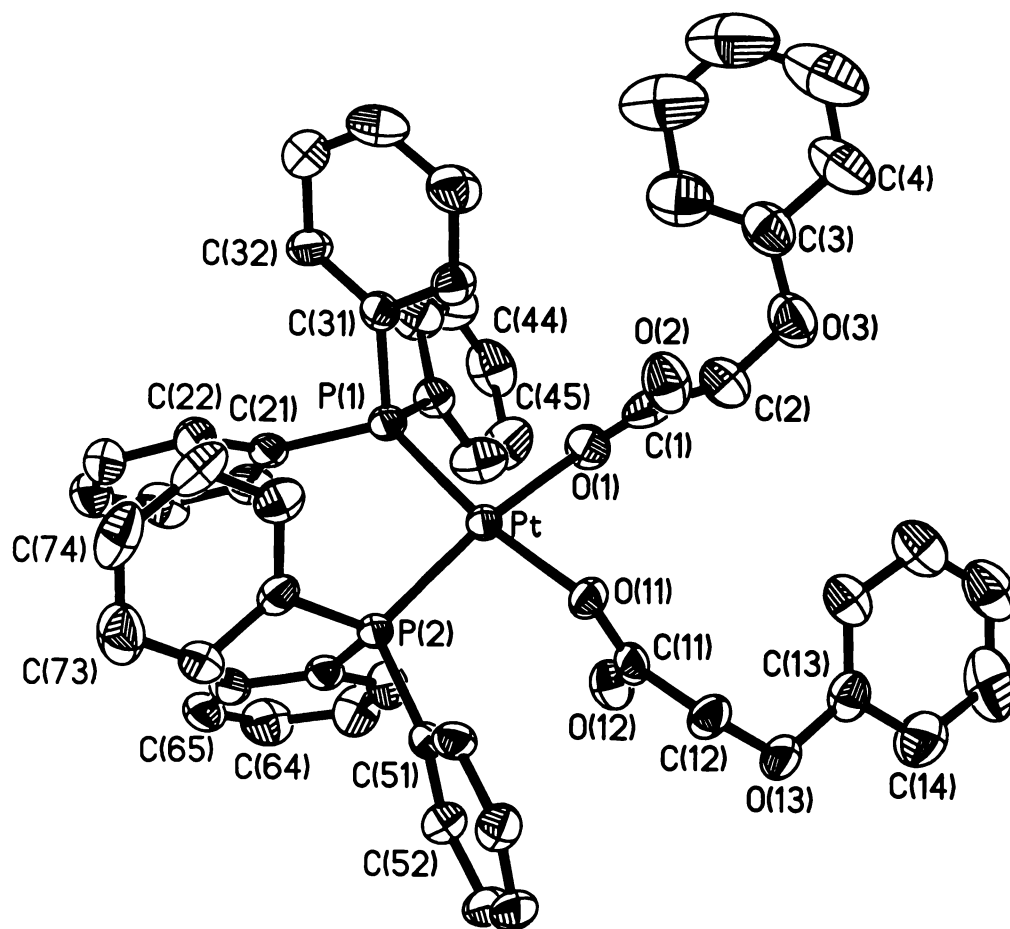


Figure 5.3 Thermal ellipsoid plot and atom labelling scheme for *cis*-[Pt(O₂CCH₂OPh)₂(PPh₃)₂] (5.9)

Thermal displacement ellipsoids are viewed at 50% probability. Hydrogen atoms and dichloromethane of crystallisation omitted for clarity.

The phenoxyacetate ligands are distorted out of the plane around the platinum. O(1) lies 0.433(6) Å above the plane defined by P(1), P(2) and Pt, while O(11) is 0.178(5) Å below the plane. This distortion is also reflected in the bond angles of the atoms *trans*-to the oxygens [167.53(16) and 170.64(14)° for O(1)–Pt–P(2) and O(11)–Pt–P(1) respectively] with respect to an ideal 180°. The Pt–O bond lengths [2.082(5) and 2.056(4) Å for Pt–O(1) and Pt–O(11), respectively] are within the ranges of the previously described platinum(II) carboxylate complexes, *cis*-[Pt(O₂CR)₂L₂] [R = Me or Ph; L₂ = (dppf); R = CF₃; L₂ = (dppm)] [2.034(6) to 2.089(6)Å],⁶ and the Pt–P bond lengths are also not unusual.

The carbonyl groups of the carboxylate ligands lie in an *anti* arrangement with respect to one another [O(2)–C(1)–C(11)–O(12) 177.9(6)°] (see Figure 5.4). This geometry has been observed in the other reported *cis*-acetato platinum(II) complexes.⁶ The O(1)–C(1) bond distance is 1.177(9) Å, fractionally shorter than that of O(2)–C(1) [1.225(9) Å], where O(1) is the oxygen coordinated to the platinum. The other coordinating oxygen [O(11)] shows more single bond nature with an O–C bond distance of 1.285(8) Å and is comparable with previously reported bond lengths [1.257(8) to 1.298(5) Å].⁶ The short, formally single-bond, C–O distances observed are unusual. Back donation of electron density from the platinum into the carboxylic group may be the cause of the reduction in the bonding distances observed. The formal single-bond shows more double-bond character and because of this back donation of electron density from the platinum more delocalisation of electron density about the carboxylic functionality could occur resulting in the observed short bond distances.

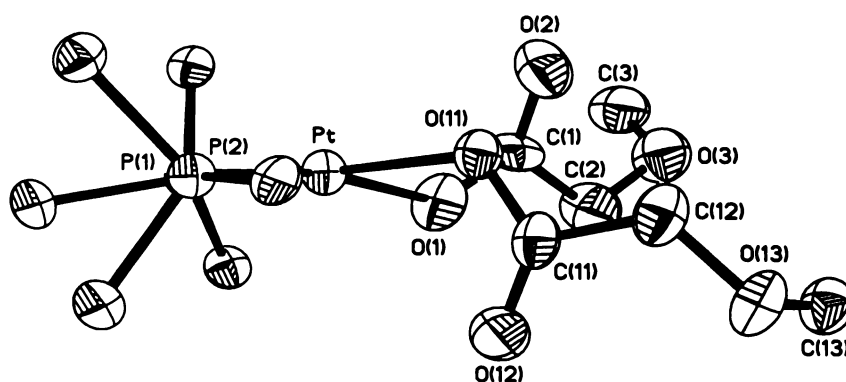


Figure 5.4 Plan view of 5.9 depicting the *anti*-arrangement of the carboxylate ligands

Thermal displacement ellipsoids are viewed at 50% probability. Only the phenyl *ipso* carbon atoms shown for clarity.

Table 5.3 Selected bond lengths (Å) and angles (°) for *cis*-[Pt(O₂CCH₂OPh)₂(PPh₃)₂] (5.9)

Pt–O(11)	2.056(4)	Pt–O(1)	2.082(5)
Pt–P(2)	2.2305(17)	Pt–P(1)	2.2501(18)
O(1)–C(1)	1.177(9)	O(2)–C(1)	1.225(9)
O(3)–C(3)	1.369(11)	O(3)–C(2)	1.396(10)
O(11)–C(11)	1.285(8)	O(12)–C(11)	1.234(9)
O(13)–C(13)	1.385(9)	O(13)–C(12)	1.414(8)
C(1)–C(2)	1.597(11)	C(11)–C(12)	1.510(10)
P(1)–C(31)	1.812(7)	P(1)–C(41)	1.829(7)
P(1)–C(21)	1.830(7)	P(2)–C(61)	1.820(7)
P(2)–C(71)	1.825(7)	P(2)–C(51)	1.833(6)
O(11)–Pt–O(1)	87.75(19)	O(11)–Pt–P(2)	89.93(14)
O(1)–Pt–P(2)	167.53(16)	O(11)–Pt–P(1)	170.64(14)
O(1)–Pt–P(1)	85.54(15)	P(2)–Pt–P(1)	98.00(6)
C(1)–O(1)–Pt	124.6(6)	C(3)–O(3)–C(2)	117.2(7)
C(11)–O(11)–Pt	118.5(4)	C(13)–O(13)–C(12)	116.7(6)
O(1)–C(1)–O(2)	134.3(9)	O(1)–C(1)–C(2)	109.8(6)
O(2)–C(1)–C(2)	115.9(8)	O(3)–C(2)–C(1)	116.0(7)
O(3)–C(3)–C(8)	124.7(9)	O(3)–C(3)–C(4)	115.0(10)
O(12)–C(11)–O(11)	125.3(7)	O(12)–C(11)–C(12)	121.9(7)
O(11)–C(11)–C(12)	112.7(7)	O(13)–C(12)–C(11)	114.5(6)
C(14)–C(13)–O(13)	115.2(7)	C(18)–C(13)–O(13)	124.4(7)

5.3.5 NMR spectroscopy

Phosphorus NMR is an efficient method for determining the outcome of silver(I) oxide reactions of bis-triphenylphosphine platinum(II) complexes. The ¹J(Pt, P) coupling constants give a great deal of information about the product. In the complexes presented here, the phosphorus atoms are magnetically and chemically identical to one another. This gives rise to the observed singlet, with platinum satellites. For *cis*-

[Pt(CH₂CN)₂(PPh₃)₂], the observed single peak with ¹J(Pt, P) satellites of 2376 Hz indicates that the phosphorus atoms are in magnetically equivalent environments, *trans* to a high *trans*-influence carbon atom and is comparable with the coupling constants observed for other complexes with a carbon atom *trans* to phosphorus [2393 – 2545 Hz].¹⁻³ As shown in the X-ray crystal structure this is the case. The platinum satellites of *cis*-[Pt(O₂CCH₂OPh)₂(PPh₃)₂] (4084 Hz) indicate that a low *trans*-influence atom is bonded to the platinum. The singlet resonance again implies that the two phosphorus atoms are equivalent. This ¹J(Pt, P) coupling constant is in accord with those observed for other complexes with a platinum-oxygen bond *trans* to an oxygen [3862 – 4230 Hz].^{1,2}

5.4 Conclusion

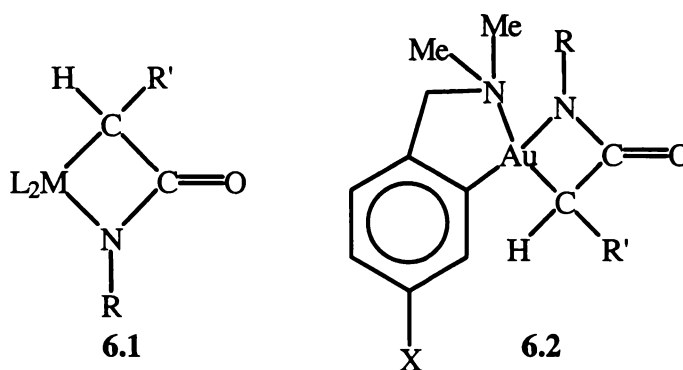
Silver(I) oxide has proven to be a useful reagent for the synthesis of a large number of metallacyclic complexes. While metallalactones can be synthesised *via* a silver(I) oxide mediated reaction with malonates, it does not appear that reaction with carboxylic acids gives such a direct result. Instead, one of two mechanisms are likely. As seen here with the *cis*-[Pt(O₂CCH₂OPh)₂(PPh₃)₂] complex which forms a simple *bis*-carboxylato complex, which intuitively one might expect to form.

The unusual result is that silver(I) oxide may be able to promote decarboxylation of carboxylic acids. Presumably, the driving force would be the formation of silver carbonate. However, it is unclear why cyanoacetic acid would undergo such a decarboxylation, while phenoxyacetic acid does not. The respective electronegativities of the cyanide and phenoxy functionalities may alter the reactivity of the carboxylic acid towards attack by silver(I) oxide, and hence alter the final product formed.

Chapter Six. Triethylamine mediated syntheses of four-membered metallalactam complexes

6.1 Introduction

A wide variety of metallalactam complexes have been synthesised from platinum(II),¹ palladium(II)^{2,3} (see also Chapter Two) (6.1) and gold(III) dihalide (refer Chapter Four) (6.2) compounds. Principally the reactions involve silver(I) oxide as a base and halide abstractor, and functionalised amides to produce the four-membered metallalactam ring system. However, these complexes have been limited in their versatility towards further functionalisation, by having substituents (Ph, CO₂Et) that stabilise the metal-nitrogen bond.



The principal driving force of these silver(I) oxide mediated reactions is the formation of insoluble silver(I) chloride. However, it is not the only reagent that can effect these reactions; triethylamine has also been used with some degree of success.⁴ One minor problem with triethylamine mediated reactions is the purification of the products if the reaction does not proceed smoothly.

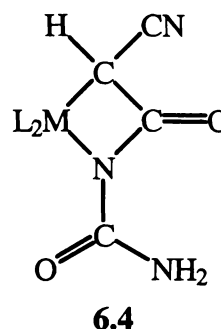
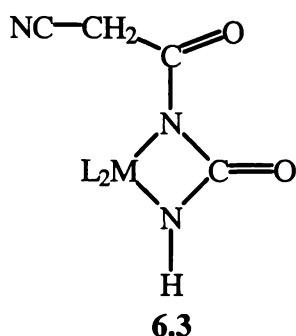
1 W. Henderson, B. K. Nicholson and A. G. Oliver, *J. Chem. Soc., Dalton Trans.*, (1994), 1831

2 W. Henderson, J. Fawcett, R. D. W. Kemmitt, C. Proctor and D. R. Russell, *J. Chem. Soc., Dalton Trans.*, (1994), 3085

3 W. Henderson, A. G. Oliver, C. E. F. Rickard and L.-J. Baker, *Inorg. Chim. Acta*, (1999), **292**, 260

4 L. J. McCaffrey, W. Henderson, B. K. Nicholson, J. E. Mackay and M. B. Dinger, *J. Chem. Soc., Dalton Trans.*, (1997), 2577

The following work describes the synthesis and characterisation of several novel complexes synthesised from palladium and platinum(II) dihalides reacted with cyanoacetylurea in the presence of triethylamine. Cyanoacetylurea, $[\text{NCCH}_2\text{C}(\text{O})\text{NHC}(\text{O})\text{NH}_2]$, has the possibility of forming one of two products, either a ureylene complex (6.3) or a metallalactam complex (6.4).



A study was made of a selection of amides which were reacted with *cis*- $[\text{PtCl}_2(\text{PPh}_3)_2]$ in the presence of triethylamine. The amides selected are known to give well-characterised and reproducible products^{1,2,3} when reacted with *cis*- $[\text{PtCl}_2(\text{PPh}_3)_2]$ in the presence of silver(I) oxide. The results of these comparative studies will also be discussed.

6.2 Experimental

All syntheses were performed in air. $[\text{PtCl}_2(\text{COD})]_5^5$ and $[\text{PdCl}_2(\text{COD})]_6^6$ were prepared by standard literature procedures. 1,2-Bis(diphenylphosphino)ethane⁷ $[\text{PtCl}_2(\text{PPh}_3)_2]$, $[\text{PtCl}_2(\text{dppe})]$ and $[\text{PdCl}_2(\text{dppe})]_5^5$ were prepared by literature methods. Triphenylphosphine (Pressure Chemical Co.), 1,5-cyclooctadiene (BDH), *N*-cyanoacetylurethane, cyanoacetylurea, 2-benzoylacetanilide and acetoacetanilide (Aldrich) were used as supplied. Triethylamine was distilled from magnesium sulfate before use. Dichloromethane was distilled from CaH_2 and diethyl ether was distilled from sodium benzophenone ketyl before use. Methanol (AR grade) was used as supplied. NMR spectra were recorded on either a Brüker AC300P (^1H , ^{13}C - $\{^1\text{H}\}$ and ^{31}P - $\{^1\text{H}\}$) or a Brüker 400DRX (^1H and ^{13}C - $\{^1\text{H}\}$). Spectra were recorded at 300.133 or

5 J. X. McDermott, J. F. White and G. M. Whitesides, *J. Am. Chem. Soc.*, (1976), **98**, 6521

6 D. Drew and J. R. Doyle, *Inorg. Synth.*, (1972), **13**, 52

7 J. Chatt and F. A. Hart, *J. Chem. Soc.*, (1960), 1378

400.131 MHz, respectively for ^1H and 75.47 or 100.61 MHz, respectively for ^{13}C - $\{^1\text{H}\}$ referenced to internal TMS (δ 0.00) with a CDCl_3 lock. ^{31}P - $\{^1\text{H}\}$ spectra were recorded at 121.74 MHz in CDCl_3 and referenced to external 85% H_3PO_4 . Infrared spectra were recorded on a Bio-Rad FTS-40 Infrared spectrometer as solid KBr discs. Melting points were obtained from a Reichert Thermopan apparatus and are uncorrected. Elemental analyses were carried out at the Microanalytical Unit at the University of Otago. Accurate X-ray intensity data were collected on a Siemens SMART CCD diffractometer at the University of Auckland. Electrospray mass spectra were collected on a VG Platform II Mass Spectrometer in positive-ion mode with either a 1:1 methanol : water or 1:1 acetonitrile : water mix as the carrier solvent.

6.2.1 Synthesis of $[\text{Pt}\{\text{N}(\text{C}(\text{O})\text{NH}_2)\text{C}(\text{O})\text{CHCN}\}(\text{PPh}_3)_2]$ (6.5)

Triethylamine (0.5 cm^3) was added to a suspension of *cis*- $[\text{PtCl}_2(\text{PPh}_3)_2]$ (0.101 g, 0.128 mmol) and cyanoacetylurea (0.022 g, 0.17 mmol) in methanol (8 cm^3). The mixture was heated at reflux for 20 min., by which time the suspension had dissolved giving a clear yellow solution. To this solution, distilled water (40 cm^3) was added forcing the precipitation of a pale yellow solid. The precipitate was left to consolidate for 18 h. and filtered by gravity. The solid was washed with distilled water and diethyl ether and dried (0.101 g, 93%). Subsequently the product was recrystallised from dichloromethane / diethyl ether, filtered and dried for analysis. The X-ray crystal structure of 6.5 showed the presence of dichloromethane. Elemental analysis indicates that some dichloromethane may be present in the matrix, even after drying.

Elemental analysis: C, 55.7; H, 4.2; N, 4.6. $\text{C}_{40}\text{H}_{33}\text{N}_3\text{O}_2\text{P}_2\text{Pt}$ requires: C, 56.9; H, 3.9; N, 5.0%. $\text{C}_{40}\text{H}_{33}\text{N}_3\text{O}_2\text{P}_2\text{Pt} \cdot \frac{1}{4}(\text{CH}_2\text{Cl}_2)$ requires: C, 55.8; H, 3.9; N, 4.8%.

IR: $\nu(\text{CN})$ 2211; $\nu(\text{CO})$ 1683, 1652 cm^{-1} .

m.p.: 213 – 216 $^\circ\text{C}$ (decomp.)

ES/MS (20 V): $[\text{M}+\text{H}]^+$ m/z 845, (100%)

^1H NMR: δ 7.54 - 7.03 (m, 30H, Ph), 6.50 (s, 1.5H, NH_2), 1.65 [dd, 1H, CH, $^3J(\text{trans P, H})$ 8, $^3J(\text{cis P, H})$ 3, $^2J(\text{Pt, H})$ 61].

^{13}C - $\{^1\text{H}\}$ NMR: δ 173.9 [d, ring C(O) $^3J(\text{P, C})$ 6], 156.0 [d, urea C(O), $^3J(\text{P, C})$ 5], 134.7 - 127.5 (m, Ph), 121.7 [d, CN, $^3J(\text{P, C})$ 7], 11.5 [dd, ring CH, $^2J(\text{trans P, C})$ 74, $^2J(\text{cis P, C})$ 2].

^{31}P - $\{^1\text{H}\}$ NMR: AB spin system δ 17.24 [d, $^1J(\text{Pt}, \text{P trans C})$ 2530, $^2J(\text{P}, \text{P})$ 18], 11.78 [d, $^1J(\text{Pt}, \text{P trans N})$ 3722, $^2J(\text{P}, \text{P})$ 18].

6.2.2 Synthesis of $[\text{Pt}\{\text{N}(\text{C}(\text{O})\text{NH}_2)\text{C}(\text{O})\text{CHCN}\}(\text{COD})]$ (6.6)

A stirred suspension of $[\text{PtCl}_2(\text{COD})]$ (0.117 g, 0.312 mmol), cyanoacetylurea (0.042 g, 0.33 mmol) and triethylamine (*ca.* 0.5 cm³) was heated under reflux in methanol (8 cm³) for 15 min. Toluene (5 cm³) and diethyl ether (30 cm³) were added to the hot solution, precipitating a white microcrystalline solid. The pale yellow product was allowed to consolidate, filtered at the pump and washed with diethyl ether and dried (yield 0.078 g, 58%). The product could only be redissolved in either a large volume of dichloromethane or in dimethylsulfoxide, which was found to degrade the product. *In situ* displacement of COD by triphenylphosphine and subsequent analysis by ^{31}P NMR gave data consistent with the complex 6.5. The complex was precipitated from a dichloromethane solution of 6.6 by the addition of diethyl ether, filtered at the pump and dried for analysis. Again, data consistent with the presence of dichloromethane was obtained.

Elemental analysis: C, 31.9; H, 4.2; N, 9.1. $\text{C}_{12}\text{H}_{15}\text{N}_3\text{O}_2\text{Pt}$ requires: C, 33.6; H, 3.5; N, 9.8%. $\text{C}_{12}\text{H}_{15}\text{N}_3\text{O}_2\text{Pt} \cdot \frac{1}{2}(\text{CH}_2\text{Cl}_2)$ requires: C, 31.8; H, 3.4; N, 8.9%.

IR: $\nu(\text{CN})$ 2211; $\nu(\text{CO})$ (br., s) 1635 cm⁻¹

m.p.: 182 – 186 °C (decomp.)

ES/MS (20 V): $[\text{M}+\text{H}]^+$ m/z 530, (100%)

6.2.2.1 Ligand displacement of COD from $[\text{Pt}\{\text{N}(\text{C}(\text{O})\text{NH}_2)\text{C}(\text{O})\text{CHCN}\}(\text{COD})]$ (6.6) by PPh_3

To a stirred suspension of $[\text{Pt}\{\text{N}(\text{C}(\text{O})\text{NH}_2)\text{C}(\text{O})\text{CHCN}\}(\text{COD})]$ (0.034 g, 0.079 mmol) in dichloromethane (2 cm³), triphenylphosphine (0.044 g, 0.16 mmol) was added. The solution was stirred for 10 min. The volume of the solvent was reduced and the product precipitated by the addition of diethyl ether (30 cm³). ^{31}P - $\{^1\text{H}\}$ NMR and ES/MS data were collected on the crude product for comparison with 6.5.

ES/MS (20 V): $[\text{M}+\text{H}]^+$ m/z 845, (100%).

^{31}P - $\{^1\text{H}\}$ NMR: AB spin system δ 20.46 [d, P *trans* C, $^1J(\text{Pt}, \text{P})$ 2599, $^2J(\text{P}, \text{P})$ 18], 10.16 [d, P *trans* N, $^1J(\text{Pt}, \text{P})$ 3314, $^2J(\text{Pt}, \text{P})$ 18].

6.2.3 Synthesis of $[\text{Pt}\{\text{N}(\text{C}(\text{O})\text{NH}_2)\text{C}(\text{O})\text{CHCN}\}(\text{dppe})]$ (6.7)

A mixture of $[\text{PtCl}_2(\text{dppe})]$ (0.088 g, 0.13 mmol), cyanoacetylurea (0.018 g, 0.15 mmol) and triethylamine (*ca* 0.5 cm³) was heated at reflux in methanol (8 cm³) for 15 min. Addition of distilled water (40 cm³) to the clear yellow solution caused the precipitation of a pale yellow solid, which was allowed to coagulate. The product was filtered at the pump and washed with water and diethyl ether and dried (0.068 g, 73%). The complex **6.7** was recrystallised from dichloromethane /diethyl ether and dried before analysis.

Elemental analysis: C, 49.6; H, 4.0; N, 5.7. C₃₀H₂₇N₃O₂P₂Pt requires: C, 50.0; H, 3.8; N, 5.8%.

IR: $\nu(\text{CN})$ 2202; $\nu(\text{CO})$ (br., s) 1616 cm⁻¹

m.p.: 151 – 154 °C (decomp.)

ES/MS (20 V) $[\text{M}+\text{H}]^+$ m/z 719, (100%)

^1H NMR: δ 7.90 – 7.36 (m, 20H, Ph), 3.52 (m, 2H, dppe CH₂) 3.33 (m, 2H, dppe CH₂), 1.64 [dd, 1H, ring CH, $^3J(\text{trans P}, \text{H})$ 8, $^3J(\text{cis P}, \text{H})$ 3].

^{13}C - $\{^1\text{H}\}$ NMR: δ 171.3 (s, ring CO), 155.8 [d, urea CO, $^3J(\text{P}, \text{C})$ 5], 129.5 – 123.3 (m, Ph), 121.3 (s, CN), 33.5 – 29.2 (m, dppe CH₂), 12.1 [d, CH, $^2J(\text{Pt}, \text{C})$ 70].

^{31}P - $\{^1\text{H}\}$ NMR: AB spin system δ 45.07 [s, $^1J(\text{Pt}, \text{P } \textit{trans} \text{ C})$ 2525, $^2J(\text{P}, \text{P})$ unresolved], 38.64 [s, $^1J(\text{Pt}, \text{P } \textit{trans} \text{ N})$ 3432, $^2J(\text{P}, \text{P})$ unresolved].

6.2.4 Synthesis of $[\text{Pd}\{\text{N}(\text{C}(\text{O})\text{NH}_2)\text{C}(\text{O})\text{CHCN}\}(\text{dppe})]$ (6.8)

Cyanoacetylurea (0.025 g, 0.20 mmol), $[\text{PdCl}_2(\text{dppe})]$ (0.098 g, 0.17 mmol), and triethylamine (*ca* 0.5 cm³) were refluxed in methanol (8 cm³) for 20 min. A yellow solid was precipitated by the addition of distilled water (40 cm³) to the hot solution. The product was allowed to settle and consolidate. Subsequently the yellow product was filtered by gravity, and washed with water and diethyl ether and dried (0.046 g, 44%). The compound was precipitated from a dichloromethane solution by the addition of diethyl ether, filtered and dried before analysis.

Elemental analysis: Found C, 54.1; H, 4.5; N, 5.4. $C_{30}H_{27}N_3O_2P_2Pd$ requires: C, 57.2; H, 4.3; N, 6.7%. $C_{30}H_{27}N_3O_2P_2Pd \cdot \frac{1}{2}(CH_2Cl_2)$ requires: C, 54.5; H, 4.1; N, 6.2%.

IR: ν (CN) 2198; ν (CO) 1616 (br., s) cm^{-1}

m.p.: 154 – 156 °C (decomp.)

ES/MS (20 V): $[M+H]^+$ m/z 630, (100%); $[2M+H]^+$ m/z 1260, (30%).

1H NMR: δ 7.90- 7.36 (m, 24H, Ph), 6.65 (br. s, 1H, NH_2), 3.94 [m, 2H, dppe CH_2], 3.21 [dd, 2H, dppe CH_2 , $^2J(H, H)$ 8, $^3J(H, H)$ 8], 2.04 [d, 1H, CH, $^3J(trans\ P, H)$ 11].

^{13}C - $\{^1H\}$ NMR: δ 171.7 (s, ring CO), 161.3 (s, urea CO), 133.8 – 128.6 (m, Ph), 127.2 (s, CN), 31.1 – 29.5 (d, dppe CH_2), 20.0 [d, ring CH, $^2J(trans\ P, C)$ 72]

^{31}P - $\{^1H\}$ NMR: AB spin system δ 57.75 [d, $^2J(P, P)$ 26], 52.55 [s, $^2J(P, P)$ 26].

6.2.5 Reaction of N-cyanoacetylurethane with *cis*- $[PtCl_2(PPh_3)_2]$ in the presence of triethylamine

A stirred suspension of *cis*- $[PtCl_2(PPh_3)_2]$ (0.062 g, 0.079 mmol), N-cyanoacetylurethane (0.013 g, 0.085 mmol) and triethylamine (*ca* 0.5 cm^3) in methanol (8 cm^3) was heated at reflux for 30 min. To the clear yellow solution, distilled water (40 cm^3) was added precipitating a white microcrystalline solid. The mixture was stirred at room temperature for 18 h, consolidating the compound. The product was filtered by gravity and washed with water and diethyl ether and allowed to dry in air. ^{31}P - $\{^1H\}$ NMR spectroscopy and ES/MS gave data consistent with the previously characterised platinalactam **6.1** ($M = Pt$, $L = PPh_3$, $R = CO_2Et$, $R' = CN$).¹

ES/MS (20 V): $[M+H]^+$ m/z 874, (100%), $[M+NEt_3+H]^+$ m/z 975, (20%).

^{31}P - $\{^1H\}$ NMR: AB spin system δ 20.10 [d, P *trans* C, $^1J(Pt, P)$ 2493, $^2J(Pt, P)$ 18], 11.33 [d, P *trans* N, $^1J(Pt, P)$ 3813, $^2J(Pt, P)$ 18].

6.2.6 Reaction of *cis*- $[PtCl_2(PPh_3)_2]$ with 2-benzoylacetylurethane in the presence of triethylamine

A mixture of *cis*- $[PtCl_2(PPh_3)_2]$ (0.037 g, 0.047 mmol), 2-benzoylacetylurethane (0.014 g, 0.057 mmol) and triethylamine (0.5 cm^3) was heated at reflux in methanol (8 cm^3) for 30 min. Distilled water (40 cm^3) was added to the hot solution forcing the precipitation of a white solid, which was left to consolidate. The precipitate was filtered by gravity and washed successively with water and diethyl ether and dried in air. Data obtained

from $^{31}\text{P}\{-^1\text{H}\}$ NMR and ES/MS was comparable with that obtained for the platinalactam **6.1** [$\text{M} = \text{Pt}$, $\text{L} = \text{PPh}_3$, $\text{R} = \text{Ph}$, $\text{R}' = \text{C}(\text{O})\text{Ph}$].³

ES/MS (20 V): $[\text{M}+\text{H}]^+$ m/z 958, (100%).

$^{31}\text{P}\{-^1\text{H}\}$ NMR: AB spin system δ 17.25 [d, P *trans* C, $^1J(\text{Pt}, \text{P})$ 2385, $^2J(\text{P}, \text{P})$ 16], 11.17 [d, P *trans* N, $^1J(\text{Pt}, \text{P})$ 3756, $^2J(\text{P}, \text{P})$ 16].

6.2.7 Reaction of *cis*- $[\text{PtCl}_2(\text{PPh}_3)_2]$ with acetoacetanilide, in the presence of triethylamine

Triethylamine (*ca* 0.5 cm³) was added to a stirred suspension of *cis*- $[\text{PtCl}_2(\text{PPh}_3)_2]$ (0.105 g, 0.133 mmol) and acetoacetanilide (0.024 g, 0.14 mmol) in methanol (8 cm³). The mixture was heated at reflux for 30 min. after which time distilled water (40 cm³) was added. The resulting precipitate was allowed to consolidate and subsequently filtered by gravity. The pale yellow powder was washed with water and diethyl ether and dried in air. ES/MS and $^{31}\text{P}\{-^1\text{H}\}$ NMR spectroscopies were used to identify the products. The presence of a ^{31}P NMR singlet resonance with $^1J(\text{Pt}, \text{P})$ satellites matching those of *cis*- $[\text{PtCl}_2(\text{PPh}_3)_2]$ and a peak at m/z 754 in the ES/MS spectrum indicates that the reaction did not go to completion. The data from the minor component was, however, consistent with that for the platinalactam **6.1** [$\text{M} = \text{Pt}$, $\text{L} = \text{PPh}_3$, $\text{R} = \text{Ph}$, $\text{R}' = \text{C}(\text{O})\text{Me}$].²

ES/MS (20 V): $[\text{PtCl}(\text{PPh}_3)_2]^+$ m/z 754, (100%); $[\text{M}+\text{H}]^+$ m/z 895, (30%).

$^{31}\text{P}\{-^1\text{H}\}$ NMR: AB spin system δ 17.52 [d, P *trans* C, $^1J(\text{Pt}, \text{P})$ 2447, $^2J(\text{P}, \text{P})$ 12], 10.72 [d, P *trans* N, $^1J(\text{Pt}, \text{P})$ 3735, $^2J(\text{P}, \text{P})$ 12], 13.33 [s, P *trans* Cl, $^1J(\text{Pt}, \text{P})$ 3950].

6.2.8 X-ray crystallography of $[\text{Pt}\{\text{N}(\text{C}(\text{O})\text{NH}_2)\text{C}(\text{O})\text{CHCN}\}(\text{PPh}_3)_2]$ (**6.5**)

X-ray crystallographic quality crystals were grown by vapour diffusion of diethyl ether into a dichloromethane solution of **6.5**. Preliminary cell parameters and the crystal orientation matrix were obtained from a collection of 45 standard frames. Accurate intensity data of **6.5** were collected over a sphere of reciprocal space and were corrected for Lorentz and polarisation effects. A linear absorption correction was applied to the

data by comparison of the intensities of equivalent reflections.⁸ The position of the platinum atom was determined by Patterson methods.⁹ All other non-hydrogen atoms were located from the electron density maps of successive refinement cycles. Electron density that was assigned to the solvates of crystallisation (dichloromethane and diethyl ether) was initially refined with a variable site occupancy factor. This indicated that the dichloromethane had about 90% occupancy, and was subsequently refined with full occupancy, while the diethyl ether had about 50% occupancy, and was modelled in the final refinement cycle with a 50% site occupancy factor. The final difference map showed significant electron density ($2.88 \text{ e.}\text{\AA}^{-3}$) located 1.14 \AA from C(84). Crystal data for the collection and refinement of $[\text{Pt}\{\text{N}(\text{C}(\text{O})\text{NH}_2)\text{C}(\text{O})\text{CHCN}\}(\text{PPh}_3)_2]$ are included in table 6.1.

Table 6.1 Crystal collection and refinement data for $[\text{Pt}\{\text{N}(\text{C}(\text{O})\text{NH}_2)\text{C}(\text{O})\text{CHCN}\}(\text{PPh}_3)_2] \cdot \text{CH}_2\text{Cl}_2 \cdot \frac{1}{2}\text{Et}_2\text{O}$ (6.5)

<i>Crystal data</i>	
Empirical formula	$\text{C}_{40}\text{H}_{33}\text{N}_3\text{P}_2\text{Pt} \cdot (\text{CH}_2\text{Cl}_2) \cdot \frac{1}{2}(\text{C}_4\text{H}_{10}\text{O})$
Formula weight	966.71
Crystal system	Triclinic
Space group	$\text{P}\bar{1}$
Unit cell dimensions	
a (Å)	10.9488(1)
b (Å)	12.8958(2)
c (Å)	17.5272(3)
α (°)	72.796(1)
β (°)	73.69(1)
γ (°)	66.19(1)
V (Å ³)	2125.65(5)
Z	2
$D(c)$ (g cm ⁻³)	1.510

⁸ R. H. Blessing, *Acta Crystallogr.*, (1995), **A51**, 33

⁹ G. M. Sheldrick, SHELXS-97, *Program for the solution of X-ray structures*, Universität Göttingen, 1997

Data Collection

Diffractometer	Siemens SMART CCD
Radiation	Mo-K α
Wavelength (Å)	0.71073
Temperature (K)	203(2)
Crystal size (mm)	0.45 x 0.40 x 0.30
θ range for data collection (°)	1.76 to 27.49
Index ranges	-13 \leq h \leq 14 -15 \leq k \leq 16, 0 \leq l \leq 22
Reflections collected	20978
Independent reflections	9205 [R(int) = 0.0202]
Absorption coefficient (mm ⁻¹)	3.541
Maximum transmission	0.4164
Minimum transmission	0.2987
F(000)	962

Structure analysis and refinement

Solution by	direct methods
Refinement method	Full-matrix least-squares on F^2
Data / restraints / parameters	9205 / 3 / 481
Goodness-of-fit on F^2	1.141
Final R indices [$I > 2\sigma(I)$]	$R_1 = 0.0348$, $wR^2 = 0.0991$
R indices (all data)	$R_1 = 0.0374$, $wR^2 = 0.1013$
Weighting Scheme:	$w = 1/[\sigma^2(F_o^2) + (0.0520P)^2 + 7.0112P]$ where $P = (F_o^2 + 2F_c^2)/3$
Largest difference peak (e.Å ⁻³)	2.881 [1.14 Å from C(84)]
Largest difference hole (e.Å ⁻³)	-2.719
Programs used	
Solution by	SHELXS-97 ⁹
Refinement by	SHELXL-97 ¹⁰

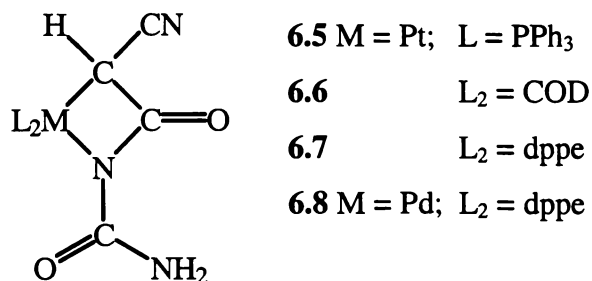
10 G. M. Sheldrick, SHELXL-97, *Program for the refinement of X-ray structures*, Universität Göttingen, 1997

6.3 Results and discussion

6.3.1 Synthesis of metallalactam complexes mediated by triethylamine

Syntheses of metallalactam complexes from reactions of the appropriate amide with metal dihalides in the presence of silver(I) oxide are well documented.^{1,2,3} In fact a wide range of novel metallacyclic complexes, including ureylene ring systems¹¹ are readily accessible by such methodology. By comparison the use of triethylamine for metallacyclic syntheses is not as well documented. In an effort to determine whether triethylamine is as effective as silver(I) oxide, reactions of *N*-cyanoacetylurethane, 2-benzoylacetylurethane and acetoacetylurethane with *cis*-[PtCl₂(PPh₃)₂] in the presence of triethylamine were performed. The products of these reactions are well characterised. From the preliminary investigations carried out here, triethylamine is also able to readily facilitate the synthesis of metallalactam complexes from these organic reagents. Indeed, it appears to be more effective than silver(I) oxide because the reaction time was only 30 minutes as opposed to 18 h for silver(I) oxide mediated reactions.

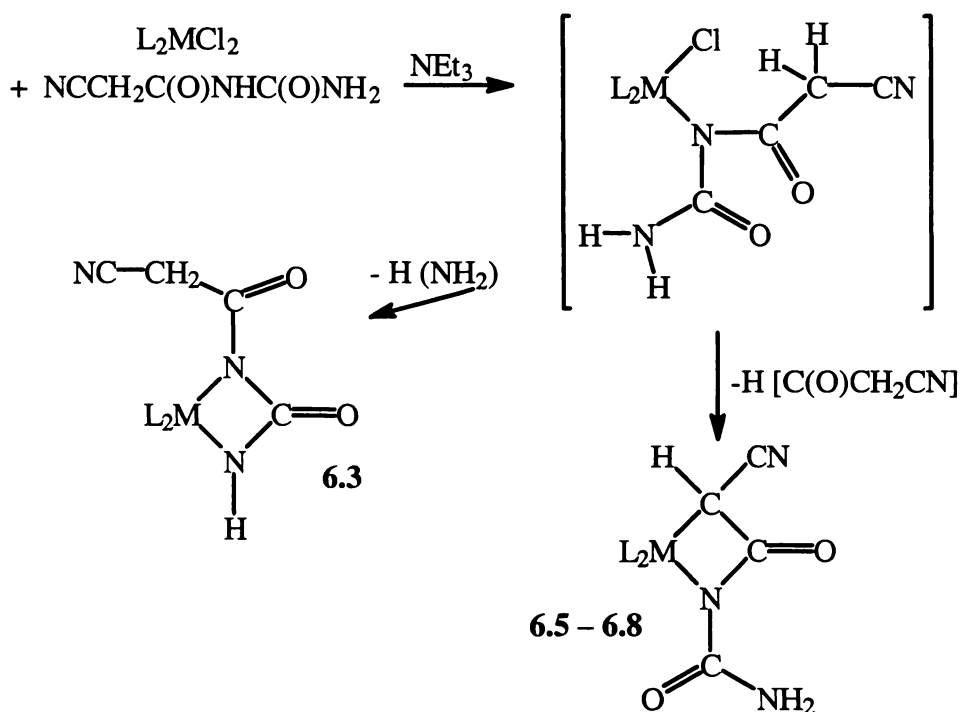
The complexes [6.5 - 6.8] can be synthesised in high yields from a refluxing methanol solution of cyanoacetylurea, triethylamine and the appropriate metal dihalide. Reactions proceed rapidly, often complete in 20 minutes, and the products can be readily purified by the addition of water to the hot reaction mix, precipitating the compounds. As with previous examples of metallalactam complexes, these new compounds are also air-stable allowing easy handling.



As mentioned previously cyanoacetylurea presents an interesting case; it may be possible for the urea to cyclise and form a ureylene complex. Presumably the nitrogen with two adjacent carbonyl groups would be the most acidic, and hence bond to the

metal first (refer Chapter 3). Either the free urea nitrogen could bond to give **6.3** (see Scheme 6.1), or the acetyl carbon could bond to the metal next to give a metallalactam (**6.5 – 6.8**).

It is interesting to note that as with the previously characterised *N*-cyanoacetylurethane derived metallalactam (**6.1**, R = CO₂Et, R' = CN),¹ the IR stretching frequency of the cyanide functionality has shifted. In the parent cyanoacetylurea, the cyanide stretch is observed at 2270 cm⁻¹, while in the metallacyclic complexes the stretching frequency is observed at 2211 to 2198 cm⁻¹. Electron density has been withdrawn from the C=O bond because the nearby N is acting as a donor ligand to the metal.



Scheme 6.1 Metallalactam or ureylene synthetic routes

6.3.2 X-ray crystal structure analysis of $[Pt\{N(C(O)NH_2)C(O)CHCN\}(PPh_3)_2] \cdot CH_2Cl_2 \cdot \frac{1}{2}[(C_2H_5)_2O]$ (**6.5**)

The complex $[Pt\{N(C(O)NH_2)C(O)CHCN\}(PPh_3)_2]$ (**6.5**) was crystallised by vapour diffusion of diethyl ether into a dichloromethane solution of the compound. The complex crystallises with one dichloromethane and one half of a diethyl ether of

crystallisation. These two molecules occupy voids in the crystal lattice and have no contacts closer than 3.257 and 3.532 Å [C(70) to O(2) and O(3) to C(22) respectively] with the metallalactam complex. Figure 6.1 shows the atom labelling scheme for the molecule. Elemental analysis of the complexes also indicates that some residual solvent was present even after drying *in vacuo*.

The geometry about the platinum atom is a distorted square plane. The N(1)–Pt–C(2) angle is acute at 65.94(17)°, but is comparable to those found in similar metallalactam structures (64 – 67°).^{1,2} The P(1)–Pt–P(2) angle is more obtuse [97.35(4)°] than an ideal 90° and accommodates the steric bulk of the triphenylphosphine ligands. The Pt–P bond lengths reflect the relative *trans*-influence of the *trans* atoms. Pt–P(1) [2.2466(11) Å] (*trans* to the low *trans*-influence nitrogen) is shorter than Pt–P(2) [2.3375(11) Å], *trans* to C(2). The Pt–N [2.071(4) Å] and Pt–C [2.105(4) Å] bonds are normal for metallalactam complexes.^{1,2} The coordination sphere about the platinum atom, and the lactam ring system, is highly planar, with no atom lying more than 0.022(2) Å from the least-squares plane. O(1) is also co-planar with the metallalactam, and lies only 0.065(7) Å from the above plane.

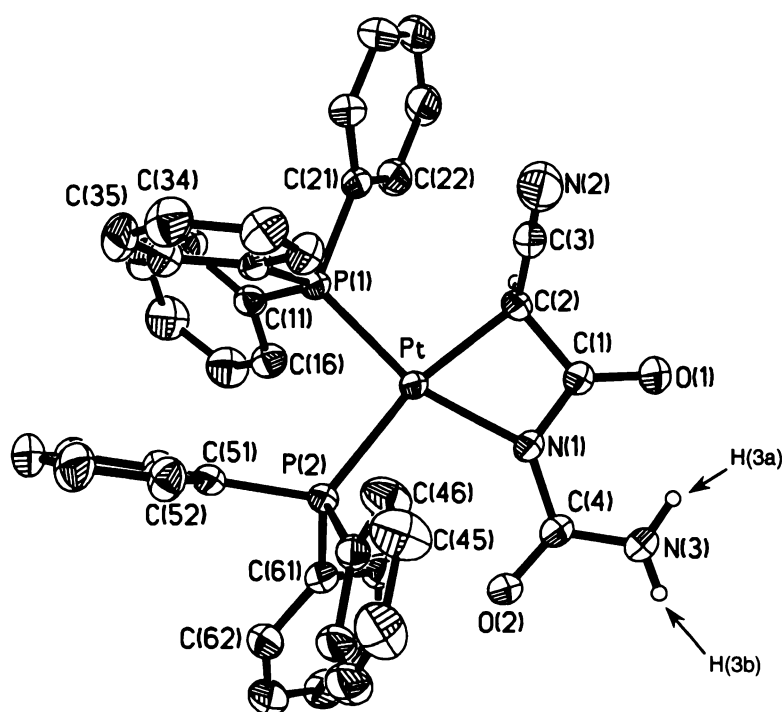


Figure 6.1 Crystal structure of *cis*-[Pt{N(C(O)NH₂)C(O)CHCN}(PPh₃)₂] (6.5)

Thermal displacement ellipsoids are depicted at 50% probability. The phenyl hydrogen atoms, dichloromethane and diethyl ether of crystallisation have been omitted for clarity.

Table 6.2 Selected bond lengths (Å) and bond angles (°) for *cis*-[Pt{N(C(O)NH₂)C(O)CHCN}(PPh₃)₂] (**6.5**)

Pt–N(1)	2.071(4)	Pt–C(2)	2.105(4)
Pt–P(1)	2.2466(11)	Pt–P(2)	2.3375(11)
N(1)–C(1)	1.371(6)	N(1)–C(4)	1.401(6)
N(2)–C(3)	1.143(7)	N(3)–C(4)	1.349(7)
O(1)–C(1)	1.220(6)	O(2)–C(4)	1.230(6)
C(1)–C(2)	1.529(6)	C(2)–C(3)	1.442(7)
P(1)–C(11)	1.826(5)	P(1)–C(21)	1.834(5)
P(1)–C(31)	1.813(5)	P(2)–C(41)	1.827(5)
P(2)–C(51)	1.841(5)	P(2)–C(61)	1.826(5)
N(1)–Pt–C(2)	65.94(17)	N(1)–Pt–P(1)	162.51(11)
C(2)–Pt–P(1)	96.62(13)	N(1)–Pt–P(2)	99.97(11)
C(2)–Pt–P(2)	165.48(13)	P(1)–Pt–P(2)	97.35(4)
C(1)–N(1)–C(4)	124.5(4)	C(1)–N(1)–Pt	98.6(3)
C(4)–N(1)–Pt	135.9(3)	O(1)–C(1)–N(1)	130.2(5)
O(1)–C(1)–C(2)	126.7(4)	N(1)–C(1)–C(2)	103.1(4)
C(3)–C(2)–C(1)	112.4(4)	C(3)–C(2)–Pt	113.8(3)
C(1)–C(2)–Pt	92.2(3)	N(2)–C(3)–C(2)	178.9(6)
O(2)–C(4)–N(3)	123.0(5)	O(2)–C(4)–N(1)	119.9(4)
N(3)–C(4)–N(1)	117.2(4)		

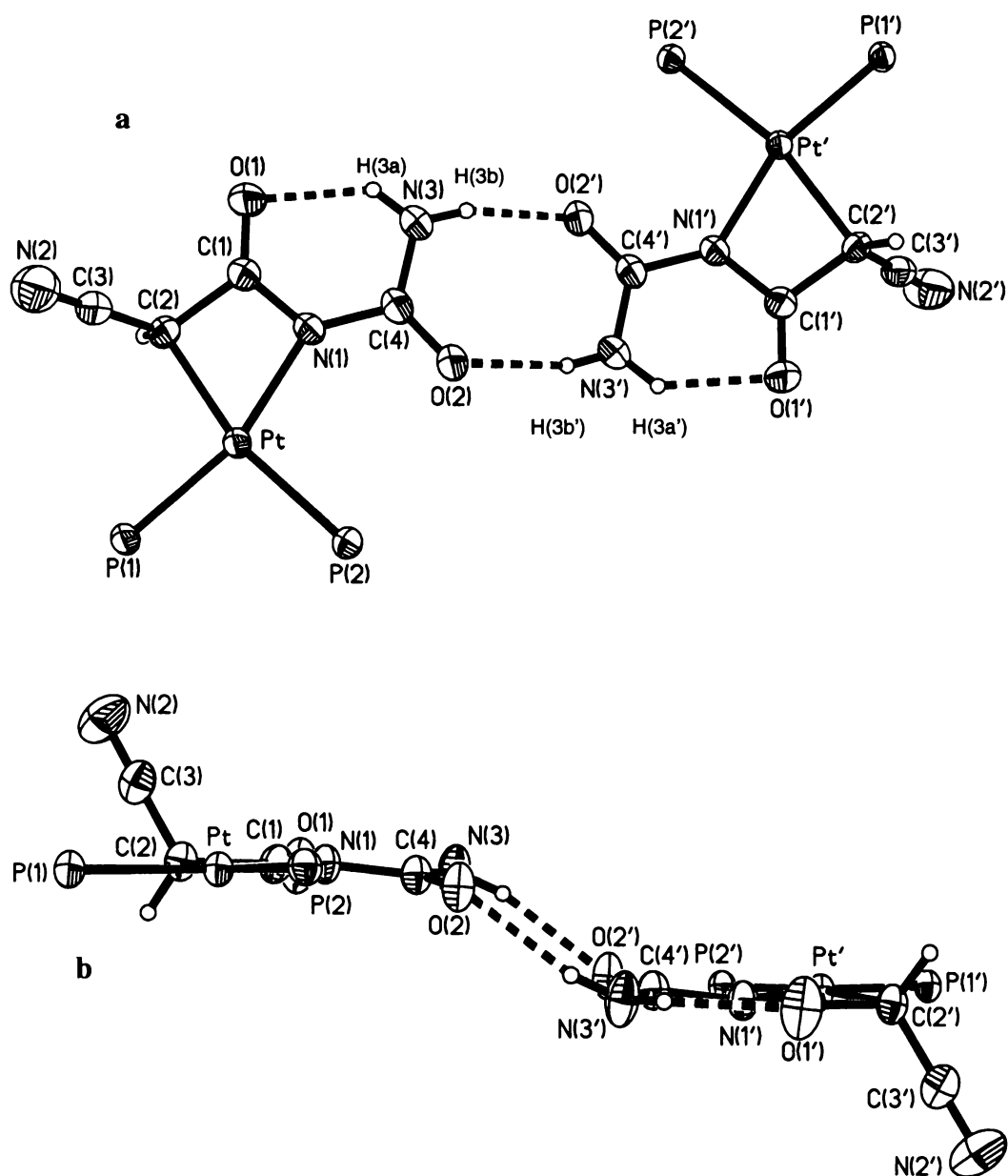


Figure 6.2 Diagrams depicting the H-bonding scheme in $\text{Pt}\{\text{N}(\text{C}(\text{O})\text{NH}_2)\text{C}(\text{O})\text{CHCN}\}(\text{PPh}_3)_2$ (6.5).

The phenyl rings have been omitted for clarity.

The geometry of the urea moiety is interesting. The urea functionality is co-planar with the ring system, with the urea nitrogen [N(3)] oriented such that H(3a) forms an intramolecular hydrogen-bond to the lactam oxygen O(1) [O(1).....H(3a) 1.988 Å]. H(3b) forms an intermolecular hydrogen bond to a symmetry equivalent of O(2) [O(2)'.....H(3b) 2.123 Å], giving rise to a loosely bound dimeric species in the solid state (see Figure 6.2a, Table 6.3). The bond lengths are not unusual for the cyanoacetylurea moiety, however, the bond angles about N(1) are distorted, presumably

to accommodate the dimerisation and intramolecular H-bond. For example, the Pt–N(1)–C(4) bond angle has distorted away from the ideal 120° to 135.9(3)°, which will allow a closer intramolecular interaction between H(3a) and O(1). However, these bond angles are comparable to those found previously for the palladalactam **2.14** (see Chapter Two). A view of the intermolecular contacts shows that the H-bonding is not in a planar arrangement, but has the molecules lying stepped to one another (Figure 6.2b). The H-bond bridge is across the inversion centre at (1, 0.5, 1). H(3a) and H(3b) were located from the residual electron density map. Because of this intermolecular interaction, H(3a) and H(3b) are not positioned opposite one another. As can be seen in Figure 6.2b, H(3b) is bent out of the plane of the metallalactam moiety, oriented so that it can more readily H-bond to O(2'). A conformational calculation of the torsion angles [O(2)–C(4)–N(3)–H] has H(3a) at 170.3(5.1)° and H(3b) at 22.1(5.6)°. If H(3b) was directly opposite H(3a) a torsion angle of about 10° for O(2)–C(4)–N(3)–H(3b) might be expected.

Table 6.3 Hydrogen bonds and angles for
 $[\text{Pt}\{\text{N}(\text{C}(\text{O})\text{NH}_2)\text{C}(\text{O})\text{CHCN}\}(\text{PPh}_3)_2]\cdot\text{CH}_2\text{Cl}_2\cdot 0.5\text{Et}_2\text{O}$ (**6.5**)

Hydrogen bonds with $\text{H}\cdots\text{A} < r(\text{A}) + 2.000$ Angstroms and $\langle\text{DHA}\rangle > 110$ deg.

D-H	(D-H) (Å)	(H \cdots A) (Å)	$\langle\text{DHA}\rangle$ (°)	(D \cdots A) (Å)	A
N(3) – H(3a)	0.901	1.988	137.45	2.721	O1
N(3) – H(3b)	0.861	2.123	161.93	2.954	O2 *

symmetry operator = [-x+2, -y+1, -z+2]

D = donor atom

A = Acceptor atom

6.3.3 NMR spectroscopy

Due to the relatively uncomplicated structure of these complexes, NMR spectroscopy only provides a limited amount of information. ^{31}P NMR spectroscopy, where relevant, provides some connectivity information, while ^1H NMR spectra have only a small amount of information, in most cases phenyl resonances are the main feature of the spectrum. These resonances are the salient feature of ^{13}C spectra also.

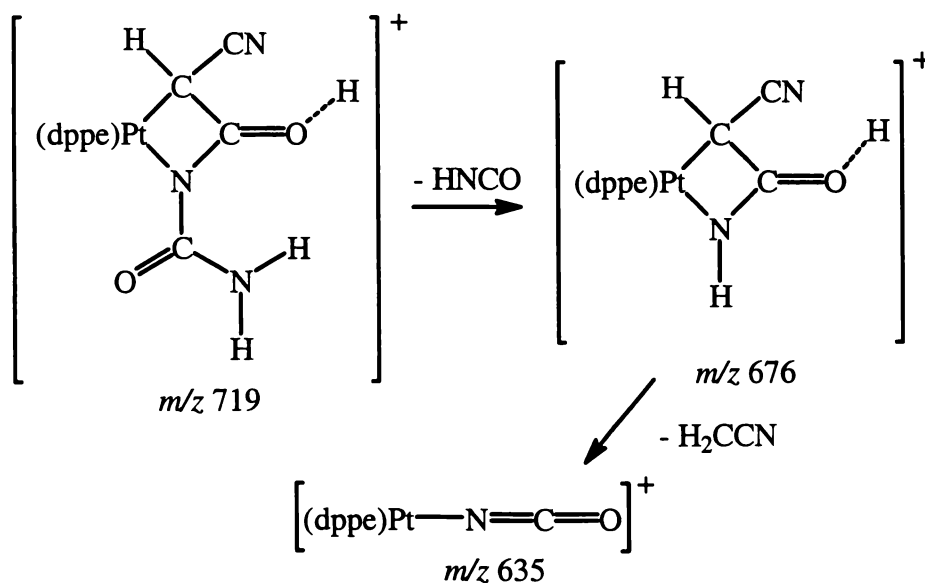
In the ^1H NMR spectrum of several of the compounds, (6.5, 6.8) a broad resonance, which has been assigned to the urea protons is observed (about δ 6.5). The urea proton resonance of the parent cyanoacetylurea was observed to be a small broad signal also, indicating that proton exchange with the deuterated solvent may be taking place. It is not unreasonable to presume that this too may occur with the metallacyclic complexes diminishing their strength.

The phosphorus NMR spectrum of the $[\text{Pt}\{\overline{\text{N}(\text{C}(\text{O})\text{NH}_2)\text{C}(\text{O})\text{CHCN}}\}(\text{PPh}_3)_2]$ (6.5) complex has the expected AB spin system characteristic of two magnetically inequivalent phosphorus atoms. The platinum satellites of these two doublets are indicative of the atom in the *trans* position. The smaller $^1J(\text{Pt}, \text{P})$ coupling constant (2543 Hz) observed for the doublet at δ 17.24 is in the expected range for a phosphorus atom *trans* to high *trans*-influence atom, for example carbon.¹⁻³ The larger $^1J(\text{Pt}, \text{P})$ coupling constant for the resonance at δ 11.78 (3742 Hz) is within the observed range of 3500 – 3800 Hz for phosphorus *trans* to nitrogen.^{1-3,11} As described earlier, the varying *trans*-influences that these atoms exert is also reflected in the Pt–P bond lengths.

6.3.4 Electrospray mass spectrometry

The metallalactams (**6.5** – **6.8**) are all easily characterised by electrospray mass spectrometry. At low cone voltages, a simple $[M+H]^+$ peak is observed. Some aggregation of the complexes is observed, usually seen as a small ($\sim 10\%$) $[2M+H]^+$ peak (Figure 6.3).

An interesting feature of these complexes, exemplified by the $[\text{Pt}\{\text{N}(\text{C}(\text{O})\text{NH}_2)\text{C}(\text{O})\text{CHCN}\}(\text{dppe})]$ (**M**) complex (**6.7**), is the degradation of these compounds. At low cone voltages (*ca* 20 V) only the parent $[M + H]^+$ peak (m/z 719) is observed. With increasing cone voltage (*ca* 50 V) the predominant peak is still the parent $[M + H]^+$ ion. Two degradation products begin to appear also, the first peak (m/z 676, 58%) is presumably due to loss of a neutral molecule (HNCO) and concomitant hydride migration to the lactam nitrogen (see Scheme 6.2). The second of these new peaks (m/z 635, 37%) is attributed to the loss of (H_2CCN). What is surprising is that at high cone voltages (*ca* 70 V) a high proportion of the parent $[M+H]^+$ ion still exists, as shown in Figure 6.3 below.



Scheme 6.2 Proposed fragmentation pathway for $[\text{Pt}\{\text{N}(\text{C}(\text{O})\text{NH}_2)\text{C}(\text{O})\text{CHCN}\}(\text{dppe})+\text{H}]^+$ (**6.7**)

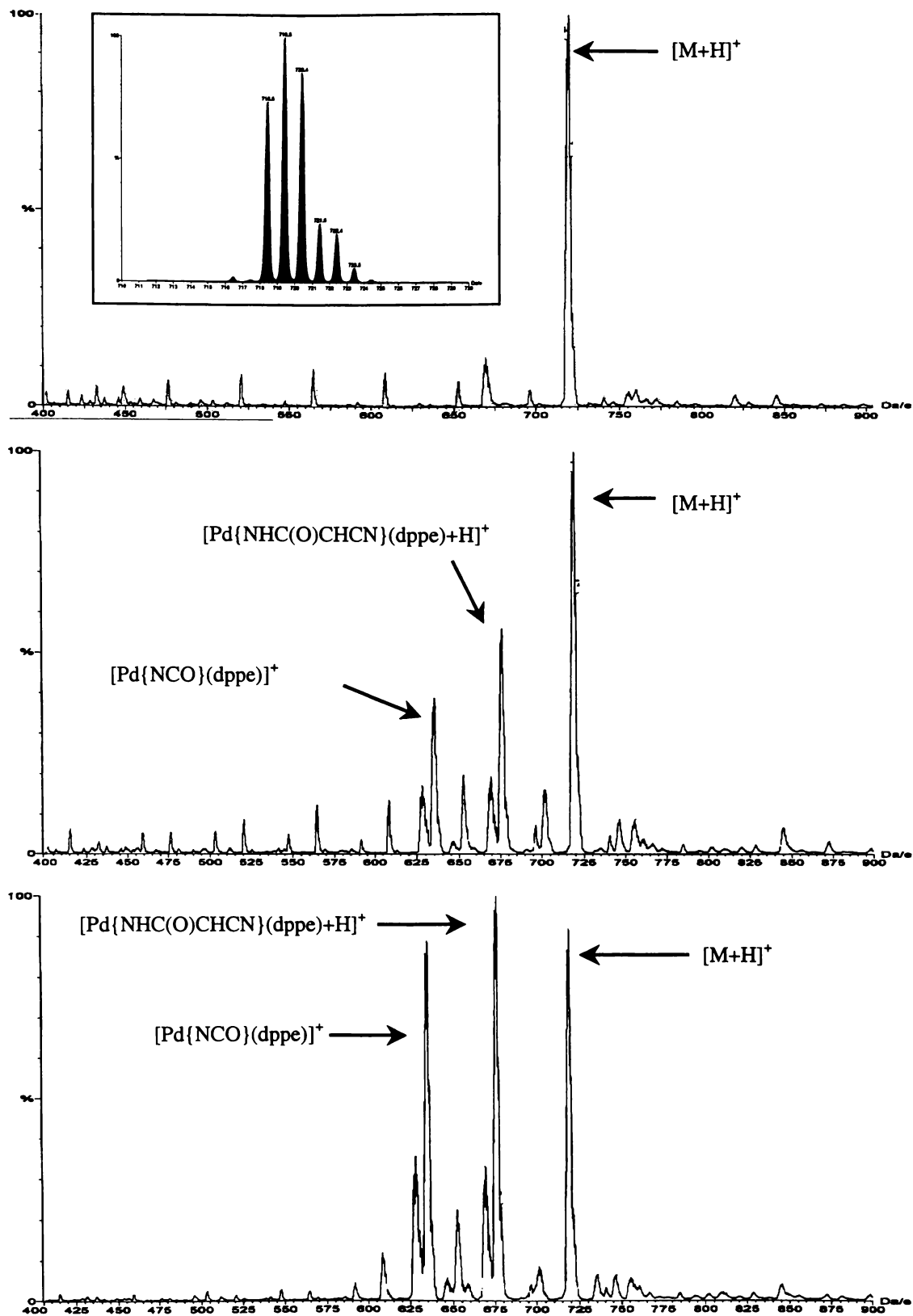


Figure 6.3 Fragmentation patterns of $[\text{Pt}\{\text{N}(\text{C}(\text{O})\text{NH}_2)\text{C}(\text{O})\text{CHCN}\}(\text{dppe})]$ at 20, 50 and 70 V

Inset shows high resolution isotope pattern of $[\text{Pt}\{\text{N}(\text{C}(\text{O})\text{NH}_2)\text{C}(\text{O})\text{CHCN}\}(\text{dppe})+\text{H}]^+$

6.4 Conclusion

Reaction of cyanoacetylurea with a variety of metal dihalide complexes, in the presence of triethylamine gave four-membered metallalactams of the type **6.1**. One of these complexes, $cis\text{-}[\text{Pt}\{\overbrace{\text{N}(\text{C}(\text{O})\text{NH}_2)\text{C}(\text{O})\text{CHCN}}\}(\text{PPh}_3)_2]$ (**6.5**), was successfully crystallised and characterised by a single crystal X-ray study. The crystal structure showed that the complex forms a dimer in the solid state, H-bonded via the urea hydrogens. Unfortunately attempts to further functionalise this complex met with failure. When compared to the reactivity of related ureylene complexes, the change of one of the ring heteroatoms from nitrogen to carbon greatly alters the reactivity of the complex towards small molecule insertion.

An interesting result of these studies is the successful synthesis of several well-characterised metallactam complexes in reactions mediated by triethylamine. The syntheses undertaken here indicate that the reaction proceeds more rapidly in the presence of triethylamine than it does in the presence of silver(I) oxide. While the reaction temperature is slightly higher in these experiments (methanol at reflux compared to dichloromethane at reflux for silver(I) oxide mediated syntheses), which will increase the reaction rate somewhat, it appears that triethylamine is an excellent alternative to silver(I) oxide for small-ring metallacycle synthesis reactions.

Electrospray mass spectrometry provided an interesting insight into the nature of this particular functionalised metallalactam. One of the proposed degradation products is an unsubstituted metallalactam (with respect to the lactam nitrogen). This indicated that an unsubstituted metallalactam could be successfully synthesised. Several attempts were made at synthesising a nitrogen-unsubstituted metallalactam from acetoacetamide [$\text{NH}_2\text{C}(\text{O})\text{CH}_2\text{C}(\text{O})\text{CH}_3$] (described in chapter two) which met with mixed results. However silver(I) oxide was used as a reaction mediator in those instances, perhaps triethylamine may prove to be more successful.

Chapter Seven. Selected X-ray crystallographic studies

7.1 Overview

The following crystallographic reports are included as part of the ongoing research at the University of Waikato in the field of metallacyclic syntheses. The complexes branch out slightly from those described in previous chapters. Predominantly the previous chapters covered the synthesis and characterisation of metallalactam complexes derived from amides, the compounds presented here have different organic ligands bonded to the metal.

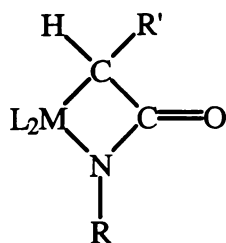
Four crystal structure studies of a selection of compounds are described. The first discussion is the structural characterisation of an iridaureylene complex. The second report details two dimeric complexes, which incorporate thiosalicylate as the coordinating ligand. Finally, the structure of a novel uranyl nitrate / platinum bis(lactam) complex is described. While these complexes were synthesised by other researchers, the structural elucidation is part of this work.

7.2 Ureylene complex

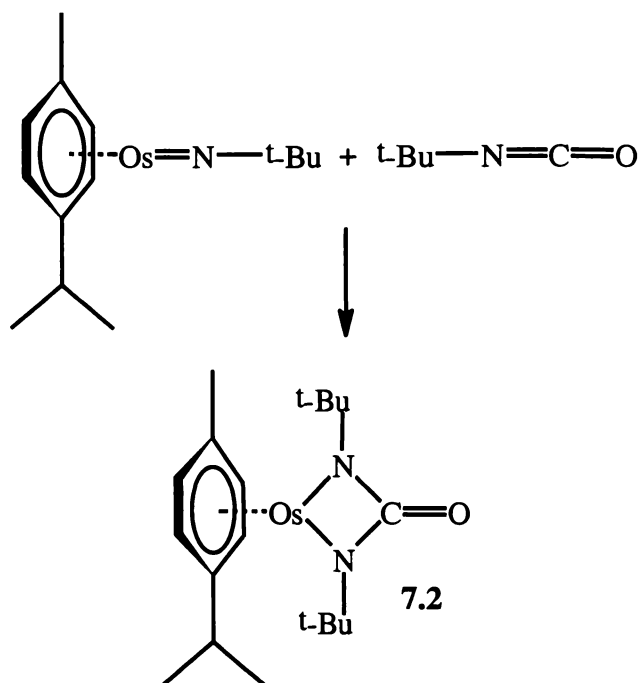
Ureylene complexes are isoelectronic with the previously described metallalactam complexes (7.1).¹ However, they differ structurally in that two nitrogen atoms are present in the heterocycle. As outlined earlier (Chapter One), a wide variety of ureylene complexes have been synthesised and characterised, covering most of the transition series. For example the cycloaddition of an organic isocyanate into a metal imido bond will form a four-membered ureylene complex (7.2).²

1 See for example: a) W. Henderson, J. Fawcett, R. D. W. Kemmitt, C. Proctor and D. R. Russell, *J. Chem. Soc., Dalton Trans.*, (1994), 3085; b) W. Henderson, A. G. Oliver and B. K. Nicholson, *J. Chem. Soc., Dalton Trans.*, (1994), 1831; c) W. Henderson, A. G. Oliver, L.-J. Baker and C. E. F. Rickard, *Inorg. Chim. Acta.*, (1999), **292**, 260

2 R. I. Michelman, R. G. Bergman and R. A. Anderson, *Organometallics*, (1993), **12**, 2741



7.1



7.2

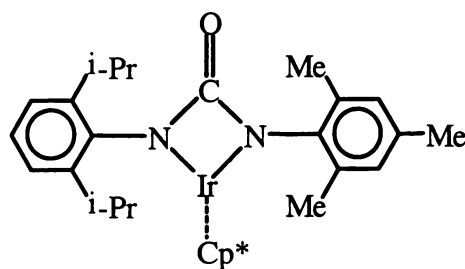
Recently, silver(I) oxide was found to promote the synthesis of ureylene complexes³ with platinum dihalide compounds, in a manner similar to that of the metallalactam complexes described previously. A wide range of these ureylene complexes were synthesised, and studies on their reactivity undertaken.⁴ Ureylene complexes have displayed quite high reactivity, and several derivatives, formed from insertion of small molecules into the ring have been successfully synthesised and characterised structurally.

This report describes the structure of an iridaureylene complex, similar to previously described platina and palladaureylenes.³ One other iridaureylene complex (7.3) has

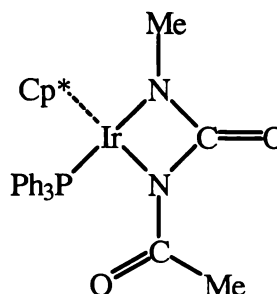
3 M. B. Dinger, W. Henderson, B. K. Nicholson and A. L. Wilkins, *J. Organomet. Chem.*, (1996), **526**, 503

4 M. B. Dinger and W. Henderson, *J. Chem. Soc., Dalton Trans.*, (1998), 1763

been described previously, however, the accuracy of that complex was rather low ($R_1 = 0.0762$).⁵ The iridium centre in that structure was however, coordinatively unsaturated.



7.3



7.4

7.3 Synthesis and structural data for $[\text{Ir}\{\text{N}(\text{Me})\text{C}(\text{O})\text{NAc}\}(\text{Cp}^*)(\text{PPh}_3)]$ (7.4)

The complex $[\text{Ir}\{\text{N}(\text{Me})\text{C}(\text{O})\text{NAc}\}(\text{Cp}^*)(\text{PPh}_3)]$ (7.4), was synthesised by Maarten Dinger, during the course of his doctoral studies. $[\text{IrCl}_2(\text{Cp}^*)(\text{PPh}_3)]$ was reacted with one equivalent of *N*-acetyl *N'*-methylurea in the presence of silver(I) oxide in dichloromethane and heated at reflux for 2 h. Silver salts were removed by filtration affording a yellow solution, the solvent was removed under reduced pressure, giving a pale orange solid. Crystals of single crystal X-ray quality were grown from a chloroform / diethyl ether solution by slow evaporation. Accurate X-ray intensity data were collected at the University of Auckland. Cell, data collection and final cycle parameter information are tabulated (Table 7.1) below.

The X-ray intensity data were corrected for Lorentz and polarisation effects and an empirical absorption correction applied by comparison of intensities of equivalent reflections.⁶ Atoms not found in the initial Fourier map were located from successive electron density difference maps. Refinement of the model was by full-matrix least-squares analysis against F^2 . All non-hydrogen atoms were assigned anisotropic thermal parameters and hydrogen atoms included as riding models. Methyl hydrogen atoms were allowed free rotation about the C–X bond and assigned thermal parameters 50%

5 A. A. Danopoulos, G. Wilkinson, T. K. N. Sweet and M. B. Hursthouse, *J. Chem. Soc., Dalton Trans.*, (1996), 3771

greater than that of the carrier atom. All other hydrogen atoms were placed geometrically and allowed to ride on the carrier atom with thermal parameters 20% greater than that of the carrier atom. The largest residual peak ($1.55 \text{ e.}\text{\AA}^{-3}$) in the difference Fourier map was located 1.37 \AA from C(13).

Table 7.1 Crystal data and structure refinement for
 $[\text{Ir}\{\text{N}(\text{Me})\text{C}(\text{O})\text{NAc}\}(\text{Cp}^*)(\text{PPh}_3)].\text{CHCl}_3$ (**7.4**).

<i>Crystal data</i>	
Empirical formula	$\text{C}_{32}\text{H}_{36}\text{IrN}_2\text{O}_2\text{P}.\text{CHCl}_3$
Formula weight	823.17
Crystal system	Monoclinic
Space group	$\text{P2}_1/\text{n}$
Unit cell dimensions	
a (Å)	12.5471(2)
b (Å)	17.0445(1)
c (Å)	16.7432(3)
β (°)	111.060(1)
Volume (Å ³)	3341.51(8)
Z	4
D(c) (g cm ⁻³)	1.636
<i>Data Collection</i>	
Diffractometer	Siemens SMART CCD
Radiation	Mo-K α
Wavelength (Å)	0.71073
Temperature (K)	203(2)
Crystal size (mm)	0.39 x 0.36 x 0.12
θ range for data collection (°)	1.76 to 27.43
Index ranges	$-15 \leq h \leq 14$ $0 \leq k \leq 22$ $0 \leq l \leq 21$
Reflections collected	19310

Independent reflections	7308 [R(int) = 0.0284]
Absorption coefficient (mm ⁻¹)	4.316
Maximum transmission	0.6255
Minimum transmission	0.2839
F(000)	1632

Structure analysis and refinement

Solution by	Direct methods
Refinement method	Full-matrix least-squares on F^2
Data / restraints / parameters	7308 / 0 / 386
Goodness-of-fit on F^2	1.067
Final R indices [$I > 2\sigma(I)$]	$R_1 = 0.0281$, $wR^2 = 0.0606$
R indices (all data)	$R_1 = 0.0397$, $wR^2 = 0.0664$
Weighting Scheme:	$w = 1/[\sigma^2(F_o^2) + (0.0215P)^2 + 5.8390P]$ where $P = (F_o^2 + 2F_c^2)/3$
Largest difference peak (e.Å ⁻³)	1.549
Largest difference hole (e.Å ⁻³)	-1.037
Programs used	
Solution by	SHELXS-97 ⁷
Refinement by	SHELXL-97 ⁸

7.4 Structural analysis of the iridaureylene complex $[\text{Ir}\{\text{N}(\text{Me})\text{C}(\text{O})\text{NAc}\}(\text{Cp}^*)(\text{PPh}_3)]$ (7.4)

The crystal structure of $[\text{Ir}\{\text{N}(\text{Me})\text{C}(\text{O})\text{NAc}\}(\text{Cp}^*)(\text{PPh}_3)]$ (Figure 7.1) shows that the molecule has adopted a pseudo-octahedral geometry, with the Cp* ligand facially coordinated, occupying three coordination sites. The triphenylphosphine and the ureylene ring occupy the three remaining coordination sites. One chloroform co-crystallises in the lattice, hydrogen-bonded to O(1) [C(50).....O(1) 2.958(6) Å].

⁷ G. M. Sheldrick, SHELXS-97, *Program for the solution of single crystal X-ray structures*, (1997), Universität Göttingen, Germany

⁸ G. M. Sheldrick, SHELXL-97, *Program for the refinement of single crystal X-ray structures*, (1997), Universität Göttingen, Germany

Structurally the four-membered ring system is similar to the previously described metallalactam rings and is, predictably, highly planar [largest deviation from the Ir, N(1), N(2), C(1) mean plane is 0.022(2) Å for C(1)]. As with many of these four-membered ring complexes which incorporate nitrogen in the ring, little folding is observed through the ring. In this case the ring dihedral angle is only 3.5(5)°.

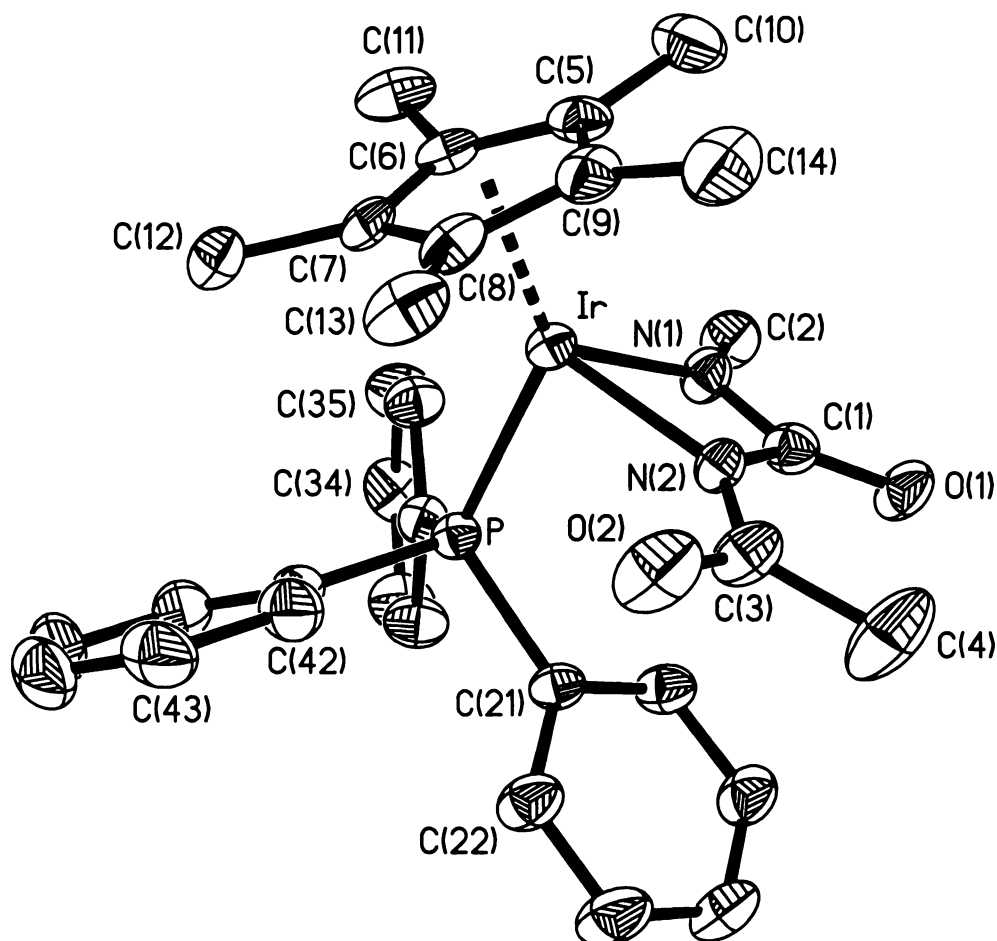


Figure 7.1 Molecular structure of $[\text{Ir}\{\text{N}(\text{Me})\text{C}(\text{O})\text{NAc}\}(\text{Cp}^*)(\text{PPh}_3)]$ (7.4).

Thermal displacement ellipsoids are shown at 50% probability. Hydrogen atoms and chloroform of crystallisation omitted for clarity.

The iridium has the expected pseudo-octahedral geometry, and is, within experimental limits, equally coordinated to the Cp* ligand [Ir–C(Cp*) bond length range 2.210(4) to 2.223(4) Å]. The Ir–N bond lengths are comparable with one another [Ir–N(1) 2.092(3) and Ir–N(2) 2.079(3) Å], though the substituents on these atoms differ quite considerably (methyl compared to acetyl). In contrast, these bonds are significantly

longer than those for the previously reported iridaureylene [1.92(2) and 2.03(2) Å].⁵ This difference may arise because the complex presented here, $[\text{Ir}\{\text{N}(\text{Me})\text{C}(\text{O})\text{NAc}\}(\text{Cp}^*)(\text{PPh}_3)]$, is coordinatively saturated, while the previous example was not. A bond length of 2.300(1) Å is normal for an iridium phosphorus bond.

Table 7.2 Selected bond lengths (Å) and angles (°) for $[\text{Ir}\{\text{N}(\text{Me})\text{C}(\text{O})\text{NAc}\}(\text{Cp}^*)(\text{PPh}_3)]$ (7.4).

Ir–N(2)	2.079(3)	Ir–N(1)	2.092(3)
Ir–P	2.300(1)	N(1)–C(1)	1.348(5)
N(1)–C(2)	1.429(5)	N(2)–C(1)	1.413(5)
N(2)–C(3)	1.349(5)	O(1)–C(1)	1.250(5)
O(2)–C(3)	1.236(5)	C(3)–C(4)	1.512(6)
Ir–C(8)	2.210(3)	Ir–C(6)	2.210(4)
Ir–C(9)	2.216(4)	Ir–C(7)	2.222(3)
Ir–C(5)	2.223(4)	P–C(21)	1.833(4)
P–C(31)	1.832(4)	P–C(41)	1.825(4)
N(2)–Ir–N(1)	62.1(1)	N(2)–Ir–P	88.8(1)
N(1)–Ir–P	87.8(1)	C(1)–N(1)–C(2)	123.8(3)
C(1)–N(1)–Ir	98.5(2)	C(2)–N(1)–Ir	137.7(3)
C(3)–N(2)–Ir	132.6(3)	C(1)–N(2)–Ir	97.0(2)
C(3)–N(2)–C(1)	129.9(3)	O(1)–C(1)–N(1)	128.3(4)
N(1)–C(1)–N(2)	102.3(3)	O(1)–C(1)–N(2)	129.5(4)
O(2)–C(3)–N(2)	121.3(4)	O(2)–C(3)–C(4)	120.6(4)
N(2)–C(3)–C(4)	118.1(4)	C(21)–P–Ir	115.8(1)
C(31)–P–Ir	114.6(1)	C(41)–P–Ir	114.2(1)

The methyl groups of the pentamethyl cyclo-pentadienyl ligand are not co-planar with the cyclo-pentadienyl ring. Indeed, three of the methyl groups [C(11), C(12) and C(13)] lie well above the mean plane [0.243(7), 0.171(7) and 0.141(7) Å, successively]. This distortion may be due to steric interaction with the triphenylphosphine ligand, over which these three atoms are oriented.

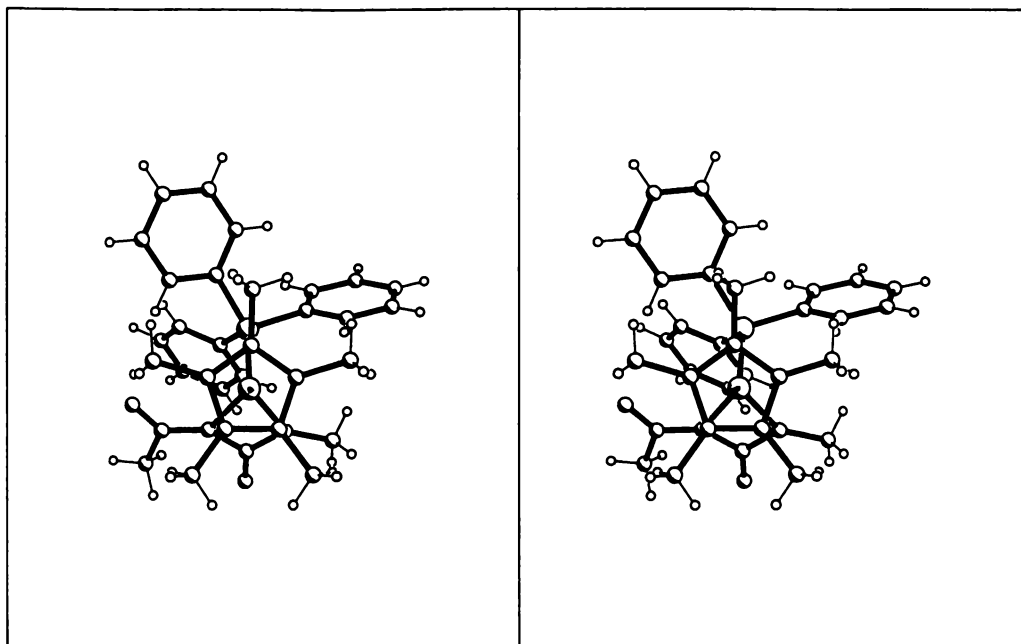


Figure 7.2 Stereoscopic view of $[\text{Ir}\{\text{N}(\text{Me})\text{C}(\text{O})\text{NAc}\}(\text{Cp}^*)(\text{PPh}_3)]$ (7.4) showing steric interactions.

Like many of these four-membered metallacycles, the bond angle at the metal is acute $[\text{N}(1)\text{--Ir--N}(2) 62.1(1)^\circ]$, as the metal can readily accommodate this distortion and allow an easing of strain throughout the rest of the metallacycle. The ureylene N–C bond lengths are quite disparate; N(1)–C(1) is longer $[1.413(5) \text{ \AA}]$ than N(2)–C(1) $[1.348(5) \text{ \AA}]$. This difference is presumably due to the different electronegativities of the groups bonded to these nitrogen atoms. Conjugation of the bonds about the four-membered ring may also be a factor in the observed differences in the bond lengths.

The orientation of the substituents on the ureylene ring is of note, the methyl group, C(2), is bent away from the iridium as reflected in the Ir–N(1)–C(2) bond angle of $137.7(3)^\circ$, though a similar distortion was observed by Danopoulos *et al.* $[\text{Ir--N--C}(\text{Ar}) 147(2) \text{ and } 138.1(4)^\circ]$.⁵ The ring interior nitrogen angles are also quite distorted from the ideal trigonal angle of 120° , and are nearly identical at $98.5(2)$ and $97.0(2)^\circ$ for C(1)–N(1)–Ir and C(1)–N(2)–Ir, respectively. The remaining interior angle $[\text{N}(1)\text{--C}(1)\text{--N}(2); 102.3(3)^\circ]$ shows that the sp^2 hybridised C(1) has undergone a slight distortion also.

The orientation of the acetyl functionality is interesting, with the carbonyl oxygen oriented *anti* to the lactam carbonyl, though it is slightly tilted with respect to the plane of the lactam [C(1)–N(2)–C(3)–O(2) dihedral angle $-171.7(4)^\circ$]. Steric interactions with the triphenylphosphine are presumably the cause of this slight rotation. It is interesting to note that the structures of the two metallalactam complexes which have a carbonyl containing functionality bonded to the ring nitrogen, $[\text{Pt}\{\text{N}(\text{CO}_2\text{Et})\text{C}(\text{O})\text{CHCN}\}(\text{COD})]^{1b}$ (7.1, $L_2 = \text{COD}$, $R = \text{CO}_2\text{Et}$, $R' = \text{CN}$) and *cis*- $[\text{Pt}\{\text{N}(\text{C}(\text{O})\text{NH}_2)\text{C}(\text{O})\text{CHCN}\}(\text{PPh}_3)_2]$ (7.1, $L = \text{PPh}_3$, $R = \text{C}(\text{O})\text{NH}_2$, $R' = \text{CN}$) (Chapter Six), also have the carbonyl oriented *anti* to the ring carbonyl. The slightly prolate nature of C(4) indicates that some thermal libration occurs about the C(3)–C(4) bond, however, the distortion is not significant enough to warrant any corrections to the positional parameters of C(4).

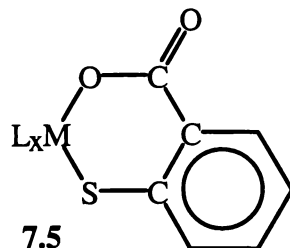
In summary, presented here is the first example of a coordinatively unsaturated iridaureylene complex. The ureylene ring system is similar to that of a previously reported coordinatively unsaturated iridaureylene, however, some differences; notably the Ir–N bond lengths, do appear. The complex is structurally analogous to previously reported platina and palladaureylene complexes.^{3,4}

7.5 Introduction to metal-thiosalicylate complexes

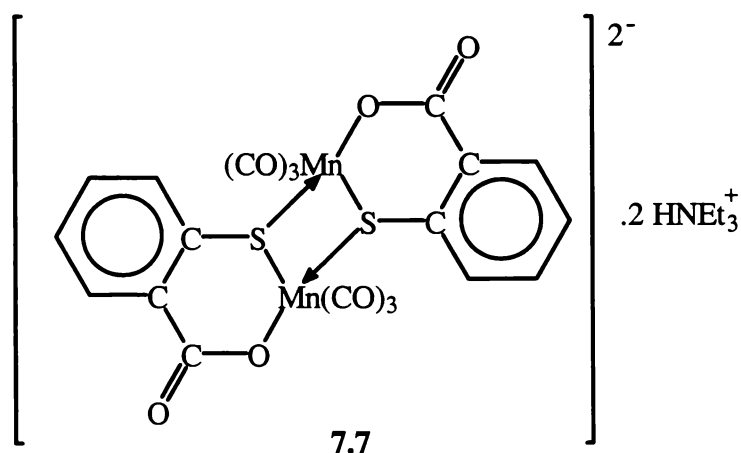
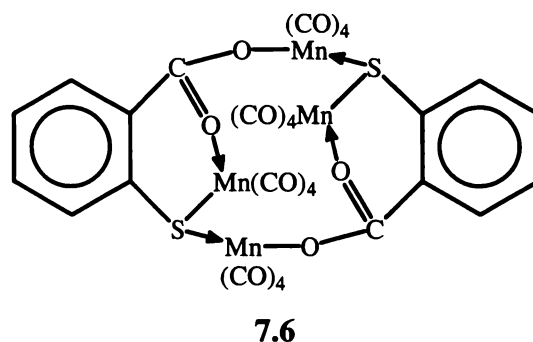
Metallacyclic complexes incorporating thiosalicylate as a ligand are well known.⁹ Predominantly, the metals are first row transition elements and the complexes formed are a simple monomeric species (7.5). Recently, silver(I) oxide has been found to promote the synthesis of late transition metal thiosalicylate complexes, which also have a monomeric structure similar to that of their first row counterparts.¹⁰

9 See for example: a) J. S. Baskin, J. C. Huffman and G. Christou, *J. Am. Chem. Soc.*, (1986), **108**, 5038; b) J. Li-Kao, O. Gonzalez, R. F. Baggio, M. T. Garland and D. Carillo, *Acta Crystallogr., Section C*, (1995), **C51**, 575; c) J. Li-Kao, O. Gonzalez, R. F. Baggio, M. T. Garland and D. Carillo, *Acta Crystallogr., Section C*, (1995), **C51**, 2486; d) K. Hegetschweiler, T. Keller, M. Baumle, G. Rihs and W. Schneider, *Inorg. Chem.*, (1991), **30**, 4342

10 a) L. J. McCaffrey, W. Henderson, B. K. Nicholson, J. E. Mackay and M. B. Dinger, *J. Chem. Soc., Dalton Trans.*, (1997), 2577; b) L. J. McCaffrey, W. Henderson and B. K. Nicholson, *Polyhedron*, (1998), 201



Two interesting results were observed during a course of study into the reactivity of *ortho*-aryl manganese carbonyl complexes. The first was that orthomanganated *N,N*-dimethylbenzylamine was found to react with SO_2 , giving a large polycyclic structure incorporating four manganese centres (7.6).¹¹ The other result, was that bromo manganese pentacarbonyl was found to react with thiosalicylic acid in the presence of triethylamine to give a novel dimeric complex (7.7).¹¹



The following two crystal structures are the rhodium and ruthenium analogues of the dimeric manganese thiosalicylate complex described above. However, they carry an overall neutral charge, while the manganese compound is an anionic species. The structures of these two compounds were solved as part of the ongoing research at

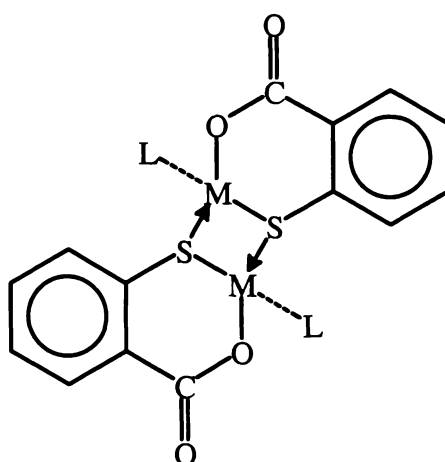
¹¹ C. V. Depree, L. Main, B. K. Nicholson and K. Roberts, *J. Organomet. Chem.*, (1996), **517**, 201

the University of Waikato into the synthesis and characterisation of metallacyclic complexes of the platinum group metals.

7.6 Synthesis of thiosalicylato complexes

$[\text{Rh}\{\text{OC}(\text{O})\text{C}_6\text{H}_4\text{-2-S}\}(\text{Cp}^*)]_2$ (7.8) was synthesised by Dr. W. Henderson at the University of Waikato. $[\text{Rh}(\text{Cp}^*)\text{Cl}_2]_2$ was reacted with two equivalents of thiosalicylic acid in the presence of silver(I) oxide in dichloromethane heated at reflux. Silver salts were removed by filtration affording a red solution, from which solvent was removed under reduced pressure. Crystals of X-ray diffraction quality were grown by vapour diffusion of diethyl ether into a dichloromethane solution of $[\text{Rh}\{\text{OC}(\text{O})\text{C}_6\text{H}_4\text{-2-S}\}(\text{Cp}^*)]_2$.

$[\text{Ru}\{\text{OC}(\text{O})\text{C}_6\text{H}_4\text{-2-S}\}(p\text{-cymene})]_2$ (7.9) was synthesised by Dr. W. Henderson at the University of Waikato. The complex $[\text{RuCl}_2(p\text{-cymene})]_2$ was reacted with two equivalents of thiosalicylic acid in the presence of triethylamine in methanol at reflux. The product was precipitated by the addition of water to the hot reaction mixture and collected by filtration. Crystals for single crystal analysis were grown by vapour diffusion of diethyl ether into a dichloromethane solution of (7.9).



7.8 M = Rh, L = Cp*

7.9 M = Ru, L = *p*-cymene

Accurate X-ray intensity data were collected at the University of Auckland on a Siemens SMART CCD diffractometer. The structures were both solved by Patterson methods and refined against F^2 . All non-hydrogen atoms were located from successive

electron density maps and allowed anisotropic thermal motion parameters. Methyl hydrogen atoms were included in calculated positions and allowed free-rotation about the C–X bond, with thermal parameters restrained to be 50% greater than U_{iso} of the atom to which they were bonded. All other hydrogen atoms were placed geometrically, with thermal parameters riding on the carrier atom and tied to be 20% greater than the U_{iso} of the carrier atom. Table 7.3 summarises the data collection, solution and final cycle refinement for $[\text{Rh}\{\text{OC}(\text{O})\text{C}_6\text{H}_4\text{-2-S}\}(\text{Cp}^*)]_2$ (7.8) and $[\text{Ru}\{\text{OC}(\text{O})\text{C}_6\text{H}_4\text{-2-S}\}(\text{p-cymene})]_2$ (7.9)

Table 7.3 Data collection and cell parameters for $[\text{Rh}\{\text{OC}(\text{O})\text{C}_6\text{H}_4\text{-2-S}\}(\text{Cp}^*)]_2$ (7.8) and $[\text{Ru}\{\text{OC}(\text{O})\text{C}_6\text{H}_4\text{-2-S}\}(\text{p-cymene})]_2$ (7.9)

<i>Crystal data</i>	7.8	7.9
Empirical formula	$\text{C}_{34}\text{H}_{28}\text{O}_4\text{Rh}_2\text{S}_2$	$\text{C}_{34}\text{H}_{36}\text{O}_4\text{Ru}_2\text{S}_2$
Formula weight	770.50	774.89
Crystal system	Monoclinic	Monoclinic
Space group	$\text{P2}_1/\text{n}$	$\text{P2}_1/\text{c}$
Unit cell dimensions		
a (Å)	11.3821(2)	9.6046(1)
b (Å)	10.2707(2)	12.8655(2)
c (Å)	13.4726(2)	12.4167(1)
β (°)	99.658(1)	105.819(1)
V (Å ³)	1552.65(5)	1476.20(3)
Z	4	2
$D(\text{c})$ (g cm ⁻³)	1.648	1.743
<i>Data Collection</i>		
Diffractometer	Siemens SMART CCD	Siemens SMART CCD
Radiation	Mo-K α	Mo-K α
Wavelength (Å)	0.71073	0.71073
Temperature (K)	203(2)	203(2)
Crystal size (mm)	0.28 x 0.20 x 0.07	0.40 x 0.18 x 0.07
θ range for data collection (°)	2.17 to 28.21	2.20 to 28.21
Index ranges	$-15 \leq h \leq 14$ $0 \leq k \leq 12,$	$-12 \leq h \leq 11$ $0 \leq k \leq 16,$

	$0 \leq l \leq 17$	$0 \leq l \leq 15$
Reflections collected	9585	9217
Independent reflections	3443 [R(int) = 0.0288]	3301 [R(int) = 0.0161]
Absorption coefficient (mm ⁻¹)	1.234	1.204
Maximum transmission	0.9186	0.9205
Minimum transmission	0.7238	0.6445
F(000)	772	784

*Structure analysis and
refinement*

Solution by	Patterson	Patterson
Refinement method	Full-matrix least-squares on F^2	Full-matrix least-squares on F^2
Data / restraints / parameters	3443 / 0 / 195	3301 / 0 / 194
Goodness-of-fit on F^2	1.078	1.029
Final R indices [$I > 2\sigma(I)$]	$R_1 = 0.0340,$ $wR^2 = 0.0738$	$R_1 = 0.0186,$ $wR^2 = 0.0471$
R indices (all data)	$R_1 = 0.0508,$ $wR^2 = 0.0814$	$R_1 = 0.0221,$ $wR^2 = 0.0482$
Weighting Scheme:	$w = 1/[\sigma^2(F_o^2) +$ $(0.0299P)^2 + 2.3859P]$ where $P = (F_o^2 + 2F_c^2)/3$	$w = 1/[\sigma^2(F_o^2) +$ $(0.0245P)^2 + 0.7557P]$ where $P = (F_o^2 + 2F_c^2)/3$
Extinction coefficient		0.00026(19)
Largest difference peak (e.A ⁻³)	0.605	0.365
Largest difference hole (e.A ⁻³)	-0.601	-0.380
Programs used		
Solution by	SHELXS-97 ⁷	SHELXS-97 ⁷
Refinement by	SHELXL-97 ⁸	SHELXL-97 ⁸

7.7 Discussion of rhodium and ruthenium thiosalicylate complexes

The two thiosalicylate structures are dimeric compounds and have adopted a distorted octahedral geometry, similar to that observed for the manganese complex 7.7. The coordinating ligand (Cp* or *p*-cymene) occupies a facial position of the octahedron, which in the manganese complex was occupied by three carbonyl ligands. The thiosalicylate ligand is coordinated such that it forms a six-membered heterocycle, bonded through the thiol sulfur and one of the carboxylate oxygen atoms to the metal. Formally the thiosalicylate ligand carries a 2⁻ charge, and the thiol sulfur is three-coordinate and bridges the two metal centres, completing the dimer.

7.7.1 Rhodium thiosalicylate complex

The single crystal X-ray structure of $[\text{Rh}\{\text{OC}(\text{O})\text{C}_6\text{H}_4\text{-2-S}\}(\text{Cp}^*)]_2$ (7.8) (Figure 7.3), shows that the complex has adopted a distorted octahedral or “bar-stool” geometry. The dimer has crystallised across the inversion centre at 0.5, 0.5, 0. Selected bond lengths and angles are summarised in Table 7.4. The coordinated thiosalicylate ligand forms a six-membered heterocycle with the rhodium. The folding of this ring predominantly occurs at the rhodium and the carboxylate, as seen from the obtuse Rh–O(1)–C(1) bond angle of 133.1(2)°. A conformational analysis of the torsion angle about the carboxylate with respect to the thiosalicylate benzene ring, shows that there is considerable twist about the C(2)–C(1) bond [torsion angle for C(3)–C(2)–C(1)–O(1) 31.4(5)°]. If the carboxylate functionality was co-planar with the benzene ring, a torsion angle of zero degrees would be expected. As might be expected the thiol sulfur is unequally coordinated to the two rhodium atoms, as seen in the different Rh–S bond lengths [Rh–S 2.350(1) Å compared to Rh–S’ 2.406(1) Å]. The Rh–S–Rh’ bond angle of 97.32(3)° is slightly larger than, though still comparable with, the manganese analogue 7.7 [Mn–S–Mn’ 96.56(4)°].¹¹ This fractional increase does not extend to the S–M–S’ bond angles [82.68(3)° for S–Rh–S compared to 83.44(4)° for S–Mn–S’], while the O–M–S bond angles are very similar [88.63(7)° for the rhodium complex and 88.2(7)° for the manganese analogue 7.7]. The acute O–M–S’ bond angles [O–Rh–S’ 77.97(7) compared to O–Mn–S’ 80.21(6)°] reflect the fact that rhodium can adopt a slightly more strained octahedral geometry than manganese. The M–S bonds for both the rhodium and the manganese complexes are, surprisingly, identical [Rh–S 2.350(1) and Mn–S

2.351(1) Å; Rh–S' 2.406(1) and Mn–S' 2.406(1) Å]. However, the M–O bonds for the two complexes differ slightly [Rh–O 2.084(2) versus Mn–O 2.031(2) Å]. The significant difference between these two complexes (rhodium and manganese) is that the manganese complex is a charged species, while the rhodium complex has an overall neutral charge.

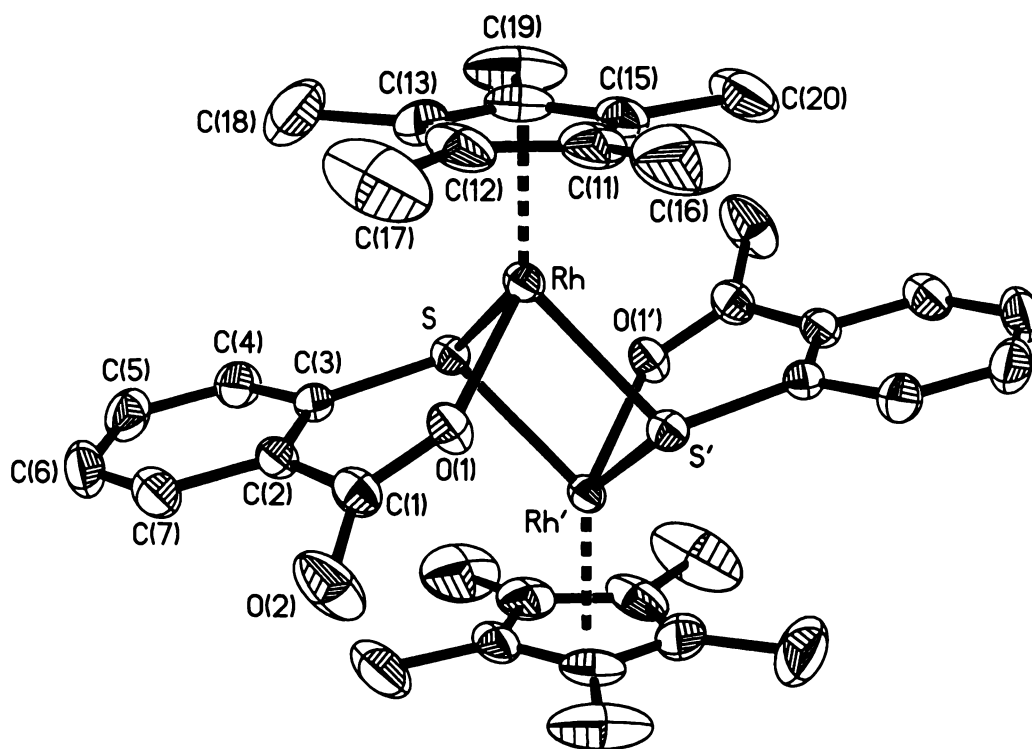


Figure 7.3 Thermal ellipsoid plot of $[\text{Rh}\{\text{OC}(\text{O})\text{C}_6\text{H}_4\text{-2-S}\}(\text{Cp}^*)]_2$ (7.8) showing molecular geometry and labelling scheme.

Thermal displacement ellipsoids are depicted at 50% probability. Hydrogen atoms are omitted for clarity.

The cyclopentadienyl ring lies almost equidistant from the rhodium, as reflected by the Rh–C bond length range of 2.144(4) to 2.186(4) Å. The methyl groups of the ligand are slightly distorted with respect to the mean plane of the cyclopentadienyl ring, C(17) and C(18) are almost coplanar with the ring [0.046(8) and 0.019(8) Å, respectively]. However C(16), C(19) and C(20) lie 0.110(8), 0.090(9) and 0.121(7) Å above the mean plane. This distortion is reflected in the Rh–C bond lengths, with C(11) [bonded to C(16)], having the longest at 2.186(4) Å. This slight tilt may arise from steric interactions with the thiosalicylate ligand.

Table 7.4 Selected bond lengths (Å) and bond angles (°) for $[\text{Rh}\{\text{OC}(\text{O})\text{C}_6\text{H}_4\text{-2-S}\}(\text{Cp}^*)]_2$ (7.8).

Rh–O(1)	2.084(2)	Rh–C(13)	2.144(4)
Rh–C(14)	2.155(4)	Rh–C(15)	2.158(4)
Rh–C(12)	2.173(4)	Rh–C(11)	2.186(4)
Rh–S	2.350(1)	Rh–S'	2.406(1)
S–C(3)	1.778(4)	S–Rh'	2.406(1)
O(1)–C(1)	1.278(4)	O(2)–C(1)	1.233(5)
C(1)–C(2)	1.511(5)	C(2)–C(3)	1.407(5)
C(2)–C(7)	1.411(5)	C(3)–C(4)	1.395(5)
C(4)–C(5)	1.380(5)	C(5)–C(6)	1.379(6)
C(6)–C(7)	1.370(6)		
O(1)–Rh–S	88.63(7)	O(1)–Rh–S'	77.97(7)
S–Rh–S'	82.68(3)	C(3)–S–Rh	103.82(12)
C(3)–S–Rh'	116.11(11)	Rh–S–Rh'	97.32(3)
C(1)–O(1)–Rh	133.1(2)	O(2)–C(1)–O(1)	121.3(4)
O(2)–C(1)–C(2)	117.2(3)	O(1)–C(1)–C(2)	121.5(3)
C(3)–C(2)–C(7)	117.8(3)	C(3)–C(2)–C(1)	125.4(3)
C(7)–C(2)–C(1)	116.7(3)	C(4)–C(3)–C(2)	119.7(3)
C(4)–C(3)–S	115.0(3)	C(2)–C(3)–S	125.3(3)
C(5)–C(4)–C(3)	120.9(4)	C(4)–C(5)–C(6)	119.9(4)
C(7)–C(6)–C(5)	120.2(4)	C(6)–C(7)–C(2)	121.5(4)

7.7.2 Ruthenium thiosalicylato complex

The ruthenium thiosalicylate complex $[\text{Ru}\{\text{OC}(\text{O})\text{C}_6\text{H}_4\text{-2-S}\}(p\text{-cymene})]_2$ (7.9) is comparable with the rhodium structure described above. The complex has a similar configuration of atoms, with the neutrally coordinating *p*-cymene bonded facially to the octahedral ruthenium. The thiosalicylate ligand is bonded in two of the three remaining vacant coordination sites, and a bond to the bridged sulfur of the dimeric partner occupies the third coordination site (Figure 7.4). The molecule has crystallised about the inversion centre at 0.5, 1, 0.

Though the metal centres of these two complexes are from different groups of the transition series, they are isoelectronic and the bond lengths about the metal are comparable and not significantly different with respect to each other. For example the Ru–O(1) bond length [2.093(1) Å] is comparable with, if fractionally longer than the Rh–O(1) bond of 2.084(2) Å. As with the rhodium compound described above, the metal does not bond equidistantly to the coordinated ligand (in this case *p*-cymene). A comparison of the Ru–C(*p*-cymene) bond lengths shows that the shortest is 2.165(2) Å for Ru–C(11), ranging to 2.264(4) Å for Ru–C(9). An analysis about a centroid of the *p*-cymene phenyl ring indicates that the ruthenium lies almost directly under the centre of the ring.

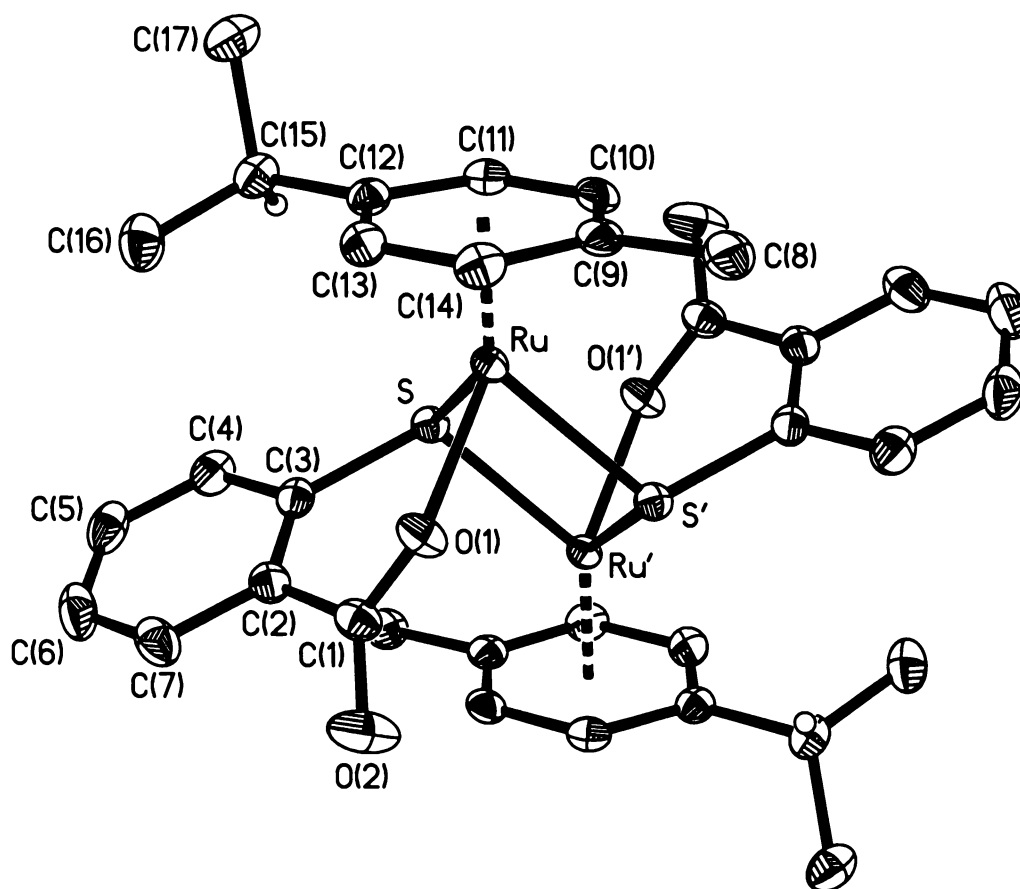


Figure 7.4 Thermal ellipsoid plot of $[\text{Ru}\{\text{OC}(\text{O})\text{C}_6\text{H}_4\text{-2-S}\}(p\text{-cymene})_2]$ (7.9) showing the atom labelling scheme.

Thermal displacement ellipsoids are shown at 50% probability and all hydrogen atoms [except H(15a) and H(15a')] have been omitted for clarity.

The primary difference between the geometries of these two complexes is the inclination angle of the thiosalicylate ligand. With the planar coordinating ligand (Cp*

or *p*-cymene) as a reference, both of which occupy an apical position in the “bar-stool” arrangement that these molecules adopt, the angle of the thiosalicylate benzene ring can be determined. The rhodium complex (7.8) is found to have the thiosalicylate tilted at 12.2(3)°. In the case of the ruthenium molecule (7.9) a significant tilt of 23.1(1)° is observed. Steric interactions between the ligands may be the cause of these distortions, though the intramolecular contacts between the atoms of either the Cp* or the *p*-cymene and the thiosalicylate ligands are quite long [closest contacts: 7.8; 3.362(7) Å for C(20).....C(2') and 3.435(4) Å for C(10).....C(3') (7.9)]. This distortion is also manifested in the torsion angles about the carboxylate functionality. The C(3)–C(2)–C(1)–O(1) dihedral angle is 41.7(3)°, considerably greater than that of 31.4(5)° observed for the rhodium analogue. The *p*-cymene ligand in 7.9 may reduce steric hindrance in this molecule as it only has two functionalities (*iso*-propyl and methyl) on the coordinating ligand allowing the thiosalicylate ligand to twist into a pocket of reduced steric interaction.

Table 7.5 Selected bond lengths (Å) and bond angles (°) for [Ru{OC(O)C₆H₄-2-S}(p-cymene)]₂ (7.9)

Ru–O(1)	2.0930(12)	Ru–C(11)	2.1648(17)
Ru–C(10)	2.1760(17)	Ru–C(13)	2.2187(17)
Ru–C(14)	2.2274(17)	Ru–C(12)	2.2313(17)
Ru–C(9)	2.2637(17)	Ru–S	2.3848(4)
Ru–S'	2.4177(4)	S–C(3)	1.7831(18)
S–Ru'	2.4177(4)	O(1)–C(1)	1.288(2)
O(2)–C(1)	1.230(2)	C(1)–C(2)	1.513(3)
C(2)–C(3)	1.402(3)	C(2)–C(7)	1.404(3)
C(3)–C(4)	1.406(2)	C(4)–C(5)	1.387(3)
C(5)–C(6)	1.387(3)	C(6)–C(7)	1.390(3)
O(1)–Ru–S'	77.80(4)	S–Ru–S'	80.714(15)
C(3)–S–Ru	104.54(6)	C(3)–S–Ru'	112.48(6)
Ru–S–Ru'	99.286(15)	C(1)–O(1)–Ru	134.03(12)
O(2)–C(1)–O(1)	122.40(17)	O(2)–C(1)–C(2)	118.15(16)
O(1)–C(1)–C(2)	119.32(15)	C(3)–C(2)–C(7)	118.44(17)
C(3)–C(2)–C(1)	124.25(16)	C(7)–C(2)–C(1)	117.31(17)

C(2)–C(3)–C(4)	119.80(17)	C(2)–C(3)–S	123.70(14)
C(4)–C(3)–S	116.48(14)	C(5)–C(4)–C(3)	120.57(19)
C(4)–C(5)–C(6)	120.08(19)	C(5)–C(6)–C(7)	119.67(19)
C(6)–C(7)–C(2)	121.41(19)		

In conclusion the thiosalicylate ligand has proven to be effective at coordinating to a range of metal centres. Discussed here are two further examples of thiosalicylate complexes, which bond in a manner similar to that of the first row transition metal manganese in the form of a dimeric species. The thiosalicylate ligand bonds to the metal in a predictable manner via the thiolate sulfur and one of the carboxylate oxygen atoms. The thiolate sulfur also bridges to the other metal of the dimeric pair, forming an $\overline{\text{M-S-M'-S}}$ four-membered ring core. Differing tilts in the plane of the thiosalicylate ligand with respect to the planar coordinating ligand were observed. It is unclear whether either steric interactions or some other mechanism causes these changes.

7.8 Lactam coordination complexes

The complexes that bis(pyridone) (7.10) and bis(lactam) (7.11) ligands form with the transition and lanthanide metals has been the subject of extensive research.¹² The structures of these complexes are often large macrocycles, ranging from eight to eighty-membered ring systems. The complexes incorporating these ligands are not restricted to purely one metal, often a mixed metal species are observed, frequently with both transition and lanthanide metals in a single macrocycle.

With the structural determination of β -propiolactam (7.12),¹³ and more recently the anion of β -propiolactam coordinated to a variety of metal centres including platinum (7.13)¹⁴ and a mixed mercury/silver complex (7.14),¹⁵ it was proposed that $\text{cis-}[\text{Pt}\{\overline{\text{NCH}_2\text{CH}_2\text{CO}}\}_2(\text{PPh}_3)_2]$ (7.13) may also coordinate in a similar fashion as

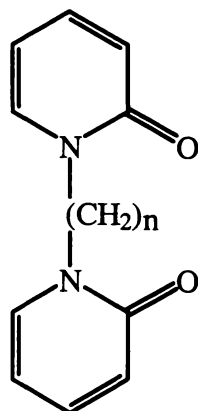
12 See for example a) D. M. L. Goodgame, S. P. W. Hill and D. J. Williams, *Polyhedron*, (1993), **12**, 2933; b) D. M. L. Goodgame, S. P. W. Hill and D. J. Williams, *J. Chem. Soc., Chem. Commun.*, (1993), 1019; c) S. Parsons and R. E. P. Winpenny, *Acc. Chem. Res.*, (1997), **30**, 89

13 Q.-C. Yang, P. Seiler and J. D. Dunitz, *Acta Crystallogr. Section C*, (1987), **C43**, 565

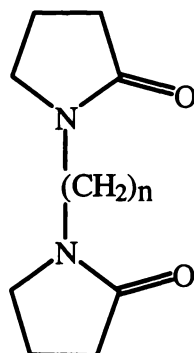
14 W. Henderson and M. Sabat, *Polyhedron*, (1997), **16**, 1663

15 D. M. L. Goodgame, S.P. W. Hill and D. J. Williams, *Polyhedron*, (1992), **11**, 1841

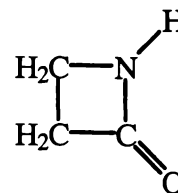
bis(lactam) (7.11) complexes. The platinum atom would act as a spacer atom, similar to the carbon chain in a bis(lactam) but would enforce a fixed (*cis*) geometry.



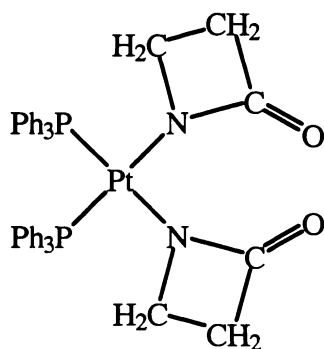
7.10



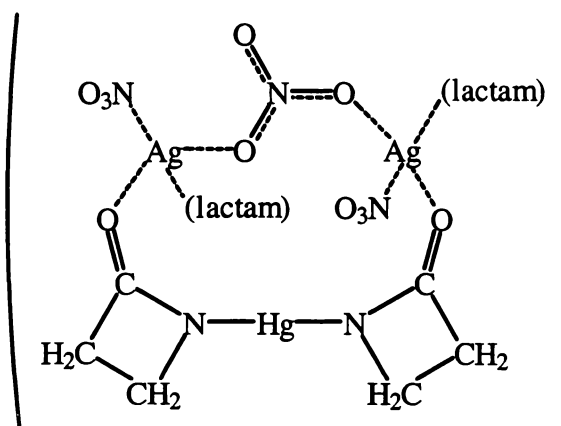
7.11



7.12



7.13



7.14

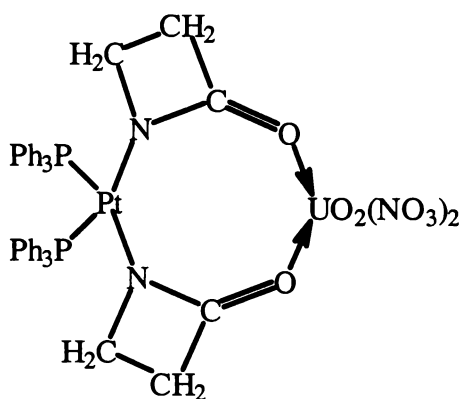
A number of complexes that incorporate a metal bis(pyridone) base unit have been synthesised and characterised.¹⁶ Several of these complexes include platinum as the metal centre. However, the molecules often have a Pt–Pt bond, or in some cases a Pt–Pt bis(pyridone) dimer.

16 see for example: a) K. Matsumoto and K. Fuma, *J. Am. Chem. Soc.*, (1982), **104**, 897; K. Matsumoto, H. Takahashi and K. Fuma, *J. Am. Chem. Soc.*, (1984), **106**, 2049; b) D. M. L. Goodgame, D. J. Williams and R. E. P. Winpenny, *J. Chem. Soc., Chem. Comm.*, (1988), 437; c) K. Matsumoto and K. Harashima, *Inorg. Chem.*, (1991), **30**, 3032; d) D. M. L. Goodgame, D. J. Williams and R. E. P. Winpenny, *Polyhedron*, (1989), **9**, 1913

7.9 Synthesis of cis -[Pt{NCH₂CH₂CO}₂(PPh₃)₂].UO₂(NO₃)₂ (7.15)

The complex cis -[Pt{NCH₂CH₂CO}₂(PPh₃)₂] (7.13) was synthesised as described.¹⁴ Uranyl nitrate (Aldrich) and methanol (LR) were used as supplied.

A solution of uranyl nitrate (0.065 g, 0.165 mmol) in methanol (5 cm³) was carefully added to a solution of cis -[Pt{NCH₂CH₂CO}₂(PPh₃)₂] (0.063 g, 0.073 mmol) in methanol (5 cm³) in a Schlenk tube. The solvent was allowed to evaporate, precipitating [Pt{NCH₂CH₂CO}₂(PPh₃)₂].UO₂(NO₃)₂ (7.15) as yellow prisms. The details of the cell parameters, data collection and final least-squares cycle analysis of the structure are given in Table 7.6



7.15

Accurate X-ray intensity data were collected at the University of Auckland on a Siemens SMART CCD diffractometer over a hemisphere of reciprocal space. The data were corrected for Lorentz and polarisation effects and an empirical correction for absorption applied.⁶ All non-hydrogen atoms were given anisotropic thermal displacement parameters. Hydrogen atoms were placed in calculated positions and assigned thermal parameters 1.2 times the U_{iso} of the atom to which they were bonded.

Table 7.6 Crystal data and structure refinement for *cis*-
[Pt{NCH₂CH₂CO}₂(PPh₃)₂].UO₂(NO₃)₂ (7.15)

<i>Crystal data</i>	
Empirical formula	C ₄₂ H ₃₈ N ₄ O ₁₀ P ₂ PtU
Formula weight	1253.82
Crystal system	Monoclinic
Space group	Cc
Unit cell dimensions	
<i>a</i> (Å)	26.7739(6)
<i>b</i> (Å)	11.1247(3)
<i>c</i> (Å)	19.3173(5)
β (°)	131.004(1)
Volume (Å ³)	4342.10(19)
Z	4
D(c) (g cm ⁻³)	1.918
<i>Data Collection</i>	
Diffractometer	Siemens SMART CCD
Radiation	Mo-Kα
Wavelength (Å)	0.71073
Temperature (K)	203(2)
Crystal size (mm)	0.34 x 0.30 x 0.23
θ range for data collection (°)	2.02 to 28.28
Index ranges	-31 ≤ h ≤ 34 0 ≤ k ≤ 14, -24 ≤ l ≤ 21
Reflections collected	12528
Independent reflections	7495 [R _(int) = 0.0240]
Absorption coefficient (mm ⁻¹)	7.078
Maximum transmission	0.2929
Minimum transmission	0.1970
F(000)	2392

Structure analysis and refinement

Solution by	direct methods
Refinement method	Full-matrix least-squares on F^2
Data / restraints / parameters	7495 / 2 / 540
Goodness-of-fit on F^2	0.855
Final R indices [$I > 2\sigma(I)$]	$R_1 = 0.0232$, $wR^2 = 0.0490$
R indices (all data)	$R_1 = 0.0258$, $wR^2 = 0.0504$
Weighting Scheme:	$w = 1/[\sigma^2(F_o^2) + (0.0000P)^2 + 0.0000P]$ where $P = (F_o^2 + 2F_c^2)/3$
Absolute structure parameter	0.009(4)
Largest difference peak ($e.\text{\AA}^{-3}$)	0.673
Largest difference hole ($e.\text{\AA}^{-3}$)	-0.966
Programs used	
Solution by	SHELXS-97 ⁷
Refinement by	SHELXL-97 ⁸

7.10 Structural analysis of $[\text{Pt}\{\overline{\text{NCH}_2\text{CH}_2\text{C}(\text{O})}\}_2(\text{PPh}_3)_2]\cdot\text{UO}_2(\text{NO}_3)_2$ (7.15)

The structure of **7.15** shows that the complex $\text{cis-}[\text{Pt}\{\overline{\text{NCH}_2\text{CH}_2\text{CO}}\}_2(\text{PPh}_3)_2]$ (**7.13**) has coordinated to uranyl nitrate via the β -lactam carbonyl oxygen atoms [O(1) and O(2)], forming an eight-membered heterocycle (Figure 7.5). This complex has a comparatively small eight-membered heterocycle compared to the previously described lanthanide lactam or pyridone complexes. This geometry is not unexpected considering that the parent platinum complex, $\text{cis-}[\text{Pt}\{\overline{\text{NCH}_2\text{CH}_2\text{CO}}\}_2(\text{PPh}_3)_2]$ (**7.13**) will force the lactams to coordinate in a *cis* fashion. A larger macrocycle, perhaps involving two or more platinum bis(lactam) and uranyl nitrate compounds could be envisioned as a reaction product. However, after initial coordination of one of the lactam carbonyl oxygen atoms to the uranium an intramolecular reaction would be favoured over further intermolecular interactions.

The uranium atom displays an eight-coordinate geometry, i.e. a distorted hexagonal bipyramid, with the nitrate ligands and β -lactam oxygens bonded to the uranium equatorially while the uranyl oxygens [O(18) and O(19)] occupy the axial positions.

The atoms (including all atoms in the nitrate ligands) about the equator of the uranium atom are all co-planar, with no atom lying more than 0.051(7) Å [N(10)] from the least-squares plane; O(13) was not included in this calculation as it is disordered over two sites. The axial oxygen atoms [O(18) and O(19)] display considerable multiple-bond character with short U–O bond lengths of 1.755(4) and 1.761(5) Å respectively and are comparable with those U–O bond lengths observed for other uranyl nitrate complexes [1.736(11) to 1.769(6) Å].¹⁷ The coordinated lactam oxygens [O(1) and O(2)] are more closely bonded to the uranium [U–O(lactam) bond lengths 2.350(5) and 2.336(5) Å, respectively] than the coordinating nitrate oxygens [U–O(nitrate) bond length range 2.512(5) to 2.535(5) Å].

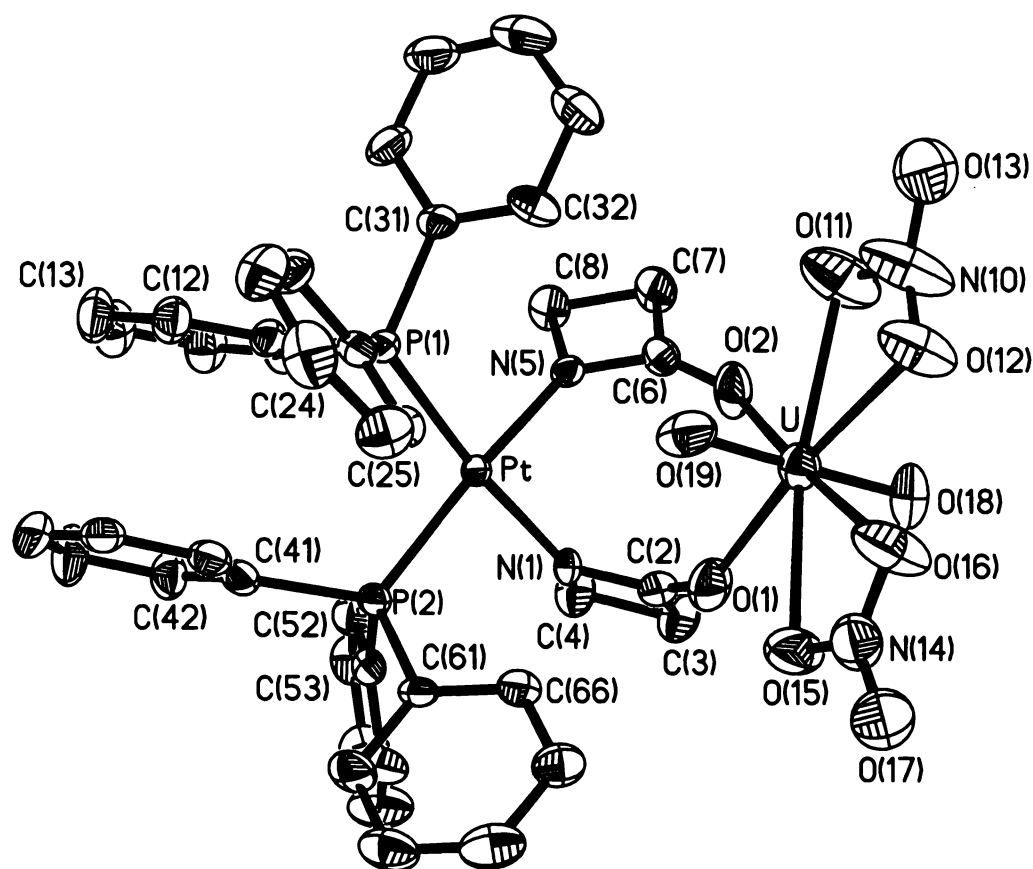


Figure 7.5 Thermal ellipsoid plot of $\overline{cis-[Pt\{NCH_2CH_2CO\}_2(PPh_3)_2].UO_2(NO_3)_2}$ (**7.15**) showing atom labelling scheme.

Thermal displacement ellipsoids are depicted at 50% probability. Hydrogen atoms and O(13') have been omitted for clarity.

¹⁷ see for example: a) P. L. Ritger, J. H. Burns and G. Bombieri, *Inorg. Chim. Acta.*, (1983), **77**, L217; b) G. Xinmin, T. Ning, W. Xin, Z. Yin and T. Minyu, *J. Coord. Chem.*, (1989), **20**, 21; c) R. Hämäläinen, U. Turpeinen and I. Mutikainen, *Acta Crystallogr.*, (1996), **C52**, 16

The platinum atom has a four-coordinate geometry normally observed for complexes of this type. The coordination sphere of the platinum is highly planar, with the largest deviation from the mean plane for N(5) [0.093(2) Å]. As would be expected for phosphorus atoms in similar environments, the Pt–P bond lengths are similar [2.262(1) and 2.282(2) Å for Pt–P(1) and Pt–P(2) respectively] and comparable with those found for the parent bis(lactam) [2.266(3) and 2.291(3) Å]. The bond angles about the platinum show the distorted square-planar nature of the metal. Often seen in bis-triphenylphosphine platinum complexes, the steric bulk of the triphenylphosphine ligands has caused an opening of the P–Pt–P bond angle [97.1(1)°], away from the ideal 90°. This obtuse angle is compensated for by a reduction in the N–Pt–N bond angle [83.3(2)°]. However, little distortion is observed for the P–Pt–N angles, which are near ideal at 90.6(1) and 88.4(1)° for P(1)–Pt–N(5) and P(2)–Pt–N(1) respectively.

Table 7.7 Selected bond lengths (Å) and bond angles (°) for $[\text{Pt}\{\overline{\text{NCH}_2\text{CH}_2\text{CO}}\}_2(\text{PPh}_3)_2]\cdot\text{UO}_2(\text{NO}_3)_2$ (**7.15**).

U–O(18)	1.755(4)	U–O(19)	1.761(5)
U–O(2)	2.336(5)	U–O(1)	2.350(5)
U–O(16)	2.512(5)	U–O(15)	2.518(5)
U–O(11)	2.523(5)	U–O(12)	2.535(5)
U.....N(10)	2.964(7)	U.....N(14)	2.967(6)
N(10)–O(13)	1.249(14)	N(10)–O(12)	1.252(9)
N(10)–O(13')	1.268(13)	N(10)–O(11)	1.296(10)
N(14)–O(17)	1.207(7)	N(14)–O(16)	1.240(7)
N(14)–O(15)	1.257(7)	Pt–N(1)	2.054(4)
Pt–N(5)	2.038(4)	Pt–P(1)	2.2616(13)
Pt–P(2)	2.2817(13)	N(1)–C(2)	1.299(7)
N(1)–C(4)	1.491(7)	O(1)–C(2)	1.244(7)
C(2)–C(3)	1.505(8)	C(2).....C(4)	2.032(9)
C(3)–C(4)	1.536(9)	O(2)–C(6)	1.252(7)
N(5)–C(6)	1.310(7)	N(5)–C(8)	1.498(7)
C(6)–C(7)	1.491(8)	C(6).....C(8)	2.026(8)
C(7)–C(8)	1.540(8)	P(1)–C(11)	1.824(6)
P(1)–C(21)	1.817(5)	P(1)–C(31)	1.825(6)

P(2)–C(41)	1.830(6)	P(2)–C(51)	1.822(5)
P(2)–C(61)	1.821(5)		
O(18)–U–O(19)	177.9(3)	O(18)–U–O(2)	89.19(19)
O(19)–U–O(2)	92.0(2)	O(18)–U–O(1)	89.6(2)
O(19)–U–O(1)	92.4(2)	O(2)–U–O(1)	71.27(17)
N(5)–Pt–P(1)	90.57(13)	N(5)–Pt–N(1)	83.34(17)
N(5)–Pt–P(2)	168.63(13)	N(1)–Pt–P(1)	173.90(13)
P(1)–Pt–P(2)	97.67(5)	N(1)–Pt–P(2)	88.39(13)
C(2)–N(1)–Pt	129.2(4)	C(2)–N(1)–C(4)	93.3(4)
C(2)–O(1)–U	141.6(4)	C(4)–N(1)–Pt	131.5(4)
O(1)–C(2)–C(3)	133.0(6)	O(1)–C(2)–N(1)	131.2(6)
N(1)–C(4)–C(3)	87.1(4)	N(1)–C(2)–C(3)	95.8(5)
C(6)–N(5)–C(8)	92.1(4)	C(2)–C(3)–C(4)	83.9(4)
C(8)–N(5)–Pt	128.7(4)	C(6)–O(2)–U	147.2(4)
O(2)–C(6)–C(7)	131.1(5)	C(6)–N(5)–Pt	137.2(4)
O(2)–C(6)–N(5)	132.2(5)	N(5)–C(6)–C(7)	96.7(5)
N(5)–C(8)–C(7)	87.3(4)	C(6)–C(7)–C(8)	83.9(4)
C(11)–P(1)–Pt	109.56(18)	C(21)–P(1)–Pt	115.91(18)
C(31)–P(1)–Pt	114.75(17)	C(41)–P(2)–Pt	120.32(18)
C(51)–P(2)–Pt	106.78(18)	C(61)–P(2)–Pt	114.47(18)

Unlike the metallalactam ring systems described previously, the β -propiolactam rings shown here have a highly strained four-membered ring. The metal, in metallalactam complexes, provides a large degree of freedom in bond geometries, predominantly observed in the acute N–M–C bond angle (typically 66 to 69°).¹ However, with β -propiolactam no metal centre is included in the ring, and hence, for the atoms in the β -propiolactam ring (carbon and nitrogen) strained geometries are observed. As noted previously, the bonds about the lactam rings of the metallated complex *cis*-[Pt{NCH₂CH₂CO}₂(PPh₃)₂] (**10**) have different bond lengths¹⁴ than those observed for the parent β -propiolactam.¹³ Coordination of the complex to uranium has not significantly altered the bond lengths and angles about the β -propiolactam ring, most significantly, the lactam carbonyl bonds [1.244(7) and 1.252(7) Å for C(2)–O(1) and

C(4)–O(2), respectively] are comparable with those found in the free platinum bis(lactam) **7.13** [1.28(1) and 1.25(10) Å].¹⁴

The β -propiolactam ligands are twisted with respect to each other, with an angle of 59.6(4)° between the least-squares planes of the two ligands. They are also rotated to differing degrees with respect to the coordination plane of the platinum. The N(1), C(2), C(3), C(4) ring is almost perpendicular to the platinum coordination plane [81.5(3)°], while the N(2), C(5), C(6) ring lies at –65.0(3)°. The crystal structure of the platinum bis(lactam) complex **7.13** showed that the carbonyl functionalities of the lactam rings were oriented in an “*anti*” arrangement.¹⁴ It was proposed that for the carbonyls to coordinate, rotation about one of the Pt–N bonds would have to occur. As can be seen here, this is precisely what has occurred.

The coordination planes of the two moieties, the platinum bis(lactam) moiety **7.13** and the uranyl nitrate equatorial plane, are inclined to one another with a “fold-angle” of 85.4(1)° through the platinum and uranium equatorial coordination planes (see Figure 7.6). This geometric constraint arises from the relatively fixed orientation that the lactam rings have to adopt to coordinate to the uranium.

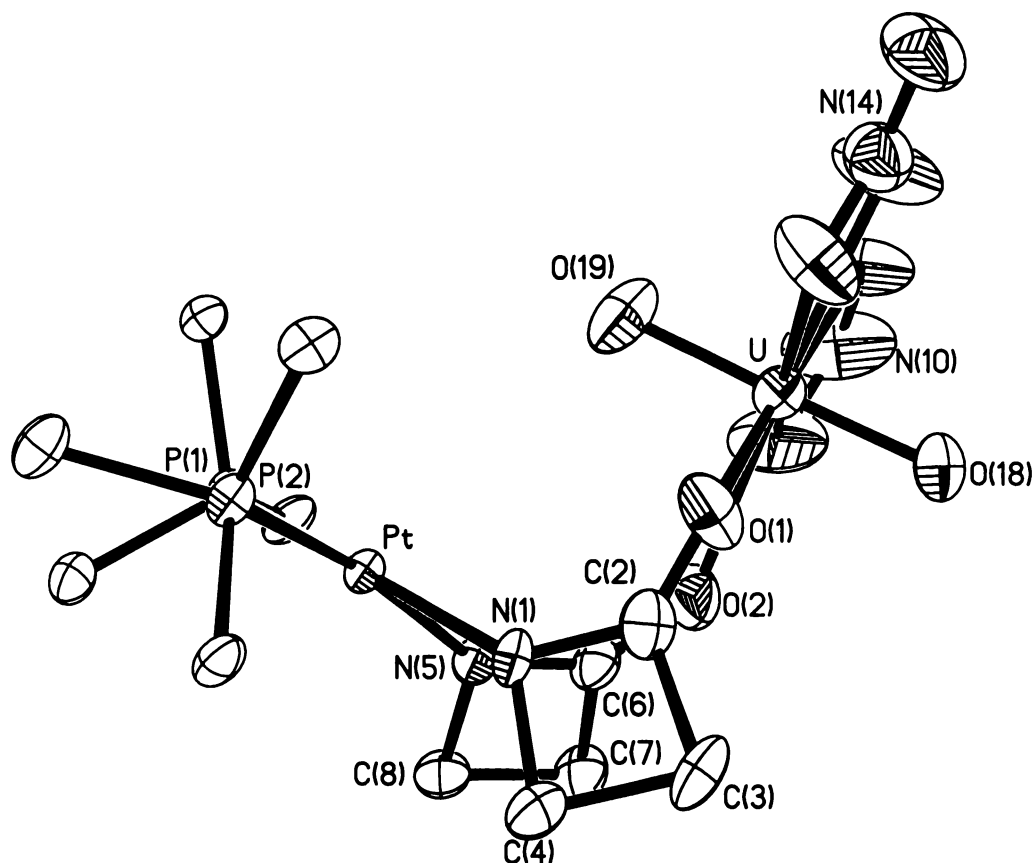


Figure 7.6 Diagram showing bonding geometry about the β -propiolactam rings of 7.15. Phenyl rings (except *ipso* carbons) and hydrogen atoms are omitted for clarity.

In summary, it has been shown that the bis(lactam) complex, *cis*-[Pt{ $\overline{\text{NCH}_2\text{CH}_2\text{CO}}$ }_2(PPh₃)₂] (7.13), can readily coordinate to an actinide series element (in this case uranium), forming an eight-membered heterocycle, similar to those observed for related bis(lactam) and bis(pyridone) actinide and lanthanide complexes. The platinum bis(lactam) coordinates in the predicted *cis* geometry, which necessarily restricts any complex formed to have an eight-membered ring.

Appendix 1 List of Publications

1.1 Chapter Two

Inorganica Chimica Acta

Platina- and palladalactam complexes derived from 2-benzoylacetanilide and X-ray structure of $[\text{Pd}\{\text{N}(\text{Ph})\text{C}(\text{O})\text{CHC}(\text{O})\text{Ph}\}\text{bipy}]\cdot\text{CH}_2\text{Cl}_2$

W. Henderson, A. G. Oliver, C. E. F. Rickard and L.-J. Baker, (1999), **292**, 260

1.2 Chapter Three

Inorganica Chimica Acta

Isolation and X-ray structure of the platinum(II)-amidate complex *cis*- $[\text{PtCl}\{\text{N}(\text{CO}_2\text{Et})\text{C}(\text{O})\text{CH}_2\text{CN}\}(\text{PPh}_3)_2]$, an intermediate in the silver(I) oxide mediated synthesis of a platinalactam complex

William Henderson, Allen G. Oliver and Brian K. Nicholson, (1999), in press

1.3 Chapter Five

Acta Crystallographica, Section C

cis-Bis(cyanomethyl) bis(triphenylphosphine) platinum(II)

William Henderson and Allen G. Oliver, (1999), **C55**, 1406

Acta Crystallographica, Section C

cis-Bis(phenoxyacetato) bis(triphenylphosphine) platinum(II)

William Henderson and Allen G. Oliver, (1999), **C55**, 1408

1.4 Chapter Seven

Acta Crystallographica, Section C

N-Acetato-*N'*-methlureato (η^5 -pentamethylcyclopentadienyl) (triphenylphosphine) iridium(III)

Maarten B. Dinger, William Henderson, Allen G. Oliver and Clifton E. F. Rickard, (1999), **C55**, 1778

Appendix 2 Crystallographic data tables

Table A-1 Atomic coordinates and equivalent isotropic displacement parameters (\AA^2) for $[\text{Pd}\{\text{N}(\text{Ph})\text{C}(\text{O})\text{CHC}(\text{O})\text{Ph}\}(\text{bipy})].\text{CH}_2\text{Cl}_2$ (**2.14**)

U(eq) is defined as one third of the trace of the orthogonalised Uij tensor.

	x	y	z	U(eq)
Pd(1)	0.08346(1)	0.1526(1)	-0.0003(1)	0.024(1)
N(1)	0.6495(5)	0.1584(5)	-0.0532(3)	0.029(1)
C(1)	0.5971(6)	0.1599(5)	0.0058(3)	0.026(1)
O(1)	0.4829(4)	0.1568(4)	0.0098(3)	0.032(1)
C(2)	0.7104(6)	0.1655(5)	0.0707(4)	0.028(1)
C(3)	0.7342(5)	0.2653(6)	0.1183(3)	0.028(1)
O(2)	0.7819(4)	0.2521(4)	0.1853(2)	0.039(1)
C(11)	0.7025(6)	0.3791(6)	0.0901(4)	0.031(2)
C(12)	0.6939(7)	0.4110(6)	0.0166(4)	0.040(2)
C(13)	0.6666(8)	0.5196(7)	-0.0044(5)	0.054(2)
C(14)	0.6451(8)	0.5975(7)	0.0463(5)	0.056(2)
C(15)	0.6527(7)	0.5674(7)	0.1182(5)	0.048(2)
C(16)	0.6828(6)	0.4598(6)	0.1407(4)	0.037(2)
C(21)	0.5769(5)	0.1460(6)	-0.1263(4)	0.030(1)
C(22)	0.5894(6)	0.2229(7)	-0.1807(4)	0.038(2)
C(23)	0.5162(7)	0.2108(8)	-0.2520(4)	0.053(2)
C(24)	0.4338(8)	0.1239(9)	-0.2691(4)	0.059(3)
C(25)	0.4222(7)	0.0450(8)	-0.2154(5)	0.051(2)
C(26)	0.4945(6)	0.0551(6)	-0.1445(4)	0.038(2)
N(2)	0.10087(5)	0.1406(5)	0.0697(3)	0.028(1)
N(3)	0.9558(5)	0.1413(5)	-0.0765(3)	0.028(1)
C(31)	0.10253(6)	0.1360(6)	0.1439(4)	0.031(2)
C(32)	0.11452(6)	0.1253(6)	0.1885(4)	0.035(2)
C(33)	0.12497(6)	0.1179(6)	0.1562(4)	0.039(2)
C(34)	0.12343(6)	0.1221(5)	0.0806(4)	0.031(2)
C(35)	0.11110(6)	0.1339(5)	0.0377(3)	0.026(1)
C(36)	0.10828(6)	0.1382(5)	-0.0433(4)	0.027(1)
C(37)	0.11764(6)	0.1371(5)	-0.0862(4)	0.029(1)
C(38)	0.11401(7)	0.1402(6)	-0.1620(4)	0.037(2)
C(39)	0.1.0113(6)	0.1442(6)	-0.1947(4)	0.036(2)
C(310)	0.9228(6)	0.1436(5)	-0.1503(4)	0.029(1)
C(101)	0.9785(10)	0.0365(8)	0.3954(6)	0.072(3)
Cl(1)	0.8936(2)	0.0862(2)	0.3110(1)	0.063(1)
Cl(2)	0.9460(3)	0.1004(2)	0.4103(2)	0.082(1)

Table A-2 Bond lengths (\AA) for $[\text{Pd}\{\text{N}(\text{Ph})\text{C}(\text{O})\text{CHC}(\text{O})\text{Ph}\}(\text{bipy})].\text{CH}_2\text{Cl}_2$ (**2.14**)

Pd(1)-N(1)	2.021(5)	Pd(1)-N(2)	2.042(5)
Pd(1)-C(2)	2.054(6)	Pd(1)-N(3)	2.104(5)
Pd(1)-C(1)	2.565(6)	N(1)-C(1)	1.324(8)
N(1)-C(21)	1.420(8)	C(1)-O(1)	1.239(8)
C(1)-C(2)	1.521(8)	C(2)-C(3)	1.483(9)
C(3)-O(2)	1.249(8)	C(3)-C(11)	1.484(9)

C(11)-C(16)	1.396(9)	C(11)-C(12)	1.397(10)
C(12)-C(13)	1.382(11)	C(13)-C(14)	1.380(13)
C(14)-C(15)	1.363(13)	C(15)-C(16)	1.382(11)
C(21)-C(22)	1.396(10)	C(21)-C(26)	1.404(10)
C(22)-C(23)	1.396(10)	C(23)-C(24)	1.366(13)
C(24)-C(25)	1.398(13)	C(25)-C(26)	1.385(10)
N(2)-C(31)	1.348(8)	N(2)-C(35)	1.349(8)
N(3)-C(310)	1.337(8)	N(3)-C(36)	1.372(8)
C(31)-C(32)	1.380(9)	C(32)-C(33)	1.374(10)
C(33)-C(34)	1.373(10)	C(34)-C(35)	1.399(9)
C(35)-C(36)	1.465(9)	C(36)-C(37)	1.397(8)
C(37)-C(38)	1.376(10)	C(38)-C(39)	1.386(10)
C(39)-C(310)	1.374(9)		
C(101)-Cl(2)	1.722(10)	C(101)-Cl(1)	1.743(9)

Table A-3 Bond angles (°) for [Pd{N(Ph)C(O)CHC(O)Ph}(bipy)].CH₂Cl₂ (**2.14**)

N(1)-Pd(1)-N(2)	169.7(2)	N(1)-Pd(1)-C(2)	67.1(2)
N(2)-Pd(1)-C(2)	103.0(2)	N(1)-Pd(1)-N(3)	110.7(2)
N(2)-Pd(1)-N(3)	79.2(2)	C(2)-Pd(1)-N(3)	177.7(2)
N(1)-Pd(1)-C(1)	30.8(2)	N(2)-Pd(1)-C(1)	139.1(2)
C(2)-Pd(1)-C(1)	36.4(2)	N(3)-Pd(1)-C(1)	141.4(2)
C(1)-N(1)-C(21)	122.9(5)	C(1)-N(1)-Pd(1)	98.0(4)
C(21)-N(1)-Pd(1)	138.3(4)	O(1)-C(1)-N(1)	129.6(6)
O(1)-C(1)-C(2)	126.1(6)	N(1)-C(1)-C(2)	104.3(5)
O(1)-C(1)-Pd(1)	176.2(5)	N(1)-C(1)-Pd(1)	51.3(3)
C(2)-C(1)-Pd(1)	53.2(3)	C(3)-C(2)-C(1)	121.1(5)
C(3)-C(2)-Pd(1)	112.7(4)	C(1)-C(2)-Pd(1)	90.4(4)
O(2)-C(3)-C(2)	118.1(6)	O(2)-C(3)-C(11)	119.0(6)
C(2)-C(3)-C(11)	123.0(5)	C(16)-C(11)-C(12)	118.0(7)
C(16)-C(11)-C(3)	117.8(6)	C(12)-C(11)-C(3)	124.2(6)
C(13)-C(12)-C(11)	120.2(8)	C(14)-C(13)-C(12)	120.7(8)
C(15)-C(14)-C(13)	119.7(8)	C(14)-C(15)-C(16)	120.5(8)
C(15)-C(16)-C(11)	120.8(7)	C(22)-C(21)-C(26)	119.7(6)
C(22)-C(21)-N(1)	120.0(6)	C(26)-C(21)-N(1)	120.3(6)
C(23)-C(22)-C(21)	119.6(7)	C(24)-C(23)-C(22)	120.6(8)
C(23)-C(24)-C(25)	120.4(7)	C(26)-C(25)-C(24)	119.9(8)
C(25)-C(26)-C(21)	119.8(7)	C(31)-N(2)-C(35)	119.6(5)
C(31)-N(2)-Pd(1)	124.1(4)	C(35)-N(2)-Pd(1)	116.2(4)
C(310)-N(3)-C(36)	119.2(5)	C(310)-N(3)-Pd(1)	127.7(4)
C(36)-N(3)-Pd(1)	113.0(4)	N(2)-C(31)-C(32)	121.7(6)
C(33)-C(32)-C(31)	119.0(6)	C(34)-C(33)-C(32)	120.1(6)
C(33)-C(34)-C(35)	118.9(6)	N(2)-C(35)-C(34)	120.7(6)
N(2)-C(35)-C(36)	115.5(5)	C(34)-C(35)-C(36)	123.8(6)
N(3)-C(36)-C(37)	120.3(6)	N(3)-C(36)-C(35)	115.8(5)
C(37)-C(36)-C(35)	123.9(6)	C(38)-C(37)-C(36)	119.5(6)
C(37)-C(38)-C(39)	119.5(6)	C(310)-C(39)-C(38)	118.9(6)
N(3)-C(310)-C(39)	122.6(6)		
Cl(2)-C(101)-Cl(1)	112.8(6)		

Table A-4 Anisotropic displacement parameters (\AA^2) for[Pd{N(Ph)C(O)CHC(O)Ph}(bipy)]CH₂Cl₂ (2.14)

The anisotropic displacement factor exponent takes the form:

$$-2\pi^2 [h^2 a^{*2} U_{11} + \dots + 2 h k a^* b^* U_{12}]$$

	U11	U22	U33	U23	U13	U12
Pd(1)	0.010(1)	0.035(1)	0.00026(1)	-0.001(1)	0.002(1)	0.001(1)
N(1)	0.017(3)	0.040(3)	0.030(3)	0.000(2)	0.004(2)	0.000(2)
C(1)	0.017(3)	0.00026(3)	0.033(3)	0.002(3)	0.002(2)	0.004(3)
O(1)	0.014(2)	0.046(3)	0.037(3)	0.003(2)	0.006(2)	0.002(2)
C(2)	0.015(3)	0.038(4)	0.032(3)	0.004(3)	0.006(3)	0.001(3)
C(3)	0.011(3)	0.044(4)	0.00028(3)	0.001(3)	0.002(2)	0.003(3)
O(2)	0.032(3)	0.057(3)	0.00025(2)	-0.001(2)	0.000(2)	0.011(2)
C(11)	0.016(3)	0.041(4)	0.033(3)	0.000(3)	-0.003(3)	0.003(3)
C(12)	0.036(4)	0.039(4)	0.040(4)	0.002(3)	-0.007(3)	0.000(3)
C(13)	0.055(5)	0.043(5)	0.055(5)	0.009(4)	-0.015(4)	-0.016(4)
C(14)	0.039(4)	0.031(4)	0.083(7)	0.009(4)	-0.019(4)	0.002(4)
C(15)	0.030(4)	0.044(5)	0.064(5)	-0.014(4)	-0.002(4)	0.009(3)
C(16)	0.026(3)	0.042(4)	0.041(4)	-0.006(3)	0.003(3)	0.001(3)
C(21)	0.011(3)	0.049(4)	0.030(3)	-0.003(3)	0.000(2)	0.005(3)
C(22)	0.027(3)	0.055(5)	0.031(4)	0.006(3)	0.005(3)	0.006(3)
C(23)	0.034(4)	0.090(7)	0.034(4)	0.011(4)	0.009(3)	0.00020(4)
C(24)	0.032(4)	0.109(8)	0.031(4)	-0.017(5)	-0.003(3)	0.00020(5)
C(25)	0.024(4)	0.070(6)	0.057(5)	-0.024(4)	0.003(3)	0.001(4)
C(26)	0.022(3)	0.050(4)	0.040(4)	-0.006(3)	0.002(3)	0.005(3)
N(2)	0.016(3)	0.037(3)	0.033(3)	0.002(2)	0.007(2)	0.001(2)
N(3)	0.017(3)	0.038(3)	0.00028(3)	-0.003(2)	0.002(2)	0.001(2)
C(31)	0.018(3)	0.042(4)	0.033(3)	0.000(3)	0.006(3)	0.005(3)
C(32)	0.030(4)	0.044(4)	0.00029(3)	0.000(3)	0.000(3)	0.007(3)
C(33)	0.018(3)	0.049(4)	0.043(4)	-0.001(3)	-0.008(3)	0.007(3)
C(34)	0.017(3)	0.036(4)	0.040(4)	-0.003(3)	0.006(3)	0.001(3)
C(35)	0.019(3)	0.030(4)	0.00028(3)	-0.001(3)	0.001(3)	0.000(3)
C(36)	0.017(3)	0.031(4)	0.035(3)	-0.002(3)	0.007(3)	-0.001(3)
C(37)	0.017(3)	0.032(4)	0.038(3)	0.000(3)	0.008(3)	0.005(3)
C(38)	0.029(4)	0.046(4)	0.042(4)	0.004(3)	0.019(3)	0.005(3)
C(39)	0.030(4)	0.049(4)	0.00029(3)	-0.003(3)	0.005(3)	0.007(3)
C(310)	0.020(3)	0.032(4)	0.034(3)	-0.008(3)	0.002(3)	0.002(3)
C(101)	0.075(7)	0.062(6)	0.070(6)	0.003(5)	-0.005(5)	0.009(5)
Cl(1)	0.065(1)	0.062(1)	0.056(1)	0.004(1)	0.001(1)	0.003(1)
Cl(2)	0.0106(2)	0.059(2)	0.082(2)	0.013(1)	0.00024(2)	0.004(2)

Table A-5 Hydrogen coordinates and isotropic displacement parameters (\AA^2) for[Pd{N(Ph)C(O)CHC(O)Ph}(bipy)].CH₂Cl₂ (2.14)

	x	y	z	U(eq)
H(2)	0.7142(6)	0.0973(5)	0.1017(4)	0.034
H(12)	0.7068(7)	0.3578(6)	-0.0191(4)	0.048
H(13)	0.6626(8)	0.5409(7)	-0.0544(5)	0.065
H(14)	0.6251(8)	0.6718(7)	0.0312(5)	0.067
H(15)	0.6372(7)	0.6209(7)	0.1531(5)	0.057

H(16)	0.6901(6)	0.4406(6)	0.1912(4)	0.045
H(22)	0.6473(6)	0.2832(7)	-0.1693(4)	0.046
H(23)	0.5238(7)	0.2636(8)	-0.2891(4)	0.063
H(24)	0.3840(8)	0.1169(9)	-0.3177(4)	0.070
H(25)	0.3648(7)	-0.0154(8)	-0.2276(5)	0.061
H(26)	0.4884(6)	0.0007(6)	-0.1082(4)	0.045
H(31)	0.9528(6)	0.1402(6)	0.1661(4)	0.037
H(32)	0.11553(6)	0.1231(6)	0.2408(4)	0.042
H(33)	0.13328(6)	0.1098(6)	0.1861(4)	0.046
H(34)	0.13061(6)	0.1171(5)	0.0579(4)	0.037
H(37)	0.12644(6)	0.1342(5)	-0.0632(4)	0.034
H(38)	0.12028(7)	0.1396(6)	-0.1917(4)	0.045
H(39)	0.9847(6)	0.1472(6)	-0.2469(4)	0.044
H(310)	0.8345(6)	0.1449(5)	-0.1729(4)	0.035
H(10A)	0.10712(10)	0.0447(8)	0.3969(6)	0.086
H(10B)	0.9572(10)	0.0819(8)	0.4358(6)	0.086

Table A-6 Atomic coordinates and equivalent isotropic displacement parameters for *cis*-[Pt{N(C(O)CH₂CN)(CO₂Et)}Cl(PPh₃)₂]. 0.5CH₂Cl₂ (3.4)

U(eq) is defined as one third of the trace of the orthogonalised U_{ij} tensor.

	x	y	z	U(eq)
Pt	0.0860(1)	0.4001(1)	0.2682(1)	0.016(1)
Cl(1)	-0.1074(2)	0.3665(2)	0.3492(1)	0.025(1)
P(1)	0.1468(2)	0.2009(2)	0.2744(1)	0.019(1)
P(2)	0.2638(2)	0.4476(2)	0.1923(1)	0.017(1)
N(1)	0.0009(7)	0.5820(6)	0.2653(4)	0.019(2)
N(2)	-0.1708(9)	0.8752(8)	0.0354(6)	0.049(3)
O(1)	-0.0654(7)	0.5932(6)	0.1512(4)	0.036(2)
O(2)	-0.0595(8)	0.7302(6)	0.3353(4)	0.048(2)
O(3)	0.0882(6)	0.5541(6)	0.3741(4)	0.030(2)
C(1)	-0.1468(10)	0.8319(9)	0.1005(8)	0.037(3)
C(2)	-0.1150(10)	0.7803(8)	0.1825(6)	0.033(3)
C(3)	-0.0603(9)	0.6442(8)	0.2002(6)	0.024(2)
C(4)	0.0039(10)	0.6317(9)	0.3250(6)	0.029(2)
C(5)	0.1057(12)	0.5976(11)	0.4389(7)	0.055(4)
C(6)	0.2176(19)	0.5114(18)	0.4721(12)	0.070(6)
C(5')	0.1057(12)	0.5976(11)	0.4389(7)	0.055(4)
C(6')	0.190(4)	0.672(4)	0.419(3)	0.091(17)
C(11)	0.1634(9)	0.1058(8)	0.3763(6)	0.025(2)
C(12)	0.1300(9)	0.1550(8)	0.4435(6)	0.027(2)
C(13)	0.1426(11)	0.0825(9)	0.5219(6)	0.041(3)
C(14)	0.1895(13)	-0.0410(11)	0.5339(7)	0.067(4)
C(15)	0.2240(13)	-0.0922(10)	0.4690(7)	0.062(4)
C(16)	0.2121(10)	-0.0203(8)	0.3912(6)	0.037(3)
C(21)	0.2939(9)	0.1322(7)	0.2145(5)	0.020(2)
C(22)	0.2921(9)	0.1136(8)	0.1390(5)	0.027(2)
C(23)	0.4037(10)	0.0611(9)	0.0956(6)	0.036(3)
C(24)	0.5178(11)	0.0236(9)	0.1250(7)	0.042(3)
C(25)	0.5200(10)	0.0411(9)	0.1983(7)	0.036(3)
C(26)	0.4087(9)	0.0950(8)	0.2442(6)	0.028(2)
C(31)	0.0235(9)	0.1686(8)	0.2380(5)	0.023(2)
C(32)	-0.0124(10)	0.0602(9)	0.2702(6)	0.032(3)
C(33)	-0.1027(11)	0.0416(11)	0.2391(7)	0.043(3)
C(34)	-0.1569(11)	0.1248(11)	0.1748(7)	0.045(3)
C(35)	-0.1228(10)	0.2323(10)	0.1429(7)	0.041(3)
C(36)	-0.0348(9)	0.2551(9)	0.1741(6)	0.028(2)
C(41)	0.3101(9)	0.4025(8)	0.0970(5)	0.025(2)
C(42)	0.2101(10)	0.4215(8)	0.0556(5)	0.028(2)
C(43)	0.2347(12)	0.3940(9)	-0.0205(6)	0.039(3)
C(44)	0.3603(13)	0.3433(10)	-0.0523(6)	0.047(3)
C(45)	0.4580(12)	0.3234(9)	-0.0106(6)	0.042(3)
C(46)	0.4349(10)	0.3516(8)	0.0645(6)	0.030(2)
C(51)	0.3988(9)	0.3926(8)	0.2468(6)	0.022(2)
C(52)	0.5138(9)	0.4274(8)	0.2101(6)	0.027(2)
C(53)	0.6122(10)	0.3912(9)	0.2533(7)	0.037(3)
C(54)	0.6022(11)	0.3194(10)	0.3331(8)	0.048(3)
C(55)	0.4883(10)	0.2871(9)	0.3696(7)	0.041(3)

C(56)	0.3889(9)	0.3223(8)	0.3268(6)	0.027(2)
C(61)	0.2455(8)	0.6118(8)	0.1586(5)	0.019(2)
C(62)	0.1977(9)	0.6826(8)	0.0864(6)	0.030(2)
C(63)	0.1777(10)	0.8056(8)	0.0638(6)	0.031(2)
C(64)	0.2058(9)	0.8625(8)	0.1126(6)	0.029(2)
C(65)	0.2541(9)	0.7943(8)	0.1833(6)	0.028(2)
C(66)	0.2733(9)	0.6696(8)	0.2071(5)	0.024(2)
C(70)	-0.3817(19)	0.630(2)	0.3565(11)	0.063(6)
Cl(2)	-0.4514(7)	0.7230(6)	0.2793(4)	0.063(2)
Cl(3)	-0.4892(14)	0.6012(13)	0.4383(9)	0.179(5)

Table A-7 Bond lengths (Å) for *cis*-[Pt{N(C(O)CH₂CN)(CO₂Et)}Cl(PPh₃)₂].
0.5CH₂Cl₂ (3.4)

Pt-N(1)	2.080(7)	Pt-P(2)	2.237(2)
Pt-P(1)	2.250(2)	Pt-Cl(1)	2.356(2)
P(1)-C(11)	1.800(9)	P(1)-C(21)	1.819(9)
P(1)-C(31)	1.835(10)	P(2)-C(51)	1.808(9)
P(2)-C(41)	1.812(9)	P(2)-C(61)	1.837(9)
N(1)-C(3)	1.351(11)	N(1)-C(4)	1.363(12)
N(2)-C(1)	1.147(13)	O(1)-C(3)	1.217(11)
O(2)-C(4)	1.214(11)	O(3)-C(4)	1.346(11)
O(3)-C(5)	1.459(12)	O(3)-C(5')	1.458(12)
C(1)-C(2)	1.448(16)	C(2)-C(3)	1.514(12)
C(5)-C(6)	1.45(2)	C(5')-C(6')	1.42(2)
C(11)-C(12)	1.393(13)	C(11)-C(16)	1.401(13)
C(12)-C(13)	1.382(13)	C(13)-C(14)	1.376(15)
C(14)-C(15)	1.370(16)	C(15)-C(16)	1.371(14)
C(21)-C(26)	1.383(13)	C(21)-C(22)	1.405(13)
C(22)-C(23)	1.365(13)	C(23)-C(24)	1.375(15)
C(24)-C(25)	1.363(15)	C(25)-C(26)	1.390(13)
C(31)-C(36)	1.391(13)	C(31)-C(32)	1.397(13)
C(32)-C(33)	1.358(15)	C(33)-C(34)	1.363(16)
C(34)-C(35)	1.377(15)	C(35)-C(36)	1.363(14)
C(41)-C(46)	1.388(13)	C(41)-C(42)	1.392(13)
C(42)-C(43)	1.407(13)	C(43)-C(44)	1.391(16)
C(44)-C(45)	1.371(16)	C(45)-C(46)	1.395(14)
C(51)-C(56)	1.384(13)	C(51)-C(52)	1.419(13)
C(52)-C(53)	1.358(14)	C(53)-C(54)	1.388(15)
C(54)-C(55)	1.395(15)	C(55)-C(56)	1.366(14)
C(61)-C(66)	1.389(12)	C(61)-C(62)	1.395(13)
C(62)-C(63)	1.366(13)	C(63)-C(64)	1.387(13)
C(64)-C(65)	1.371(13)	C(65)-C(66)	1.386(13)
C(70)-Cl(2)	1.631(16)	C(70)-Cl(3)	1.651(17)

Table A-8 Bond angles (°) for *cis*-[Pt{N(C(O)CH₂CN)(CO₂Et)}Cl(PPh₃)₂].
0.5CH₂Cl₂ (3.4)

N(1)-Pt-P(2)	89.7(2)	N(1)-Pt-P(1)	171.1(2)
P(2)-Pt-P(1)	98.30(9)	N(1)-Pt-Cl(1)	85.7(2)
P(2)-Pt-Cl(1)	175.32(9)	P(1)-Pt-Cl(1)	86.36(9)

C(11)-P(1)-C(21)	102.0(4)	C(11)-P(1)-C(31)	108.6(4)
C(21)-P(1)-C(31)	102.7(4)	C(11)-P(1)-Pt	113.2(3)
C(21)-P(1)-Pt	122.0(3)	C(31)-P(1)-Pt	107.4(3)
C(51)-P(2)-C(41)	109.8(4)	C(51)-P(2)-C(61)	102.6(4)
C(41)-P(2)-C(61)	103.3(4)	C(51)-P(2)-Pt	113.8(3)
C(41)-P(2)-Pt	113.6(3)	C(61)-P(2)-Pt	112.7(3)
C(3)-N(1)-C(4)	123.7(8)	C(3)-N(1)-Pt	113.4(6)
C(4)-N(1)-Pt	122.8(6)	C(4)-O(3)-C(5)	116.1(7)
N(2)-C(1)-C(2)	178.3(11)	C(1)-C(2)-C(3)	111.7(8)
O(1)-C(3)-N(1)	120.7(8)	O(1)-C(3)-C(2)	118.2(8)
N(1)-C(3)-C(2)	120.9(8)	O(2)-C(4)-O(3)	123.0(9)
O(2)-C(4)-N(1)	126.9(9)	O(3)-C(4)-N(1)	110.0(8)
C(6)-C(5)-O(3)	106.2(11)	C(6')-C(5')-O(3)	119(2)
C(12)-C(11)-C(16)	117.3(9)	C(12)-C(11)-P(1)	121.2(7)
C(16)-C(11)-P(1)	121.5(7)	C(13)-C(12)-C(11)	121.5(9)
C(14)-C(13)-C(12)	119.3(10)	C(15)-C(14)-C(13)	120.6(10)
C(14)-C(15)-C(16)	120.1(10)	C(15)-C(16)-C(11)	121.2(10)
C(26)-C(21)-C(22)	119.4(9)	C(26)-C(21)-P(1)	119.9(7)
C(22)-C(21)-P(1)	120.7(7)	C(23)-C(22)-C(21)	119.6(10)
C(22)-C(23)-C(24)	121.1(10)	C(25)-C(24)-C(23)	119.5(10)
C(24)-C(25)-C(26)	121.1(10)	C(21)-C(26)-C(25)	119.3(9)
C(36)-C(31)-C(32)	118.5(9)	C(36)-C(31)-P(1)	118.4(7)
C(32)-C(31)-P(1)	123.1(8)	C(33)-C(32)-C(31)	119.9(10)
C(32)-C(33)-C(34)	121.6(11)	C(33)-C(34)-C(35)	118.9(11)
C(36)-C(35)-C(34)	120.9(11)	C(35)-C(36)-C(31)	120.1(9)
C(46)-C(41)-C(42)	119.7(9)	C(46)-C(41)-P(2)	124.8(8)
C(42)-C(41)-P(2)	115.5(7)	C(41)-C(42)-C(43)	120.7(10)
C(44)-C(43)-C(42)	118.8(11)	C(45)-C(44)-C(43)	120.1(10)
C(44)-C(45)-C(46)	121.5(11)	C(41)-C(46)-C(45)	119.1(10)
C(56)-C(51)-C(52)	119.0(9)	C(56)-C(51)-P(2)	120.5(7)
C(52)-C(51)-P(2)	120.4(7)	C(53)-C(52)-C(51)	120.0(9)
C(52)-C(53)-C(54)	120.8(10)	C(53)-C(54)-C(55)	119.2(10)
C(56)-C(55)-C(54)	120.7(10)	C(55)-C(56)-C(51)	120.4(10)
C(66)-C(61)-C(62)	118.2(8)	C(66)-C(61)-P(2)	120.2(7)
C(62)-C(61)-P(2)	121.5(7)	C(63)-C(62)-C(61)	121.4(9)
C(62)-C(63)-C(64)	120.0(9)	C(65)-C(64)-C(63)	119.5(9)
C(64)-C(65)-C(66)	120.8(9)	C(65)-C(66)-C(61)	120.1(9)
Cl(2)-C(70)-Cl(3)	110.5(13)		

Table A-9 Anisotropic displacement parameters (\AA^2) for for *cis*-
[Pt{N(C(O)CH₂CN)(CO₂Et)}Cl(PPh₃)₂]. 0.5CH₂Cl₂ (**3.4**)

The anisotropic displacement factor exponent takes the form:

$$-2\pi^2 [h^2 a^{*2} U_{11} + \dots + 2 h k a^* b^* U_{12}].$$

	U11	U22	U33	U23	U13	U12
Pt	0.020(1)	0.012(1)	0.014(1)	-0.004(1)	0.000(1)	-0.005(1)
Cl(1)	0.021(1)	0.026(1)	0.026(1)	-0.011(1)	0.006(1)	-0.008(1)
P(1)	0.024(1)	0.014(1)	0.015(1)	-0.004(1)	0.003(1)	-0.006(1)
P(2)	0.024(1)	0.014(1)	0.013(1)	0.000(1)	-0.001(1)	-0.008(1)
N(1)	0.024(4)	0.019(4)	0.014(4)	-0.006(3)	-0.001(3)	-0.005(3)

N(2)	0.058(7)	0.031(6)	0.043(6)	0.010(5)	-0.011(5)	-0.010(5)
O(1)	0.056(5)	0.020(4)	0.034(4)	-0.003(3)	-0.023(4)	-0.006(3)
O(2)	0.076(6)	0.025(4)	0.037(4)	-0.020(4)	-0.015(4)	0.010(4)
O(3)	0.034(4)	0.030(4)	0.030(4)	-0.018(3)	-0.010(3)	-0.001(3)
C(1)	0.033(6)	0.013(5)	0.056(8)	-0.007(6)	-0.002(6)	-0.002(5)
C(2)	0.036(6)	0.021(5)	0.038(7)	0.001(5)	-0.014(5)	-0.004(5)
C(3)	0.032(6)	0.014(5)	0.026(6)	0.001(4)	-0.011(5)	-0.005(4)
C(4)	0.039(6)	0.025(6)	0.021(6)	-0.010(5)	0.001(5)	-0.002(5)
C(5)	0.059(8)	0.068(9)	0.040(7)	-0.037(7)	-0.023(6)	0.012(7)
C(5')	0.059(8)	0.068(9)	0.040(7)	-0.037(7)	-0.023(6)	0.012(7)
C(11)	0.026(5)	0.018(5)	0.024(6)	0.000(4)	0.002(4)	-0.006(4)
C(12)	0.029(6)	0.017(5)	0.024(6)	-0.002(4)	-0.001(4)	0.004(4)
C(13)	0.058(8)	0.032(6)	0.019(6)	-0.007(5)	-0.004(5)	0.004(6)
C(14)	0.091(11)	0.041(8)	0.022(7)	0.010(6)	0.005(7)	0.014(7)
C(15)	0.093(10)	0.026(6)	0.025(7)	0.010(5)	0.005(7)	0.015(6)
C(16)	0.047(7)	0.017(6)	0.033(6)	-0.010(5)	0.012(5)	-0.001(5)
C(21)	0.032(6)	0.010(5)	0.020(5)	-0.006(4)	0.004(4)	-0.010(4)
C(22)	0.034(6)	0.023(5)	0.022(5)	-0.006(4)	0.007(5)	-0.014(5)
C(23)	0.036(7)	0.042(7)	0.033(6)	-0.026(5)	0.014(5)	-0.013(5)
C(24)	0.043(8)	0.032(6)	0.045(7)	-0.020(6)	0.022(6)	-0.011(5)
C(25)	0.022(6)	0.035(6)	0.049(7)	-0.012(6)	-0.002(5)	-0.008(5)
C(26)	0.026(6)	0.022(5)	0.032(6)	-0.011(5)	-0.002(5)	0.000(4)
C(31)	0.030(6)	0.018(5)	0.022(5)	-0.010(4)	0.006(4)	-0.011(4)
C(32)	0.039(6)	0.026(6)	0.030(6)	-0.010(5)	0.009(5)	-0.016(5)
C(33)	0.048(7)	0.050(7)	0.039(7)	-0.028(6)	0.025(6)	-0.032(6)
C(34)	0.052(8)	0.074(9)	0.034(7)	-0.032(7)	0.012(6)	-0.045(7)
C(35)	0.038(7)	0.054(8)	0.037(7)	-0.014(6)	-0.005(5)	-0.019(6)
C(36)	0.030(6)	0.032(6)	0.029(6)	-0.007(5)	-0.003(5)	-0.018(5)
C(41)	0.042(6)	0.015(5)	0.020(5)	0.000(4)	0.003(5)	-0.018(5)
C(42)	0.048(7)	0.021(5)	0.018(5)	0.001(4)	-0.003(5)	-0.023(5)
C(43)	0.075(9)	0.031(6)	0.020(6)	0.000(5)	-0.007(6)	-0.033(6)
C(44)	0.089(10)	0.049(7)	0.015(6)	-0.012(5)	0.018(7)	-0.048(7)
C(45)	0.067(8)	0.035(7)	0.027(6)	-0.013(5)	0.024(6)	-0.034(6)
C(46)	0.039(6)	0.026(6)	0.025(6)	-0.005(5)	0.007(5)	-0.021(5)
C(51)	0.026(5)	0.013(5)	0.028(6)	-0.009(4)	-0.001(4)	-0.007(4)
C(52)	0.030(6)	0.023(5)	0.029(6)	-0.010(5)	-0.007(5)	-0.005(5)
C(53)	0.030(7)	0.025(6)	0.053(8)	-0.012(6)	0.005(6)	-0.008(5)
C(54)	0.036(7)	0.034(7)	0.079(10)	-0.007(7)	-0.035(7)	-0.007(6)
C(55)	0.045(7)	0.029(6)	0.047(7)	0.003(5)	-0.014(6)	-0.011(5)
C(56)	0.033(6)	0.021(5)	0.030(6)	-0.004(5)	-0.012(5)	-0.009(5)
C(61)	0.019(5)	0.025(5)	0.014(5)	-0.002(4)	0.007(4)	-0.018(4)
C(62)	0.041(6)	0.024(6)	0.028(6)	-0.003(5)	-0.008(5)	-0.016(5)
C(63)	0.051(7)	0.018(6)	0.025(6)	0.004(4)	-0.015(5)	-0.013(5)
C(64)	0.042(6)	0.015(5)	0.028(6)	-0.001(5)	0.001(5)	-0.013(5)
C(65)	0.033(6)	0.019(5)	0.034(6)	-0.009(5)	-0.004(5)	-0.007(5)
C(66)	0.036(6)	0.024(6)	0.017(5)	-0.009(4)	-0.008(4)	-0.007(5)

Table A-10 Hydrogen coordinates and isotropic displacement parameters (\AA^2) for *cis*-
[Pt{N(C(O)CH₂CN)(CO₂Et)}Cl(PPh₃)₂]. 0.5CH₂Cl₂ (**3.4**)

	x	Y	z	U(eq)
H(2A)	-0.1930	0.7998	0.2227	0.040
H(2B)	-0.0518	0.8172	0.1889	0.040
H(5A)	0.1196	0.6796	0.4164	0.066
H(5B)	0.0294	0.6014	0.4820	0.066
H(6A)	0.2322	0.5354	0.5172	0.105
H(6B)	0.2927	0.5102	0.4291	0.105
H(6C)	0.2034	0.4304	0.4926	0.105
H(5'A)	0.0206	0.6434	0.4613	0.066
H(5'B)	0.1358	0.5259	0.4834	0.066
H(6'A)	0.1924	0.6936	0.4687	0.136
H(6'B)	0.1606	0.7454	0.3771	0.136
H(6'C)	0.2764	0.6272	0.3992	0.136
H(12)	0.0978	0.2403	0.4353	0.033
H(13)	0.1191	0.1177	0.5670	0.049
H(14)	0.1981	-0.0913	0.5877	0.080
H(15)	0.2561	-0.1776	0.4779	0.075
H(16)	0.2375	-0.0566	0.3465	0.044
H(22)	0.2137	0.1375	0.1184	0.032
H(23)	0.4024	0.0501	0.0440	0.043
H(24)	0.5945	-0.0141	0.0946	0.051
H(25)	0.5990	0.0160	0.2184	0.043
H(26)	0.4113	0.1062	0.2954	0.033
H(32)	0.0263	-0.0004	0.3138	0.038
H(33)	-0.1286	-0.0312	0.2627	0.052
H(34)	-0.2174	0.1089	0.1523	0.054
H(35)	-0.1610	0.2913	0.0987	0.049
H(36)	-0.0132	0.3302	0.1520	0.034
H(42)	0.1244	0.4534	0.0789	0.033
H(43)	0.1666	0.4097	-0.0496	0.047
H(44)	0.3785	0.3225	-0.1030	0.057
H(45)	0.5435	0.2896	-0.0333	0.051
H(46)	0.5036	0.3362	0.0929	0.035
H(52)	0.5220	0.4759	0.1553	0.032
H(53)	0.6886	0.4153	0.2285	0.045
H(54)	0.6721	0.2927	0.3626	0.057
H(55)	0.4799	0.2400	0.4249	0.050
H(56)	0.3124	0.2984	0.3522	0.032
H(62)	0.1786	0.6444	0.0524	0.035
H(63)	0.1446	0.8521	0.0146	0.037
H(64)	0.1917	0.9480	0.0972	0.035
H(65)	0.2747	0.8330	0.2164	0.034
H(66)	0.3055	0.6236	0.2566	0.029

Table A-11 Atomic coordinates and equivalent isotropic displacement parameters for $[\text{C}_6\text{H}_4(\text{CH}_2\text{NMe}_2)\text{-2}]\text{Au}\{\text{N}(\text{Ph})\text{C}(\text{O})\text{CHC}(\text{O})\text{CH}_3\}$ (4.13)

U(eq) is defined as one third of the trace of the orthogonalised Uij tensor.

	x	y	z	U(eq)
Au	0.0252(1)	0.2210(1)	0.4983(1)	0.025(1)
O(1)	-0.1122(3)	-0.1227(3)	0.7784(3)	0.043(1)
O(2)	-0.3968(3)	0.2633(4)	0.6335(3)	0.057(1)
N(1)	0.2364(3)	0.3005(3)	0.3955(3)	0.029(1)
N(2)	0.0822(3)	0.0203(3)	0.6689(3)	0.032(1)
C(1)	-0.0644(4)	-0.0125(4)	0.6944(3)	0.030(1)
C(2)	-0.1683(4)	0.1258(4)	0.5988(4)	0.031(1)
C(3)	-0.2665(4)	0.1982(4)	0.6728(4)	0.036(1)
C(4)	-0.2006(6)	0.1911(6)	0.7973(5)	0.051(1)
C(11)	-0.0734(4)	0.4056(4)	0.3408(3)	0.029(1)
C(12)	0.0328(4)	0.4699(4)	0.2329(3)	0.030(1)
C(13)	-0.0171(4)	0.5995(4)	0.1183(4)	0.036(1)
C(14)	-0.1710(5)	0.6660(4)	0.1115(4)	0.041(1)
C(15)	-0.2757(4)	0.6022(4)	0.2176(4)	0.039(1)
C(16)	-0.2282(4)	0.4719(4)	0.3323(3)	0.031(1)
C(17)	0.1960(4)	0.3898(4)	0.2449(3)	0.032(1)
C(18)	0.3696(4)	0.1851(4)	0.4139(4)	0.037(1)
C(19)	0.2797(5)	0.3932(4)	0.4490(4)	0.039(1)
C(21)	0.2127(4)	-0.0707(4)	0.7510(3)	0.029(1)
C(22)	0.3225(4)	-0.0116(4)	0.7839(4)	0.036(1)
C(23)	0.4500(5)	-0.0991(5)	0.8654(4)	0.045(1)
C(24)	0.4682(4)	-0.2452(5)	0.9159(4)	0.041(1)
C(25)	0.3611(4)	-0.3042(4)	0.8841(4)	0.039(1)
C(26)	0.2336(4)	-0.2183(4)	0.8007(4)	0.032(1)

Table A-12 Bond lengths (Å) for $[\text{C}_6\text{H}_4(\text{CH}_2\text{NMe}_2)\text{-2}]\text{Au}\{\text{N}(\text{Ph})\text{C}(\text{O})\text{CHC}(\text{O})\text{CH}_3\}$ (4.13)

Au-C(11)	2.027(3)	Au-C(2)	2.076(3)
Au-N(2)	2.097(3)	Au-N(1)	2.157(3)
Au.....C(1)	2.616(3)	O(1)-C(1)	1.226(4)
O(2)-C(3)	1.220(5)	N(1)-C(18)	1.491(4)
N(1)-C(19)	1.494(5)	N(1)-C(17)	1.511(4)
N(2)-C(1)	1.356(4)	N(2)-C(21)	1.425(4)
C(1)-C(2)	1.536(5)	C(2)-C(3)	1.495(5)
C(3)-C(4)	1.504(6)	C(11)-C(16)	1.397(5)
C(11)-C(12)	1.409(5)	C(12)-C(13)	1.397(5)
C(12)-C(17)	1.507(5)	C(13)-C(14)	1.393(5)
C(14)-C(15)	1.390(6)	C(15)-C(16)	1.396(5)
C(21)-C(26)	1.398(5)	C(21)-C(22)	1.401(5)
C(22)-C(23)	1.395(5)	C(23)-C(24)	1.383(6)
C(24)-C(25)	1.375(6)	C(25)-C(26)	1.399(5)

Table A-13 Bond Angles (°) for $[\text{C}_6\text{H}_4(\text{CH}_2\text{NMe}_2)\text{-}2]\text{Au}\{\text{N}(\text{Ph})\text{C}(\text{O})\text{CHC}(\text{O})\text{CH}_3\}$

(4.13)

C(11)-Au-C(2)	102.06(13)	C(11)-Au-N(2)	168.64(12)
C(2)-Au-N(2)	66.65(12)	C(11)-Au-N(1)	81.74(12)
C(2)-Au-N(1)	174.54(12)	N(2)-Au-N(1)	109.42(11)
C(11)-Au.....C(1)	137.61(12)	C(2)-Au.....C(1)	35.95(12)
N(2)-Au.....C(1)	31.04(10)	N(1)-Au.....C(1)	139.67(10)
C(18)-N(1)-C(19)	109.4(3)	C(18)-N(1)-C(17)	110.4(3)
C(19)-N(1)-C(17)	109.4(3)	C(18)-N(1)-Au	113.2(2)
C(19)-N(1)-Au	108.9(2)	C(17)-N(1)-Au	105.54(19)
C(1)-N(2)-C(21)	123.4(3)	C(1)-N(2)-Au	96.1(2)
C(21)-N(2)-Au	140.5(2)	O(1)-C(1)-N(2)	130.3(3)
O(1)-C(1)-C(2)	124.9(3)	N(2)-C(1)-C(2)	104.7(3)
O(1)-C(1).....Au	174.9(3)	N(2)-C(1).....Au	52.85(17)
C(2)-C(1).....Au	52.50(16)	C(3)-C(2)-C(1)	113.7(3)
C(3)-C(2)-Au	113.8(2)	C(1)-C(2)-Au	91.5(2)
O(2)-C(3)-C(2)	121.5(4)	O(2)-C(3)-C(4)	120.0(4)
C(2)-C(3)-C(4)	118.5(3)	C(16)-C(11)-C(12)	119.8(3)
C(16)-C(11)-Au	127.1(3)	C(12)-C(11)-Au	113.2(2)
C(13)-C(12)-C(11)	119.9(3)	C(13)-C(12)-C(17)	122.8(3)
C(11)-C(12)-C(17)	117.3(3)	C(14)-C(13)-C(12)	120.0(3)
C(15)-C(14)-C(13)	120.0(3)	C(14)-C(15)-C(16)	120.7(3)
C(15)-C(16)-C(11)	119.6(3)	C(12)-C(17)-N(1)	109.1(3)
C(26)-C(21)-C(22)	118.9(3)	C(26)-C(21)-N(2)	121.6(3)
C(22)-C(21)-N(2)	119.5(3)	C(23)-C(22)-C(21)	120.4(4)
C(24)-C(23)-C(22)	120.2(4)	C(25)-C(24)-C(23)	119.9(3)
C(24)-C(25)-C(26)	120.9(4)	C(21)-C(26)-C(25)	119.7(3)

Table A-14 Anisotropic displacement parameters (\AA^2) for $[\text{C}_6\text{H}_4(\text{CH}_2\text{NMe}_2)\text{-}2]\text{Au}\{\text{N}(\text{Ph})\text{C}(\text{O})\text{CHC}(\text{O})\text{CH}_3\}$ (4.13)

The anisotropic displacement factor exponent takes the form:

$$-2\pi^2 [h^2 a^{*2} U_{11} + \dots + 2 h k a^* b^* U_{12}]$$

	U11	U22	U33	U23	U13	U12
Au	0.022(1)	0.027(1)	0.021(1)	-0.010(1)	0.001(1)	-0.003(1)
O(1)	0.036(1)	0.034(1)	0.046(2)	-0.006(1)	0.002(1)	-0.011(1)
O(2)	0.029(1)	0.070(2)	0.056(2)	-0.023(2)	0.004(1)	0.008(1)
N(1)	0.027(1)	0.031(1)	0.026(1)	-0.012(1)	0.002(1)	-0.004(1)
N(2)	0.027(1)	0.031(1)	0.031(1)	-0.008(1)	-0.001(1)	-0.007(1)
C(1)	0.028(2)	0.032(2)	0.028(2)	-0.013(1)	0.002(1)	-0.004(1)
C(2)	0.027(2)	0.033(2)	0.027(2)	-0.010(1)	0.000(1)	-0.007(1)
C(3)	0.030(2)	0.036(2)	0.031(2)	-0.007(2)	0.008(1)	-0.007(1)
C(4)	0.053(3)	0.058(3)	0.043(2)	-0.028(2)	0.008(2)	-0.004(2)
C(11)	0.031(2)	0.030(2)	0.024(2)	-0.012(1)	-0.002(1)	-0.003(1)
C(12)	0.033(2)	0.032(2)	0.024(2)	-0.011(1)	0.000(1)	-0.006(1)
C(13)	0.037(2)	0.038(2)	0.025(2)	-0.007(2)	0.000(1)	-0.007(1)
C(14)	0.047(2)	0.036(2)	0.026(2)	-0.004(2)	-0.010(2)	-0.002(2)
C(15)	0.034(2)	0.047(2)	0.033(2)	-0.018(2)	-0.008(2)	0.004(2)
C(16)	0.030(2)	0.039(2)	0.023(2)	-0.014(1)	0.000(1)	-0.002(1)

C(17)	0.032(2)	0.037(2)	0.022(2)	-0.008(1)	0.004(1)	-0.009(1)
C(18)	0.025(2)	0.045(2)	0.034(2)	-0.015(2)	0.003(1)	0.002(2)
C(19)	0.037(2)	0.043(2)	0.042(2)	-0.021(2)	-0.005(2)	-0.009(2)
C(21)	0.026(2)	0.035(2)	0.023(2)	-0.010(1)	0.001(1)	-0.003(1)
C(22)	0.035(2)	0.039(2)	0.033(2)	-0.016(2)	-0.004(1)	-0.005(2)
C(23)	0.037(2)	0.063(3)	0.036(2)	-0.023(2)	-0.005(2)	-0.009(2)
C(24)	0.030(2)	0.055(2)	0.027(2)	-0.014(2)	-0.006(1)	0.007(2)
C(25)	0.038(2)	0.037(2)	0.031(2)	-0.010(2)	0.001(1)	0.005(2)
C(26)	0.029(2)	0.035(2)	0.029(2)	-0.012(1)	0.001(1)	-0.002(1)

Table A-15 Hydrogen coordinates and isotropic displacement parameters (\AA^2) for $[\text{C}_6\text{H}_4(\text{CH}_2\text{NMe}_2)\text{-2}]\text{Au}\{\text{N}(\text{Ph})\text{C}(\text{O})\text{CHC}(\text{O})\text{CH}_3\}$ (4.13)

	x	y	z	U(eq)
H(2)	-0.233(5)	0.122(4)	0.531(4)	0.037
H(4A)	-0.101(6)	0.207(6)	0.785(5)	0.061
H(4B)	-0.277(6)	0.257(6)	0.829(5)	0.061
H(4C)	-0.184(6)	0.092(6)	0.875(6)	0.061
H(13)	0.055(5)	0.645(5)	0.042(5)	0.043
H(14)	-0.201(5)	0.750(5)	0.035(5)	0.049
H(15)	-0.382(5)	0.650(5)	0.223(5)	0.047
H(16)	-0.300(5)	0.431(4)	0.405(4)	0.038
H(17A)	0.197(5)	0.325(5)	0.210(5)	0.039
H(17B)	0.276(5)	0.453(5)	0.203(4)	0.039
H(18A)	0.396(5)	0.134(5)	0.503(5)	0.045
H(18B)	0.458(5)	0.226(5)	0.371(5)	0.045
H(18C)	0.332(5)	0.119(5)	0.381(5)	0.045
H(19A)	0.379(5)	0.440(5)	0.388(5)	0.047
H(19B)	0.310(5)	0.335(5)	0.551(5)	0.047
H(19C)	0.191(5)	0.462(5)	0.444(5)	0.047
H(22)	0.303(5)	0.085(5)	0.758(5)	0.043
H(23)	0.520(5)	-0.054(5)	0.885(5)	0.054
H(24)	0.544(5)	-0.299(5)	0.961(5)	0.049
H(25)	0.378(5)	-0.408(5)	0.920(5)	0.047
H(26)	0.163(5)	-0.256(5)	0.774(4)	0.039

Table A-16 Atomic coordinates and equivalent isotropic displacement parameters (\AA^2) for $[\{C_6H_3(CH_2NMe_2)-2-(OMe)-5\}Au\{N(CO_2Et)C(O)CHCN\}]_2 \cdot 2CDCl_3$ (**4.15**)

U(eq) is defined as one third of the trace of the orthogonalised Uij tensor.

	x	y	z	U(eq)
Au	0.1700(1)	0.0999(1)	0.5138(1)	0.016(1)
N(1)	0.2596(2)	0.1948(2)	0.6454(2)	0.022(1)
N(2)	-0.0389(3)	-0.1119(2)	0.8139(3)	0.036(1)
N(3)	0.0189(2)	0.0924(2)	0.5528(2)	0.018(1)
O(1)	0.4642(2)	0.0679(2)	0.2908(2)	0.033(1)
O(2)	0.1191(2)	-0.0058(2)	0.6913(2)	0.022(1)
O(3)	-0.1791(2)	0.1354(2)	0.4882(2)	0.028(1)
O(4)	-0.0538(2)	0.1950(2)	0.4175(2)	0.026(1)
C(1)	-0.0604(3)	-0.0688(2)	0.7325(3)	0.024(1)
C(2)	-0.0906(3)	-0.0147(2)	0.6280(3)	0.019(1)
C(3)	0.0222(2)	0.0254(2)	0.6275(2)	0.018(1)
C(4)	-0.0818(3)	0.1394(2)	0.4868(3)	0.020(1)
C(5)	-0.1522(3)	0.2418(3)	0.3310(4)	0.041(1)
C(6)	-0.1014(4)	0.3055(3)	0.2722(4)	0.055(1)
C(10)	0.5750(3)	0.0825(3)	0.2822(3)	0.036(1)
C(11)	0.3228(2)	0.1066(2)	0.4899(3)	0.020(1)
C(12)	0.4145(3)	0.1464(2)	0.5855(3)	0.025(1)
C(13)	0.5242(3)	0.1595(3)	0.5810(3)	0.033(1)
C(14)	0.5461(3)	0.1340(2)	0.4847(3)	0.030(1)
C(15)	0.4551(3)	0.0944(2)	0.3907(3)	0.023(1)
C(16)	0.3441(3)	0.0803(2)	0.3938(3)	0.021(1)
C(17)	0.3878(3)	0.1713(2)	0.6880(3)	0.028(1)
C(18)	0.2227(3)	0.1976(2)	0.7447(3)	0.028(1)
C(19)	0.2383(3)	0.2835(2)	0.5889(3)	0.032(1)
C(20)	-0.2511(1)	0.0476(1)	0.0360(1)	0.040(1)
Cl(1)	-0.3221(1)	0.1503(1)	0.0018(1)	0.082(1)
Cl(2)	-0.1791(1)	0.0192(1)	-0.0551(1)	0.063(1)
Cl(3)	-0.3577(1)	-0.0345(1)	0.0244(1)	0.052(1)

Table A-17 Bond lengths [\AA] for $[\{C_6H_3(CH_2NMe_2)-2-(OMe)-5\}Au\{N(CO_2Et)C(O)CHCN\}]_2 \cdot 2CDCl_3$ (**4.15**)

Au-C(11)	2.031(3)	Au-C(2')	2.098(3)
Au-N(3)	2.116(3)	Au-N(1)	2.137(3)
N(1)-C(18)	1.492(4)	N(1)-C(19)	1.495(4)
N(1)-C(17)	1.497(4)	N(2)-C(1)	1.152(5)
N(3)-C(3)	1.374(4)	N(3)-C(4)	1.384(4)
O(1)-C(15)	1.366(4)	O(1)-C(10)	1.433(4)
O(2)-C(3)	1.237(4)	O(3)-C(4)	1.211(4)
O(4)-C(4)	1.353(4)	O(4)-C(5)	1.450(4)
C(1)-C(2)	1.464(4)	C(2)-C(3)	1.523(4)
C(2)-Au'	2.098(3)	C(5)-C(6)	1.499(5)
C(11)-C(16)	1.394(4)	C(11)-C(12)	1.413(4)
C(12)-C(13)	1.394(4)	C(12)-C(17)	1.501(5)
C(13)-C(14)	1.396(5)	C(14)-C(15)	1.397(5)

C(15)-C(16)	1.404(4)		
C(20)-Cl(1)	1.7568	C(20)-Cl(2)	1.7620
C(20)-Cl(3)	1.7764		

Symmetry transformations used to generate equivalent atoms: #’ -x,-y,-z+1

Table A-18 Bond angles (°) for [$\{C_6H_3(CH_2NMe_2)-2-(OMe)-$
 $\overline{5}\}Au\{N(CO_2Et)C(O)CHCN\}]_2 \cdot 2CDCl_3$ (**4.15**)

C(11)-Au-C(2’)	92.89(12)	C(11)-Au-N(3)	175.52(10)
C(2’)-Au-N(3)	90.53(10)	C(11)-Au-N(1)	81.78(11)
C(2’)-Au-N(1)	173.03(10)	N(3)-Au-N(1)	95.04(9)
C(18)-N(1)-C(19)	108.5(3)	C(18)-N(1)-C(17)	110.1(3)
C(19)-N(1)-C(17)	110.1(3)	C(18)-N(1)-Au	115.36(19)
C(19)-N(1)-Au	107.59(19)	C(17)-N(1)-Au	105.05(19)
C(3)-N(3)-C(4)	124.3(2)	C(3)-N(3)-Au	114.33(19)
C(4)-N(3)-Au	119.84(19)	C(15)-O(1)-C(10)	117.3(3)
C(4)-O(4)-C(5)	115.7(2)	N(2)-C(1)-C(2)	178.7(3)
C(1)-C(2)-C(3)	108.9(2)	C(1)-C(2)-Au’	106.2(2)
C(3)-C(2)-Au’	111.02(19)	O(2)-C(3)-N(3)	118.7(3)
O(2)-C(3)-C(2)	119.6(3)	N(3)-C(3)-C(2)	121.6(3)
O(3)-C(4)-O(4)	123.6(3)	O(3)-C(4)-N(3)	128.5(3)
O(4)-C(4)-N(3)	107.8(2)	O(4)-C(5)-C(6)	107.1(3)
C(16)-C(11)-C(12)	119.5(3)	C(16)-C(11)-Au	128.6(2)
C(12)-C(11)-Au	111.8(2)	C(13)-C(12)-C(11)	119.1(3)
C(13)-C(12)-C(17)	123.5(3)	C(11)-C(12)-C(17)	117.3(3)
C(12)-C(13)-C(14)	121.7(3)	C(13)-C(14)-C(15)	118.8(3)
O(1)-C(15)-C(14)	124.6(3)	O(1)-C(15)-C(16)	115.1(3)
C(14)-C(15)-C(16)	120.3(3)	C(11)-C(16)-C(15)	120.5(3)
N(1)-C(17)-C(12)	108.7(3)		
Cl(1)-C(20)-Cl(2)	113.0	Cl(1)-C(20)-Cl(3)	108.7
Cl(2)-C(20)-Cl(3)	109.1		

Symmetry transformations used to generate equivalent atoms: #’ -x,-y,-z+1

Table A-19 Anisotropic displacement parameters (\AA^2) for [$\{C_6H_3(CH_2NMe_2)-2-(OMe)-$
 $\overline{5}\}Au\{N(CO_2Et)C(O)CHCN\}]_2 \cdot 2CDCl_3$ (**4.15**)

The anisotropic displacement factor exponent takes the form:

$$-2\pi^2 [h^2 a^{*2} U_{11} + \dots + 2 h k a^* b^* U_{12}]$$

	U11	U22	U33	U23	U13	U12
Au	0.012(1)	0.017(1)	0.019(1)	-0.001(1)	0.007(1)	-0.003(1)
N(1)	0.019(1)	0.023(1)	0.026(1)	-0.005(1)	0.011(1)	-0.006(1)
N(2)	0.033(2)	0.048(2)	0.027(2)	0.007(1)	0.010(1)	-0.011(1)
N(3)	0.014(1)	0.020(1)	0.021(1)	-0.001(1)	0.009(1)	-0.003(1)

O(1)	0.020(1)	0.054(2)	0.030(1)	-0.003(1)	0.014(1)	-0.003(1)
O(2)	0.017(1)	0.025(1)	0.023(1)	0.001(1)	0.007(1)	-0.002(1)
O(3)	0.019(1)	0.036(1)	0.034(1)	0.005(1)	0.014(1)	0.002(1)
O(4)	0.022(1)	0.027(1)	0.033(1)	0.010(1)	0.013(1)	0.003(1)
C(1)	0.019(1)	0.032(2)	0.023(2)	-0.006(1)	0.009(1)	-0.011(1)
C(2)	0.016(1)	0.022(2)	0.021(1)	-0.002(1)	0.009(1)	-0.006(1)
C(3)	0.017(1)	0.018(1)	0.020(1)	-0.005(1)	0.009(1)	-0.004(1)
C(4)	0.016(1)	0.022(2)	0.022(1)	-0.003(1)	0.009(1)	-0.001(1)
C(5)	0.034(2)	0.044(2)	0.048(2)	0.024(2)	0.018(2)	0.016(2)
C(6)	0.053(3)	0.055(3)	0.065(3)	0.037(2)	0.032(2)	0.014(2)
C(10)	0.023(2)	0.055(2)	0.035(2)	0.000(2)	0.019(2)	-0.001(2)
C(11)	0.014(1)	0.020(2)	0.026(2)	0.001(1)	0.009(1)	-0.002(1)
C(12)	0.017(1)	0.028(2)	0.030(2)	-0.005(1)	0.009(1)	-0.002(1)
C(13)	0.016(2)	0.043(2)	0.037(2)	-0.012(2)	0.008(1)	-0.008(1)
C(14)	0.013(1)	0.038(2)	0.040(2)	-0.005(2)	0.011(1)	-0.008(1)
C(15)	0.017(1)	0.029(2)	0.024(2)	0.005(1)	0.010(1)	0.004(1)
C(16)	0.014(1)	0.023(1)	0.024(2)	0.001(1)	0.008(1)	-0.002(1)
C(17)	0.017(1)	0.038(2)	0.028(2)	-0.009(1)	0.007(1)	-0.006(1)
C(18)	0.031(2)	0.032(2)	0.027(2)	-0.009(1)	0.016(1)	-0.009(1)
C(19)	0.039(2)	0.022(2)	0.040(2)	-0.005(1)	0.019(2)	-0.006(1)
C(20)	0.042(2)	0.042(2)	0.034(2)	-0.002(2)	0.014(2)	0.006(2)
Cl(1)	0.122(1)	0.049(1)	0.082(1)	0.014(1)	0.049(1)	0.030(1)
Cl(2)	0.059(1)	0.078(1)	0.063(1)	-0.030(1)	0.037(1)	-0.020(1)
Cl(3)	0.041(1)	0.065(1)	0.050(1)	-0.004(1)	0.018(1)	-0.001(1)

Table A-20 Hydrogen coordinates and isotropic displacement parameters (\AA^2) for
 $[\{\text{C}_6\text{H}_3(\text{CH}_2\text{NMe}_2)\text{-2-(OMe)-5}\}\text{Au}\{\text{N}(\text{CO}_2\text{Et})\text{C}(\text{O})\text{CHCN}\}]_2 \cdot 2\text{CDCl}_3$ (**4.15**)

	x	y	z	U(eq)
H(2A)	-0.151(3)	0.028(2)	0.621(3)	0.023
H(5A)	-0.1969	0.2734	0.3681	0.049
H(5B)	-0.2055	0.2004	0.2741	0.049
H(6A)	-0.1648	0.3394	0.2152	0.083
H(6B)	-0.0596	0.2733	0.2338	0.083
H(6C)	-0.0471	0.3450	0.3297	0.083
H(10A)	0.5695	0.0628	0.2068	0.053
H(10B)	0.6366	0.0497	0.3428	0.053
H(10C)	0.5938	0.1448	0.2912	0.053
H(13A)	0.5851	0.1862	0.6445	0.040
H(14A)	0.6206	0.1434	0.4831	0.036
H(16A)	0.2836	0.0530	0.3305	0.025
H(17A)	0.4057	0.1218	0.7425	0.034
H(17B)	0.4367	0.2216	0.7286	0.034
H(18A)	0.2764	0.2350	0.8056	0.042
H(18B)	0.2246	0.1385	0.7748	0.042
H(18C)	0.1431	0.2209	0.7183	0.042
H(19A)	0.2804	0.3278	0.6461	0.049
H(19B)	0.1543	0.2963	0.5569	0.049
H(19C)	0.2662	0.2838	0.5270	0.049
H(20)	-0.1917	0.0492	0.1173	0.048

Table A-21 Atomic coordinates and equivalent isotropic displacement parameters (\AA^2) for *cis*-[Pt(CH₂CN)₂(PPh₃)₂].0.6CH₂Cl₂ (5.7)

U(eq) is defined as one third of the trace of the orthogonalised Uij tensor.

	x	y	z	U(eq)
Pt	0.8760(1)	0.9117(1)	0.7216(1)	0.031(1)
P(1)	0.9117(2)	0.7515(2)	0.6321(1)	0.031(1)
P(2)	0.9860(2)	0.7778(2)	0.8118(1)	0.030(1)
N(1)	0.5204(8)	1.0782(13)	0.6661(5)	0.112(4)
C(1)	0.6338(9)	1.0731(10)	0.6597(5)	0.059(2)
C(2)	0.7764(7)	1.0591(7)	0.6502(4)	0.038(2)
N(2)	0.5854(9)	1.1847(10)	0.8325(5)	0.086(3)
C(3)	0.7005(9)	1.1364(8)	0.8171(4)	0.048(2)
C(4)	0.8430(7)	1.0718(7)	0.7982(4)	0.037(2)
C(11)	1.0942(7)	0.6720(7)	0.6092(4)	0.034(2)
C(12)	1.1549(8)	0.5363(9)	0.6058(4)	0.047(2)
C(13)	1.2970(9)	0.4910(10)	0.5894(4)	0.060(3)
C(14)	1.3773(9)	0.5801(14)	0.5764(5)	0.078(4)
C(15)	1.3197(8)	0.7133(12)	0.5800(5)	0.064(3)
C(16)	1.1782(7)	0.7628(10)	0.5960(4)	0.052(2)
C(21)	0.8579(7)	0.8059(7)	0.5405(4)	0.034(2)
C(22)	0.7179(8)	0.8342(9)	0.5339(4)	0.050(2)
C(23)	0.6724(8)	0.8711(9)	0.4663(4)	0.053(2)
C(24)	0.7639(8)	0.8822(9)	0.4029(4)	0.051(2)
C(25)	0.9013(9)	0.8569(10)	0.4090(4)	0.057(2)
C(26)	0.9480(8)	0.8198(9)	0.4770(4)	0.048(2)
C(31)	0.8172(7)	0.6247(7)	0.6543(4)	0.034(2)
C(32)	0.7192(7)	0.6404(8)	0.7186(4)	0.041(2)
C(33)	0.6403(8)	0.5470(9)	0.7333(4)	0.053(2)
C(34)	0.6560(8)	0.4447(9)	0.6865(5)	0.056(2)
C(35)	0.7488(8)	0.4311(8)	0.6205(5)	0.049(2)
C(36)	0.8288(8)	0.5206(8)	0.6056(4)	0.043(2)
C(41)	1.0823(7)	0.6031(7)	0.7975(3)	0.032(2)
C(42)	1.0103(8)	0.5072(8)	0.7945(4)	0.041(2)
C(43)	1.0799(10)	0.3720(8)	0.7840(5)	0.055(2)
C(44)	1.2219(10)	0.3346(10)	0.7763(4)	0.060(2)
C(45)	1.2916(9)	0.4283(9)	0.7795(4)	0.056(2)
C(46)	1.2249(7)	0.5602(8)	0.7897(4)	0.044(2)
C(51)	1.1122(7)	0.8575(8)	0.8389(4)	0.036(2)
C(52)	1.2107(8)	0.8842(9)	0.7816(4)	0.049(2)
C(53)	1.3102(8)	0.9436(9)	0.7987(5)	0.054(2)
C(54)	1.3101(8)	0.9801(9)	0.8702(5)	0.057(2)
C(55)	1.2125(9)	0.9582(10)	0.9268(5)	0.060(2)
C(56)	1.1149(8)	0.8945(9)	0.9118(4)	0.051(2)
C(61)	0.8704(7)	0.7631(7)	0.8967(4)	0.036(2)
C(62)	0.7294(7)	0.8263(7)	0.9021(4)	0.038(2)
C(63)	0.6423(8)	0.8117(8)	0.9671(4)	0.043(2)
C(64)	0.6931(8)	0.7345(8)	1.0254(4)	0.046(2)
C(65)	0.8294(9)	0.6718(9)	1.0207(4)	0.051(2)
C(66)	0.9193(7)	0.6846(8)	0.9564(4)	0.042(2)

Table A-22 Bond lengths (Å) for *cis*-[Pt(CH₂CN)₂(PPh₃)₂].0.6CH₂Cl₂ (5.7)

Pt-C(2)	2.104(7)	Pt-C(4)	2.138(7)
Pt-P(1)	2.2953(18)	Pt-P(2)	2.3161(18)
P(1)-C(31)	1.822(7)	P(1)-C(11)	1.826(7)
P(1)-C(21)	1.840(7)	P(2)-C(61)	1.824(7)
P(2)-C(41)	1.830(7)	P(2)-C(51)	1.836(7)
N(1)-C(1)	1.136(10)	C(1)-C(2)	1.413(10)
N(2)-C(3)	1.150(10)	C(3)-C(4)	1.433(10)
C(11)-C(12)	1.381(11)	C(11)-C(16)	1.422(10)
C(12)-C(13)	1.396(11)	C(13)-C(14)	1.379(14)
C(14)-C(15)	1.351(15)	C(15)-C(16)	1.394(11)
C(21)-C(26)	1.391(9)	C(21)-C(22)	1.407(9)
C(22)-C(23)	1.374(10)	C(23)-C(24)	1.392(11)
C(24)-C(25)	1.380(11)	C(25)-C(26)	1.386(10)
C(31)-C(36)	1.395(10)	C(31)-C(32)	1.405(9)
C(32)-C(33)	1.407(10)	C(33)-C(34)	1.349(12)
C(34)-C(35)	1.401(11)	C(35)-C(36)	1.382(10)
C(41)-C(42)	1.390(10)	C(41)-C(46)	1.397(10)
C(42)-C(43)	1.403(11)	C(43)-C(44)	1.389(12)
C(44)-C(45)	1.354(13)	C(45)-C(46)	1.365(11)
C(51)-C(56)	1.396(10)	C(51)-C(52)	1.407(10)
C(52)-C(53)	1.396(10)	C(53)-C(54)	1.364(12)
C(54)-C(55)	1.376(12)	C(55)-C(56)	1.395(11)
C(61)-C(66)	1.395(10)	C(61)-C(62)	1.410(9)
C(62)-C(63)	1.395(9)	C(63)-C(64)	1.375(11)
C(64)-C(65)	1.367(11)	C(65)-C(66)	1.397(10)

Table A-23 Bond angles (°) for *cis*-[Pt(CH₂CN)₂(PPh₃)₂].0.6CH₂Cl₂ (5.7)

C(2)-Pt-C(4)	85.3(3)	C(2)-Pt-P(1)	90.9(2)
C(4)-Pt-P(1)	175.7(2)	C(2)-Pt-P(2)	170.8(2)
C(4)-Pt-P(2)	85.6(2)	P(1)-Pt-P(2)	98.09(6)
C(31)-P(1)-C(11)	110.1(3)	C(31)-P(1)-C(21)	98.8(3)
C(11)-P(1)-C(21)	103.4(3)	C(31)-P(1)-Pt	115.3(2)
C(11)-P(1)-Pt	110.4(2)	C(21)-P(1)-Pt	117.7(2)
C(61)-P(2)-C(41)	100.8(3)	C(61)-P(2)-C(51)	106.4(3)
C(41)-P(2)-C(51)	103.4(3)	C(61)-P(2)-Pt	112.8(2)
C(41)-P(2)-Pt	124.2(2)	C(51)-P(2)-Pt	107.8(2)
N(1)-C(1)-C(2)	176.7(12)	C(1)-C(2)-Pt	112.1(5)
N(2)-C(3)-C(4)	178.0(9)	C(3)-C(4)-Pt	111.8(5)
C(12)-C(11)-C(16)	119.1(7)	C(12)-C(11)-P(1)	126.4(6)
C(16)-C(11)-P(1)	114.5(6)	C(11)-C(12)-C(13)	119.5(8)
C(14)-C(13)-C(12)	120.8(9)	C(15)-C(14)-C(13)	120.4(8)
C(14)-C(15)-C(16)	120.6(9)	C(15)-C(16)-C(11)	119.5(9)
C(26)-C(21)-C(22)	117.8(6)	C(26)-C(21)-P(1)	123.8(5)
C(22)-C(21)-P(1)	118.4(5)	C(23)-C(22)-C(21)	120.9(7)
C(22)-C(23)-C(24)	120.6(7)	C(25)-C(24)-C(23)	119.0(7)
C(24)-C(25)-C(26)	120.7(7)	C(25)-C(26)-C(21)	120.9(7)
C(36)-C(31)-C(32)	118.9(6)	C(36)-C(31)-P(1)	122.0(5)
C(32)-C(31)-P(1)	118.8(5)	C(31)-C(32)-C(33)	118.9(7)
C(34)-C(33)-C(32)	121.2(7)	C(33)-C(34)-C(35)	120.6(7)

C(36)-C(35)-C(34)	119.0(7)	C(35)-C(36)-C(31)	121.3(7)
C(42)-C(41)-C(46)	117.8(7)	C(42)-C(41)-P(2)	118.6(5)
C(46)-C(41)-P(2)	123.6(6)	C(41)-C(42)-C(43)	120.5(7)
C(44)-C(43)-C(42)	119.4(8)	C(45)-C(44)-C(43)	119.9(8)
C(44)-C(45)-C(46)	121.2(8)	C(45)-C(46)-C(41)	121.2(8)
C(56)-C(51)-C(52)	118.7(6)	C(56)-C(51)-P(2)	124.3(5)
C(52)-C(51)-P(2)	117.0(5)	C(53)-C(52)-C(51)	119.7(7)
C(54)-C(53)-C(52)	120.5(8)	C(53)-C(54)-C(55)	120.7(7)
C(54)-C(55)-C(56)	120.0(8)	C(55)-C(56)-C(51)	120.3(8)
C(66)-C(61)-C(62)	118.8(6)	C(66)-C(61)-P(2)	120.4(5)
C(62)-C(61)-P(2)	120.8(5)	C(63)-C(62)-C(61)	119.9(7)
C(64)-C(63)-C(62)	120.3(7)	C(65)-C(64)-C(63)	120.5(7)
C(64)-C(65)-C(66)	120.6(8)	C(61)-C(66)-C(65)	120.0(7)

Table A-24 Anisotropic displacement parameters (\AA^2) for *cis*-
[Pt(CH₂CN)₂(PPh₃)₂].0.6CH₂Cl₂ (**5.7**)

The anisotropic displacement factor exponent takes the form:

$$-2 \pi^2 [h^2 a^2 U_{11} + \dots + 2 h k a^* b^* U_{12}]$$

	U11	U22	U33	U23	U13	U12
Pt	0.025(1)	0.039(1)	0.026(1)	-0.003(1)	0.002(1)	-0.005(1)
P(1)	0.029(1)	0.040(1)	0.023(1)	-0.001(1)	-0.001(1)	-0.007(1)
P(2)	0.027(1)	0.038(1)	0.024(1)	-0.005(1)	-0.001(1)	-0.007(1)
N(1)	0.039(5)	0.212(13)	0.078(6)	0.014(7)	-0.014(5)	-0.018(6)
C(1)	0.045(5)	0.080(7)	0.041(5)	0.001(4)	-0.009(4)	0.003(4)
C(2)	0.034(4)	0.032(4)	0.042(4)	0.001(3)	0.001(3)	-0.004(3)
N(2)	0.058(5)	0.093(7)	0.086(6)	-0.021(5)	0.014(5)	0.008(5)
C(3)	0.053(5)	0.041(5)	0.043(5)	-0.012(4)	-0.001(4)	-0.003(4)
C(4)	0.033(4)	0.034(4)	0.042(4)	-0.003(3)	-0.004(3)	-0.007(3)
C(11)	0.028(3)	0.047(5)	0.021(3)	-0.005(3)	0.001(3)	-0.002(3)
C(12)	0.045(4)	0.063(6)	0.028(4)	-0.006(4)	-0.005(3)	-0.002(4)
C(13)	0.050(5)	0.078(7)	0.032(4)	-0.017(4)	-0.007(4)	0.021(5)
C(14)	0.035(5)	0.144(11)	0.036(5)	-0.023(6)	0.002(4)	0.009(6)
C(15)	0.027(4)	0.114(9)	0.048(5)	-0.015(5)	0.005(4)	-0.016(5)
C(16)	0.032(4)	0.086(7)	0.038(4)	-0.014(4)	0.003(3)	-0.016(4)
C(21)	0.032(4)	0.049(5)	0.023(3)	-0.003(3)	0.000(3)	-0.012(3)
C(22)	0.038(4)	0.082(7)	0.030(4)	0.007(4)	-0.007(3)	-0.013(4)
C(23)	0.040(4)	0.075(6)	0.043(5)	0.003(4)	-0.012(4)	-0.010(4)
C(24)	0.060(5)	0.063(6)	0.031(4)	-0.002(4)	-0.013(4)	-0.013(4)
C(25)	0.055(5)	0.088(7)	0.025(4)	0.008(4)	0.007(4)	-0.024(5)
C(26)	0.037(4)	0.076(6)	0.033(4)	0.010(4)	-0.003(3)	-0.018(4)
C(31)	0.032(4)	0.045(4)	0.027(3)	0.000(3)	-0.004(3)	-0.013(3)
C(32)	0.038(4)	0.052(5)	0.034(4)	-0.004(3)	0.000(3)	-0.013(4)
C(33)	0.044(5)	0.075(7)	0.040(5)	0.001(4)	0.008(4)	-0.025(4)
C(34)	0.047(5)	0.060(6)	0.065(6)	0.004(5)	-0.002(4)	-0.025(4)
C(35)	0.059(5)	0.045(5)	0.048(5)	-0.008(4)	-0.009(4)	-0.019(4)
C(36)	0.044(4)	0.048(5)	0.033(4)	-0.002(3)	0.002(3)	-0.011(4)
C(41)	0.035(4)	0.040(4)	0.017(3)	0.000(3)	-0.001(3)	-0.003(3)
C(42)	0.047(4)	0.046(5)	0.030(4)	0.001(3)	-0.010(3)	-0.010(4)
C(43)	0.090(7)	0.036(5)	0.044(5)	-0.003(4)	-0.016(5)	-0.019(5)

C(44)	0.075(6)	0.054(6)	0.031(4)	-0.003(4)	0.003(4)	0.013(5)
C(45)	0.056(5)	0.053(6)	0.038(5)	0.007(4)	0.013(4)	0.010(4)
C(46)	0.040(4)	0.052(5)	0.035(4)	0.003(4)	-0.002(3)	-0.005(4)
C(51)	0.030(4)	0.048(5)	0.029(4)	-0.001(3)	-0.005(3)	-0.009(3)
C(52)	0.044(4)	0.065(6)	0.040(4)	0.006(4)	-0.010(4)	-0.018(4)
C(53)	0.051(5)	0.059(6)	0.056(5)	0.013(4)	-0.007(4)	-0.025(4)
C(54)	0.046(5)	0.056(6)	0.077(6)	-0.007(5)	-0.015(5)	-0.021(4)
C(55)	0.055(5)	0.077(7)	0.054(5)	-0.021(5)	-0.012(4)	-0.021(5)
C(56)	0.046(5)	0.069(6)	0.042(5)	-0.012(4)	-0.001(4)	-0.022(4)
C(61)	0.035(4)	0.046(5)	0.027(3)	-0.010(3)	0.001(3)	-0.015(3)
C(62)	0.036(4)	0.045(5)	0.031(4)	-0.002(3)	-0.004(3)	-0.009(3)
C(63)	0.037(4)	0.048(5)	0.042(4)	-0.005(4)	0.005(3)	-0.011(3)
C(64)	0.051(5)	0.057(5)	0.030(4)	-0.009(4)	0.011(3)	-0.020(4)
C(65)	0.064(5)	0.059(6)	0.027(4)	-0.006(4)	0.000(4)	-0.012(4)
C(66)	0.038(4)	0.052(5)	0.032(4)	0.003(3)	-0.004(3)	-0.007(3)

Table A-25 Hydrogen coordinates and isotropic displacement parameters (\AA^2) for *cis*- $[\text{Pt}(\text{CH}_2\text{CN})_2(\text{PPh}_3)_2] \cdot 0.6\text{CH}_2\text{Cl}_2$ (**5.7**)

	x	y	z	U(eq)
H(2A)	0.7936	1.1449	0.6602	0.045
H(2B)	0.8145	1.0354	0.5983	0.045
H(4A)	0.8815	1.0368	0.8438	0.044
H(4B)	0.8911	1.1376	0.7759	0.044
H(12A)	1.1010	0.4748	0.6143	0.057
H(13A)	1.3385	0.3987	0.5873	0.072
H(14A)	1.4727	0.5480	0.5648	0.093
H(15A)	1.3755	0.7730	0.5718	0.077
H(16A)	1.1386	0.8555	0.5979	0.063
H(22A)	0.6546	0.8278	0.5762	0.060
H(23A)	0.5784	0.8891	0.4629	0.063
H(24A)	0.7326	0.9065	0.3566	0.061
H(25A)	0.9639	0.8650	0.3666	0.068
H(26A)	1.0418	0.8038	0.4802	0.058
H(32A)	0.7066	0.7121	0.7511	0.050
H(33A)	0.5755	0.5561	0.7766	0.063
H(34A)	0.6041	0.3820	0.6984	0.067
H(35A)	0.7566	0.3621	0.5869	0.059
H(36A)	0.8922	0.5111	0.5617	0.051
H(42A)	0.9142	0.5331	0.7996	0.049
H(43A)	1.0310	0.3073	0.7822	0.066
H(44A)	1.2695	0.2444	0.7688	0.072
H(45A)	1.3876	0.4021	0.7746	0.067
H(46A)	1.2759	0.6232	0.7914	0.053
H(52A)	1.2096	0.8620	0.7320	0.059
H(53A)	1.3778	0.9587	0.7607	0.065
H(54A)	1.3773	1.0206	0.8810	0.069
H(55A)	1.2116	0.9862	0.9756	0.072
H(56A)	1.0507	0.8764	0.9509	0.062
H(62A)	0.6942	0.8781	0.8621	0.045
H(63A)	0.5485	0.8549	0.9710	0.052

H(64A)	0.6337	0.7246	1.0689	0.056
H(65A)	0.8630	0.6196	1.0611	0.061
H(66A)	1.0127	0.6404	0.9535	0.050

Table A-26 Atomic coordinates and equivalent isotropic displacement parameters (\AA^2) for *cis*-[Pt(O₂CCH₂OPh)₂(PPh₃)₂].CH₂Cl₂ (**5.9**)U(eq) is defined as one third of the trace of the orthogonalised U_{ij} tensor.

	x	y	z	U(eq)
Pt	0.0808(1)	0.5663(1)	0.3508(1)	0.028(1)
P(1)	0.1320(2)	0.5172(1)	0.2706(1)	0.029(1)
P(2)	0.2329(2)	0.5227(1)	0.4161(1)	0.026(1)
O(1)	-0.0417(5)	0.6289(3)	0.2931(2)	0.045(1)
O(2)	-0.2121(5)	0.5858(3)	0.3105(3)	0.058(2)
O(3)	-0.3294(5)	0.6936(3)	0.2369(3)	0.062(2)
O(11)	0.0059(4)	0.6088(3)	0.4170(2)	0.033(1)
O(12)	0.1068(5)	0.7156(3)	0.4174(2)	0.043(1)
O(13)	-0.0384(5)	0.7768(3)	0.4897(2)	0.044(1)
C(1)	-0.1451(8)	0.6270(4)	0.2905(3)	0.040(2)
C(2)	-0.2060(7)	0.6964(5)	0.2535(4)	0.055(2)
C(3)	-0.3752(8)	0.6483(5)	0.1910(4)	0.060(2)
C(4)	-0.4977(9)	0.6544(6)	0.1714(5)	0.082(3)
C(5)	-0.5502(13)	0.6131(9)	0.1268(8)	0.123(6)
C(6)	-0.4855(18)	0.5609(9)	0.0984(7)	0.133(6)
C(7)	-0.3675(16)	0.5562(8)	0.1175(6)	0.116(5)
C(8)	-0.3096(11)	0.5998(6)	0.1643(4)	0.075(3)
C(11)	0.0340(6)	0.6753(4)	0.4350(3)	0.033(2)
C(12)	-0.0266(7)	0.6988(4)	0.4840(3)	0.038(2)
C(13)	-0.1305(7)	0.8107(4)	0.4518(3)	0.040(2)
C(14)	-0.1490(9)	0.8847(5)	0.4633(4)	0.069(3)
C(15)	-0.2417(10)	0.9224(5)	0.4278(5)	0.077(3)
C(16)	-0.3129(9)	0.8869(7)	0.3829(4)	0.067(3)
C(17)	-0.2915(8)	0.8151(6)	0.3721(4)	0.057(2)
C(18)	-0.2006(7)	0.7759(5)	0.4066(3)	0.044(2)
C(21)	0.2772(6)	0.4751(4)	0.2704(3)	0.031(2)
C(22)	0.2997(7)	0.4015(4)	0.2886(3)	0.037(2)
C(23)	0.4105(7)	0.3703(4)	0.2888(3)	0.043(2)
C(24)	0.4988(7)	0.4117(5)	0.2726(4)	0.048(2)
C(25)	0.4788(7)	0.4842(5)	0.2553(3)	0.049(2)
C(26)	0.3681(7)	0.5169(5)	0.2544(3)	0.041(2)
C(31)	0.0262(6)	0.4464(4)	0.2395(3)	0.031(2)
C(32)	0.0519(7)	0.3946(4)	0.1994(3)	0.041(2)
C(33)	-0.0332(8)	0.3427(5)	0.1717(4)	0.051(2)
C(34)	-0.1441(8)	0.3457(5)	0.1846(4)	0.055(2)
C(35)	-0.1728(7)	0.3979(5)	0.2238(4)	0.048(2)
C(36)	-0.0876(6)	0.4476(4)	0.2519(3)	0.035(2)
C(41)	0.1248(6)	0.5889(4)	0.2145(3)	0.036(2)
C(42)	0.0956(8)	0.5702(5)	0.1557(3)	0.053(2)
C(43)	0.0957(9)	0.6252(6)	0.1132(4)	0.067(3)
C(44)	0.1272(9)	0.6977(6)	0.1310(4)	0.064(3)
C(45)	0.1556(9)	0.7161(5)	0.1877(4)	0.063(3)
C(46)	0.1532(8)	0.6609(5)	0.2299(3)	0.053(2)
C(51)	0.2322(6)	0.5549(3)	0.4904(3)	0.025(1)
C(52)	0.3017(6)	0.6145(4)	0.5158(3)	0.036(2)
C(53)	0.2961(7)	0.6377(4)	0.5715(3)	0.042(2)

C(54)	0.2211(7)	0.6019(5)	0.6019(3)	0.045(2)
C(55)	0.1529(7)	0.5440(4)	0.5780(3)	0.039(2)
C(56)	0.1571(6)	0.5202(4)	0.5217(3)	0.032(2)
C(61)	0.3682(6)	0.5617(4)	0.3986(3)	0.031(2)
C(62)	0.3618(7)	0.6370(4)	0.3820(3)	0.039(2)
C(63)	0.4583(7)	0.6701(5)	0.3662(4)	0.049(2)
C(64)	0.5605(7)	0.6296(5)	0.3646(4)	0.052(2)
C(65)	0.5674(7)	0.5562(5)	0.3816(4)	0.048(2)
C(66)	0.4726(6)	0.5216(4)	0.3985(3)	0.037(2)
C(71)	0.2468(6)	0.4219(4)	0.4253(3)	0.032(2)
C(72)	0.3407(7)	0.3902(4)	0.4650(3)	0.039(2)
C(73)	0.3511(8)	0.3140(5)	0.4704(4)	0.052(2)
C(74)	0.2677(9)	0.2689(4)	0.4382(4)	0.051(2)
C(75)	0.1726(8)	0.2991(4)	0.4008(3)	0.044(2)
C(76)	0.1611(7)	0.3758(4)	0.3949(3)	0.038(2)
C(80)	0.2569(15)	0.8408(10)	0.4813(8)	0.144(6)
Cl(1)	0.1951(6)	0.9264(3)	0.4685(3)	0.198(2)
Cl(2)	0.3977(6)	0.8399(4)	0.4518(3)	0.216(3)

Table A-27 Bond lengths (Å) for *cis*-[Pt(O₂CCH₂OPh)₂(PPh₃)₂].CH₂Cl₂ (**5.9**)

Pt-O(11)	2.056(4)	Pt-O(1)	2.082(5)
Pt-P(2)	2.2305(17)	Pt-P(1)	2.2501(18)
P(1)-C(31)	1.812(7)	P(1)-C(41)	1.829(7)
P(1)-C(21)	1.830(7)	P(2)-C(61)	1.820(7)
P(2)-C(71)	1.825(7)	P(2)-C(51)	1.833(6)
O(1)-C(1)	1.177(9)	O(2)-C(1)	1.225(9)
O(3)-C(3)	1.369(11)	O(3)-C(2)	1.396(10)
O(11)-C(11)	1.285(8)	O(12)-C(11)	1.234(9)
O(13)-C(13)	1.385(9)	O(13)-C(12)	1.414(8)
C(1)-C(2)	1.597(11)	C(3)-C(8)	1.376(14)
C(3)-C(4)	1.398(13)	C(4)-C(5)	1.327(18)
C(5)-C(6)	1.43(2)	C(6)-C(7)	1.35(2)
C(7)-C(8)	1.405(16)	C(11)-C(12)	1.510(10)
C(13)-C(18)	1.353(11)	C(13)-C(14)	1.379(11)
C(14)-C(15)	1.394(13)	C(15)-C(16)	1.359(14)
C(16)-C(17)	1.344(13)	C(17)-C(18)	1.383(11)
C(21)-C(26)	1.394(10)	C(21)-C(22)	1.396(10)
C(22)-C(23)	1.389(10)	C(23)-C(24)	1.367(11)
C(24)-C(25)	1.369(12)	C(25)-C(26)	1.396(11)
C(31)-C(32)	1.392(10)	C(31)-C(36)	1.390(10)
C(32)-C(33)	1.414(11)	C(33)-C(34)	1.365(12)
C(34)-C(35)	1.394(12)	C(35)-C(36)	1.393(10)
C(41)-C(46)	1.363(11)	C(41)-C(42)	1.394(11)
C(42)-C(43)	1.400(12)	C(43)-C(44)	1.392(13)
C(44)-C(45)	1.345(13)	C(45)-C(46)	1.403(11)
C(51)-C(56)	1.382(9)	C(51)-C(52)	1.397(9)
C(52)-C(53)	1.382(10)	C(53)-C(54)	1.377(11)
C(54)-C(55)	1.356(11)	C(55)-C(56)	1.392(10)
C(61)-C(66)	1.398(9)	C(61)-C(62)	1.403(10)
C(62)-C(63)	1.369(10)	C(63)-C(64)	1.386(11)
C(64)-C(65)	1.373(12)	C(65)-C(66)	1.375(10)

C(71)-C(76)	1.376(10)	C(71)-C(72)	1.402(10)
C(72)-C(73)	1.376(11)	C(73)-C(74)	1.365(12)
C(74)-C(75)	1.372(12)	C(75)-C(76)	1.388(10)
C(80)-Cl(1)	1.695(16)	C(80)-Cl(2)	1.874(17)

Table A-28 Bond angles (°) for *cis*-[Pt(O₂CCH₂OPh)₂(PPh₃)₂].CH₂Cl₂ (**5.9**)

O(11)-Pt-O(1)	87.75(19)	O(11)-Pt-P(2)	89.93(14)
O(1)-Pt-P(2)	167.53(16)	O(11)-Pt-P(1)	170.64(14)
O(1)-Pt-P(1)	85.54(15)	P(2)-Pt-P(1)	98.00(6)
C(31)-P(1)-C(41)	105.7(3)	C(31)-P(1)-C(21)	104.6(3)
C(41)-P(1)-C(21)	101.8(3)	C(31)-P(1)-Pt	110.3(2)
C(41)-P(1)-Pt	109.9(2)	C(21)-P(1)-Pt	123.1(2)
C(61)-P(2)-C(71)	110.4(3)	C(61)-P(2)-C(51)	104.5(3)
C(71)-P(2)-C(51)	102.5(3)	C(61)-P(2)-Pt	107.6(2)
C(71)-P(2)-Pt	117.9(2)	C(51)-P(2)-Pt	113.2(2)
C(1)-O(1)-Pt	124.6(6)	C(3)-O(3)-C(2)	117.2(7)
C(11)-O(11)-Pt	118.5(4)	C(13)-O(13)-C(12)	116.7(6)
O(1)-C(1)-O(2)	134.3(9)	O(1)-C(1)-C(2)	109.8(6)
O(2)-C(1)-C(2)	115.9(8)	O(3)-C(2)-C(1)	116.0(7)
O(3)-C(3)-C(8)	124.7(9)	O(3)-C(3)-C(4)	115.0(10)
C(8)-C(3)-C(4)	120.3(11)	C(5)-C(4)-C(3)	119.4(13)
C(4)-C(5)-C(6)	122.1(14)	C(7)-C(6)-C(5)	117.7(14)
C(6)-C(7)-C(8)	121.3(16)	C(3)-C(8)-C(7)	119.2(12)
O(12)-C(11)-O(11)	125.3(7)	O(12)-C(11)-C(12)	121.9(7)
O(11)-C(11)-C(12)	112.7(7)	O(13)-C(12)-C(11)	114.5(6)
C(18)-C(13)-C(14)	120.4(8)	C(18)-C(13)-O(13)	124.4(7)
C(14)-C(13)-O(13)	115.2(7)	C(13)-C(14)-C(15)	118.6(9)
C(16)-C(15)-C(14)	120.8(9)	C(17)-C(16)-C(15)	119.3(9)
C(16)-C(17)-C(18)	121.5(9)	C(13)-C(18)-C(17)	119.4(8)
C(26)-C(21)-C(22)	119.1(7)	C(26)-C(21)-P(1)	120.5(6)
C(22)-C(21)-P(1)	120.3(5)	C(23)-C(22)-C(21)	119.9(7)
C(24)-C(23)-C(22)	120.5(8)	C(23)-C(24)-C(25)	120.4(8)
C(24)-C(25)-C(26)	120.3(8)	C(21)-C(26)-C(25)	119.7(7)
C(32)-C(31)-C(36)	118.7(6)	C(32)-C(31)-P(1)	121.8(5)
C(36)-C(31)-P(1)	119.3(5)	C(31)-C(32)-C(33)	122.1(7)
C(34)-C(33)-C(32)	117.7(8)	C(33)-C(34)-C(35)	121.3(8)
C(34)-C(35)-C(36)	120.5(8)	C(35)-C(36)-C(31)	119.7(7)
C(46)-C(41)-C(42)	119.3(7)	C(46)-C(41)-P(1)	120.0(6)
C(42)-C(41)-P(1)	120.6(6)	C(41)-C(42)-C(43)	120.0(8)
C(44)-C(43)-C(42)	118.7(9)	C(45)-C(44)-C(43)	121.7(8)
C(44)-C(45)-C(46)	119.1(9)	C(41)-C(46)-C(45)	121.2(8)
C(56)-C(51)-C(52)	118.8(6)	C(56)-C(51)-P(2)	118.6(5)
C(52)-C(51)-P(2)	122.7(5)	C(53)-C(52)-C(51)	120.5(7)
C(54)-C(53)-C(52)	119.5(7)	C(55)-C(54)-C(53)	120.9(7)
C(54)-C(55)-C(56)	120.3(7)	C(51)-C(56)-C(55)	120.1(7)
C(66)-C(61)-C(62)	119.6(7)	C(66)-C(61)-P(2)	124.9(6)
C(62)-C(61)-P(2)	115.5(5)	C(63)-C(62)-C(61)	119.4(7)
C(62)-C(63)-C(64)	120.7(8)	C(65)-C(64)-C(63)	119.9(8)
C(66)-C(65)-C(64)	120.7(7)	C(65)-C(66)-C(61)	119.6(7)
C(76)-C(71)-C(72)	118.9(7)	C(76)-C(71)-P(2)	119.8(6)
C(72)-C(71)-P(2)	121.3(5)	C(73)-C(72)-C(71)	120.3(7)

C(74)-C(73)-C(72)	120.0(8)	C(73)-C(74)-C(75)	120.5(7)
C(74)-C(75)-C(76)	120.2(8)	C(71)-C(76)-C(75)	120.0(8)
Cl(1)-C(80)-Cl(2)	107.7(10)		

Table A-29 Anisotropic displacement parameters (\AA^2) for *cis*-[Pt(O₂CCH₂OPh)₂(PPh₃)₂].CH₂Cl₂ (**5.9**)

The anisotropic displacement factor exponent takes the form:

$$-2\pi^2 [h^2 a^{*2} U_{11} + \dots + 2 h k a^* b^* U_{12}]$$

	U11	U22	U33	U23	U13	U12
Pt	0.029(1)	0.033(1)	0.021(1)	-0.001(1)	0.004(1)	0.004(1)
P(1)	0.031(1)	0.035(1)	0.021(1)	-0.001(1)	0.004(1)	0.002(1)
P(2)	0.027(1)	0.029(1)	0.022(1)	-0.002(1)	0.004(1)	0.002(1)
O(1)	0.056(4)	0.049(3)	0.025(3)	0.006(2)	-0.002(3)	0.016(3)
O(2)	0.051(4)	0.073(4)	0.055(4)	0.015(3)	0.019(3)	0.014(3)
O(3)	0.050(4)	0.060(4)	0.073(4)	0.006(3)	0.001(3)	0.010(3)
O(11)	0.036(3)	0.034(3)	0.030(3)	-0.004(2)	0.011(2)	0.005(2)
O(12)	0.044(3)	0.044(3)	0.041(3)	0.009(2)	0.008(3)	0.004(3)
O(13)	0.055(3)	0.037(3)	0.036(3)	-0.008(2)	0.002(3)	0.015(2)
C(1)	0.057(5)	0.045(5)	0.026(4)	-0.010(3)	0.026(4)	-0.020(4)
C(2)	0.044(5)	0.056(5)	0.062(6)	0.010(4)	0.005(4)	0.003(4)
C(3)	0.050(6)	0.054(6)	0.073(7)	0.012(5)	0.005(5)	0.001(5)
C(4)	0.053(6)	0.076(7)	0.105(9)	0.016(7)	-0.017(6)	-0.011(6)
C(5)	0.087(10)	0.111(12)	0.148(14)	0.024(11)	-0.036(10)	-0.028(9)
C(6)	0.156(17)	0.119(13)	0.098(12)	-0.013(9)	-0.040(11)	-0.033(12)
C(7)	0.155(15)	0.110(11)	0.066(9)	-0.010(8)	-0.019(9)	-(10)
C(8)	0.081(8)	0.083(7)	0.055(7)	0.013(6)	0.002(6)	-0.006(6)
C(11)	0.037(4)	0.039(4)	0.022(4)	0.007(3)	0.000(3)	0.015(3)
C(12)	0.054(5)	0.042(4)	0.018(4)	-0.001(3)	0.004(3)	0.012(4)
C(13)	0.051(5)	0.039(4)	0.031(5)	0.005(3)	0.009(4)	0.010(4)
C(14)	0.082(7)	0.049(6)	0.073(7)	-0.011(5)	0.007(6)	0.011(5)
C(15)	0.076(7)	0.044(6)	0.111(10)	0.030(6)	0.015(7)	0.025(5)
C(16)	0.051(6)	0.096(8)	0.051(6)	0.024(6)	0.003(5)	0.012(6)
C(17)	0.048(5)	0.068(6)	0.054(6)	0.016(5)	0.007(4)	-0.001(5)
C(18)	0.036(4)	0.054(5)	0.042(5)	0.015(4)	0.008(4)	0.000(4)
C(21)	0.030(4)	0.044(4)	0.018(4)	-0.007(3)	0.006(3)	0.004(3)
C(22)	0.038(4)	0.046(4)	0.029(4)	-0.002(3)	0.009(3)	0.003(3)
C(23)	0.044(5)	0.045(5)	0.038(5)	-0.004(4)	0.004(4)	0.007(4)
C(24)	0.035(4)	0.066(6)	0.041(5)	-0.010(4)	0.005(4)	0.007(4)
C(25)	0.031(4)	0.077(6)	0.043(5)	0.003(4)	0.015(4)	-0.007(4)
C(26)	0.047(5)	0.051(5)	0.024(4)	0.001(3)	0.005(3)	-0.007(4)
C(31)	0.036(4)	0.035(4)	0.020(4)	0.003(3)	0.001(3)	0.004(3)
C(32)	0.031(4)	0.056(5)	0.034(5)	-0.014(4)	0.002(3)	-0.005(4)
C(33)	0.053(5)	0.050(5)	0.048(5)	-0.009(4)	0.006(4)	0.003(4)
C(34)	0.049(5)	0.063(6)	0.047(6)	-0.005(4)	-0.003(4)	-0.023(4)
C(35)	0.038(5)	0.064(5)	0.044(5)	-0.005(4)	0.010(4)	-0.010(4)
C(36)	0.034(4)	0.040(4)	0.033(4)	-0.004(3)	0.011(3)	-0.002(3)
C(41)	0.035(4)	0.038(4)	0.036(5)	0.005(3)	0.011(3)	0.002(3)
C(42)	0.072(6)	0.061(5)	0.022(5)	0.004(4)	0.002(4)	0.006(5)
C(43)	0.087(8)	0.084(7)	0.030(5)	0.014(5)	0.005(5)	0.007(6)

C(44)	0.068(6)	0.076(7)	0.049(6)	0.031(5)	0.012(5)	0.014(5)
C(45)	0.093(8)	0.050(5)	0.047(6)	0.005(4)	0.018(5)	0.001(5)
C(46)	0.077(6)	0.060(5)	0.019(5)	0.010(4)	0.005(4)	-0.010(5)
C(51)	0.030(3)	0.029(4)	0.014(4)	0.002(3)	-0.001(3)	0.006(3)
C(52)	0.039(4)	0.032(4)	0.035(5)	-0.003(3)	0.009(3)	-0.002(3)
C(53)	0.052(5)	0.045(4)	0.026(5)	-0.009(3)	-0.002(4)	-0.002(4)
C(54)	0.056(5)	0.050(5)	0.029(4)	-0.006(4)	0.007(4)	0.009(4)
C(55)	0.049(5)	0.036(4)	0.032(5)	0.004(3)	0.013(4)	0.006(3)
C(56)	0.035(4)	0.031(4)	0.028(4)	0.001(3)	0.003(3)	0.001(3)
C(61)	0.028(3)	0.036(4)	0.030(4)	-0.004(3)	0.007(3)	0.000(3)
C(62)	0.033(4)	0.046(5)	0.040(5)	0.004(3)	0.012(3)	-0.002(3)
C(63)	0.050(5)	0.046(5)	0.056(6)	-0.001(4)	0.020(4)	-0.010(4)
C(64)	0.037(5)	0.070(6)	0.050(6)	-0.008(4)	0.014(4)	-0.013(4)
C(65)	0.025(4)	0.064(6)	0.053(5)	-0.014(4)	0.004(3)	0.003(4)
C(66)	0.030(4)	0.048(5)	0.033(4)	-0.006(3)	0.004(3)	0.001(3)
C(71)	0.040(4)	0.029(4)	0.029(4)	-0.004(3)	0.012(3)	0.001(3)
C(72)	0.040(4)	0.043(4)	0.030(4)	0.002(3)	0.000(3)	0.005(4)
C(73)	0.063(6)	0.049(5)	0.042(5)	0.013(4)	0.005(4)	0.017(4)
C(74)	0.084(7)	0.036(4)	0.041(5)	0.006(4)	0.027(5)	0.013(5)
C(75)	0.074(6)	0.034(4)	0.031(5)	-0.007(3)	0.025(4)	-0.011(4)
C(76)	0.044(4)	0.040(4)	0.034(4)	-0.002(3)	0.015(3)	-0.003(3)

Table A-30 Hydrogen coordinates and isotropic displacement parameters (\AA^2) for *cis*-
[Pt(O₂CCH₂OPh)₂(PPh₃)₂].CH₂Cl₂ (**5.9**)

	x	y	z	U(eq)
H(2)	-0.1849	0.7418	0.2765	0.066
H(2)	-0.1720	0.7007	0.2183	0.066
H(4)	-0.5426	0.6874	0.1898	0.098
H(5)	-0.6323	0.6182	0.1134	0.147
H(6)	-0.5243	0.5310	0.0676	0.159
H(7)	-0.3229	0.5231	0.0991	0.139
H(8)	-0.2271	0.5959	0.1772	0.089
H(12A)	-0.1058	0.6762	0.4777	0.046
H(12B)	0.0185	0.6790	0.5206	0.046
H(14)	-0.1000	0.9093	0.4944	0.083
H(15)	-0.2552	0.9729	0.4349	0.092
H(16)	-0.3764	0.9123	0.3596	0.081
H(17)	-0.3394	0.7910	0.3404	0.069
H(18)	-0.1875	0.7255	0.3987	0.052
H(22)	0.2399	0.3731	0.3006	0.045
H(23)	0.4248	0.3204	0.3001	0.052
H(24)	0.5738	0.3902	0.2735	0.058
H(25)	0.5399	0.5121	0.2439	0.059
H(26)	0.3549	0.5669	0.2429	0.049
H(32)	0.1283	0.3942	0.1904	0.049
H(33)	-0.0140	0.3074	0.1453	0.061
H(34)	-0.2024	0.3119	0.1667	0.065
H(35)	-0.2503	0.3995	0.2314	0.058
H(36)	-0.1068	0.4819	0.2790	0.042
H(42)	0.0758	0.5208	0.1445	0.063

H(43)	0.0750	0.6133	0.0734	0.081
H(44)	0.1287	0.7347	0.1028	0.077
H(45)	0.1767	0.7654	0.1989	0.075
H(46)	0.1715	0.6738	0.2696	0.063
H(52)	0.3527	0.6389	0.4949	0.043
H(53)	0.3432	0.6778	0.5885	0.051
H(54)	0.2172	0.6177	0.6398	0.054
H(55)	0.1025	0.5199	0.5994	0.046
H(56)	0.1088	0.4805	0.5051	0.038
H(62)	0.2919	0.6644	0.3817	0.047
H(63)	0.4553	0.7210	0.3563	0.059
H(64)	0.6249	0.6523	0.3520	0.062
H(65)	0.6378	0.5293	0.3816	0.057
H(66)	0.4780	0.4713	0.4099	0.044
H(72)	0.3968	0.4212	0.4882	0.046
H(73)	0.4156	0.2930	0.4961	0.062
H(74)	0.2754	0.2169	0.4416	0.062
H(75)	0.1150	0.2676	0.3792	0.053
H(76)	0.0948	0.3963	0.3700	0.046
H(80A)	0.2023	0.8025	0.4619	0.173
H(80B)	0.2739	0.8304	0.5232	0.173

Table A-31 Atomic coordinates and equivalent isotropic displacement parameters (\AA^2)for $[\text{Pt}\{\text{N}(\text{C}(\text{O})\text{NH}_2)\text{C}(\text{O})\text{CHCN}\}(\text{PPh}_3)_2]\cdot\text{CH}_2\text{Cl}_2\cdot 0.5\text{Et}_2\text{O}$ (**6.5**)

U(eq) is defined as one third of the trace of the orthogonalised Uij tensor.

	x	y	z	U(eq)
Pt	0.8068(1)	0.7131(1)	0.7460(1)	0.022(1)
P(1)	0.6707(1)	0.8062(1)	0.6535(1)	0.024(1)
P(2)	0.6765(1)	0.8223(1)	0.8450(1)	0.024(1)
N(1)	0.9703(4)	0.6037(3)	0.8020(2)	0.028(1)
N(2)	1.0862(6)	0.7092(5)	0.5479(4)	0.061(2)
N(3)	1.1193(5)	0.4916(5)	0.8934(3)	0.044(1)
O(1)	1.1522(4)	0.4605(4)	0.7410(2)	0.048(1)
O(2)	0.9159(4)	0.6245(3)	0.9334(2)	0.037(1)
C(1)	1.0453(5)	0.5425(4)	0.7423(3)	0.031(1)
C(2)	0.9622(5)	0.6017(4)	0.6743(3)	0.028(1)
C(3)	1.0316(5)	0.6609(5)	0.6034(3)	0.036(1)
C(4)	0.9988(5)	0.5744(4)	0.8804(3)	0.031(1)
C(11)	0.5034(5)	0.7923(4)	0.6818(3)	0.030(1)
C(12)	0.4082(6)	0.8498(5)	0.6307(3)	0.040(1)
C(13)	0.2851(6)	0.8309(7)	0.6518(4)	0.056(2)
C(14)	0.2586(7)	0.7530(7)	0.7220(4)	0.055(2)
C(15)	0.3540(6)	0.6924(6)	0.7712(4)	0.048(1)
C(16)	0.4765(6)	0.7120(5)	0.7516(3)	0.036(1)
C(21)	0.7337(5)	0.7530(4)	0.5586(3)	0.030(1)
C(22)	0.7400(6)	0.6417(5)	0.5616(4)	0.040(1)
C(23)	0.7849(7)	0.5972(6)	0.4918(4)	0.051(2)
C(24)	0.8214(7)	0.6638(6)	0.4180(4)	0.057(2)
C(25)	0.8157(7)	0.7751(6)	0.4137(4)	0.054(2)
C(26)	0.7714(6)	0.8199(5)	0.4841(3)	0.038(1)
C(31)	0.6577(5)	0.9569(4)	0.6204(3)	0.028(1)
C(32)	0.7823(6)	0.9750(5)	0.6003(3)	0.037(1)
C(33)	0.7870(7)	1.0859(5)	0.5698(4)	0.045(1)
C(34)	0.6680(7)	1.1798(5)	0.5608(4)	0.049(1)
C(35)	0.5430(7)	1.1644(5)	0.5827(4)	0.048(1)
C(36)	0.5383(6)	1.0522(4)	0.6122(3)	0.036(1)
C(41)	0.7810(5)	0.8834(4)	0.8702(3)	0.029(1)
C(42)	0.7578(5)	0.9111(5)	0.9455(3)	0.037(1)
C(43)	0.8271(6)	0.9736(6)	0.9566(4)	0.047(1)
C(44)	0.9195(6)	1.0070(6)	0.8946(5)	0.055(2)
C(45)	0.9469(7)	0.9776(7)	0.8198(4)	0.059(2)
C(46)	0.8782(6)	0.9157(6)	0.8078(4)	0.045(1)
C(51)	0.5282(5)	0.9534(4)	0.8236(3)	0.027(1)
C(52)	0.5345(6)	1.0646(4)	0.8046(4)	0.040(1)
C(53)	0.4187(7)	1.1625(5)	0.7908(4)	0.051(2)
C(54)	0.2982(7)	1.1515(5)	0.7944(4)	0.051(2)
C(55)	0.2903(6)	1.0421(6)	0.8127(4)	0.044(1)
C(56)	0.4040(5)	0.9438(4)	0.8278(3)	0.034(1)
C(61)	0.6030(5)	0.7432(4)	0.9391(3)	0.028(1)
C(62)	0.5093(5)	0.7989(5)	0.9996(3)	0.035(1)
C(63)	0.4585(6)	0.7368(5)	1.0709(3)	0.045(1)
C(64)	0.4991(6)	0.6164(5)	1.0825(4)	0.047(1)

C(65)	0.5895(6)	0.5607(5)	1.0225(4)	0.042(1)
C(66)	0.6407(5)	0.6225(4)	0.9508(3)	0.032(1)
C(70)	0.9146(12)	0.3020(10)	0.9786(6)	0.100(3)
Cl(1)	0.7982(3)	0.2329(2)	1.0346(2)	0.086(1)
Cl(2)	0.9124(5)	0.3291(3)	0.8751(3)	0.173(2)
O(3)	0.6185(9)	0.4103(8)	0.6575(6)	0.053(2)
C(81)	0.5078(13)	0.4432(12)	0.6662(8)	0.053(3)
C(82)	0.439(2)	0.5287(17)	0.6027(12)	0.090(6)
C(83)	0.6940(18)	0.3408(17)	0.6942(12)	0.085(5)
C(84)	0.8371(18)	0.3028(18)	0.6828(13)	0.088(5)

Table A-32 Bond lengths (Å) for $[\text{Pt}\{\text{N}(\text{C}(\text{O})\text{NH}_2)\text{C}(\text{O})\text{CHCN}\}(\text{PPh}_3)_2]\cdot\text{CH}_2\text{Cl}_2$.

0.5Et₂O (6.5)

Pt–N(1)	2.071(4)	Pt–C(2)	2.105(4)
Pt–P(1)	2.2467(11)	Pt–P(2)	2.3375(11)
P(1)–C(31)	1.813(5)	P(1)–C(11)	1.826(5)
P(1)–C(21)	1.834(5)	P(2)–C(61)	1.826(5)
P(2)–C(41)	1.827(5)	P(2)–C(51)	1.841(5)
N(1)–C(1)	1.371(6)	N(1)–C(4)	1.401(6)
N(2)–C(3)	1.143(7)	N(3)–C(4)	1.349(7)
O(1)–C(1)	1.220(6)	O(2)–C(4)	1.230(6)
C(1)–C(2)	1.529(6)	C(2)–C(3)	1.442(7)
C(11)–C(12)	1.395(7)	C(11)–C(16)	1.396(7)
C(12)–C(13)	1.394(8)	C(13)–C(14)	1.383(10)
C(14)–C(15)	1.377(10)	C(15)–C(16)	1.395(8)
C(21)–C(26)	1.393(7)	C(21)–C(22)	1.395(7)
C(22)–C(23)	1.386(8)	C(23)–C(24)	1.378(10)
C(24)–C(25)	1.392(10)	C(25)–C(26)	1.396(8)
C(31)–C(36)	1.395(7)	C(31)–C(32)	1.406(7)
C(32)–C(33)	1.387(7)	C(33)–C(34)	1.385(9)
C(34)–C(35)	1.392(9)	C(35)–C(36)	1.403(8)
C(41)–C(46)	1.391(7)	C(41)–C(42)	1.397(7)
C(42)–C(43)	1.390(8)	C(43)–C(44)	1.358(9)
C(44)–C(45)	1.391(9)	C(45)–C(46)	1.386(8)
C(51)–C(56)	1.395(7)	C(51)–C(52)	1.398(7)
C(52)–C(53)	1.399(8)	C(53)–C(54)	1.365(10)
C(54)–C(55)	1.384(9)	C(55)–C(56)	1.392(7)
C(61)–C(62)	1.392(7)	C(61)–C(66)	1.405(6)
C(62)–C(63)	1.374(8)	C(63)–C(64)	1.399(9)
C(64)–C(65)	1.375(9)	C(65)–C(66)	1.379(7)
C(70)–Cl(2)	1.748(10)	C(70)–Cl(1)	1.755(10)
O(3)–C(81)	1.091(13)	O(3)–C(83)	1.122(15)
C(81)–C(82)	1.450(19)	C(81)–C(83)	2.04(2)
C(83)–C(84)	1.41(2)		

Table A-33 Bond angles ($^{\circ}$) for $[\text{Pt}\{\text{N}(\text{C}(\text{O})\text{NH}_2)\text{C}(\text{O})\text{CHCN}\}(\text{PPh}_3)_2]\cdot\text{CH}_2\text{Cl}_2\cdot 0.5\text{Et}_2\text{O}$
(6.5)

N(1)–Pt–C(2)	65.94(17)	N(1)–Pt–P(1)	162.51(11)
C(2)–Pt–P(1)	96.62(13)	N(1)–Pt–P(2)	99.97(11)
C(2)–Pt–P(2)	165.48(13)	P(1)–Pt–P(2)	97.35(4)
C(31)–P(1)–C(11)	111.4(2)	C(31)–P(1)–C(21)	103.4(2)
C(11)–P(1)–C(21)	99.8(2)	C(31)–P(1)–Pt	110.34(15)
C(11)–P(1)–Pt	116.33(16)	C(21)–P(1)–Pt	114.52(15)
C(61)–P(2)–C(41)	108.2(2)	C(61)–P(2)–C(51)	101.1(2)
C(41)–P(2)–C(51)	100.5(2)	C(61)–P(2)–Pt	115.18(16)
C(41)–P(2)–Pt	109.27(16)	C(51)–P(2)–Pt	121.07(15)
C(1)–N(1)–C(4)	124.5(4)	C(1)–N(1)–Pt	98.6(3)
C(4)–N(1)–Pt	135.9(3)	O(1)–C(1)–N(1)	130.2(5)
O(1)–C(1)–C(2)	126.7(4)	N(1)–C(1)–C(2)	103.1(4)
C(3)–C(2)–C(1)	112.4(4)	C(3)–C(2)–Pt	113.8(3)
C(1)–C(2)–Pt	92.2(3)	N(2)–C(3)–C(2)	178.9(6)
O(2)–C(4)–N(3)	123.0(5)	O(2)–C(4)–N(1)	119.9(4)
N(3)–C(4)–N(1)	117.2(4)	C(12)–C(11)–C(16)	119.2(5)
C(12)–C(11)–P(1)	121.5(4)	C(16)–C(11)–P(1)	118.8(4)
C(13)–C(12)–C(11)	119.8(5)	C(14)–C(13)–C(12)	120.3(6)
C(15)–C(14)–C(13)	120.3(6)	C(14)–C(15)–C(16)	120.0(6)
C(15)–C(16)–C(11)	120.3(5)	C(26)–C(21)–C(22)	119.1(5)
C(26)–C(21)–P(1)	122.9(4)	C(22)–C(21)–P(1)	118.0(4)
C(23)–C(22)–C(21)	120.7(6)	C(24)–C(23)–C(22)	120.1(6)
C(23)–C(24)–C(25)	120.1(5)	C(24)–C(25)–C(26)	120.0(6)
C(21)–C(26)–C(25)	120.0(6)	C(36)–C(31)–C(32)	119.2(5)
C(36)–C(31)–P(1)	126.0(4)	C(32)–C(31)–P(1)	114.9(4)
C(33)–C(32)–C(31)	120.5(5)	C(34)–C(33)–C(32)	119.8(6)
C(33)–C(34)–C(35)	120.8(5)	C(34)–C(35)–C(36)	119.4(5)
C(31)–C(36)–C(35)	120.2(5)	C(46)–C(41)–C(42)	118.7(5)
C(46)–C(41)–P(2)	117.5(4)	C(42)–C(41)–P(2)	123.4(4)
C(43)–C(42)–C(41)	120.3(5)	C(44)–C(43)–C(42)	120.4(5)
C(43)–C(44)–C(45)	120.2(5)	C(46)–C(45)–C(44)	120.0(6)
C(45)–C(46)–C(41)	120.2(5)	C(56)–C(51)–C(52)	118.0(5)
C(56)–C(51)–P(2)	120.0(4)	C(52)–C(51)–P(2)	122.0(4)
C(51)–C(52)–C(53)	120.5(5)	C(54)–C(53)–C(52)	120.8(6)
C(53)–C(54)–C(55)	119.5(5)	C(54)–C(55)–C(56)	120.5(5)
C(55)–C(56)–C(51)	120.8(5)	C(62)–C(61)–C(66)	118.8(4)
C(62)–C(61)–P(2)	122.0(4)	C(66)–C(61)–P(2)	119.2(4)
C(63)–C(62)–C(61)	120.8(5)	C(62)–C(63)–C(64)	119.8(5)
C(65)–C(64)–C(63)	119.8(5)	C(64)–C(65)–C(66)	120.6(5)
C(65)–C(66)–C(61)	120.1(5)		
Cl(2)–C(70)–Cl(1)	109.3(6)		
C(81)–O(3)–C(83)	133.8(16)	O(3)–C(81)–C(82)	120.6(15)
O(3)–C(81)–C(83)	23.4(8)	C(82)–C(81)–C(83)	143.9(13)
O(3)–C(83)–C(84)	133(2)	O(3)–C(83)–C(81)	22.8(8)
C(84)–C(83)–C(81)	155.2(16)		

Table A-34 Anisotropic displacement parameters (\AA^2) for
 $[\text{Pt}\{\text{N}(\text{C}(\text{O})\text{NH}_2)\text{C}(\text{O})\text{CHCN}\}(\text{PPh}_3)_2]\cdot\text{CH}_2\text{Cl}_2\cdot 0.5\text{Et}_2\text{O}$ (6.5)

The anisotropic displacement factor exponent takes the form:

$$-2\pi^2 [h^2 a^{*2} U_{11} + \dots + 2 h k a^* b^* U_{12}]$$

	U11	U22	U33	U23	U13	U12
Pt	0.024(1)	0.021(1)	0.020(1)	-0.005(1)	-0.006(1)	-0.005(1)
P(1)	0.026(1)	0.024(1)	0.022(1)	-0.005(1)	-0.007(1)	-0.006(1)
P(2)	0.025(1)	0.024(1)	0.023(1)	-0.007(1)	-0.004(1)	-0.007(1)
N(1)	0.028(2)	0.027(2)	0.026(2)	-0.005(2)	-0.010(2)	-0.003(2)
N(2)	0.046(3)	0.063(4)	0.053(3)	0.007(3)	0.000(3)	-0.017(3)
N(3)	0.036(2)	0.052(3)	0.031(2)	-0.009(2)	-0.014(2)	0.003(2)
O(1)	0.041(2)	0.048(2)	0.039(2)	-0.017(2)	-0.013(2)	0.012(2)
O(2)	0.038(2)	0.040(2)	0.027(2)	-0.010(1)	-0.012(2)	-0.002(2)
C(1)	0.030(2)	0.028(2)	0.028(2)	-0.005(2)	-0.008(2)	-0.004(2)
C(2)	0.030(2)	0.025(2)	0.025(2)	-0.010(2)	-0.004(2)	-0.002(2)
C(3)	0.029(2)	0.038(3)	0.032(3)	-0.005(2)	-0.005(2)	-0.003(2)
C(4)	0.032(2)	0.033(2)	0.027(2)	-0.004(2)	-0.011(2)	-0.009(2)
C(11)	0.030(2)	0.034(2)	0.028(2)	-0.010(2)	-0.006(2)	-0.010(2)
C(12)	0.038(3)	0.049(3)	0.036(3)	-0.004(2)	-0.014(2)	-0.015(2)
C(13)	0.038(3)	0.078(5)	0.056(4)	-0.011(3)	-0.018(3)	-0.021(3)
C(14)	0.040(3)	0.073(4)	0.059(4)	-0.015(3)	-0.007(3)	-0.029(3)
C(15)	0.046(3)	0.055(4)	0.047(3)	-0.008(3)	-0.001(3)	-0.028(3)
C(16)	0.042(3)	0.036(3)	0.034(3)	-0.006(2)	-0.010(2)	-0.016(2)
C(21)	0.027(2)	0.034(2)	0.027(2)	-0.011(2)	-0.010(2)	-0.003(2)
C(22)	0.042(3)	0.037(3)	0.041(3)	-0.016(2)	-0.011(2)	-0.005(2)
C(23)	0.056(4)	0.045(3)	0.054(4)	-0.028(3)	-0.023(3)	0.003(3)
C(24)	0.054(4)	0.066(4)	0.043(3)	-0.035(3)	-0.017(3)	0.007(3)
C(25)	0.050(3)	0.069(4)	0.028(3)	-0.015(3)	-0.005(2)	-0.006(3)
C(26)	0.040(3)	0.041(3)	0.027(2)	-0.008(2)	-0.008(2)	-0.007(2)
C(31)	0.035(2)	0.026(2)	0.021(2)	-0.003(2)	-0.008(2)	-0.008(2)
C(32)	0.037(3)	0.032(2)	0.040(3)	-0.002(2)	-0.012(2)	-0.011(2)
C(33)	0.052(3)	0.040(3)	0.047(3)	-0.002(2)	-0.013(3)	-0.023(3)
C(34)	0.063(4)	0.030(3)	0.052(3)	-0.001(2)	-0.014(3)	-0.017(3)
C(35)	0.049(3)	0.030(3)	0.051(3)	-0.001(2)	-0.014(3)	-0.002(2)
C(36)	0.038(3)	0.032(2)	0.034(3)	-0.005(2)	-0.009(2)	-0.007(2)
C(41)	0.028(2)	0.029(2)	0.033(2)	-0.011(2)	-0.008(2)	-0.008(2)
C(42)	0.035(3)	0.044(3)	0.037(3)	-0.018(2)	-0.007(2)	-0.012(2)
C(43)	0.043(3)	0.059(4)	0.050(3)	-0.030(3)	-0.010(3)	-0.016(3)
C(44)	0.043(3)	0.065(4)	0.076(5)	-0.035(4)	-0.007(3)	-0.026(3)
C(45)	0.056(4)	0.085(5)	0.056(4)	-0.027(4)	0.005(3)	-0.047(4)
C(46)	0.044(3)	0.061(4)	0.042(3)	-0.022(3)	0.001(2)	-0.028(3)
C(51)	0.031(2)	0.025(2)	0.024(2)	-0.007(2)	-0.005(2)	-0.006(2)
C(52)	0.044(3)	0.028(2)	0.047(3)	-0.006(2)	-0.015(2)	-0.010(2)
C(53)	0.063(4)	0.026(3)	0.057(4)	-0.007(2)	-0.022(3)	-0.004(3)
C(54)	0.047(3)	0.041(3)	0.049(3)	-0.015(3)	-0.016(3)	0.008(3)
C(55)	0.031(3)	0.058(4)	0.038(3)	-0.014(3)	-0.009(2)	-0.005(2)
C(56)	0.031(2)	0.034(2)	0.034(3)	-0.009(2)	-0.005(2)	-0.010(2)
C(61)	0.031(2)	0.028(2)	0.026(2)	-0.004(2)	-0.007(2)	-0.011(2)
C(62)	0.039(3)	0.034(2)	0.032(3)	-0.009(2)	-0.003(2)	-0.013(2)
C(63)	0.045(3)	0.052(3)	0.032(3)	-0.010(2)	0.001(2)	-0.017(3)

C(64)	0.051(3)	0.049(3)	0.037(3)	0.005(2)	-0.007(2)	-0.024(3)
C(65)	0.046(3)	0.033(3)	0.044(3)	0.001(2)	-0.012(2)	-0.015(2)
C(66)	0.032(2)	0.028(2)	0.033(2)	-0.005(2)	-0.009(2)	-0.008(2)
Cl(1)	0.101(2)	0.070(1)	0.081(1)	-0.019(1)	-0.007(1)	-0.026(1)
Cl(2)	0.218(5)	0.116(3)	0.162(4)	-0.051(3)	0.086(3)	-0.101(3)

Table A-35 Hydrogen coordinates and isotropic displacement parameters (\AA^2) for
 $[\text{Pt}\{\text{N}(\text{C}(\text{O})\text{NH}_2)\text{C}(\text{O})\text{CHCN}\}(\text{PPh}_3)_2]\cdot\text{CH}_2\text{Cl}_2\cdot 0.5\text{Et}_2\text{O}$ (**6.5**)

	x	y	z	U(eq)
H(2A)	0.9310	0.5482	0.6610	0.034
H(3A)	1.167(7)	0.452(6)	0.853(5)	0.053
H(3B)	1.128(7)	0.455(6)	0.943(5)	0.053
H(12)	0.4269	0.9012	0.5821	0.048
H(13)	0.2199	0.8713	0.6181	0.067
H(14)	0.1751	0.7412	0.7361	0.066
H(15)	0.3366	0.6379	0.8181	0.058
H(16)	0.5413	0.6710	0.7855	0.044
H(22)	0.7134	0.5964	0.6115	0.048
H(23)	0.7905	0.5214	0.4947	0.062
H(24)	0.8501	0.6340	0.3705	0.068
H(25)	0.8418	0.8201	0.3635	0.064
H(26)	0.7671	0.8952	0.4811	0.046
H(32)	0.8629	0.9116	0.6075	0.044
H(33)	0.8708	1.0973	0.5553	0.054
H(34)	0.6716	1.2547	0.5396	0.058
H(35)	0.4624	1.2288	0.5779	0.058
H(36)	0.4543	1.0411	0.6264	0.044
H(42)	0.6951	0.8873	0.9889	0.044
H(43)	0.8100	0.9928	1.0072	0.056
H(44)	0.9651	1.0501	0.9023	0.066
H(45)	1.0120	0.9997	0.7774	0.071
H(46)	0.8973	0.8954	0.7573	0.054
H(52)	0.6170	1.0737	0.8011	0.047
H(53)	0.4240	1.2368	0.7790	0.061
H(54)	0.2212	1.2177	0.7846	0.061
H(55)	0.2077	1.0341	0.8150	0.053
H(56)	0.3970	0.8700	0.8408	0.040
H(62)	0.4804	0.8799	0.9916	0.042
H(63)	0.3965	0.7752	1.1118	0.054
H(64)	0.4647	0.5736	1.1313	0.057
H(65)	0.6167	0.4798	1.0304	0.050
H(66)	0.7010	0.5839	0.9096	0.038
H(70A)	0.8902	0.3751	0.9953	0.120
H(70B)	1.0060	0.2526	0.9890	0.120
H(81A)	0.4733	0.4763	0.7150	0.064
H(81B)	0.4792	0.3763	0.6783	0.064
H(82A)	0.4396	0.6041	0.6015	0.135
H(82B)	0.3453	0.5320	0.6135	0.135
H(82C)	0.4844	0.5073	0.5506	0.135
H(83A)	0.6751	0.2704	0.7001	0.102

H(83B)	0.6628	0.3594	0.7483	0.102
H(84A)	0.8735	0.3287	0.6263	0.132
H(84B)	0.8735	0.2188	0.6972	0.132
H(84C)	0.8625	0.3347	0.7170	0.132

Table A-36 Atomic coordinates and equivalent isotropic displacement parameters (\AA^2)for $[\text{Ir}\{\text{N}(\text{Me})\text{C}(\text{O})\text{NAc}\}(\text{Cp}^*)(\text{PPh}_3)].\text{CHCl}_3$ (7.4)

U(eq) is defined as one third of the trace of the orthogonalised Uij tensor.

	x	y	z	U(eq)
Ir	0.4133(1)	0.1459(1)	0.7799(1)	0.021(1)
P	0.4505(1)	0.0859(1)	0.6697(1)	0.023(1)
N(1)	0.3154(3)	0.0478(2)	0.7841(2)	0.030(1)
N(2)	0.2409(3)	0.1468(2)	0.7039(2)	0.025(1)
O(1)	0.1181(2)	0.0403(2)	0.7106(2)	0.039(1)
O(2)	0.2194(3)	0.2533(2)	0.6197(2)	0.054(1)
C(1)	0.2130(3)	0.0734(2)	0.7305(2)	0.030(1)
C(2)	0.3326(4)	-0.0265(2)	0.8263(3)	0.038(1)
C(3)	0.1773(4)	0.1950(2)	0.6408(3)	0.037(1)
C(4)	0.0519(4)	0.1761(3)	0.5968(4)	0.065(2)
C(5)	0.4525(4)	0.1825(2)	0.9149(2)	0.033(1)
C(6)	0.5574(3)	0.1637(2)	0.9021(2)	0.030(1)
C(7)	0.5694(3)	0.2180(2)	0.8398(2)	0.027(1)
C(8)	0.4704(3)	0.2684(2)	0.8122(3)	0.032(1)
C(9)	0.3992(4)	0.2460(2)	0.8600(3)	0.035(1)
C(10)	0.4084(5)	0.1412(3)	0.9763(3)	0.049(1)
C(11)	0.6495(4)	0.1109(3)	0.9582(3)	0.044(1)
C(12)	0.6739(4)	0.2247(3)	0.8163(3)	0.040(1)
C(13)	0.4508(4)	0.3388(2)	0.7546(3)	0.044(1)
C(14)	0.2871(4)	0.2840(3)	0.8517(3)	0.054(1)
C(21)	0.3251(3)	0.0585(2)	0.5766(2)	0.026(1)
C(22)	0.2947(4)	0.0965(3)	0.4982(3)	0.039(1)
C(23)	0.1975(4)	0.0746(3)	0.4301(3)	0.049(1)
C(24)	0.1274(4)	0.0157(3)	0.4392(3)	0.046(1)
C(25)	0.1572(4)	-0.0230(3)	0.5171(3)	0.040(1)
C(26)	0.2555(4)	-0.0029(2)	0.5844(2)	0.033(1)
C(31)	0.5250(3)	-0.0084(2)	0.6977(2)	0.027(1)
C(32)	0.5172(4)	-0.0656(2)	0.6360(3)	0.038(1)
C(33)	0.5687(4)	-0.1388(3)	0.6608(3)	0.046(1)
C(34)	0.6278(4)	-0.1546(3)	0.7465(3)	0.044(1)
C(35)	0.6369(4)	-0.0987(3)	0.8072(3)	0.044(1)
C(36)	0.5850(4)	-0.0257(2)	0.7829(3)	0.035(1)
C(41)	0.5349(3)	0.1452(2)	0.6235(2)	0.030(1)
C(42)	0.4959(4)	0.2221(2)	0.5986(3)	0.039(1)
C(43)	0.5565(5)	0.2710(3)	0.5631(3)	0.048(1)
C(44)	0.6549(5)	0.2441(3)	0.5541(3)	0.056(1)
C(45)	0.6945(5)	0.1700(3)	0.5791(3)	0.054(1)
C(46)	0.6343(4)	0.1192(3)	0.6136(3)	0.040(1)
C(50)	0.0074(5)	0.0498(3)	0.8393(3)	0.054(1)
Cl(1)	-0.1269(1)	0.0060(1)	0.8176(1)	0.077(1)
Cl(2)	-0.0053(2)	0.1529(1)	0.8363(2)	0.097(1)
Cl(3)	0.1032(2)	0.0206(1)	0.9399(1)	0.098(1)

Table A-37 Bond lengths (Å) for $[\text{Ir}\{\text{N}(\text{Me})\text{C}(\text{O})\text{NAc}\}(\text{Cp}^*)(\text{PPh}_3)].\text{CHCl}_3$ (7.4)

Ir–N(2)	2.079(3)	Ir–N(1)	2.092(3)
Ir–C(8)	2.210(3)	Ir–C(6)	2.210(4)
Ir–C(9)	2.216(4)	Ir–C(7)	2.222(3)
Ir–C(5)	2.223(4)	Ir–P	2.3001(9)
P–C(41)	1.825(4)	P–C(31)	1.832(4)
P–C(21)	1.833(4)	N(1)–C(1)	1.348(5)
N(1)–C(2)	1.429(5)	N(2)–C(3)	1.349(5)
N(2)–C(1)	1.413(5)	O(1)–C(1)	1.250(5)
O(2)–C(3)	1.236(5)	C(3)–C(4)	1.512(6)
C(5)–C(9)	1.422(6)	C(5)–C(6)	1.444(6)
C(5)–C(10)	1.505(6)	C(6)–C(7)	1.442(5)
C(6)–C(11)	1.500(6)	C(7)–C(8)	1.443(5)
C(7)–C(12)	1.502(6)	C(8)–C(9)	1.449(6)
C(8)–C(13)	1.505(5)	C(9)–C(14)	1.508(6)
C(21)–C(22)	1.389(5)	C(21)–C(26)	1.398(5)
C(22)–C(23)	1.388(6)	C(23)–C(24)	1.379(6)
C(24)–C(25)	1.387(6)	C(25)–C(26)	1.382(6)
C(31)–C(36)	1.386(5)	C(31)–C(32)	1.399(5)
C(32)–C(33)	1.398(6)	C(33)–C(34)	1.385(7)
C(34)–C(35)	1.368(6)	C(35)–C(36)	1.396(6)
C(41)–C(46)	1.389(6)	C(41)–C(42)	1.409(6)
C(42)–C(43)	1.397(6)	C(43)–C(44)	1.375(7)
C(44)–C(45)	1.367(7)	C(45)–C(46)	1.402(6)
C(50)–Cl(3)	1.754(6)	C(50)–Cl(1)	1.758(6)
C(50)–Cl(2)	1.763(5)		

Table A-38 Bond angles (°) for $[\text{Ir}\{\text{N}(\text{Me})\text{C}(\text{O})\text{NAc}\}(\text{Cp}^*)(\text{PPh}_3)].\text{CHCl}_3$ (7.4)

N(2)–Ir–N(1)	62.08(12)	N(2)–Ir–C(8)	108.49(13)
N(1)–Ir–C(8)	152.83(14)	N(2)–Ir–C(6)	152.94(14)
N(1)–Ir–C(6)	111.92(13)	C(8)–Ir–C(6)	63.83(14)
N(2)–Ir–C(9)	94.17(14)	N(1)–Ir–C(9)	114.79(14)
C(8)–Ir–C(9)	38.22(15)	C(6)–Ir–C(9)	63.33(15)
N(2)–Ir–C(7)	145.74(12)	N(1)–Ir–C(7)	149.32(13)
C(8)–Ir–C(7)	37.99(14)	C(6)–Ir–C(7)	37.98(14)
C(9)–Ir–C(7)	63.29(15)	N(2)–Ir–C(5)	114.93(14)
N(1)–Ir–C(5)	96.19(14)	C(8)–Ir–C(5)	63.42(15)
C(6)–Ir–C(5)	38.02(15)	C(9)–Ir–C(5)	37.36(15)
C(7)–Ir–C(5)	63.20(15)	N(2)–Ir–P	88.79(9)
N(1)–Ir–P	87.84(9)	C(8)–Ir–P	118.38(11)
C(6)–Ir–P	117.98(11)	C(9)–Ir–P	155.73(11)
C(7)–Ir–P	102.01(10)	C(5)–Ir–P	154.99(12)
C(41)–P–C(31)	105.89(18)	C(41)–P–C(21)	103.44(17)
C(31)–P–C(21)	101.41(17)	C(41)–P–Ir	114.17(12)
C(31)–P–Ir	114.62(12)	C(21)–P–Ir	115.80(12)
C(1)–N(1)–C(2)	123.8(3)	C(1)–N(1)–Ir	98.5(2)
C(2)–N(1)–Ir	137.7(3)	C(3)–N(2)–C(1)	129.9(3)
C(3)–N(2)–Ir	132.6(3)	C(1)–N(2)–Ir	97.0(2)
O(1)–C(1)–N(1)	128.3(4)	O(1)–C(1)–N(2)	129.5(4)

N(1)–C(1)–N(2)	102.3(3)	O(2)–C(3)–N(2)	121.3(4)
O(2)–C(3)–C(4)	120.6(4)	N(2)–C(3)–C(4)	118.1(4)
C(9)–C(5)–C(6)	108.4(3)	C(9)–C(5)–C(10)	126.5(4)
C(6)–C(5)–C(10)	125.2(4)	C(9)–C(5)–Ir	71.1(2)
C(6)–C(5)–Ir	70.5(2)	C(10)–C(5)–Ir	124.2(3)
C(7)–C(6)–C(5)	107.6(3)	C(7)–C(6)–C(11)	125.5(4)
C(5)–C(6)–C(11)	125.4(4)	C(7)–C(6)–Ir	71.5(2)
C(5)–C(6)–Ir	71.5(2)	C(11)–C(6)–Ir	133.5(3)
C(6)–C(7)–C(8)	108.2(3)	C(6)–C(7)–C(12)	124.4(4)
C(8)–C(7)–C(12)	127.1(4)	C(6)–C(7)–Ir	70.6(2)
C(8)–C(7)–Ir	70.5(2)	C(12)–C(7)–Ir	129.4(3)
C(7)–C(8)–C(9)	107.3(3)	C(7)–C(8)–C(13)	127.2(4)
C(9)–C(8)–C(13)	125.0(4)	C(7)–C(8)–Ir	71.47(19)
C(9)–C(8)–Ir	71.1(2)	C(13)–C(8)–Ir	129.3(3)
C(5)–C(9)–C(8)	108.5(4)	C(5)–C(9)–C(14)	126.4(4)
C(8)–C(9)–C(14)	125.1(4)	C(5)–C(9)–Ir	71.6(2)
C(8)–C(9)–Ir	70.6(2)	C(14)–C(9)–Ir	123.3(3)
C(22)–C(21)–C(26)	117.9(3)	C(22)–C(21)–P	123.0(3)
C(26)–C(21)–P	119.1(3)	C(23)–C(22)–C(21)	120.8(4)
C(24)–C(23)–C(22)	120.8(4)	C(23)–C(24)–C(25)	118.9(4)
C(26)–C(25)–C(24)	120.5(4)	C(25)–C(26)–C(21)	121.0(4)
C(36)–C(31)–C(32)	118.7(4)	C(36)–C(31)–P	119.3(3)
C(32)–C(31)–P	121.9(3)	C(33)–C(32)–C(31)	120.1(4)
C(34)–C(33)–C(32)	120.0(4)	C(35)–C(34)–C(33)	120.4(4)
C(34)–C(35)–C(36)	119.9(4)	C(31)–C(36)–C(35)	121.0(4)
C(46)–C(41)–C(42)	119.5(4)	C(46)–C(41)–P	123.8(3)
C(42)–C(41)–P	116.6(3)	C(43)–C(42)–C(41)	119.8(4)
C(44)–C(43)–C(42)	119.6(5)	C(45)–C(44)–C(43)	121.1(4)
C(44)–C(45)–C(46)	120.4(5)	C(41)–C(46)–C(45)	119.5(5)
Cl(3)–C(50)–Cl(1)	110.7(3)	Cl(3)–C(50)–Cl(2)	109.5(3)
Cl(1)–C(50)–Cl(2)	110.4(3)		

Table A-39 Anisotropic displacement parameters (\AA^2) for

$[\text{Ir}\{\text{N}(\text{Me})\text{C}(\text{O})\text{NAc}\}(\text{Cp}^*)(\text{PPh}_3)].\text{CHCl}_3$ (**7.4**)

The anisotropic displacement factor exponent takes the form:

$$-2\pi^2 [h^2 a^{*2} U_{11} + \dots + 2 h k a^* b^* U_{12}]$$

	U11	U22	U33	U23	U13	U12
Ir	0.024(1)	0.016(1)	0.022(1)	0.000(1)	0.005(1)	-0.001(1)
P	0.026(1)	0.021(1)	0.023(1)	0.000(1)	0.007(1)	-0.001(1)
N(1)	0.027(2)	0.027(2)	0.033(2)	0.003(1)	0.008(1)	-0.005(1)
N(2)	0.023(2)	0.022(1)	0.028(2)	0.001(1)	0.006(1)	-0.002(1)
O(1)	0.033(2)	0.041(2)	0.036(2)	0.003(1)	0.004(1)	-0.017(1)
O(2)	0.056(2)	0.036(2)	0.052(2)	0.021(2)	-0.001(2)	-0.004(2)
C(1)	0.033(2)	0.027(2)	0.027(2)	-0.003(2)	0.010(2)	-0.003(2)
C(2)	0.040(2)	0.036(2)	0.036(2)	0.007(2)	0.010(2)	-0.003(2)
C(3)	0.035(2)	0.030(2)	0.036(2)	0.005(2)	0.000(2)	0.002(2)
C(4)	0.043(3)	0.050(3)	0.072(4)	0.023(3)	-0.014(3)	-0.001(2)
C(5)	0.044(2)	0.028(2)	0.024(2)	-0.009(2)	0.011(2)	-0.008(2)

C(6)	0.032(2)	0.026(2)	0.023(2)	-0.006(1)	0.000(2)	-0.003(2)
C(7)	0.026(2)	0.020(2)	0.030(2)	-0.004(1)	0.003(2)	-0.009(1)
C(8)	0.033(2)	0.016(2)	0.038(2)	-0.006(2)	0.003(2)	-0.004(2)
C(9)	0.037(2)	0.026(2)	0.038(2)	-0.014(2)	0.011(2)	-0.004(2)
C(10)	0.067(3)	0.048(3)	0.037(2)	-0.006(2)	0.026(2)	-0.013(2)
C(11)	0.053(3)	0.034(2)	0.030(2)	-0.001(2)	-0.003(2)	0.005(2)
C(12)	0.032(2)	0.043(2)	0.042(2)	-0.008(2)	0.011(2)	-0.012(2)
C(13)	0.050(3)	0.024(2)	0.045(3)	0.002(2)	0.001(2)	-0.004(2)
C(14)	0.043(3)	0.047(3)	0.068(3)	-0.027(2)	0.014(2)	0.006(2)
C(21)	0.030(2)	0.022(2)	0.023(2)	-0.002(1)	0.006(2)	-0.001(1)
C(22)	0.040(2)	0.036(2)	0.032(2)	0.007(2)	0.002(2)	-0.008(2)
C(23)	0.049(3)	0.050(3)	0.034(2)	0.012(2)	-0.004(2)	-0.008(2)
C(24)	0.036(2)	0.046(3)	0.039(2)	-0.002(2)	-0.005(2)	-0.006(2)
C(25)	0.037(2)	0.036(2)	0.042(2)	-0.006(2)	0.009(2)	-0.012(2)
C(26)	0.039(2)	0.029(2)	0.027(2)	-0.001(2)	0.008(2)	-0.004(2)
C(31)	0.027(2)	0.024(2)	0.030(2)	-0.002(2)	0.010(2)	0.000(1)
C(32)	0.047(3)	0.033(2)	0.033(2)	-0.002(2)	0.013(2)	0.005(2)
C(33)	0.055(3)	0.034(2)	0.050(3)	-0.008(2)	0.021(2)	0.010(2)
C(34)	0.049(3)	0.036(2)	0.053(3)	0.009(2)	0.023(2)	0.018(2)
C(35)	0.047(3)	0.044(3)	0.036(2)	0.009(2)	0.009(2)	0.016(2)
C(36)	0.037(2)	0.032(2)	0.032(2)	-0.002(2)	0.008(2)	0.004(2)
C(41)	0.032(2)	0.031(2)	0.025(2)	-0.004(2)	0.009(2)	-0.007(2)
C(42)	0.046(3)	0.035(2)	0.036(2)	0.001(2)	0.016(2)	-0.010(2)
C(43)	0.069(3)	0.039(2)	0.038(2)	0.000(2)	0.021(2)	-0.016(2)
C(44)	0.073(4)	0.055(3)	0.050(3)	-0.012(2)	0.036(3)	-0.032(3)
C(45)	0.051(3)	0.067(3)	0.057(3)	-0.015(3)	0.034(3)	-0.019(3)
C(46)	0.042(3)	0.042(2)	0.039(2)	-0.011(2)	0.018(2)	-0.009(2)
C(50)	0.053(3)	0.059(3)	0.057(3)	-0.001(2)	0.027(3)	0.005(2)
Cl(1)	0.056(1)	0.096(1)	0.083(1)	-0.007(1)	0.028(1)	-0.009(1)
Cl(2)	0.121(2)	0.055(1)	0.122(2)	-0.014(1)	0.052(1)	0.006(1)
Cl(3)	0.063(1)	0.152(2)	0.073(1)	0.031(1)	0.017(1)	0.016(1)

Table A-40 Hydrogen coordinates and isotropic displacement parameters (\AA^2) for
 $[\text{Ir}\{\text{N}(\text{Me})\text{C}(\text{O})\text{NAc}\}(\text{Cp}^*)(\text{PPh}_3)]\cdot\text{CHCl}_3$ (**7.4**)

	x	y	z	U(eq)
H(2A)	0.2655	-0.0402	0.8393	0.057
H(2B)	0.3985	-0.0237	0.8791	0.057
H(2C)	0.3455	-0.0663	0.7893	0.057
H(4A)	0.0250	0.1976	0.5394	0.097
H(4B)	0.0089	0.1988	0.6290	0.097
H(4C)	0.0416	0.1196	0.5939	0.097
H(10A)	0.4435	0.1638	1.0329	0.073
H(10B)	0.4273	0.0859	0.9783	0.073
H(10C)	0.3262	0.1474	0.9572	0.073
H(11A)	0.6905	0.1374	1.0118	0.066
H(11B)	0.7021	0.0981	0.9296	0.066
H(11C)	0.6156	0.0631	0.9697	0.066
H(12A)	0.7329	0.2529	0.8610	0.059
H(12B)	0.6549	0.2529	0.7627	0.059
H(12C)	0.7012	0.1727	0.8101	0.059

H(13A)	0.4557	0.3862	0.7878	0.066
H(13B)	0.3757	0.3354	0.7102	0.066
H(13C)	0.5084	0.3403	0.7285	0.066
H(14A)	0.3000	0.3236	0.8958	0.082
H(14B)	0.2351	0.2445	0.8581	0.082
H(14C)	0.2542	0.3083	0.7958	0.082
H(22)	0.3405	0.1376	0.4911	0.047
H(23)	0.1792	0.1002	0.3772	0.059
H(24)	0.0606	0.0019	0.3934	0.055
H(25)	0.1101	-0.0633	0.5242	0.048
H(26)	0.2759	-0.0309	0.6361	0.039
H(32)	0.4774	-0.0548	0.5777	0.046
H(33)	0.5631	-0.1773	0.6193	0.055
H(34)	0.6619	-0.2040	0.7630	0.053
H(35)	0.6781	-0.1094	0.8653	0.053
H(36)	0.5908	0.0123	0.8250	0.042
H(42)	0.4293	0.2404	0.6059	0.046
H(43)	0.5302	0.3221	0.5455	0.058
H(44)	0.6955	0.2772	0.5303	0.067
H(45)	0.7625	0.1529	0.5732	0.065
H(46)	0.6610	0.0679	0.6299	0.048
H(50)	0.0378	0.0331	0.7950	0.065

Table A-41 Atomic coordinates and equivalent isotropic displacement parameters (\AA^2) for $[\text{Rh}\{\text{OC}(\text{O})\text{C}_6\text{H}_4\text{-2-S}\}(\text{Cp}^*)]_2$ (7.8)

$U(\text{eq})$ is defined as one third of the trace of the orthogonalised U_{ij} tensor.

	x	y	z	$U(\text{eq})$
Rh	0.4071(1)	0.5501(1)	0.0874(1)	0.023(1)
S	0.3912(1)	0.5197(1)	-0.0872(1)	0.024(1)
O(1)	0.3937(2)	0.3490(2)	0.1032(2)	0.030(1)
O(2)	0.3496(3)	0.1442(3)	0.0707(2)	0.060(1)
C(1)	0.3409(3)	0.2600(4)	0.0461(3)	0.031(1)
C(2)	0.2628(3)	0.2922(3)	-0.0529(3)	0.026(1)
C(3)	0.2793(3)	0.3982(3)	-0.1153(3)	0.026(1)
C(4)	0.2038(3)	0.4135(4)	-0.2075(3)	0.032(1)
C(5)	0.1111(3)	0.3280(4)	-0.2372(3)	0.040(1)
C(6)	0.0943(4)	0.2235(4)	-0.1768(3)	0.042(1)
C(7)	0.1688(3)	0.2051(4)	-0.0869(3)	0.036(1)
C(11)	0.3948(4)	0.6431(4)	0.2313(3)	0.043(1)
C(12)	0.2811(4)	0.5905(4)	0.1881(4)	0.052(1)
C(13)	0.2431(4)	0.6497(5)	0.0939(4)	0.047(1)
C(14)	0.3301(4)	0.7422(4)	0.0776(3)	0.045(1)
C(15)	0.4231(4)	0.7379(4)	0.1603(4)	0.040(1)
C(16)	0.4602(6)	0.6130(6)	0.3327(4)	0.086(2)
C(17)	0.2178(7)	0.4835(6)	0.2338(6)	0.103(3)
C(18)	0.1268(4)	0.6243(7)	0.0236(5)	0.092(2)
C(19)	0.3219(7)	0.8334(5)	-0.0096(4)	0.083(2)
C(20)	0.5293(5)	0.8261(5)	0.1797(5)	0.078(2)

Table A-42 Bond lengths (\AA) for $[\text{Rh}\{\text{OC}(\text{O})\text{C}_6\text{H}_4\text{-2-S}\}(\text{Cp}^*)]_2$ (7.8)

Rh–O(1)	2.084(2)	Rh–C(13)	2.144(4)
Rh–C(14)	2.155(4)	Rh–C(15)	2.158(4)
Rh–C(12)	2.173(4)	Rh–C(11)	2.186(4)
Rh–S	2.3498(9)	Rh–S'	2.4056(9)
S–C(3)	1.778(4)	S–Rh'	2.4056(9)
O(1)–C(1)	1.278(4)	O(2)–C(1)	1.233(5)
C(1)–C(2)	1.511(5)	C(2)–C(3)	1.407(5)
C(2)–C(7)	1.411(5)	C(3)–C(4)	1.395(5)
C(4)–C(5)	1.380(5)	C(5)–C(6)	1.379(6)
C(6)–C(7)	1.370(6)	C(11)–C(12)	1.433(6)
C(11)–C(15)	1.438(6)	C(11)–C(16)	1.475(7)
C(12)–C(13)	1.408(7)	C(12)–C(17)	1.502(7)
C(13)–C(14)	1.416(6)	C(13)–C(18)	1.515(7)
C(14)–C(15)	1.404(6)	C(14)–C(19)	1.493(7)
C(15)–C(20)	1.499(6)		

Symmetry transformations used to generate equivalent atoms:

#' $-x+1, -y+1, -z$

Table A-43 Bond angles (°) for $[\text{Rh}\{\text{OC}(\text{O})\text{C}_6\text{H}_4\text{-2-S}\}(\text{Cp}^*)]_2$ (7.8)

O(1)–Rh–C(13)	112.90(15)	O(1)–Rh–C(14)	151.35(15)
C(13)–Rh–C(14)	38.47(17)	O(1)–Rh–C(15)	147.26(15)
C(13)–Rh–C(15)	64.04(16)	C(14)–Rh–C(15)	37.98(17)
O(1)–Rh–C(12)	93.33(14)	C(13)–Rh–C(12)	38.07(19)
C(14)–Rh–C(12)	63.83(18)	C(15)–Rh–C(12)	63.85(15)
O(1)–Rh–C(11)	109.02(14)	C(13)–Rh–C(11)	64.49(17)
C(14)–Rh–C(11)	64.43(16)	C(15)–Rh–C(11)	38.65(16)
C(12)–Rh–C(11)	38.37(17)	O(1)–Rh–S	88.63(7)
C(13)–Rh–S	100.51(13)	C(14)–Rh–S	95.59(12)
C(15)–Rh–S	124.09(13)	C(12)–Rh–S	134.58(16)
C(11)–Rh–S	160.01(12)	O(1)–Rh–S'	77.97(7)
C(13)–Rh–S'	168.59(13)	C(14)–Rh–S'	130.66(13)
C(15)–Rh–S'	105.04(11)	C(12)–Rh–S'	141.99(16)
C(11)–Rh–S'	109.56(12)	S–Rh–S'	82.68(3)
C(3)–S–Rh	103.82(12)	C(3)–S–Rh'	116.11(11)
Rh–S–Rh'	97.32(3)	C(1)–O(1)–Rh	133.1(2)
O(2)–C(1)–O(1)	121.3(4)	O(2)–C(1)–C(2)	117.2(3)
O(1)–C(1)–C(2)	121.5(3)	C(3)–C(2)–C(7)	117.8(3)
C(3)–C(2)–C(1)	125.4(3)	C(7)–C(2)–C(1)	116.7(3)
C(4)–C(3)–C(2)	119.7(3)	C(4)–C(3)–S	115.0(3)
C(2)–C(3)–S	125.3(3)	C(5)–C(4)–C(3)	120.9(4)
C(4)–C(5)–C(6)	119.9(4)	C(7)–C(6)–C(5)	120.2(4)
C(6)–C(7)–C(2)	121.5(4)	C(12)–C(11)–C(15)	105.9(4)
C(12)–C(11)–C(16)	125.3(5)	C(15)–C(11)–C(16)	128.6(5)
C(12)–C(11)–Rh	70.3(2)	C(15)–C(11)–Rh	69.6(2)
C(16)–C(11)–Rh	129.2(3)	C(13)–C(12)–C(11)	108.8(4)
C(13)–C(12)–C(17)	126.1(5)	C(11)–C(12)–C(17)	124.9(6)
C(13)–C(12)–Rh	69.8(2)	C(11)–C(12)–Rh	71.3(2)
C(17)–C(12)–Rh	121.9(3)	C(12)–C(13)–C(14)	108.2(4)
C(12)–C(13)–C(18)	126.4(5)	C(14)–C(13)–C(18)	125.3(5)
C(12)–C(13)–Rh	72.1(2)	C(14)–C(13)–Rh	71.2(2)
C(18)–C(13)–Rh	124.6(3)	C(15)–C(14)–C(13)	108.0(4)
C(15)–C(14)–C(19)	125.7(5)	C(13)–C(14)–C(19)	126.2(5)
C(15)–C(14)–Rh	71.1(2)	C(13)–C(14)–Rh	70.4(2)
C(19)–C(14)–Rh	126.4(3)	C(14)–C(15)–C(11)	109.0(4)
C(14)–C(15)–C(20)	126.8(5)	C(11)–C(15)–C(20)	123.9(5)
C(14)–C(15)–Rh	70.9(2)	C(11)–C(15)–Rh	71.7(2)
C(20)–C(15)–Rh	128.6(3)		

Symmetry transformations used to generate equivalent atoms:

#' -x+1,-y+1,-z

Table A-44 Anisotropic displacement parameters (\AA^2) for $[\text{Rh}\{\text{OC}(\text{O})\text{C}_6\text{H}_4\text{-2-S}\}(\text{Cp}^*)]_2$ (7.8)

The anisotropic displacement factor exponent takes the form:

$$-2\pi^2 [h^2 a^{*2} U_{11} + \dots + 2 h k a^* b^* U_{12}]$$

	U11	U22	U33	U23	U13	U12
Rh	0.023(1)	0.021(1)	0.025(1)	-0.004(1)	0.007(1)	-0.003(1)
S	0.025(1)	0.022(1)	0.024(1)	-0.001(1)	0.005(1)	-0.001(1)
O(1)	0.036(1)	0.024(1)	0.028(1)	0.000(1)	-0.001(1)	-0.006(1)
O(2)	0.092(3)	0.028(2)	0.051(2)	0.009(1)	-0.014(2)	-0.012(2)
C(1)	0.034(2)	0.024(2)	0.035(2)	0.001(2)	0.007(2)	-0.005(2)
C(2)	0.025(2)	0.023(2)	0.031(2)	-0.005(1)	0.007(2)	-0.002(1)
C(3)	0.022(2)	0.025(2)	0.030(2)	-0.006(1)	0.006(1)	0.001(1)
C(4)	0.031(2)	0.034(2)	0.029(2)	-0.001(2)	-0.002(2)	0.003(2)
C(5)	0.028(2)	0.053(3)	0.036(2)	-0.010(2)	-0.004(2)	0.003(2)
C(6)	0.030(2)	0.047(3)	0.049(3)	-0.019(2)	0.005(2)	-0.012(2)
C(7)	0.038(2)	0.032(2)	0.040(2)	-0.007(2)	0.014(2)	-0.007(2)
C(11)	0.057(3)	0.043(2)	0.032(2)	-0.014(2)	0.011(2)	0.012(2)
C(12)	0.060(3)	0.035(2)	0.074(3)	-0.023(2)	0.050(3)	-0.014(2)
C(13)	0.032(2)	0.053(3)	0.058(3)	-0.025(2)	0.011(2)	0.008(2)
C(14)	0.060(3)	0.030(2)	0.047(3)	-0.007(2)	0.019(2)	0.016(2)
C(15)	0.033(2)	0.032(2)	0.060(3)	-0.022(2)	0.024(2)	-0.005(2)
C(16)	0.120(6)	0.090(4)	0.043(3)	-0.025(3)	0.002(3)	0.033(4)
C(17)	0.143(7)	0.068(4)	0.129(6)	-0.028(4)	0.111(6)	-0.040(4)
C(18)	0.032(3)	0.123(6)	0.115(5)	-0.058(5)	-0.003(3)	0.017(3)
C(19)	0.142(6)	0.050(3)	0.062(4)	0.012(3)	0.033(4)	0.048(4)
C(20)	0.060(3)	0.049(3)	0.137(6)	-0.051(3)	0.050(4)	-0.024(3)

Table A-45 Hydrogen coordinates and isotropic displacement parameters (\AA^2) for $[\text{Rh}\{\text{OC}(\text{O})\text{C}_6\text{H}_4\text{-2-S}\}(\text{Cp}^*)]_2$ (7.8)

	X	y	z	U(eq)
H(4A)	0.2163	0.4830	-0.2498	0.039
H(5A)	0.0594	0.3409	-0.2986	0.048
H(6A)	0.0316	0.1647	-0.1974	0.051
H(7A)	0.1569	0.1329	-0.0469	0.043
H(16A)	0.4417	0.6780	0.3800	0.129
H(16B)	0.5451	0.6136	0.3315	0.129
H(16C)	0.4367	0.5277	0.3532	0.129
H(17A)	0.1640	0.5211	0.2747	0.154
H(17B)	0.2757	0.4290	0.2756	0.154
H(17C)	0.1726	0.4312	0.1807	0.154
H(18A)	0.0714	0.6946	0.0293	0.138
H(18B)	0.0930	0.5427	0.0417	0.138
H(18C)	0.1415	0.6193	-0.0451	0.138
H(19A)	0.2774	0.9103	0.0034	0.124
H(19B)	0.2816	0.7906	-0.0700	0.124
H(19C)	0.4015	0.8586	-0.0190	0.124
H(20A)	0.5163	0.8928	0.2277	0.117
H(20B)	0.5410	0.8668	0.1171	0.117
H(20C)	0.5995	0.7758	0.2069	0.117

Table A-46 Atomic coordinates and equivalent isotropic displacement parameters (\AA^2)for $[\text{Ru}\{\text{OC}(\text{O})\text{C}_6\text{H}_4\text{-2-S}\}(p\text{-cymene})]_2$ (**7.9**)

U(eq) is defined as one third of the trace of the orthogonalised Uij tensor.

	X	y	z	U(eq)
Ru	0.5884(1)	0.0739(1)	0.9112(1)	0.016(1)
S	0.4635(1)	0.1040(1)	1.0500(1)	0.018(1)
O(1)	0.3866(1)	0.0491(1)	0.7965(1)	0.024(1)
O(2)	0.1540(2)	0.0107(1)	0.7418(1)	0.041(1)
C(1)	0.2548(2)	0.0622(1)	0.7996(2)	0.023(1)
C(2)	0.2199(2)	0.1486(1)	0.8707(2)	0.022(1)
C(3)	0.3049(2)	0.1739(1)	0.9784(2)	0.021(1)
C(4)	0.2644(2)	0.2571(2)	1.0367(2)	0.028(1)
C(5)	0.1407(2)	0.3144(2)	0.9888(2)	0.033(1)
C(6)	0.0550(2)	0.2893(2)	0.8828(2)	0.036(1)
C(7)	0.0938(2)	0.2066(2)	0.8249(2)	0.030(1)
C(8)	0.8439(2)	-0.0566(2)	0.8131(2)	0.029(1)
C(9)	0.7884(2)	0.0407(1)	0.8539(2)	0.022(1)
C(10)	0.8231(2)	0.0655(1)	0.9711(2)	0.021(1)
C(11)	0.7750(2)	0.1588(1)	1.0086(2)	0.021(1)
C(12)	0.6882(2)	0.2318(1)	0.9306(1)	0.020(1)
C(13)	0.6487(2)	0.2044(1)	0.8162(2)	0.022(1)
C(14)	0.6979(2)	0.1096(2)	0.7789(2)	0.023(1)
C(15)	0.6385(2)	0.3316(1)	0.9735(2)	0.023(1)
C(16)	0.5078(2)	0.3808(2)	0.8910(2)	0.032(1)
C(17)	0.7671(2)	0.4076(2)	1.0047(2)	0.032(1)

Table A-47 Bond lengths (\AA) for $[\text{Ru}\{\text{OC}(\text{O})\text{C}_6\text{H}_4\text{-2-S}\}(p\text{-cymene})]_2$ (**7.9**)

Ru–O(1)	2.0930(12)	Ru–C(11)	2.1648(17)
Ru–C(10)	2.1760(17)	Ru–C(13)	2.2187(17)
Ru–C(14)	2.2274(17)	Ru–C(12)	2.2313(17)
Ru–C(9)	2.2637(17)	Ru–S	2.3848(4)
Ru–S'	2.4177(4)	S–C(3)	1.7831(18)
S–Ru'	2.4177(4)	O(1)–C(1)	1.288(2)
O(2)–C(1)	1.230(2)	C(1)–C(2)	1.513(3)
C(2)–C(3)	1.402(3)	C(2)–C(7)	1.404(3)
C(3)–C(4)	1.406(2)	C(4)–C(5)	1.387(3)
C(5)–C(6)	1.387(3)	C(6)–C(7)	1.390(3)
C(8)–C(9)	1.502(3)	C(9)–C(14)	1.402(3)
C(9)–C(10)	1.437(3)	C(10)–C(11)	1.410(2)
C(11)–C(12)	1.440(2)	C(12)–C(13)	1.412(2)
C(12)–C(15)	1.516(2)	C(13)–C(14)	1.430(3)
C(15)–C(16)	1.524(3)	C(15)–C(17)	1.540(3)

Symmetry transformations used to generate equivalent atoms:

#' -x+1,-y,-z+2

Table A-48 Bond angles (°) for $[\text{Ru}\{\text{OC}(\text{O})\text{C}_6\text{H}_4\text{-2-S}\}(p\text{-cymene})]_2$ (**7.9**)

O(1)–Ru–C(11)	158.26(6)	O(1)–Ru–C(10)	154.95(6)
C(11)–Ru–C(10)	37.91(7)	O(1)–Ru–C(13)	94.64(6)
C(11)–Ru–C(13)	67.56(7)	C(10)–Ru–C(13)	79.78(7)
O(1)–Ru–C(14)	93.74(6)	C(11)–Ru–C(14)	79.75(7)
C(10)–Ru–C(14)	66.94(7)	C(13)–Ru–C(14)	37.53(7)
O(1)–Ru–C(12)	120.20(6)	C(11)–Ru–C(12)	38.19(6)
C(10)–Ru–C(12)	68.49(6)	C(13)–Ru–C(12)	37.00(6)
C(14)–Ru–C(12)	67.44(6)	O(1)–Ru–C(9)	117.71(6)
C(11)–Ru–C(9)	68.05(7)	C(10)–Ru–C(9)	37.71(7)
C(13)–Ru–C(9)	66.93(7)	C(14)–Ru–C(9)	36.37(7)
C(12)–Ru–C(9)	80.14(6)	O(1)–Ru–S	87.80(4)
C(11)–Ru–S	91.01(5)	C(10)–Ru–S	116.09(5)
C(13)–Ru–S	121.15(5)	C(14)–Ru–S	158.68(5)
C(12)–Ru–S	93.45(4)	C(9)–Ru–S	153.52(5)
O(1)–Ru–S'	77.80(4)	C(11)–Ru–S'	123.41(5)
C(10)–Ru–S'	97.79(5)	C(13)–Ru–S'	156.93(5)
C(14)–Ru–S'	120.41(5)	C(12)–Ru–S'	161.07(5)
C(9)–Ru–S'	97.04(5)	S–Ru–S'	80.714(15)
C(3)–S–Ru	104.54(6)	C(3)–S–Ru'	112.48(6)
Ru–S–Ru'	99.286(15)	C(1)–O(1)–Ru	134.03(12)
O(2)–C(1)–O(1)	122.40(17)	O(2)–C(1)–C(2)	118.15(16)
O(1)–C(1)–C(2)	119.32(15)	C(3)–C(2)–C(7)	118.44(17)
C(3)–C(2)–C(1)	124.25(16)	C(7)–C(2)–C(1)	117.31(17)
C(2)–C(3)–C(4)	119.80(17)	C(2)–C(3)–S	123.70(14)
C(4)–C(3)–S	116.48(14)	C(5)–C(4)–C(3)	120.57(19)
C(4)–C(5)–C(6)	120.08(19)	C(5)–C(6)–C(7)	119.67(19)
C(6)–C(7)–C(2)	121.41(19)	C(14)–C(9)–C(10)	117.61(16)
C(14)–C(9)–C(8)	121.01(17)	C(10)–C(9)–C(8)	121.37(17)
C(14)–C(9)–Ru	70.40(10)	C(10)–C(9)–Ru	67.83(9)
C(8)–C(9)–Ru	132.27(12)	C(11)–C(10)–C(9)	121.08(17)
C(11)–C(10)–Ru	70.61(10)	C(9)–C(10)–Ru	74.45(10)
C(10)–C(11)–C(12)	121.02(16)	C(10)–C(11)–Ru	71.47(10)
C(12)–C(11)–Ru	73.41(10)	C(13)–C(12)–C(11)	117.48(16)
C(13)–C(12)–C(15)	122.70(16)	C(11)–C(12)–C(15)	119.78(15)
C(13)–C(12)–Ru	71.02(10)	C(11)–C(12)–Ru	68.40(10)
C(15)–C(12)–Ru	129.93(12)	C(12)–C(13)–C(14)	121.11(16)
C(12)–C(13)–Ru	71.99(10)	C(14)–C(13)–Ru	71.56(10)
C(9)–C(14)–C(13)	121.56(16)	C(9)–C(14)–Ru	73.22(10)
C(13)–C(14)–Ru	70.91(9)	C(12)–C(15)–C(16)	113.37(15)
C(12)–C(15)–C(17)	108.59(15)	C(16)–C(15)–C(17)	111.25(16)

Symmetry transformations used to generate equivalent atoms:

#' -x+1,-y,-z+2

Table A-49 Anisotropic displacement parameters (\AA^2) for $[\text{Ru}\{\text{OC}(\text{O})\text{C}_6\text{H}_4\text{-2-S}\}(p\text{-cymene})]_2$ (**7.9**)

The anisotropic displacement factor exponent takes the form:

$$-2\pi^2 [h^2 a^{*2} U_{11} + \dots + 2 h k a^* b^* U_{12}]$$

	U11	U22	U33	U23	U13	U12
Ru	0.014(1)	0.018(1)	0.015(1)	0.000(1)	0.006(1)	0.001(1)
S	0.017(1)	0.019(1)	0.018(1)	-0.002(1)	0.007(1)	0.000(1)
O(1)	0.017(1)	0.034(1)	0.021(1)	-0.005(1)	0.004(1)	0.002(1)
O(2)	0.024(1)	0.058(1)	0.041(1)	-0.020(1)	0.010(1)	-0.012(1)
C(1)	0.019(1)	0.029(1)	0.020(1)	0.002(1)	0.006(1)	-0.001(1)
C(2)	0.018(1)	0.023(1)	0.027(1)	0.005(1)	0.010(1)	0.000(1)
C(3)	0.020(1)	0.018(1)	0.026(1)	0.003(1)	0.012(1)	0.001(1)
C(4)	0.030(1)	0.024(1)	0.035(1)	-0.002(1)	0.018(1)	-0.001(1)
C(5)	0.036(1)	0.021(1)	0.053(1)	0.003(1)	0.028(1)	0.005(1)
C(6)	0.028(1)	0.032(1)	0.053(1)	0.017(1)	0.020(1)	0.012(1)
C(7)	0.021(1)	0.035(1)	0.034(1)	0.010(1)	0.010(1)	0.003(1)
C(8)	0.023(1)	0.029(1)	0.039(1)	-0.006(1)	0.014(1)	0.000(1)
C(9)	0.016(1)	0.024(1)	0.030(1)	-0.002(1)	0.012(1)	-0.003(1)
C(10)	0.014(1)	0.025(1)	0.026(1)	0.002(1)	0.007(1)	-0.002(1)
C(11)	0.018(1)	0.025(1)	0.019(1)	-0.001(1)	0.005(1)	-0.004(1)
C(12)	0.020(1)	0.020(1)	0.023(1)	0.000(1)	0.009(1)	-0.003(1)
C(13)	0.023(1)	0.024(1)	0.021(1)	0.004(1)	0.009(1)	-0.001(1)
C(14)	0.025(1)	0.026(1)	0.020(1)	-0.001(1)	0.012(1)	-0.003(1)
C(15)	0.028(1)	0.021(1)	0.025(1)	-0.001(1)	0.013(1)	-0.001(1)
C(16)	0.035(1)	0.028(1)	0.037(1)	0.002(1)	0.015(1)	0.009(1)
C(17)	0.037(1)	0.025(1)	0.040(1)	-0.007(1)	0.021(1)	-0.008(1)

Table A-50 Hydrogen coordinates and isotropic displacement parameters (\AA^2) for $[\text{Ru}\{\text{OC}(\text{O})\text{C}_6\text{H}_4\text{-2-S}\}(p\text{-cymene})]_2$ (**7.9**)

	x	y	z	U(eq)
H(4A)	0.3217	0.2742	1.1088	0.033
H(5A)	0.1149	0.3703	1.0282	0.040
H(6A)	-0.0289	0.3280	0.8502	0.043
H(7A)	0.0343	0.1892	0.7537	0.036
H(8A)	0.9309	-0.0408	0.7910	0.044
H(8B)	0.7707	-0.0839	0.7493	0.044
H(8C)	0.8657	-0.1079	0.8726	0.044
H(10A)	0.8680	0.0116	1.0266	0.026
H(11A)	0.7876	0.1688	1.0897	0.025
H(13A)	0.5710	0.2442	0.7635	0.026
H(14A)	0.6523	0.0858	0.7015	0.027
H(15A)	0.6108	0.3149	1.0427	0.028
H(16A)	0.4317	0.3293	0.8676	0.049
H(16B)	0.5356	0.4058	0.8261	0.049
H(16C)	0.4730	0.4384	0.9268	0.049
H(17A)	0.8480	0.3748	1.0582	0.048
H(17B)	0.7389	0.4698	1.0377	0.048
H(17C)	0.7955	0.4261	0.9380	0.048

Table A-51 Atomic coordinates and equivalent isotropic displacement parameters (\AA^2) for $[\text{Pt}\{\overline{\text{NCH}_2\text{CH}_2\text{CO}}\}_2(\text{PPh}_3)_2]\cdot\text{UO}_2(\text{NO}_3)_2$ (**7.15**)

U(eq) is defined as one third of the trace of the orthogonalised Uij tensor.

	x	y	z	U(eq)
U	-0.0659(1)	0.1110(1)	0.2798(1)	0.033(1)
N(10)	-0.1273(4)	-0.0756(8)	0.3127(5)	0.087(3)
O(11)	-0.1226(3)	-0.0875(5)	0.2504(4)	0.076(2)
O(12)	-0.0996(3)	0.0152(5)	0.3628(4)	0.064(2)
O(13)	-0.1416(7)	-0.1741(13)	0.3270(9)	0.068(4)
O(13')	-0.1640(6)	-0.1340(11)	0.3206(8)	0.055(3)
N(14)	-0.0129(3)	0.3083(5)	0.4152(4)	0.046(1)
O(15)	-0.0088(3)	0.3083(4)	0.3540(4)	0.057(1)
O(16)	-0.0406(3)	0.2181(5)	0.4142(4)	0.070(2)
O(17)	0.0081(3)	0.3885(5)	0.4702(4)	0.065(2)
O(18)	-0.1436(2)	0.1817(5)	0.2091(3)	0.051(1)
O(19)	0.0114(2)	0.0384(4)	0.3533(3)	0.051(1)
Pt	0.0662(1)	0.0146(1)	0.2162(1)	0.018(1)
P(1)	0.1206(1)	-0.1588(1)	0.2881(1)	0.022(1)
P(2)	0.1565(1)	0.1311(1)	0.2753(1)	0.022(1)
N(1)	0.0077(2)	0.1617(4)	0.1435(3)	0.024(1)
O(1)	-0.0357(3)	0.2233(4)	0.2093(3)	0.048(1)
C(2)	-0.0333(3)	0.2169(5)	0.1472(4)	0.032(1)
C(3)	-0.0760(3)	0.2679(6)	0.0517(4)	0.042(2)
C(4)	-0.0278(3)	0.2012(6)	0.0476(4)	0.039(2)
O(2)	-0.0970(2)	0.0047(4)	0.1524(3)	0.046(1)
N(5)	-0.0222(2)	-0.0733(4)	0.1395(3)	0.022(1)
C(6)	-0.0792(3)	-0.0602(5)	0.1191(4)	0.028(1)
C(7)	-0.1173(3)	-0.1452(6)	0.0400(4)	0.039(2)
C(8)	-0.0509(3)	-0.1599(6)	0.0622(4)	0.034(1)
C(11)	0.1631(3)	-0.2096(5)	0.2488(4)	0.026(1)
C(12)	0.2261(3)	-0.2580(5)	0.3042(4)	0.036(1)
C(13)	0.2528(3)	-0.2946(6)	0.2659(5)	0.048(2)
C(14)	0.2185(4)	-0.2819(7)	0.1749(5)	0.050(2)
C(15)	0.1555(3)	-0.2309(6)	0.1185(4)	0.041(2)
C(16)	0.1279(3)	-0.1949(6)	0.1559(4)	0.033(1)
C(21)	0.1760(2)	-0.1562(5)	0.4126(3)	0.023(1)
C(22)	0.2140(3)	-0.2566(5)	0.4646(4)	0.033(1)
C(23)	0.2569(3)	-0.2536(6)	0.5585(4)	0.041(2)
C(24)	0.2611(3)	-0.1523(7)	0.6020(4)	0.045(2)
C(25)	0.2212(3)	-0.0537(6)	0.5520(4)	0.041(2)
C(26)	0.1790(3)	-0.0556(5)	0.4576(4)	0.028(1)
C(31)	0.0676(3)	-0.2846(5)	0.2644(4)	0.028(1)
C(32)	0.0248(3)	-0.2679(6)	0.2806(4)	0.036(1)
C(33)	-0.0162(3)	-0.3635(7)	0.2629(5)	0.047(2)
C(34)	-0.0124(4)	-0.4730(7)	0.2316(5)	0.056(2)
C(35)	0.0295(4)	-0.4862(6)	0.2157(6)	0.054(2)
C(36)	0.0699(3)	-0.3943(5)	0.2315(5)	0.042(2)
C(41)	0.2368(3)	0.0615(5)	0.3307(4)	0.029(1)
C(42)	0.2583(3)	0.0377(6)	0.2844(4)	0.036(1)
C(43)	0.3173(4)	-0.0197(7)	0.3253(6)	0.052(2)

C(44)	0.3575(3)	-0.0535(6)	0.4178(5)	0.046(2)
C(45)	0.3367(3)	-0.0303(5)	0.4650(5)	0.038(2)
C(46)	0.2769(3)	0.0282(5)	0.4229(4)	0.029(1)
C(51)	0.1381(3)	0.2145(5)	0.1796(4)	0.024(1)
C(52)	0.1123(3)	0.1515(6)	0.0997(4)	0.036(1)
C(53)	0.0961(3)	0.2117(6)	0.0254(4)	0.041(2)
C(54)	0.1042(4)	0.3330(7)	0.0276(5)	0.052(2)
C(55)	0.1291(4)	0.3966(6)	0.1065(5)	0.059(2)
C(56)	0.1462(3)	0.3369(6)	0.1817(5)	0.041(2)
C(61)	0.1746(3)	0.2433(5)	0.3577(4)	0.024(1)
C(62)	0.2340(3)	0.3069(6)	0.4093(4)	0.037(2)
C(63)	0.2472(3)	0.3933(6)	0.4724(5)	0.044(2)
C(64)	0.2015(4)	0.4162(6)	0.4812(4)	0.043(2)
C(65)	0.1422(3)	0.3559(5)	0.4288(4)	0.037(1)
C(66)	0.1295(3)	0.2680(5)	0.3687(4)	0.030(1)

Table A-52 Bond lengths (Å) for $[\text{Pt}\{\text{NCH}_2\text{CH}_2\text{CO}\}_2(\text{PPh}_3)_2]\cdot\text{UO}_2(\text{NO}_3)_2$ (**7.15**)

U–O(18)	1.755(4)	U–O(19)	1.761(5)
U–O(2)	2.336(5)	U–O(1)	2.350(5)
U–O(16)	2.512(5)	U–O(15)	2.518(5)
U–O(11)	2.523(5)	U–O(12)	2.535(5)
U–N(10)	2.964(7)	U–N(14)	2.967(6)
N(10)–O(13)	1.249(14)	N(10)–O(12)	1.252(9)
N(10)–O(13')	1.268(13)	N(10)–O(11)	1.296(10)
N(14)–O(17)	1.207(7)	N(14)–O(16)	1.240(7)
N(14)–O(15)	1.257(7)	Pt–N(5)	2.038(4)
Pt–N(1)	2.054(4)	Pt–P(1)	2.2616(13)
Pt–P(2)	2.2817(13)	P(1)–C(21)	1.817(5)
P(1)–C(11)	1.824(6)	P(1)–C(31)	1.825(6)
P(2)–C(61)	1.821(5)	P(2)–C(51)	1.822(5)
P(2)–C(41)	1.830(6)	N(1)–C(2)	1.299(7)
N(1)–C(4)	1.491(7)	O(1)–C(2)	1.244(7)
C(2)–C(3)	1.505(8)	C(2)–C(4)	2.032(9)
C(3)–C(4)	1.536(9)	O(2)–C(6)	1.252(7)
N(5)–C(6)	1.310(7)	N(5)–C(8)	1.498(7)
C(6)–C(7)	1.491(8)	C(6)–C(8)	2.026(8)
C(7)–C(8)	1.540(8)	C(11)–C(12)	1.382(8)
C(11)–C(16)	1.384(8)	C(12)–C(13)	1.385(9)
C(13)–C(14)	1.354(10)	C(14)–C(15)	1.394(9)
C(15)–C(16)	1.389(8)	C(21)–C(26)	1.387(8)
C(21)–C(22)	1.396(7)	C(22)–C(23)	1.370(8)
C(23)–C(24)	1.366(10)	C(24)–C(25)	1.386(9)
C(25)–C(26)	1.377(8)	C(31)–C(32)	1.384(8)
C(31)–C(36)	1.396(8)	C(32)–C(33)	1.401(9)
C(33)–C(34)	1.392(12)	C(34)–C(35)	1.350(12)
C(35)–C(36)	1.370(9)	C(41)–C(42)	1.369(8)
C(41)–C(46)	1.398(8)	C(42)–C(43)	1.375(9)
C(43)–C(44)	1.403(10)	C(44)–C(45)	1.370(10)
C(45)–C(46)	1.393(8)	C(51)–C(56)	1.375(8)
C(51)–C(52)	1.398(8)	C(52)–C(53)	1.371(8)
C(53)–C(54)	1.363(10)	C(54)–C(55)	1.392(11)

C(55)–C(56)	1.374(9)	C(61)–C(66)	1.385(8)
C(61)–C(62)	1.392(8)	C(62)–C(63)	1.403(9)
C(63)–C(64)	1.365(10)	C(64)–C(65)	1.373(9)
C(65)–C(66)	1.378(8)		

Table A-53 Bond angles (°) for [Pt{NCH₂CH₂CO} ²₂(PPh₃)₂].UO₂(NO₃)₂ (7.15)

O(18)–U–O(19)	177.9(3)	O(18)–U–O(2)	89.19(19)
O(19)–U–O(2)	92.0(2)	O(18)–U–O(1)	89.6(2)
O(19)–U–O(1)	92.4(2)	O(2)–U–O(1)	71.27(17)
O(18)–U–O(16)	88.3(2)	O(19)–U–O(16)	90.4(2)
O(2)–U–O(16)	175.35(17)	O(1)–U–O(16)	112.61(16)
O(18)–U–O(15)	91.1(2)	O(19)–U–O(15)	89.3(2)
O(2)–U–O(15)	134.80(17)	O(1)–U–O(15)	63.53(16)
O(16)–U–O(15)	49.18(15)	O(18)–U–O(11)	89.3(2)
O(19)–U–O(11)	89.7(2)	O(2)–U–O(11)	64.81(19)
O(1)–U–O(11)	136.07(18)	O(16)–U–O(11)	111.25(18)
O(15)–U–O(11)	160.39(18)	O(18)–U–O(12)	87.1(2)
O(19)–U–O(12)	90.9(2)	O(2)–U–O(12)	115.18(17)
O(1)–U–O(12)	172.69(18)	O(16)–U–O(12)	60.80(16)
O(15)–U–O(12)	109.98(17)	O(11)–U–O(12)	50.46(19)
O(18)–U–N(10)	86.6(3)	O(19)–U–N(10)	91.7(3)
O(2)–U–N(10)	90.4(2)	O(1)–U–N(10)	161.3(2)
O(16)–U–N(10)	85.6(2)	O(15)–U–N(10)	134.7(2)
O(11)–U–N(10)	25.8(2)	O(12)–U–N(10)	24.77(19)
O(18)–U–N(14)	89.5(2)	O(19)–U–N(14)	89.93(19)
O(2)–U–N(14)	159.50(17)	O(1)–U–N(14)	88.27(17)
O(16)–U–N(14)	24.38(15)	O(15)–U–N(14)	24.80(15)
O(11)–U–N(14)	135.62(18)	O(12)–U–N(14)	85.18(17)
N(10)–U–N(14)	109.9(2)	O(13)–N(10)–O(12)	130.4(10)
O(13)–N(10)–O(13')	31.8(7)	O(12)–N(10)–O(13')	115.6(10)
O(13)–N(10)–O(11)	110.3(10)	O(12)–N(10)–O(11)	115.5(6)
O(13')–N(10)–O(11)	128.0(9)	O(13)–N(10)–U	162.6(10)
O(12)–N(10)–U	58.0(4)	O(13')–N(10)–U	165.3(9)
O(11)–N(10)–U	57.7(3)	N(10)–O(11)–U	96.5(4)
N(10)–O(12)–U	97.2(5)	O(17)–N(14)–O(16)	122.7(6)
O(17)–N(14)–O(15)	123.4(6)	O(16)–N(14)–O(15)	113.9(6)
O(17)–N(14)–U	179.3(5)	O(16)–N(14)–U	56.8(3)
O(15)–N(14)–U	57.2(3)	N(14)–O(15)–U	98.0(4)
N(14)–O(16)–U	98.8(4)	N(5)–Pt–N(1)	83.34(17)
N(5)–Pt–P(1)	90.57(13)	N(1)–Pt–P(1)	173.90(13)
N(5)–Pt–P(2)	168.63(13)	N(1)–Pt–P(2)	88.39(13)
P(1)–Pt–P(2)	97.67(5)	C(21)–P(1)–C(11)	111.4(3)
C(21)–P(1)–C(31)	99.8(2)	C(11)–P(1)–C(31)	104.6(3)
C(21)–P(1)–Pt	115.91(18)	C(11)–P(1)–Pt	109.56(18)
C(31)–P(1)–Pt	114.75(17)	C(61)–P(2)–C(51)	106.1(3)
C(61)–P(2)–C(41)	104.0(3)	C(51)–P(2)–C(41)	103.9(3)
C(61)–P(2)–Pt	114.47(18)	C(51)–P(2)–Pt	106.78(18)
C(41)–P(2)–Pt	120.32(18)	C(2)–N(1)–C(4)	93.3(4)
C(2)–N(1)–Pt	129.2(4)	C(4)–N(1)–Pt	131.5(4)
C(2)–O(1)–U	141.6(4)	O(1)–C(2)–N(1)	131.2(6)
O(1)–C(2)–C(3)	133.0(6)	N(1)–C(2)–C(3)	95.8(5)

O(1)–C(2)–C(4)	178.1(5)	N(1)–C(2)–C(4)	47.1(3)
C(3)–C(2)–C(4)	48.7(3)	C(2)–C(3)–C(4)	83.9(4)
N(1)–C(4)–C(3)	87.1(4)	N(1)–C(4)–C(2)	39.7(3)
C(3)–C(4)–C(2)	47.4(3)	C(6)–O(2)–U	147.2(4)
C(6)–N(5)–C(8)	92.1(4)	C(6)–N(5)–Pt	137.2(4)
C(8)–N(5)–Pt	128.7(4)	O(2)–C(6)–N(5)	132.2(5)
O(2)–C(6)–C(7)	131.1(5)	N(5)–C(6)–C(7)	96.7(5)
O(2)–C(6)–C(8)	177.8(5)	N(5)–C(6)–C(8)	47.6(3)
C(7)–C(6)–C(8)	49.1(3)	C(6)–C(7)–C(8)	83.9(4)
N(5)–C(8)–C(7)	87.3(4)	N(5)–C(8)–C(6)	40.3(3)
C(7)–C(8)–C(6)	47.0(3)	C(12)–C(11)–C(16)	119.8(6)
C(12)–C(11)–P(1)	125.2(5)	C(16)–C(11)–P(1)	115.0(4)
C(11)–C(12)–C(13)	119.8(6)	C(14)–C(13)–C(12)	121.0(6)
C(13)–C(14)–C(15)	120.0(6)	C(16)–C(15)–C(14)	119.6(6)
C(11)–C(16)–C(15)	119.8(6)	C(26)–C(21)–C(22)	118.7(5)
C(26)–C(21)–P(1)	120.2(4)	C(22)–C(21)–P(1)	121.1(4)
C(23)–C(22)–C(21)	121.0(6)	C(24)–C(23)–C(22)	119.6(6)
C(23)–C(24)–C(25)	120.6(6)	C(26)–C(25)–C(24)	119.9(6)
C(25)–C(26)–C(21)	120.1(6)	C(32)–C(31)–C(36)	120.7(6)
C(32)–C(31)–P(1)	117.6(4)	C(36)–C(31)–P(1)	121.7(5)
C(31)–C(32)–C(33)	118.4(7)	C(34)–C(33)–C(32)	120.1(8)
C(35)–C(34)–C(33)	120.2(7)	C(34)–C(35)–C(36)	121.3(7)
C(35)–C(36)–C(31)	119.3(7)	C(42)–C(41)–C(46)	118.7(5)
C(42)–C(41)–P(2)	122.4(4)	C(46)–C(41)–P(2)	118.9(5)
C(41)–C(42)–C(43)	122.0(6)	C(42)–C(43)–C(44)	119.4(7)
C(45)–C(44)–C(43)	119.2(6)	C(44)–C(45)–C(46)	120.9(6)
C(45)–C(46)–C(41)	119.7(6)	C(56)–C(51)–C(52)	118.8(6)
C(56)–C(51)–P(2)	122.8(5)	C(52)–C(51)–P(2)	118.3(4)
C(53)–C(52)–C(51)	120.0(6)	C(54)–C(53)–C(52)	121.1(6)
C(53)–C(54)–C(55)	119.3(6)	C(56)–C(55)–C(54)	120.0(6)
C(55)–C(56)–C(51)	120.8(6)	C(66)–C(61)–C(62)	119.4(5)
C(66)–C(61)–P(2)	120.7(4)	C(62)–C(61)–P(2)	119.9(5)
C(61)–C(62)–C(63)	119.3(7)	C(64)–C(63)–C(62)	120.0(6)
C(63)–C(64)–C(65)	120.9(6)	C(64)–C(65)–C(66)	119.7(6)
C(65)–C(66)–C(61)	120.7(5)		

Table A-54 Anisotropic displacement parameters (\AA^2) for
 $[\text{Pt}\{\overline{\text{NCH}_2\text{CH}_2\text{CO}}\}_2(\text{PPh}_3)_2]\cdot\text{UO}_2(\text{NO}_3)_2$ (**7.15**)

The anisotropic displacement factor exponent takes the form:

$$-2\pi^2 [h^2 a^{*2} U_{11} + \dots + 2 h k a^* b^* U_{12}]$$

	U11	U22	U33	U23	U13	U12
U	0.027(1)	0.038(1)	0.030(1)	-0.002(1)	0.016(1)	0.001(1)
N(10)	0.096(6)	0.085(6)	0.059(5)	-0.010(5)	0.043(5)	-0.057(5)
O(11)	0.074(4)	0.085(5)	0.054(4)	-0.028(3)	0.035(3)	-0.050(3)
O(12)	0.080(4)	0.069(4)	0.044(3)	-0.015(3)	0.041(3)	-0.039(3)
N(14)	0.044(3)	0.051(4)	0.048(3)	-0.005(3)	0.032(3)	-0.003(3)
O(15)	0.087(4)	0.041(3)	0.084(4)	-0.014(3)	0.073(4)	-0.017(3)
O(16)	0.105(5)	0.071(4)	0.069(4)	-0.034(3)	0.072(4)	-0.053(3)
O(17)	0.063(3)	0.062(4)	0.071(4)	-0.038(3)	0.045(3)	-0.022(3)

O(18)	0.035(2)	0.071(4)	0.049(3)	0.001(2)	0.029(2)	0.012(2)
O(19)	0.032(2)	0.032(3)	0.049(3)	0.001(2)	0.010(2)	0.001(2)
Pt	0.015(1)	0.018(1)	0.018(1)	0.001(1)	0.009(1)	0.001(1)
P(1)	0.019(1)	0.018(1)	0.023(1)	0.001(1)	0.012(1)	0.002(1)
P(2)	0.017(1)	0.020(1)	0.023(1)	0.002(1)	0.011(1)	0.000(1)
N(1)	0.015(2)	0.025(3)	0.028(2)	0.002(2)	0.013(2)	0.004(2)
O(1)	0.060(3)	0.047(3)	0.059(3)	-0.002(2)	0.049(3)	0.006(2)
C(2)	0.032(3)	0.022(3)	0.042(3)	0.002(2)	0.025(3)	0.001(2)
C(3)	0.027(3)	0.039(4)	0.040(4)	0.015(3)	0.014(3)	0.016(3)
C(4)	0.033(3)	0.048(4)	0.028(3)	0.013(3)	0.017(3)	0.013(3)
O(2)	0.025(2)	0.060(3)	0.045(3)	-0.019(2)	0.020(2)	-0.004(2)
N(5)	0.020(2)	0.018(2)	0.023(2)	-0.004(2)	0.012(2)	-0.001(2)
C(6)	0.018(2)	0.031(3)	0.026(3)	-0.003(2)	0.010(2)	-0.003(2)
C(7)	0.023(3)	0.044(4)	0.037(3)	-0.012(3)	0.013(3)	-0.007(3)
C(8)	0.027(3)	0.039(4)	0.024(3)	-0.015(3)	0.011(3)	-0.007(3)
C(11)	0.022(3)	0.024(3)	0.028(3)	0.000(2)	0.014(2)	0.002(2)
C(12)	0.026(3)	0.037(4)	0.037(3)	-0.004(3)	0.018(3)	0.003(3)
C(13)	0.034(3)	0.052(5)	0.060(5)	-0.003(4)	0.031(4)	0.008(3)
C(14)	0.046(4)	0.061(5)	0.049(4)	-0.016(4)	0.033(4)	0.000(3)
C(15)	0.040(4)	0.050(4)	0.037(4)	-0.011(3)	0.027(3)	0.002(3)
C(16)	0.027(3)	0.039(4)	0.031(3)	-0.002(3)	0.018(3)	-0.001(3)
C(21)	0.020(2)	0.024(3)	0.022(3)	0.002(2)	0.012(2)	-0.003(2)
C(22)	0.032(3)	0.029(3)	0.030(3)	0.005(2)	0.016(3)	0.005(2)
C(23)	0.039(3)	0.043(4)	0.029(3)	0.015(3)	0.017(3)	0.014(3)
C(24)	0.034(3)	0.067(5)	0.028(3)	0.005(3)	0.017(3)	0.003(3)
C(25)	0.050(4)	0.039(4)	0.035(4)	-0.007(3)	0.028(3)	-0.002(3)
C(26)	0.026(3)	0.028(3)	0.032(3)	-0.001(2)	0.020(3)	-0.002(2)
C(31)	0.022(3)	0.022(3)	0.024(3)	0.009(2)	0.009(2)	0.002(2)
C(32)	0.044(4)	0.038(4)	0.033(3)	0.000(3)	0.027(3)	-0.013(3)
C(33)	0.035(4)	0.054(5)	0.047(4)	0.008(4)	0.025(3)	-0.010(3)
C(34)	0.044(4)	0.040(5)	0.053(5)	0.011(4)	0.018(4)	-0.014(3)
C(35)	0.045(4)	0.027(4)	0.066(5)	0.003(3)	0.026(4)	-0.005(3)
C(36)	0.040(4)	0.023(3)	0.053(4)	-0.001(3)	0.026(3)	0.006(3)
C(41)	0.020(3)	0.024(3)	0.031(3)	0.005(2)	0.012(2)	-0.002(2)
C(42)	0.026(3)	0.040(4)	0.037(3)	0.010(3)	0.019(3)	0.008(3)
C(43)	0.041(4)	0.065(5)	0.064(5)	0.013(4)	0.041(4)	0.018(4)
C(44)	0.027(3)	0.032(4)	0.059(4)	0.006(3)	0.020(3)	0.010(3)
C(45)	0.025(3)	0.021(3)	0.044(4)	0.005(3)	0.013(3)	-0.002(2)
C(46)	0.023(3)	0.023(3)	0.030(3)	0.002(2)	0.013(2)	-0.004(2)
C(51)	0.018(2)	0.026(3)	0.019(3)	0.008(2)	0.009(2)	0.004(2)
C(52)	0.039(3)	0.035(3)	0.036(3)	0.005(3)	0.025(3)	0.003(3)
C(53)	0.042(4)	0.054(4)	0.031(3)	0.007(3)	0.026(3)	0.006(3)
C(54)	0.056(4)	0.059(5)	0.044(4)	0.028(4)	0.034(4)	0.011(4)
C(55)	0.080(6)	0.034(4)	0.054(5)	0.020(3)	0.040(4)	-0.002(4)
C(56)	0.045(4)	0.032(4)	0.041(4)	-0.002(3)	0.026(3)	-0.012(3)
C(61)	0.025(3)	0.015(3)	0.025(3)	0.000(2)	0.014(2)	-0.003(2)
C(62)	0.022(3)	0.033(4)	0.033(3)	-0.003(3)	0.009(3)	-0.006(2)
C(63)	0.038(4)	0.035(4)	0.034(4)	-0.005(3)	0.013(3)	-0.013(3)
C(64)	0.060(4)	0.031(4)	0.033(3)	-0.002(3)	0.027(3)	-0.005(3)
C(65)	0.047(4)	0.031(3)	0.032(3)	-0.005(3)	0.026(3)	-0.004(3)
C(66)	0.030(3)	0.024(3)	0.033(3)	-0.003(2)	0.020(3)	-0.005(2)

Table A-55 Hydrogen coordinates and isotropic displacement parameters (\AA^2) for
 $[\text{Pt}\{\text{NCH}_2\text{CH}_2\text{CO}\}_2(\text{PPh}_3)_2]\cdot\text{UO}_2(\text{NO}_3)_2$ (**7.15**)

	x	y	z	U(eq)
H(3A)	-0.0747	0.3557	0.0489	0.050
H(3B)	-0.1214	0.2372	0.0096	0.050
H(4A)	-0.0480	0.1355	0.0028	0.046
H(4B)	-0.0017	0.2540	0.0411	0.046
H(7A)	-0.1525	-0.1079	-0.0195	0.047
H(7B)	-0.1328	-0.2177	0.0497	0.047
H(8A)	-0.0322	-0.2410	0.0818	0.041
H(8B)	-0.0513	-0.1301	0.0140	0.041
H(12)	0.2507	-0.2661	0.3676	0.043
H(13)	0.2953	-0.3288	0.3036	0.058
H(14)	0.2372	-0.3074	0.1499	0.060
H(15)	0.1318	-0.2210	0.0555	0.049
H(16)	0.0853	-0.1606	0.1182	0.039
H(22)	0.2102	-0.3273	0.4347	0.040
H(23)	0.2833	-0.3209	0.5928	0.049
H(24)	0.2912	-0.1494	0.6664	0.054
H(25)	0.2230	0.0143	0.5824	0.049
H(26)	0.1522	0.0115	0.4236	0.034
H(32)	0.0232	-0.1941	0.3029	0.044
H(33)	-0.0464	-0.3538	0.2721	0.056
H(34)	-0.0390	-0.5378	0.2216	0.068
H(35)	0.0309	-0.5600	0.1933	0.065
H(36)	0.0989	-0.4050	0.2202	0.051
H(42)	0.2318	0.0613	0.2227	0.043
H(43)	0.3305	-0.0361	0.2917	0.063
H(44)	0.3984	-0.0917	0.4470	0.055
H(45)	0.3631	-0.0543	0.5266	0.045
H(46)	0.2636	0.0452	0.4564	0.035
H(52)	0.1061	0.0679	0.0969	0.043
H(53)	0.0790	0.1686	-0.0280	0.049
H(54)	0.0932	0.3732	-0.0237	0.063
H(55)	0.1343	0.4805	0.1084	0.070
H(56)	0.1635	0.3802	0.2351	0.049
H(62)	0.2648	0.2921	0.4019	0.044
H(63)	0.2876	0.4354	0.5086	0.052
H(64)	0.2107	0.4742	0.5236	0.052
H(65)	0.1105	0.3744	0.4339	0.044
H(66)	0.0897	0.2243	0.3349	0.036